JGRG23

Proceedings of
the 23rd Workshop on General Relativity
and Gravitation in Japan

5—8 November 2013

50th Anniversary Auditorium, Hirosaki University

Aomori, Japan

Volume 4

Oral Presentations: Fourth Day
Poster Presentations

Contents

Oral Presentations: Fourth Day 694

"Graviton oscillation in bi-gravity theory" by Takahiro Tanaka [JGRG23(2013)110801] 695

"F(T) gravity from the Kaluza-Klein and Randall-Sundrum theories and cosmology" by Kazuharu Bamba [JGRG23(2013)110802] 704

"Observational Upper Bound on the Cosmic Abundances of Negative-mass Compact Objects and Ellis Wormholes from the SDSS Quasar Lens Search" by Ryuichi Takahashi [JGRG23(2013)110803] 733

"Analytic formula for the threshold of primordial black hole formation" by Tomohiro Harada [JGRG23(2013)110804] 747

"First—Quantized Theory of Expanding Universe from Quantum Field in Mini—Superspace" by Daisuke Ida [JGRG23(2013)110805] 760

"Constraining the small scale perturbations in our big universe" by Christian Byrnes (invited) [JGRG23(2013)110806] 773

Poster Presentations 786

"Wormhole solutions in higher dimensional space-time and their linear stability analysis" by Takashi Torii [JGRG23(2013)P01] 789

"Gauged Q-balls" by Takashi Tamaki [JGRG23(2013)P02] 795

"Bound states of extreme Type-I cosmic strings in two-dimensional space" by Takashi Hiramatsu [JGRG23(2013)P03] 806

"Gravitational lensing shear by an exotic lens object with negative convergence or negative mass" by Koji Izumi [JGRG23(2013)P04] 815

"Shapiro delay by an exotic lens object with negative convergence or negative mass" by Koki Nakajima [JGRG23(2013)P05] 817

"Gravitational field of a rotating ring around a Schwarzschild black hole" by Yasumichi Sano [JGRG23(2013)P06] 819

"Demagnification by an exotic lens object with negative mass" by Chisaki Hagiwara [JGRG23(2013)P07] 831

"Wormholes in higher dimensional space-time: Dynamics" by Hisaaki Shinkai [JGRG23(2013)P09] 833

"General Relativistic Sitnikov 3-Body Problem" by Hideyoshi Arakida [JGRG23(2013)P10] 835

"Black Hole Universe with Lambda" by Chulmoon Yoo [JGRG23(2013)P11] 837

“Modeling of the secular evolution of a inspiral orbit around a Kerr black hole” by Norichika Sago [JGRG23(2013)P12] 846

“Spin-Regge-Wheeler-Zerilli formalism and gravitational waves” by Hiroyuki Nakano [JGRG23(2013)P13] 854

“3+1 gauge-invariant variables for perturbations on Schwarzschild spacetime” by Kouji Nakamura [JGRG23(2013)P14] 863

“How can we detect BHs ?” by Hiromi Saida [JGRG23(2013)P15] 874

“A new numerical scheme for Einstein equations with discrete variational derivative method” by Takuya Tsuchiya [JGRG23(2013)P17] 881

“Cosmological matching conditions in Horndeski's theory” by Sakine Nishi [JGRG23(2013)P20] 883

“21cm signature of minihaloes from cosmic string wakes” by Naoya Kitajima [JGRG23(2013)P23] 885

“Liquid bridges and black strings in general dimensions: Stability” by Umpei Miyamoto [JGRG23(2013)P24] 894

“(In-)stability of naked singularity formation in gravitational collapse” by Seiju Ohashi [JGRG23(2013)P26] 902

“Issues on curvaton scenario with the thermal effect” by Shuichiro Yokoyama [JGRG23(2013)P27] 911

“Monte Carlo simulation of quantum cosmology” by Hiroshi Suenobu [JGRG23(2013)P28] 919

“Magnetic Penrose Process in a Black Hole Magnetosphere” by Masaaki Takahashi [JGRG23(2013)P29] 921

“Gravitational waves generated during slow-roll inflation in Lorentz-violating Weyl gravity” by Kohji Yajima [JGRG23(2013)P31] 934

“An exact solution describing a closed membrane without spherical symmetry” by Hiroshi Kozaki [JGRG23(2013)P32] 936

Oral Presentations: Fourth Day

Friday 8 November

Morning 1 [Chair: Jiro Soda]

9:30 Takahiro Tanaka (YITP, Kyoto University)
"Graviton oscillation in bi-gravity theory"
[JGRG23(2013)110801]

9:50 Kazuharu Bamba (Kobayashi-Maskawa Institute for the Origin of Particles and the Universe, Nagoya University)
"$F(T)$ gravity from the Kaluza-Klein and Randall-Sundrum theories and cosmology"
[JGRG23(2013)110802]

10:10 Ryuichi Takahashi (Hirosaki University)
"Observational Upper Bound on the Cosmic Abundances of Negative-mass Compact Objects and Ellis Wormholes from the SDSS Quasar Lens Search"
[JGRG23(2013)110803]

10:30 Tomohiro Harada (Department of Physics, Rikkyo University)
"Analytic formula for the threshold of primordial black hole formation"
[JGRG23(2013)110804]

10:50 Daisuke Ida (Department of Physics, Gakushuin University)
"First—Quantized Theory of Expanding Universe from Quantum Field in Mini—Superspace"
[JGRG23(2013)110805]

11:10-30 Break

Morning 2 [Chair: Misao Sasaki]

11:30 Christian Byrnes (University of Sussex) [Invited]
"Constraining the small scale perturbations in our big universe"
[JGRG23(2013)110806]

12:30 Kei-ichi Maeda (Waseda University)
Closing remarks
[*]

“Graviton oscillation in bi-gravity theory”

by Takahiro Tanaka

[JGRG23(2013)110801]

Graviton Oscillation in viable bigravity models

Takahiro Tanaka (YITP)
with
Antonio De Felice and Takashi Nakamura
arXiv:1304.3920
partly work with Yasuho Yamashita

Gravitation waves will be detected soon!!!

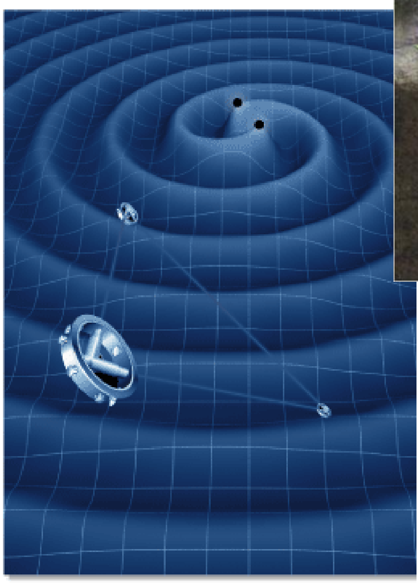

eLISA(NGO)
⇒DECIGO/BBO

LIGO⇒adv LIGO

GW generation is almost confirmed

Pulsar : ideal clock

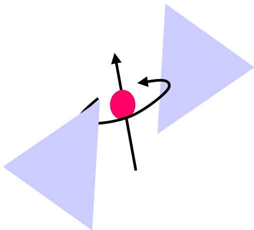

Test of GR by pulsar binaries

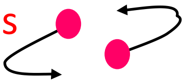

Periastron advance due to GW emission

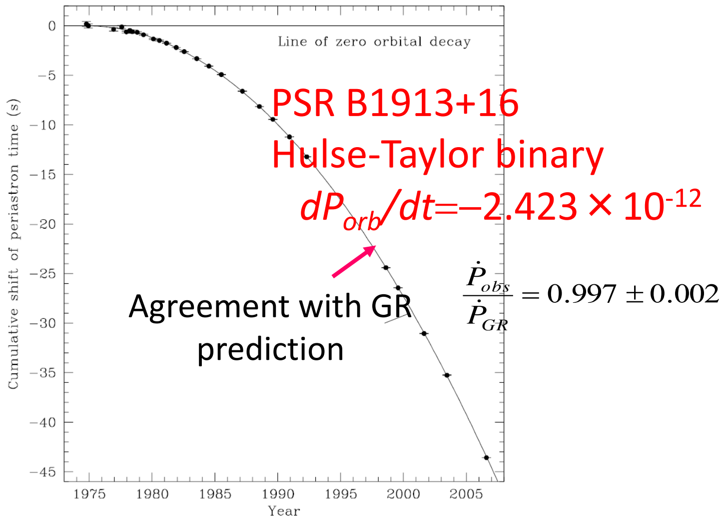

(J.M. Weisberg, Nice and J.H. Taylor, arXiv:1011.0718)

We know that GWs are emitted from binaries.

What is the possible big surprise when we directly detect GWs?

Is there possibility that graviton disappears during its propagation over cosmological distance?

Braneworld

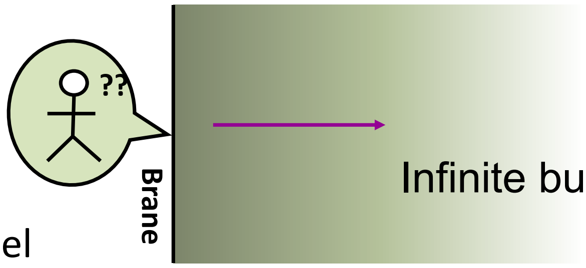

Infinite extra-dimension

RS-II model, DGP model

Modification of GW propagation is small even if sources are placed at cosmological distances.

Chern-Simons Modified Gravity

$$S \supset \frac{\alpha}{4}\int d^4x\sqrt{-g}\,\theta\,\varepsilon^{\mu\nu\rho\sigma}R_{\mu\nu}{}^{\alpha\beta}R_{\alpha\beta\rho\sigma}$$

Right-handed and left-handed gravitational waves are magnified differently during propagation, depending on frequencies.

However, the effect is large only in the strong coupling regime, outside the validity range of EFT.

Massive gravity

$$\Box h_{\mu\nu} = 0 \quad \Longrightarrow \quad \left(\Box - m^2\right)h_{\mu\nu} = 0$$

Just adding mass to graviton seems theoretically inconsistent → ghost, instability, etc.

⇨ Bi-gravity

$$\frac{L}{M_G^2} = \frac{\sqrt{-g}\,R}{16\pi} + \frac{\sqrt{-\tilde{g}}\,\tilde{R}}{16\pi\kappa} + \frac{L_{matter}(g,\phi)}{M_G^2} + \cdots$$

Both massive and massless gravitons exist.

$\rightarrow$ ν oscillation-like phenomena?

First question is whether or not we can construct a viable cosmological model.

Ghost free bi-gravity

When $\tilde{g}$ is fixed, de Rham-Gabadadze-Tolley massive gravity.

$$\frac{L}{M_G^2} = \frac{\sqrt{-g}R}{2} + \frac{\sqrt{-\tilde{g}}\tilde{R}}{2\kappa} + \frac{\sqrt{-g}}{2}\sum_{n=0}^{4} c_n V_n + \frac{L_{matter}}{M_G^2}$$

$$V_0 = 1,\ V_1 = \tau_1, V_2 = \tau_1^2 - \tau_2,\ \cdots \quad \tau_n \equiv Tr\left[\gamma^n\right] \quad \gamma^i_j \equiv \sqrt{g^{ik}\tilde{g}_{kj}}$$

Even if $\tilde{g}$ is promoted to a dynamical field, the model remains to be free from ghost.

(Hassan, Rosen (2012))

FLRW background

(Comelli, Crisostomi, Nesti, Pilo (2012))

Generic homogeneous isotropic metrics

$$ds^2 = a^2(t)\left(-dt^2 + dx^2\right)$$
$$d\tilde{s}^2 = b^2(t)\left(-c^2(t)dt^2 + dx^2\right) \qquad \xi \equiv b/a$$

$$\Rightarrow \quad \underbrace{\left(6c_3\xi^2 + 4c_2\xi + c_1\right)}_{\text{branch 1}}\underbrace{\left(cba' - ab'\right)}_{\text{branch 2}} = 0$$

branch 1 : Pathological:

Strong coupling

Unstable for the homogeneous anisotropic mode.

branch 2 : Healthy

Branch 2 background

A very simple relation holds:

$$\frac{\rho}{M_G^2} + f - \tilde{f}/\kappa\xi^2 = 0 \qquad f(\log \xi) := c_0 + 3c_1\xi + 6c_2\xi^2 + 6c_3\xi^3$$

$$\tilde{f}(\log \xi) := c_1\xi + 6c_2\xi^2 + 18c_3\xi^3 + 24c_4\xi^4$$

$\xi \equiv b/a$ is algebraically determined as a function of ρ.

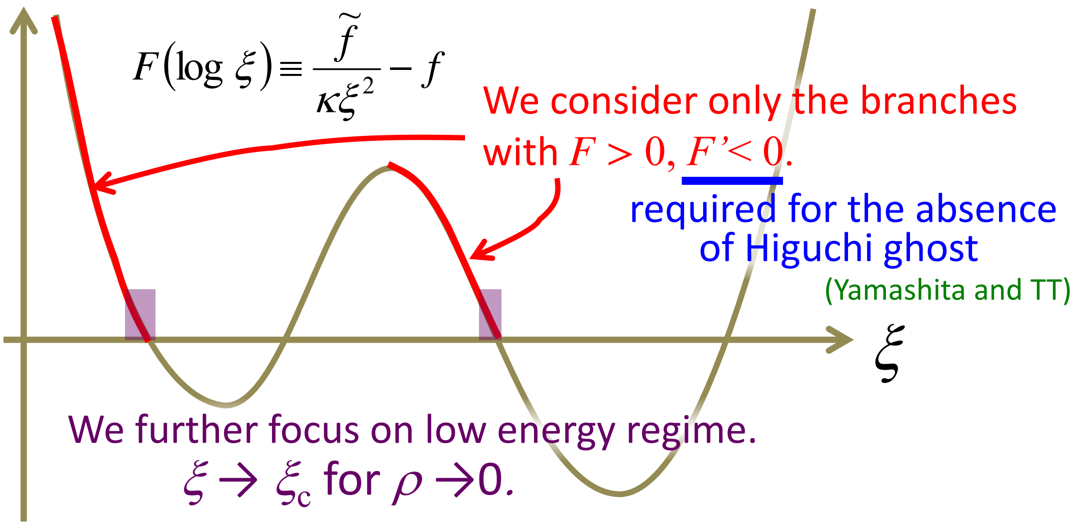

Branch 2 background

We expand with respect to $\delta\xi = \xi - \xi_c$.

$$H^2 = \frac{\rho}{3M_G^2} + \frac{f}{3} \Rightarrow H^2 = \frac{\rho}{3(1+\kappa\xi_c^2)M_G^2}$$

effective energy density due to mass term

Effective gravitational coupling is weaker because of the dilution to the hidden sector.

$$\frac{1}{c-1}\frac{\xi'}{\xi} = \frac{a'}{a} \Rightarrow c - 1 = \frac{3(\rho + P)}{\mu^2 M_G^2}$$

Effective graviton mass

$$\mu^2 = \left(1 + \frac{1}{\kappa\xi_c^2}\right) f_c'$$

natural tuning to coincident light cones (c=1)
at low energies ($\rho \to 0$)!

Why do we have this attractor behavior, $c \to 1$ and $\xi \to \xi_c$, at low energies? (→Yamashita-san's talk)

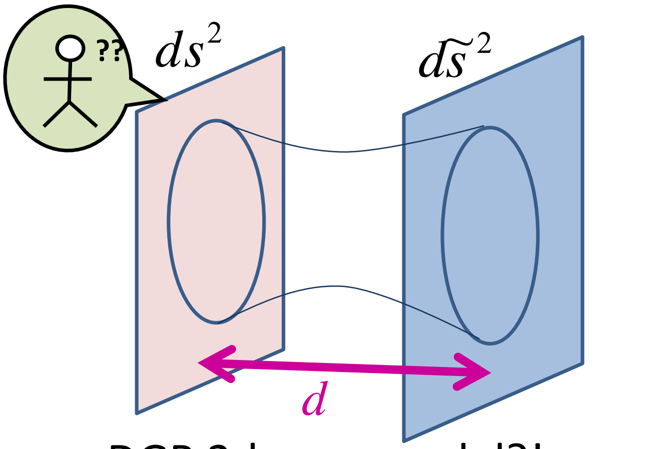

DGP 2-brane model?!

$$+\int d^4x\sqrt{-g}R \;\&\; \int d^4x\sqrt{-\tilde{g}}\tilde{R}$$

$\approx$

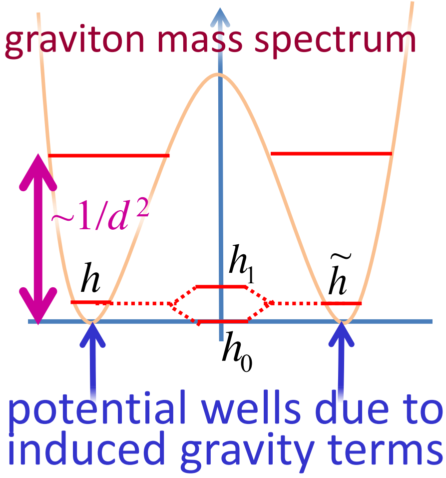

$d \to 0$ ⇨ Only first two modes remain at low energy

⇨ $d\tilde{s}^2 = \xi_c^2 ds^2$ ⇨ identical light cone $c = 1$

Solar system constraint

Ordinary Vainshtein mechanism is not good enough!

$$G_{\mu\nu} = M_G^{-2}\left(T_{\mu\nu} + T_{\mu\nu}^{(\mathrm{int})}\right)$$

Ordinary Vainshtain mechanism tells that $T_{\mu\nu}^{(\mathrm{int})}$ can be simply neglected on small length scales for $T_{\mu\nu}^{(\mathrm{int})} \to 0$.

Then, however,

"local effective gravitational coupling M_G^2"

≠ "cosmological one $\left(1+\kappa\xi_c^2\right)M_G^2$"

Here, we do not send $T_{\mu\nu}^{(\mathrm{int})} \to 0$,

but we only tune the graviton mass to be small: $\mu^2 << c_i$

⇨ $h_{\mu\nu} \approx \tilde{h}_{\mu\nu}$

"local effective gravitational coupling"= $\left(1+\kappa\xi_c^2\right)M_G^2$

Gravitational wave propagation

Short wavelength approximation :

$$k \gg m_g \gg H$$

$$h'' - \underline{\Delta h} + \underline{m_g^2}\left(h - \tilde{h}\right) = 0$$

$$\tilde{h}'' - \underline{c^2 \Delta \tilde{h}} - \frac{c m_g^2}{\underline{\kappa \xi_c^2}}\left(h - \tilde{h}\right) = 0$$

$$m_g^2 = \frac{f'}{3} + \frac{(c-1)}{6}\left(f'' - f'\right)$$

(Comelli, Crisostomi, Pilo (2012))

$$\mu^2 := m_g^2 \frac{1 + \kappa \xi^2}{\kappa \xi^2} \qquad k_c := \frac{\mu}{\sqrt{2(c-1)}} \qquad k$$

mass term is important.

Eigenmodes are

$$h + \tilde{h}, \quad \underline{\kappa \xi_c^2 h - \tilde{h}}$$

modified dispersion relation
due to the effect of mass

$C \neq 1$ is important.

Eigenmodes are

$$h, \quad \underline{\tilde{h}}$$

modified dispersion relation
due to different light cone

At the GW generation, both h and $\tilde{h}$ are equally excited.

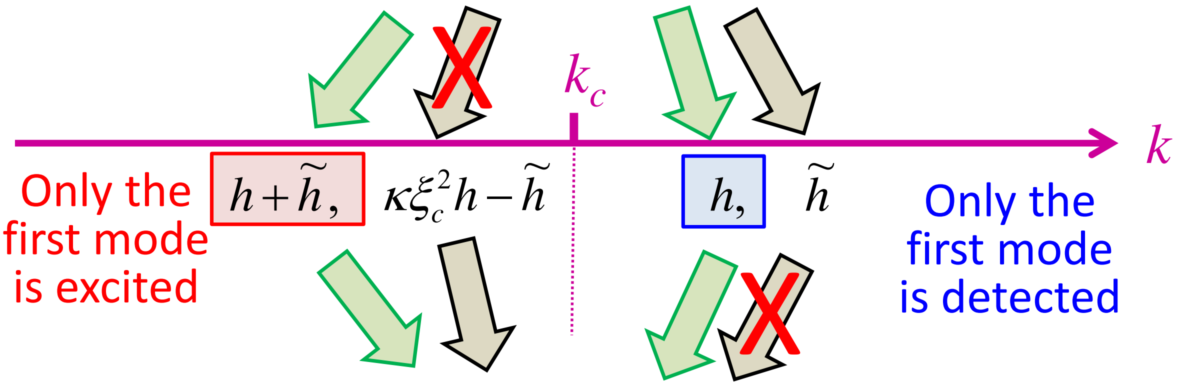

We can detect only h.

Only modes with $k \sim k_c$ picks up the non-trivial dispersion relation of the second mode.

Interference between two modes. ⇨ Graviton oscillations

If the effect appears ubiquitously, the model would be already ruled out.

Summary

Gravitational wave observations open up a new window for modified gravity.

Even graviton oscillations are not immediately denied, and hence we may find something similar to the case of solar neutrino experiment in near future.

Although space GW antenna is advantageous for the gravity test in many respects, we should be able to find more that can be tested by KAGRA.

“$F(T)$ gravity from the Kaluza-Klein and Randall-Sundrum theories and cosmology”

by Kazuharu Bamba

[JGRG23(2013)110802]

$F(T)$ gravity from the Kaluza-Klein and Randall-Sundrum theories and cosmology [110802]

Main reference: **Phys. Lett. B 725, 368 (2013) [arXiv:1304.6191 [gr-qc]].**

JGRG23
The 23rd Workshop on General Relativity and Gravitation in Japan
8th November, 2013
50th Anniversary Auditrium
Hirosaki University

Kobayashi-Maskawa Institute
for the Origin of Particles and the Universe

Presenter : **Kazuharu Bamba** (*KMI, Nagoya University*)

Collaborators : **Shin'ichi Nojiri** (*KMI and Dep. of Phys., Nagoya University*)
Sergei D. Odintsov (*ICREA and CSIC-IEEC, Spain*)

2

Contents

I. Introduction
Current cosmic accelerated expansion

II. $F(T)$ gravity

III. From the Kaluza-Klein (KK) theory

IV. From the Randall-Sundrum (RS) theory

V. Summary

3

I. Introduction

Current cosmic accelerated expansion

4

- Recent observations of Type Ia Supernova (SNe Ia) has supported that the current expansion of the universe is accelerating.

[Perlmutter *et al.* [Supernova Cosmology Project Collaboration], Astrophys. J. 517, 565 (1999)]

[Riess *et al.* [Supernova Search Team Collaboration], Astron. J. 116, 1009 (1998)]

2011 Nobel Prize in Physics

- Suppose that the universe is strictly homogeneous and isotropic.

There are two approaches to explain the current accelerated expansion of the universe.

Reviews: E.g.,

[Copeland, Sami and Tsujikawa, Int. J. Mod. Phys. D 15, 1753 (2006)]

[Nojiri and Odintsov, Phys. Rept. 505, 59 (2011); Int. J. Geom. Meth. Mod. Phys. 4, 115 (2007)]

[Capozziello and Faraoni, *Beyond Einstein Gravity* (Springer, 2010)]

[De Felice and Tsujikawa, Living Rev. Rel. 13, 3 (2010)]

[Clifton, Ferreira, Padilla and Skordis, Phys. Rept. 513, 1 (2012)]

[KB, Capozziello, Nojiri and Odintsov, Astrophys. Space Sci. 342, 155 (2012)]

Gravitational field equation

$$G_{\mu\nu} = \kappa^2 T_{\mu\nu}$$

Gravity **Matter**

$G_{\mu\nu}$: Einstein tensor

$T_{\mu\nu}$: Energy-momentum tensor

$\kappa^2 \equiv 8\pi / {M_{\mathrm{Pl}}}^2$

M_{Pl} : Planck mass

(1) **General relativistic approach** $\longrightarrow$ **Dark Energy**

(2) **Extension of gravitational theory**

(1) Candidates for dark energy

Cosmological constant, Scalar field, Fluid

(2) Extension of gravitational theory

- ***F*(*R*) gravity** $F(R)$: Arbitrary function of the Ricci scalar R
- **DGP braneworld scenario**
- **Galileon gravity**
- **Massive gravity**
- **Bimetric gravity**
- **Extended teleparallel gravity (*F*(*T*) gravity)**

$F(T)$: Arbitrary function of the torsion scalar T

Condition for accelerated expansion

Flat Friedmann-Lemaî tre-Robertson-Walker (FLRW) space-time

$$ds^2 = dt^2 - a^2(t) \sum_{i=1,2,3} \left(dx^i\right)^2$$

$a(>0)$: Scale factor

Equation of $a(t)$ for a single perfect fluid

$$\frac{\ddot{a}}{a} = -\frac{\kappa^2}{6} \underline{(1+3w)\,\rho}$$

ρ : Energy density

P : Pressure

$\dot{} = \partial/\partial t$

$\ddot{a} > 0$: **Accelerated expansion**

Cf. $w = -1$

: Cosmological constant

$$\Rightarrow \boxed{w \equiv \frac{P}{\rho} < -\frac{1}{3}}$$

w : **Equation of state (EoS) parameter**

9

PLANCK data for the current w (=constant)

[Ade *et al.* [Planck Collaboration], arXiv:1303.5076 [astro-ph.CO]]

$w = -1.13^{+0.24}_{-0.25}$ (95%; *Planck*+WP+BAO)

$w = -1.09 \pm 0.17$ (95%; *Planck*+WP+Union2.1)

$w = -1.13^{+0.13}_{-0.14}$ (95%; *Planck*+WP+SNLS)

$w = -1.24^{+0.18}_{-0.19}$ (95%; *Planck*+WP+H_0)

WP: WMAP, BAO: Baryon Acoustic Oscillation

Hubble constant (H_0) measurement

10

PLANCK data for the time-dependent w

2D Marginalized posterior distribution

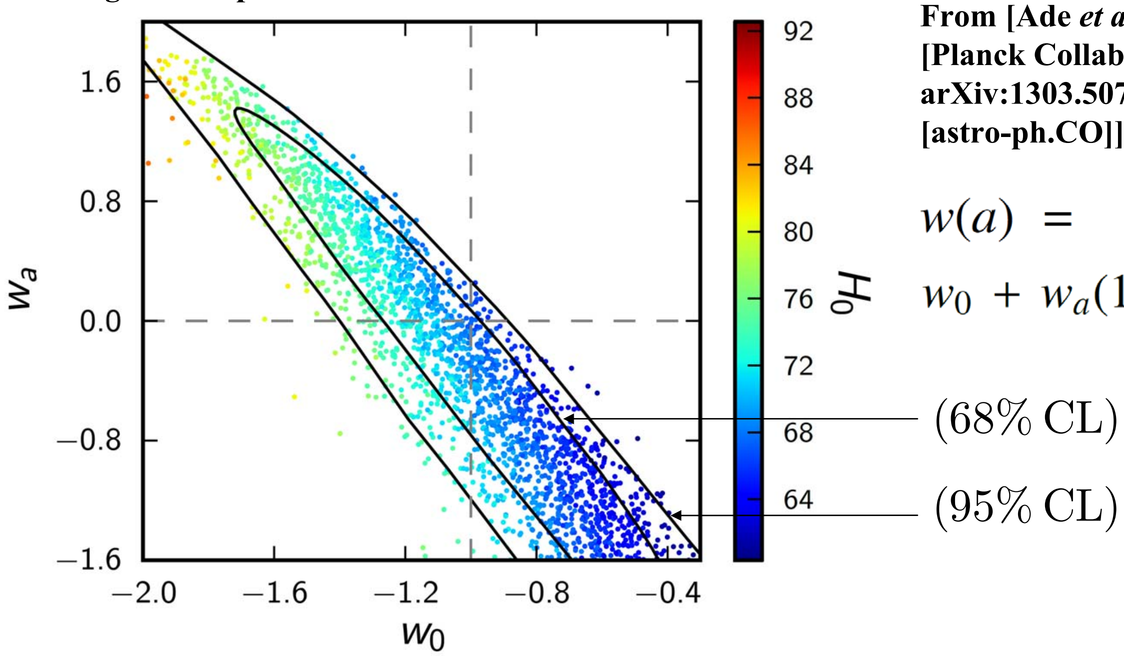

From [Ade *et al.* [Planck Collaboration], arXiv:1303.5076 [astro-ph.CO]].

$w(a) = w_0 + w_a(1 - a)$

$w_0 = -1.04^{+0.72}_{-0.69}$ (95%; *Planck*+WP+BAO)

$w_a < 1.32$ (95%; *Planck*+WP+BAO)

Motivation and Subject

- **It is meaningful to investigate theoretical features and cosmological aspects of modified gravity theories.**

→ **We explore the four-dimensional effective $F(T)$ gravity originating from higher-dimensional space-time theories, in particular the Kaluza-Klein (KK) and Randall-Sundrum (RS) theories.**

II. $F(T)$ gravity

13

Teleparallelism

- $g_{\mu\nu} = \eta_{AB} e^A_\mu e^B_\nu$

η_{AB} : Minkowski metric

$e_A(x^\mu)$: Orthonormal tetrad components

- $T^\rho_{\mu\nu} \equiv \Gamma^{\rho(W)}_{\mu\nu} - \Gamma^{\rho(W)}_{\nu\mu} = e^\rho_A \left(\partial_\mu e^A_\nu - \partial_\nu e^A_\mu\right)$: **Torsion tensor**

$\Gamma^{\rho(W)}_{\mu\nu} \equiv e^\rho_A \partial_\mu e^A_\nu$: Weitzenböck connection

* μ and ν are coordinate indices on the manifold and also run over 0, 1, 2, 3, and $e_A(x^\mu)$ forms the tangent vector of the manifold.

* An index A runs over 0, 1, 2, 3 for the tangent space at each point x^μ of the manifold.

14

$T \equiv S_\rho{}^{\mu\nu} T^\rho{}_{\mu\nu}$: **Torsion scalar**

$$K^{\mu\nu}{}_\rho \equiv -\frac{1}{2}\left(T^{\mu\nu}{}_\rho - T^{\nu\mu}{}_\rho - T_\rho{}^{\mu\nu}\right)$$: Contorsion tensor

$$S_\rho{}^{\mu\nu} \equiv \frac{1}{2}\left(K^{\mu\nu}{}_\rho + \delta^\mu_\rho\, T^{\alpha\nu}{}_\alpha - \delta^\nu_\rho\, T^{\alpha\mu}{}_\alpha\right)$$

[Hehl, Von Der Heyde, Kerlick and Nester, Rev. Mod. Phys. 48, 393 (1976)]

[Hayashi and Shirafuji, Phys. Rev. D 19, 3529 (1979)
[Addendum-ibid. D 24, 3312 (1981)]]

Extended teleparallel gravity

Action

$$S = \int d^4x|e| \left(\underline{\frac{F(T)}{2\kappa^2}} + \mathcal{L}_{\mathrm{M}} \right)$$: ***F*(*T*) gravity**

Cf. $F(T) = T$: Teleparallelism

$$|e| = \det\left(e^A_\mu\right) = \sqrt{-g}$$

$\mathcal{L}_{\mathrm{M}}$: Matter Lagrangian

${T^{(\mathrm{M})}}_\rho{}^\nu$: Energy-momentum tensor of matter

Gravitational field equation

$$\frac{1}{e}\partial_\mu\left(e{S_A}^{\mu\nu}\right)F' - e^\lambda_A {T^\rho}_{\mu\lambda}{S_\rho}^{\nu\mu}F' + {S_A}^{\mu\nu}\partial_\mu(T)F'' + \frac{1}{4}e^\nu_A F = \frac{\kappa^2}{2}e^\rho_A {T^{(\mathrm{M})}}_\rho{}^\nu$$

* A prime denotes a derivative with respect to T.

[Bengochea and Ferraro, Phys. Rev. D 79, 124019 (2009)]

- **Gravitational field equation in *F*(*T*) gravity is 2nd order, while it is 4th order in *F*(*R*) gravity.**

- For the flat FLRW space-time with the metric:

$$ds^2 = dt^2 - a^2(t)\sum_{i=1,2,3}\left(dx^i\right)^2 \Rightarrow \underline{T = -6H^2}$$

$$g_{\mu\nu} = \mathrm{diag}(1, -a^2, -a^2, -a^2)$$

$$e^A_\mu = (1, a, a, a)$$

$H \equiv \frac{\dot{a}}{a}$: Hubble parameter

17

Gravitational field equations

ρ_{DE} : Dark energy density

P_{DE} : Pressure of dark energy

ρ_{M}, P_{M}

: Energy density and pressure of dark energy

$$H^2 = \frac{\kappa^2}{3}\left(\rho_{\mathrm{M}} + \rho_{\mathrm{DE}}\right)$$

$$\dot{H} = -\frac{\kappa^2}{2}\left(\rho_{\mathrm{M}} + P_{\mathrm{M}} + \rho_{\mathrm{DE}} + P_{\mathrm{DE}}\right)$$

$$\rho_{\mathrm{DE}} = \frac{1}{2\kappa^2}\left(-T - F + 2TF'\right)$$

$$P_{\mathrm{DE}} = -\frac{1}{2\kappa^2}\left[4\left(1 - F' - 2TF''\right)\dot{H} - T - F + 2TF'\right]$$

Continuity equation

$$\dot{\rho}_{\mathrm{DE}} + 3H\left(\rho_{\mathrm{DE}} + P_{\mathrm{DE}}\right) = 0$$

18

Example of *F*(*T*) gravity model

$$F(T) = T + \gamma\left[T_0\left(\frac{uT_0}{T}\right)^{-1/2}\ln\left(\frac{uT_0}{T}\right) - T\left(1 - \mathrm{e}^{uT_0/T}\right)\right]$$

[KB, Geng, Lee and Luo, JCAP 1101, 021 (2011)]

$$\gamma \equiv \frac{1 - \Omega_{\mathrm{m}}^{(0)}}{2u^{-1/2} + \left[1 - (1 - 2u)\,\mathrm{e}^{u}\right]}$$

$u(>0)$: Positive constant

$$\Omega_{\mathrm{m}}^{(0)} \equiv \rho_{\mathrm{m}}^{(0)} / \rho_{\mathrm{crit}}^{(0)}\,, \qquad T_0 = T(z=0)$$

$$\rho_{\mathrm{crit}}^{(0)} = 3H_0^2 / \kappa^2 \qquad z = \frac{1}{a} - 1$$

: Redshift

Cf. **For the cosmological dynamics, see also, e.g., [Wu and Yu, Phys. Lett. B 692, 176 (2010); 693, 415 (2010)].**

Cosmological evolutions of w_{DE}

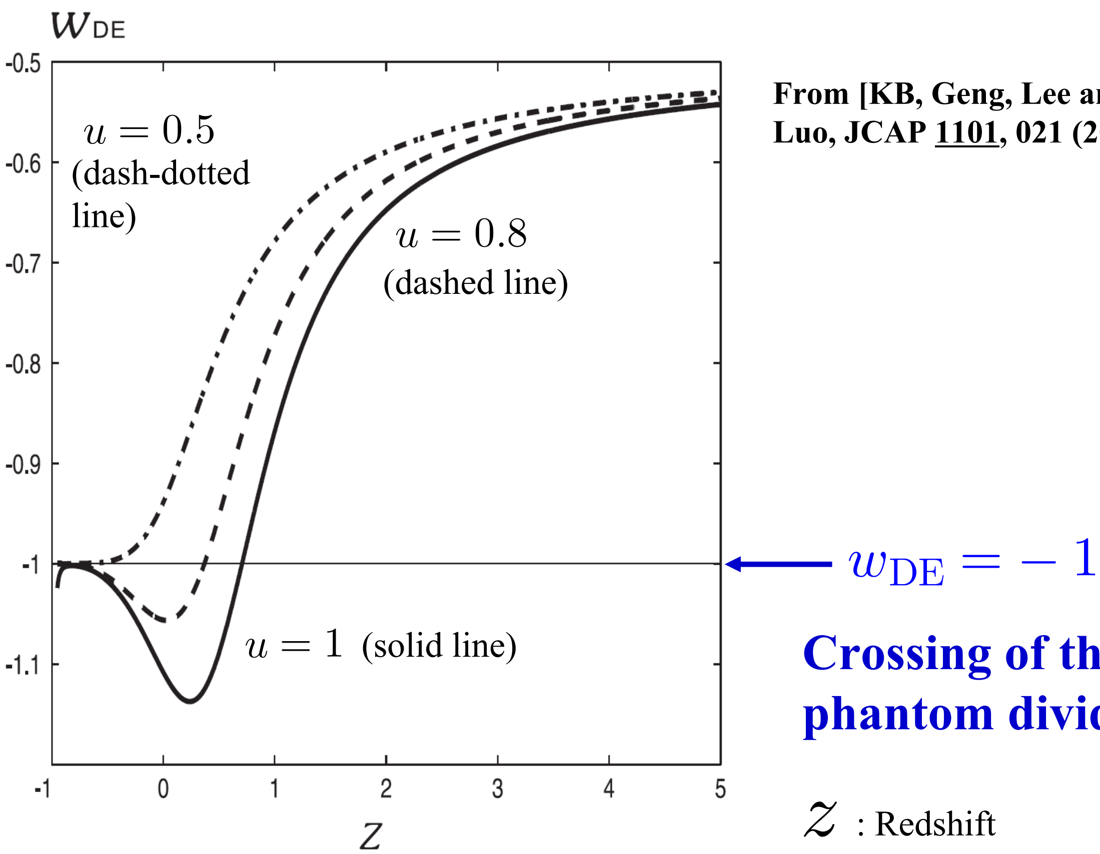

From [KB, Geng, Lee and Luo, JCAP 1101, 021 (2011)].

Crossing of the phantom divide

z : Redshift

III. From Kaluza-Klein (KK) theory

21

Action in five-dimensional space-time

$$^{(5)}S = \int d^5x \left| ^{(5)}e \right| \frac{F(^{(5)}T)}{2\kappa_5^2}$$

$$^{(5)}T \equiv \frac{1}{4}T^{abc}T_{abc} + \frac{1}{2}T^{abc}T_{cba} - T_{ab}{}^{a}T^{cb}{}_{c}$$

$$^{(5)}e = \sqrt{^{(5)}g}$$

* $a, b, \ldots$ run over $0, 1, 2, 3, 5$.

$$\kappa_5^2 \equiv 8\pi G_5 = \left(^{(5)}M_{\mathrm{Pl}}\right)^{-3}$$

* "5" denotes the component of the fifth coordinate.

- **The superscript or subscript of (5) or 5 mean the quantities in the five-dimensional space-time.**

[Capozziello, Gonzalez, Saridakis and Vasquez, JHEP 1302, 039 (2013)]

22

Original KK compactification scenario

- One of the dimensions of space is compactified to a small circle and the four-dimensional space-time is extended infinitely.
- The radius of the fifth dimension is taken to be of order of the Planck length in order for the KK effects not to be seen.

⇨ **The size of the circle is so small that phenomena in sufficiently low energies cannot be detected.**

[Appelquist, Chodos and Freund, *Modern Kaluza-Klein Theories* (Addison-Wesley, Reading, 1987)]

[Fujii and Maeda, The Scalar-Tensor Theory of Gravitation (Cambridge University Press, Cambridge, United Kingdom, 2003)]

23

Effective action in the four-dimensional space-time

Metric in five-dimensional space-time

$$ {}^{(5)}g_{ab} = \begin{pmatrix} g_{\mu\nu} & 0 \\ 0 & -\phi^2 \end{pmatrix} $$

ϕ : Dimensionless homogeneous scalar field

$$ e_a^A = \mathrm{diag}(1,1,1,1,\phi)\,, \quad \eta_{ab} = \mathrm{diag}(1,-1,-1,-1,-1) $$

$$ \Longrightarrow S_{\mathrm{KK}}^{\mathrm{eff}} = \int d^4x|e|\frac{1}{2\kappa^2}\phi F(T+\phi^{-2}\partial_\mu\phi\partial^\mu\phi) $$

$$ |{}^{(5)}e| = \phi|e| $$

* Our KK reduced action is compatible with the results in the reference: **[Fiorini, Gonzalez and Vasquez, arXiv:1304.1912 [gr-qc]].**

24

Teleparallelism with a positive cosmological constant

- $F(T) = T - 2\Lambda_4\,, \quad \Lambda_4(>0)$: Cosmological constant

- We define σ as $\phi \equiv \xi\sigma^2\,, \quad \xi = 1/4$

$$ \Longrightarrow S_{\mathrm{KK}}^{\mathrm{eff}}|_{F(T)=T-2\Lambda_4} = $$

$$ \int d^4x|e|\left(1/\kappa^2\right)\left[(1/8)\,\sigma^2 T + \underline{(1/2)\,\partial_\mu\sigma\partial^\mu\sigma} - \Lambda_4\right] $$

Canonical kinetic term

Cosmology in the flat FLRW space-time

Gravitational field equations

$$(1/2)\,\dot{\sigma}^2 \;-\; (3/4)\,H^2\sigma^2 \;+\; \Lambda_4 \;=\; 0$$

$$\dot{\sigma}^2 \;+\; H\sigma\dot{\sigma} \;+\; (1/2)\,\dot{H}\sigma^2 \;=\; 0$$

$$\Longrightarrow \quad (3/2)\,H^2\sigma^2 - 2\Lambda_4 + H\sigma\dot{\sigma} + (1/2)\,\dot{H}\sigma^2 = 0$$

Equation of motion of σ

$$\ddot{\sigma} + 3H\dot{\sigma} + (3/2)\,H^2\sigma = 0$$

Cf. [Geng, Lee, Saridakis and Wu, Phys. Lett. B 704, 384 (2011)]

Solution

$$H = H_{\mathrm{inf}} = \mathrm{constant}(>0)$$

$$\sigma \;=\; b_1\,(t/t_1) + b_2 \qquad\qquad b_1,\quad b_2(>0),\quad t_1$$: Constants

- In the limit $t \;\longrightarrow\; 0$, we can find approximate expressions

$$H_{\mathrm{inf}} \approx (2/b_2)\,\sqrt{\Lambda_4/3}$$

$$\sigma \approx b_2$$

$$b_1 \;\approx\; -\,(1/2)\,b_2 H_{\mathrm{inf}} t_1 \;\approx\; -\sqrt{\Lambda_4/3}\,t_1$$

$$a \approx \bar{a}\exp\left(H_{\mathrm{inf}} t\right), \qquad \bar{a}(>0)$$

$\Longrightarrow$ **An exponential inflation can be realized.**

IV. From the Randall-Sundrum (RS) theory

The RS type-I and II models

- In the RS type-I model, there are a positive tension brane at $y = 0$ and a negative one at $y = \tilde{s}$, where y is the fifth direction.

$$ds^2 = e^{-2|y|/l} g_{\mu\nu}(x) dx^\mu dx^\nu + dy^2, \quad l = \sqrt{-6/\Lambda_5}$$

$e^{-2|y|/l}$: Warp factor

$\Lambda_5 (< 0)$: Negative cosmological constant in the bulk

$\tilde{s} \to \infty$

- In the RS type-II model, there is only one brane with the positive tension floating in the anti-de Sitter bulk space.

[Randall and Sundrum, Phys. Rev. Lett. 83, 3370 (1999); 4690 (1999)]

Cf. [Garriga and Tanaka, Phys. Rev. Lett. 84, 2778 (2000)]

Procedures in the RS type-II model

Pioneering work:

[Shiromizu, Maeda and Sasaki, Phys. Rev. D 62, 024012 (2000)]

Application to teleparallelism:

[Nozari, Behboodi and Akhshabi, Phys. Lett. B 723, 201 (2013)]

(i) The induced equations (Gauss-Codazzi equations) on the brane are examined by using the projection vierbein of the five-dimensional space-time quantities into the four-dimensional space-time brane.

(ii) The Israel's junction conditions to connect the left-side and right-side bulk spaces sandwiching the brane are investigated.

(iii) Provided that there exists Z_2 symmetry, i.e., $y \leftrightarrow -y$, in the five-dimensional space-time, the quantities on the left and right sides of the brane are explored.

31

Cosmology in the flat FLRW space-time

Friedmann equation on the brane

$$H^2 \frac{dF(T)}{dT} = -\frac{1}{12}\left[F(T) \underline{- 4\Lambda} - 2\kappa^2 \rho_{\mathrm{M}} \underline{- \left(\frac{\kappa_5^2}{2}\right)^2 \mathcal{Q} \rho_{\mathrm{M}}^2}\right]$$

$$\mathcal{Q} \equiv \left(11 - 60 w_{\mathrm{M}} + 93 w_{\mathrm{M}}^2\right)/4 \longleftarrow$$

includes the contributions from teleparallelism, which do not exist in general relativity.

$$w_{\mathrm{M}} \equiv P_{\mathrm{M}}/\rho_{\mathrm{M}}$$

$\Lambda \equiv \Lambda_5 + \left(\kappa_5^2/2\right)^2 \lambda^2$: Eeffective cosmological constant in the brane

$\lambda(> 0)$: Tension of the brane

$$G = \left[1/\left(3\pi\right)\right]\left(\kappa_5^2/2\right)^2 \lambda$$

32

Case (1)

$$F(T) = T - 2\Lambda_5$$

$$\longrightarrow H = H_{\mathrm{DE}} = \sqrt{\Lambda_5 + \kappa_5^4 \lambda^2/6} = \mathrm{constant}$$

$$a(t) = a_{\mathrm{DE}} \exp\left(H_{\mathrm{DE}} t\right), \quad a_{\mathrm{DE}}(> 0)$$

⇨ **An approximate de Sitter solution on the brane can be realized.**

* At the dark energy completely dominated stage, we can consider that $w_{\mathrm{M}} = 0$.

Case (2)

$$F(T) = T^2/\bar{M}^2 + \alpha\Lambda_5$$

$\bar{M}$: Mass scale

α : Constant

$$\longrightarrow \quad H = H_{\mathrm{DE}} = \left[\left(\bar{M}^2/108\right)\mathcal{J}\right]^{1/4} = \text{constant}$$

$$\mathcal{J} \equiv (\alpha - 4)\,\Lambda_5 - 4\left(\kappa_5^2/2\right)^2 \lambda^2$$

$$a(t) = a_{\mathrm{DE}} \exp\left(H_{\mathrm{DE}} t\right), \qquad a_{\mathrm{DE}}(> 0)$$

⇨ **Similar approximate de Sitter solution on the brane can be obtained.**

V. Summary

- Four-dimensional effective $F(T)$ gravity coming from the five-dimensional KK and RS space-time theories have been studied.

- **With the KK reduction, the four-dimensional effective theory of $F(T)$ gravity coupling to a scalar field has been built.**

- **For the RS type-II model, the contribution of $F(T)$ gravity appears on the four-dimensional FLRW brane.**

- **Inflation and the dark energy dominated stage can be realized in the KK and RS theories, respectively, due to the effect of only the torsion in teleparallelism without that of the curvature.**

Backup Slides

No. 6

General relativistic approach

(i) Cosmological constant

(ii) Scalar field :

- **x-matter, Quintessence** ⟵ **Canonical field**

[Chiba, Sugiyama and Nakamura, Mon. Not. Roy. Astron. Soc. 289, L5 (1997)]
[Caldwell, Dave and Steinhardt, Phys. Rev. Lett. 80, 1582 (1998)]
Cf. Pioneering work: [Fujii, Phys. Rev. D 26, 2580 (1982)]

- **Phantom** ⟵ **Wrong sign kinetic term**

[Caldwell, Phys. Lett. B 545, 23 (2002)]

- **K-essence** ⟵ **Non canonical kinetic term**

[Chiba, Okabe and Yamaguchi, Phys. Rev. D 62, 023511 (2000)]
[Armendariz-Picon, Mukhanov and Steinhardt, Phys. Rev. Lett. 85, 4438 (2000)]

- **Tachyon** ⟵ **String theories** ⁎ **The mass squared is negative.**

[Padmanabhan, Phys. Rev. D 66, 021301 (2002)]

5

PLANCK 2013 results of SNLS

Magnitude residuals of the Λ CDM model that best fits the SNLS combined sample

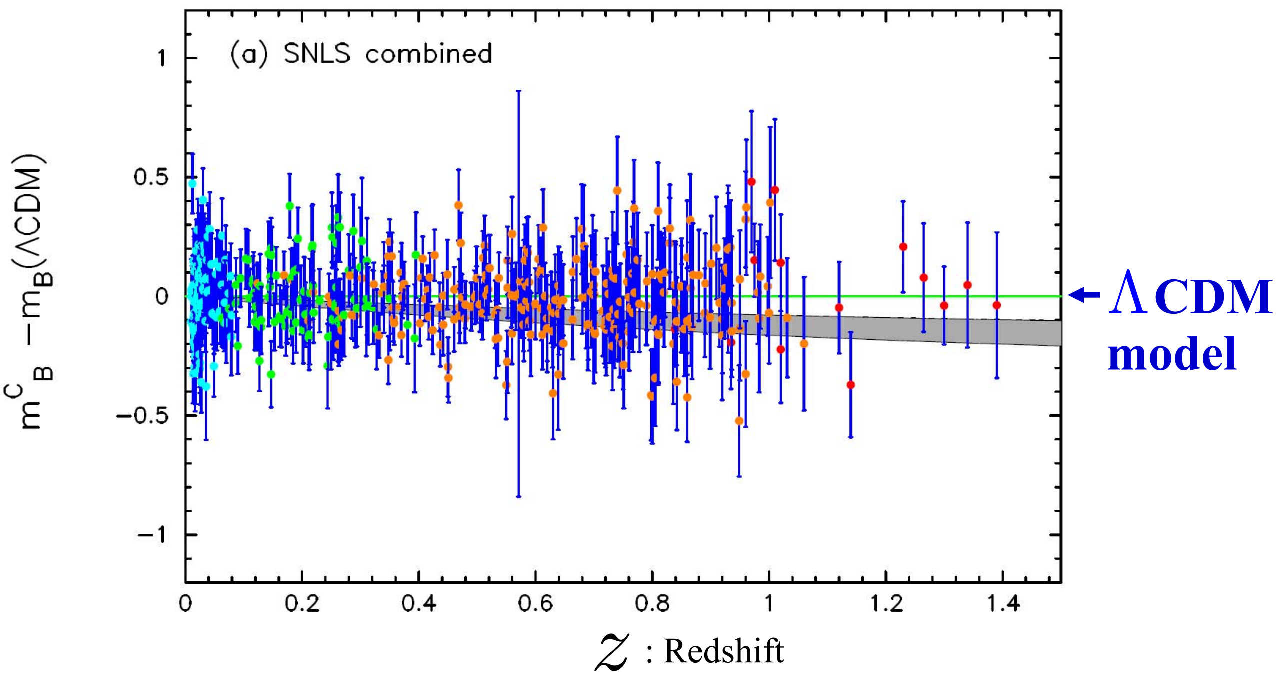

From [Ade *et al.* [Planck Collaboration], arXiv:1303.5076 [astro-ph.CO]].

SNLS data

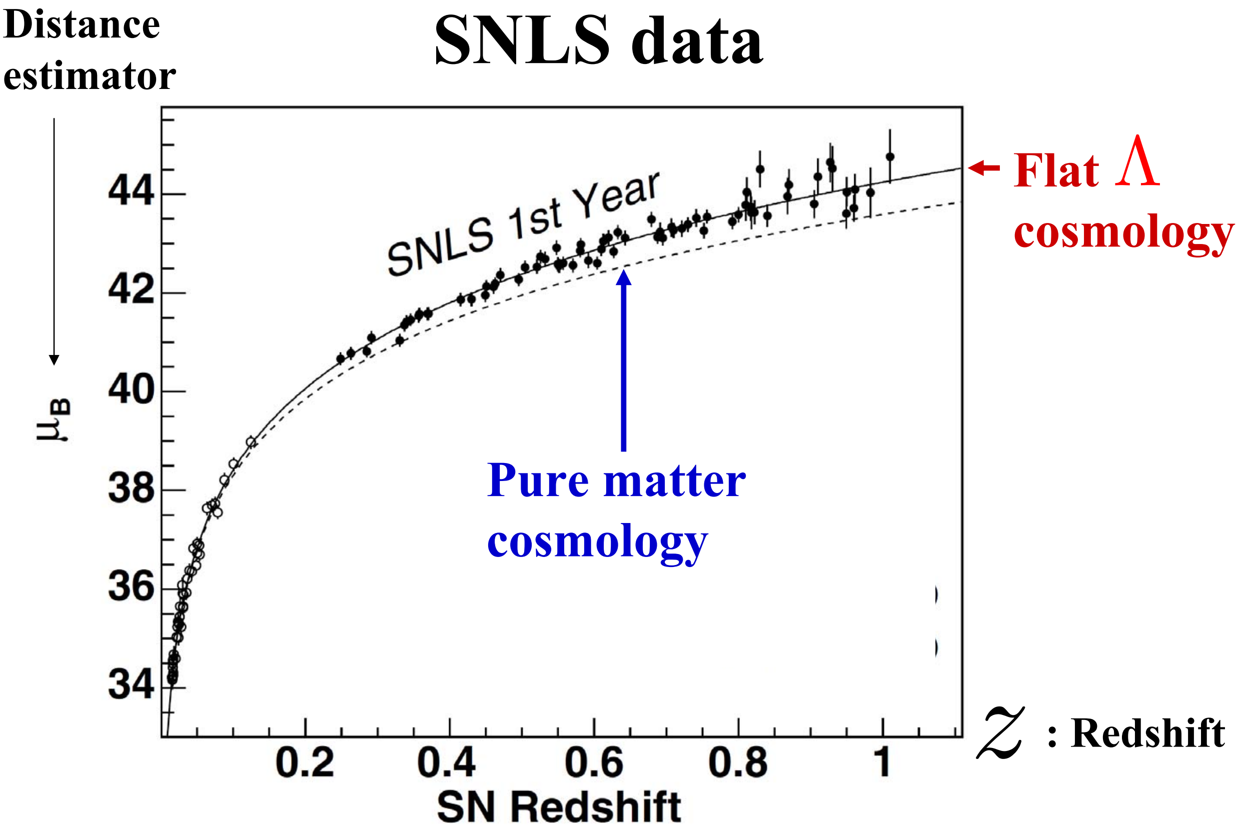

From [Astier *et al.* [The SNLS Collaboration], Astron. Astrophys. 447, 31 (2006)].

No. 14

Baryon acoustic oscillation (BAO)

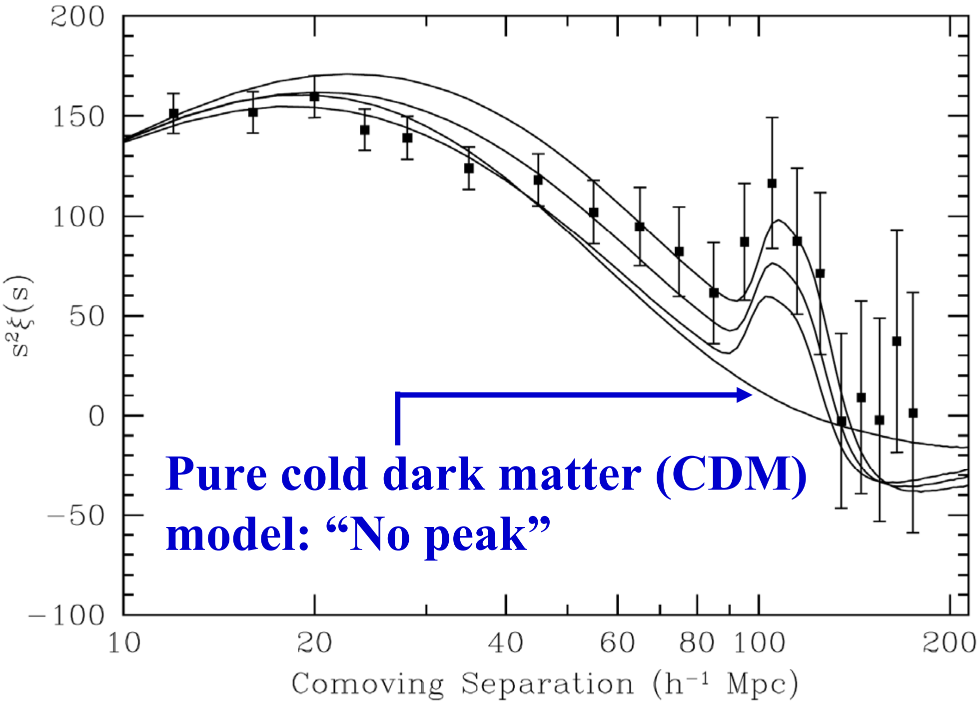

Special pattern in the large-scale correlation function of Sloan Digital Sky Survey (SDSS) luminous red galaxies

From [Eisenstein *et al.* [SDSS Collaboration], Astrophys. J. 633, 560 (2005)].

Cf. [Yamamoto, astro-ph/0110596; Astrophys. J. 595, 577 (2003)]
[Matsubara and Szalay, Phys. Rev. Lett. 90, 021302 (2003)]

PLANCK data for the current w

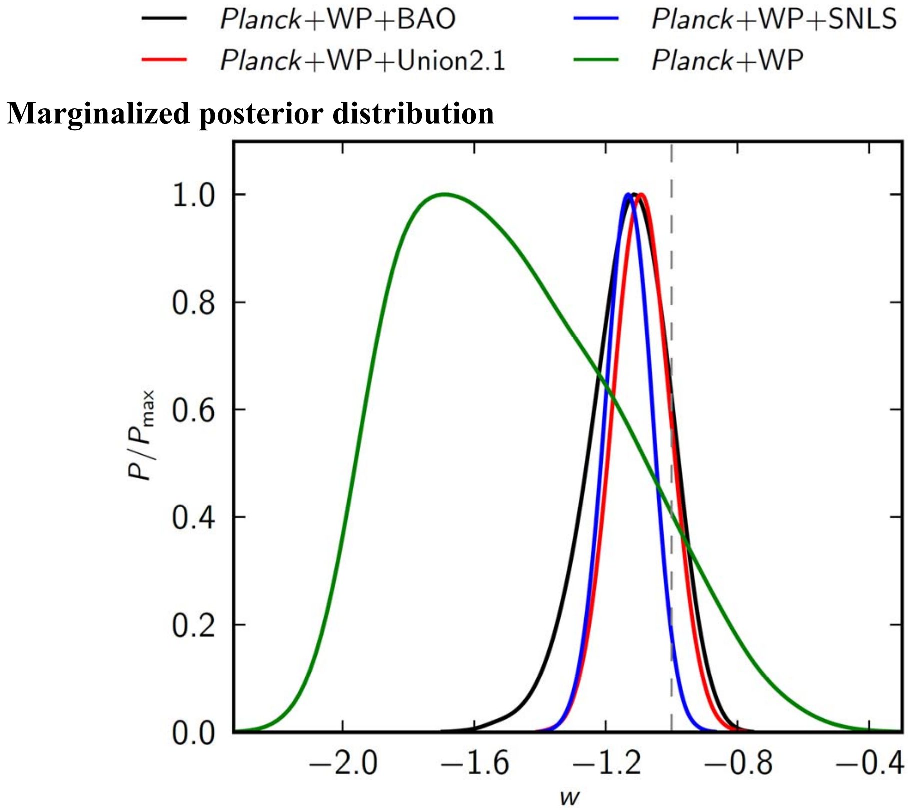

From [Ade *et al.* [Planck Collaboration], arXiv:1303.5076 [astro-ph.CO]].

$w = \mathrm{constant}$

WP: WMAP

BAO: Baryon Acoustic Oscillation

No. 15

9-year WMAP data of current w

[Hinshaw *et al.*, arXiv:1212.5226 [astro-ph.CO]]

For constant w :

$$w = \begin{cases} -1.084 \pm 0.063 & (\text{flat}) \\ -1.122^{+0.068}_{-0.067} & (\text{non-flat}) \end{cases} \quad (68\%\ \mathrm{CL})$$

(From $WMAP$+eCMB+BAO+H_0+SNe.)

* Hubble constant (H_0) measurement

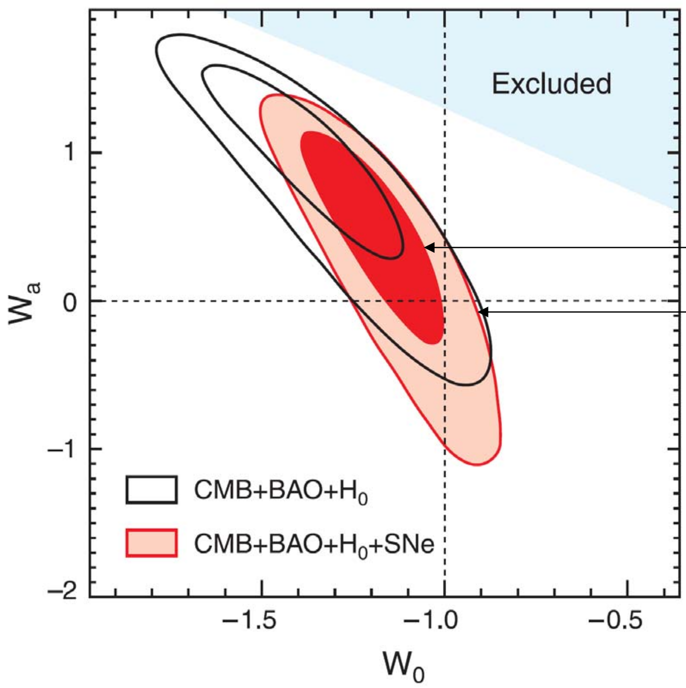

No. 16

Time-dependent w

$$w(a) = w_0 + w_a(1 - a)$$

From [Hinshaw *et al.*, arXiv:1212.5226 [astro-ph.CO]].

w_0 : Current value of w

(From $WMAP$+eCMB +BAO+H_0+SNe.)

For the flat universe:

$$w_0 = -1.17^{+0.13}_{-0.12}, \quad w_a = 0.35^{+0.50}_{-0.49} \quad \text{(68\% CL)}$$

No. 7

(iii) Fluid :

- **(Generalized) Chaplygin gas**

Equation of state (EoS): $P = -A/\rho^u$

$A > 0, \ u$: Constants

ρ : Energy density

P : Pressure

[Kamenshchik, Moschella and Pasquier, Phys. Lett. B 511, 265 (2001)] $\longleftarrow (u = 1)$

[Bento, Bertolami and Sen, Phys. Rev. D 66, 043507 (2002)]

No. 8

Extension of gravitational theory

- ***F*(*R*) gravity** $\longleftarrow$ $F(R)$: Arbitrary function of the Ricci scalar R

Cf. Application to inflation: **[Starobinsky, Phys. Lett. B 91, 99 (1980)]**

[Capozziello, Cardone, Carloni and Troisi, Int. J. Mod. Phys. D 12, 1969 (2003)]
[Carroll, Duvvuri, Trodden and Turner, Phys. Rev. D 70, 043528 (2004)]
[Nojiri and Odintsov, Phys. Rev. D 68, 123512 (2003)]

- **Scalar-tensor theories** $\longleftarrow$ $f_1(\phi)R$

$f_i(\phi)\ (i=1,2)$: Arbitrary function of a scalar field ϕ

[Boisseau, Esposito-Farese, Polarski and Starobinsky, Phys. Rev. Lett. 85, 2236 (2000)]
[Gannouji, Polarski, Ranquet and Starobinsky, JCAP 0609, 016 (2006)]

No. 9

- **Ghost condensates scenario**

[Arkani-Hamed, Cheng, Luty and Mukohyama, JHEP 0405, 074 (2004)]

- **Higher-order curvature term**

Gauss-Bonnet invariant with a coupling to a scalar field: $f_2(\phi)\mathcal{G}$

$\mathcal{G} \equiv R^2 - 4R_{\mu\nu}R^{\mu\nu} + R_{\mu\nu\rho\sigma}R^{\mu\nu\rho\sigma}$: Gauss-Bonnet invariant

$R_{\mu\nu}$: Ricci curvature tensor

$R_{\mu\nu\rho\sigma}$: Riemann tensor

[Nojiri, Odintsov and Sasaki, Phys. Rev. D 71, 123509 (2005)]

- $f(\mathcal{G})$ **gravity** $\longleftarrow$ $\frac{R}{2\kappa^2} + f(\mathcal{G})$

$\kappa^2 \equiv 8\pi G$

G : Gravitational constant

[Nojiri and Odintsov, Phys. Lett. B 631, 1 (2005)]

No. 10

- **DGP braneworld scenario**

[Dvali, Gabadadze and Porrati, Phys. Lett B 485, 208 (2000)]
[Deffayet, Dvali and Gabadadze, Phys. Rev. D 65, 044023 (2002)]

- **Non-local gravity** ⟵ $\frac{1}{2\kappa^2} f(\Box^{-1} R)$ **: Quantum effects**

[Deser and Woodard, Phys. Rev. Lett. 99, 111301 (2007)]
$\Box$: Covariant d'Alembertian
[Nojiri and Odintsov, Phys. Lett. B 659, 821 (2008)]

- ***F*(*T*) gravity** ⟵ **Extended teleparallel Lagrangian described by the torsion scalar T.**

[Bengochea and Ferraro, Phys. Rev. D 79, 124019 (2009)]
[Linder, Phys. Rev. D 81, 127301 (2010) [Erratum-ibid. D 82, 109902 (2010)]]

* "Teleparallelism" : One could use the Weitzenböck connection, which has no curvature but torsion, rather than the curvature defined by the Levi-Civita connection.

[Hayashi and Shirafuji, Phys. Rev. D 19, 3524 (1979) [Addendum-ibid. D 24, 3312 (1982)]]

No. 11

- **Galileon gravity** ⟵ $\Box\phi\,(\partial^\mu\phi\partial_\mu\phi)$

Longitudinal graviton (a branebending mode ϕ)

[Nicolis, Rattazzi and Trincherini, Phys. Rev. D 79, 064036 (2009)]

- **Massive gravity** ⟵ **Graviton with a non-zero mass**

[de Rham and Gabadadze, Phys. Rev. D 82, 044020 (2010)]
[de Rham and Gabadadze and Tolley, Phys. Rev. Lett. 106, 231101 (2011)]
Review: [Hinterbichler, Rev. Mod. Phys. 84, 671 (2012)]

Example of *F*(*T*) gravity model

- **The model contains only one parameter u if one has the value of $\Omega_{\mathrm{m}}^{(0)}$.**

[KB, Geng, Lee and Luo, JCAP 1101, 021 (2011)]

Cosmological evolutions of Ω_{DE} , Ω_{m} and Ω_{r}

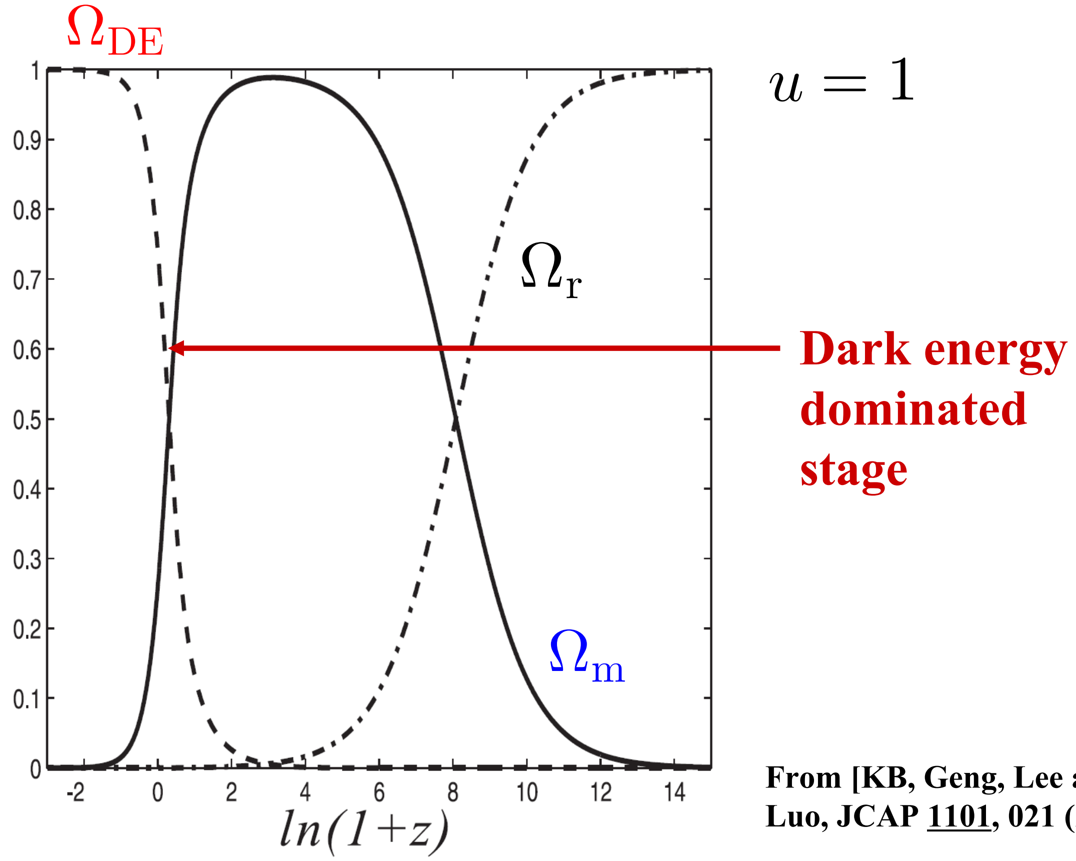

From [KB, Geng, Lee and Luo, JCAP 1101, 021 (2011)].

25

Metric in five-dimensional space-time

$$^{(5)}g_{ab} = \begin{pmatrix} g_{\mu\nu} & 0 \\ 0 & -\phi^2 \end{pmatrix},$$

$\phi \equiv \varphi/\varphi_*$: Dimensionless homogeneous scalar field

φ_* : Fiducial value of φ

$$\phi^2 = \mathcal{R}^2\theta^2$$

$\mathcal{R}$: Rradius of the compactified space

θ : Dimensionless coordinates such as an angle

$$\sqrt{^{(5)}g} = \sqrt{-g}\mathcal{R}\sqrt{\hat{g}}$$

$\hat{g}$: Determinant of the metric corresponding to the pure geometrical part represented by θ

$V_{\rm com} = \int \hat{g} d\theta$: Compactified space volume

31

Settings in the RS type-II model

- We start with the equation in the five-dimensional space-time with the brane whose tension is a positive constant.

- We consider that the vacuum solution in the five-dimensional space-time is the AdS one, and that the brane configuration is consistent with the equation in the five-dimensional space-time.

⇨ This implies that the brane configuration with a positive constant tension connecting two vacuum solutions in the five-dimensional space-time, namely, the condition of the configuration is nothing but the equation for the brane.

35

(ii) The Israel's junction conditions to connect the left-side and right-side bulk spaces sandwiching the brane are investigated.

- The first junction condition is that the vierbeins induced on the brane from the left side and right side of the brane should be the same with each other.

- Moreover, the second junction condition is that the difference of the tensor $S_{\rho}{}^{\mu\nu}$ between the left side and right side of the brane comes from the energy-momentum tensor of matter, which is confined in the brane.

(iii) Provided that there exists Z_2 symmetry, i.e., $y \leftrightarrow -y$, in the five-dimensional space-time, the quantities on the left and right sides of the brane are explored.

36

- The difference between the scalar curvature and the torsion scalar is a total derivative of the torsion tensor.

  $\longrightarrow$ This may affect the boundary.

- It has been shown that in comparison with the gravitational field equations in general relativity, the induced gravitational field equations on the brane have new terms, which comes from the additional degrees of freedom in teleparallelism.

- These extra terms correspond to the projection on the brane of the vector portion of the torsion tensor in the bulk.

Cf. Other solution

For $F(T) = T$, $\Lambda = 0$, $\mathcal{Q} = 8/3$, and $w_{\mathrm{M}} = -5.5 \times 10^{-3}$,

$$H^2 = \left(\kappa^2/3\right) \rho_{\mathrm{M}} \left[1 + \rho_{\mathrm{M}}/\left(2\lambda\right)\right]$$

[Astashenok, Elizalde, de Haro, Odintsov and Yurov, Astrophys. Space Sci. 347, 1 (2013)]

Case (2)

$\bar{M}$: Mass scale

α : Constant

$$F(T) = T^2/\bar{M}^2 + \alpha\Lambda_5$$

$$\longrightarrow \quad H = H_{\mathrm{DE}} = \left[\left(\bar{M}^2/108\right)\mathcal{J}\right]^{1/4} = \text{constant}$$

$$\mathcal{J} \equiv (\alpha - 4)\Lambda_5 - 4\left(\kappa_5^2/2\right)^2 \lambda^2$$

$$a(t) = a_{\mathrm{DE}} \exp\left(H_{\mathrm{DE}} t\right), \qquad a_{\mathrm{DE}} (> 0)$$

$$\mathcal{J}(\geq 0) \Longrightarrow \alpha \geq 4 + \left(\kappa_5^2 \lambda^2\right)/\Lambda_5$$

“Observational Upper Bound on the Cosmic Abundances of Negative-mass Compact Objects and Ellis Wormholes from the SDSS Quasar Lens Search”

by Ryuichi Takahashi

[JGRG23(2013)110803]

Observational Upper Bound on the Cosmic Abundances of Negative-mass Compact Objects and Ellis Wormholes from the SDSS Quasar Lens Search

Ryuichi Takahashi & Hideki Asada
(Hirosaki U)

RT & Asada 2013, ApJL, 768, 16

0. Abstract

Observational constraints on cosmic abundances of negative-mass compact objects & Ellis wormholes from SDSS quasar lens survey

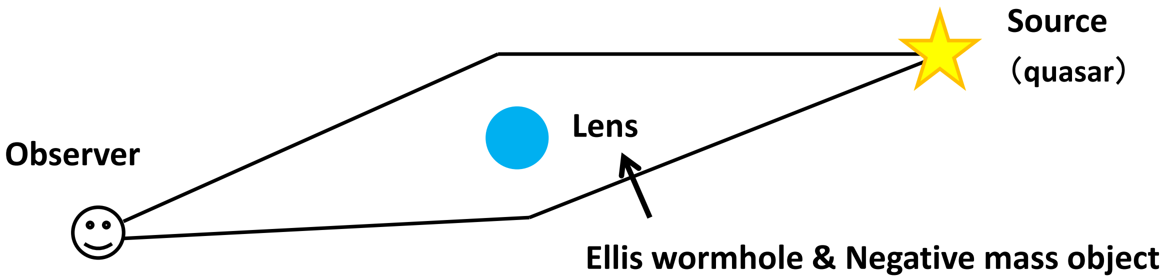

If there are Negative masses or Ellis wormholes in the Universe

- Distant quasars seen as multiple images by gravitational lensing
- SDSS quasar survey didn't find such multiple images
- As a result, we can set an observational upper bound

1. Introduction

Negative Mass Object （Bondi 1957; Jammer 1961,1999）

: Source of repulsive gravitational force

It has “negative” gravitational mass
The inertial mass can be positive or negative

$$m_{\mathrm{I}} a = G \frac{m_{\mathrm{G}} M_{\mathrm{G}}}{r^2} \quad \text{(Eq. of Motion)}$$

: Theoretical hypothetical object

: Possible ideas have been discussed since 19th century in analogy with electric charge

: It have not been found observationally

Motion of Negative Mass in Newtonian Mechanics

N Negative mass （“negative” gravitational mass & “positive” inertial mass）

Ordinary matter （positive gravitational & inertial masses）

- Negative mass and Ordinary matter

- Two Negative masses

“attractive”

Negative-Masses Clustering in the Universe

Negative mass   Ordinary matter

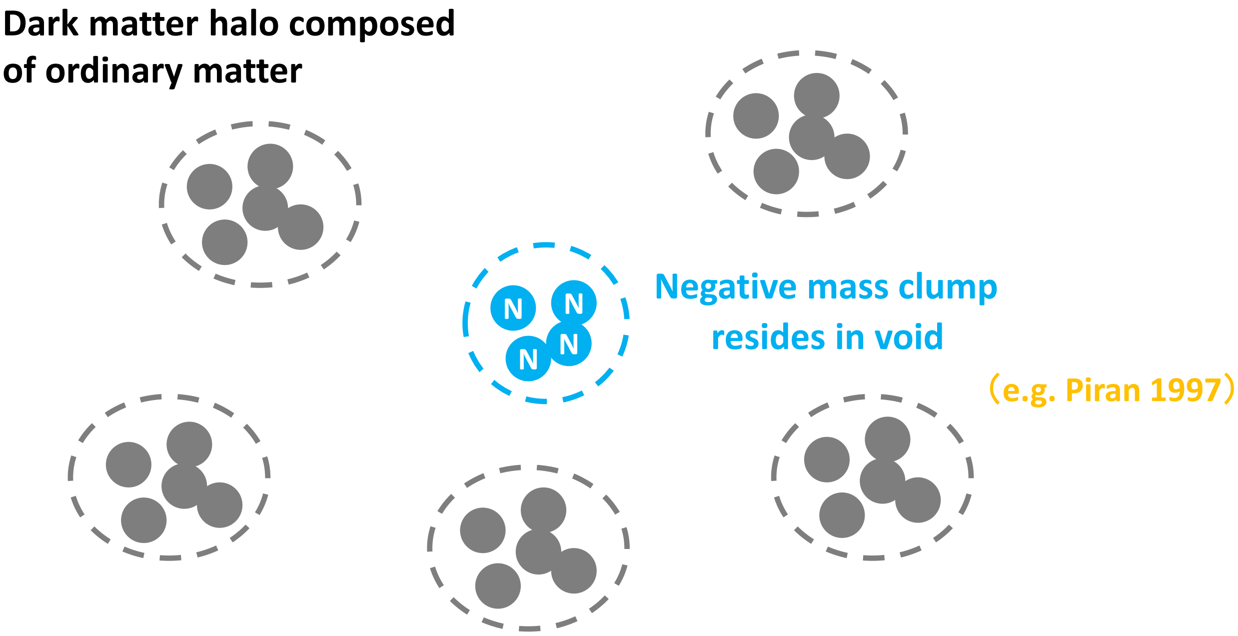

Motion of Negative Mass in Newtonian Mechanics

Negative mass (“negative” gravitational mass
& “negative” inertial mass)

Ordinary matter (positive gravitational & inertial masses)

- **Ordinary matter and Negative mass**

- **Two Negative masses**

Negative-Masses Clustering in the Univesers

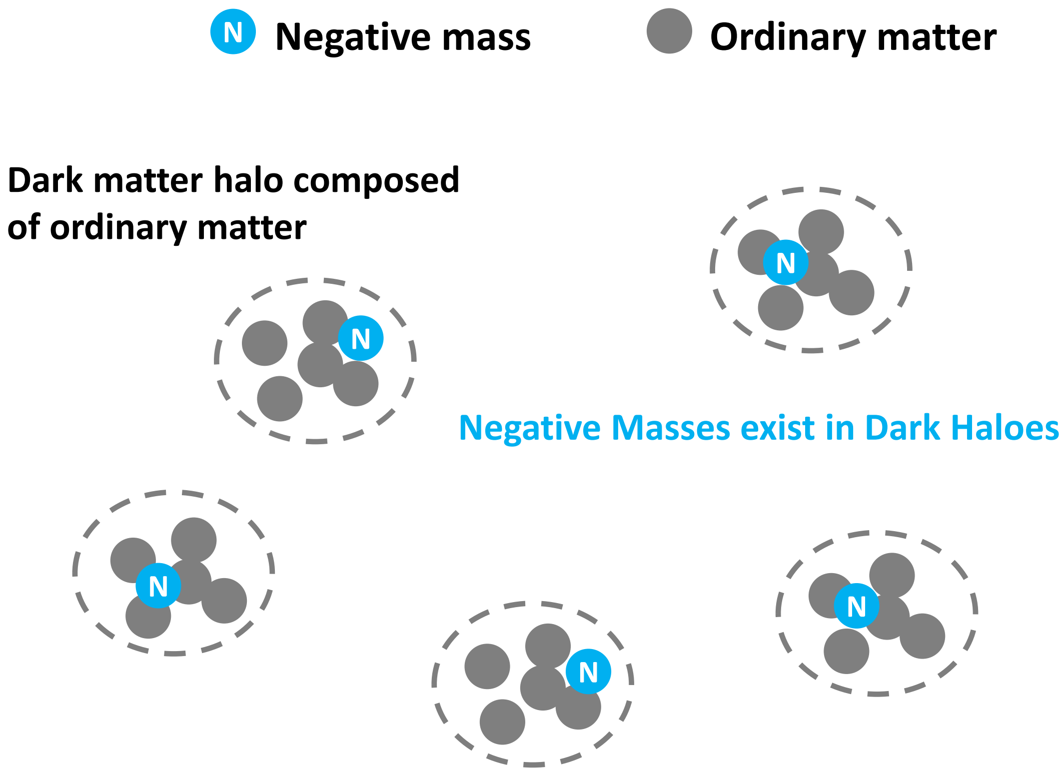

Wormhole

(Morris & Thorne 1988; Morris+ 1988)

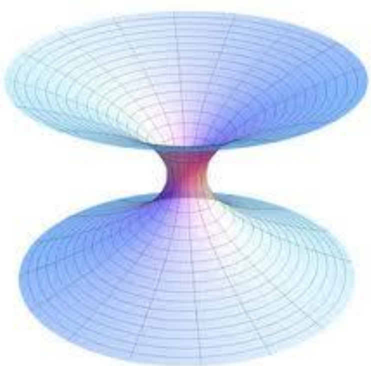

"Tunnel" connects distant space-time

theoretical prediction of general relativity

A solution of Einstein Eq.

Ellis wormhole (Ellis 1973)

- a solution of Einstein eq.
- massless scalar field

a : throat radius

Metric

$$ds^2 = dt^2 - dr^2 - (r^2 + a^2)(d\theta^2 + \sin^2\theta d\varphi^2)$$

no interaction with matters

no light emission

light ray path is deflected by gravitational lensing

Previous upper bound on abundance of negative masses

Cramer+ 1995

Gravitational microlensing by negative masses in our galaxy

Magnification curve

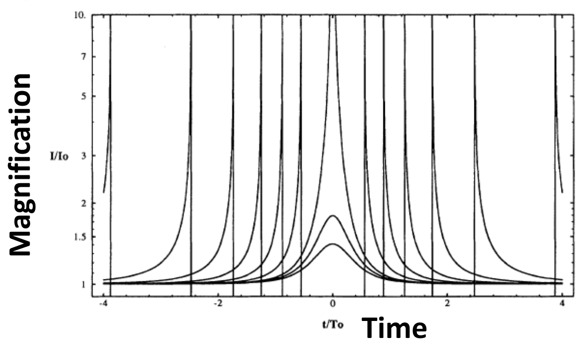

FIG. 3. Intensity profile of a gravitationally negative anomalous compact halo object (GNACHO) as it passes near the source-detector axis DS. The several curves correspond to minimum dimensionless impact parameter values $B_0 = 0.50$ (at edge of plot), 0.75, 1.00, 1.25, 1.50, 1.75, 2.00, 2.10, and 2.20 (small central bump). (See text for definitions of the variables.)

Torres+ 1998

Gravitational lensing of distant AGNs (Active Galactic Nuclei) by negative masses

$|\rho| < 10^{-36}\ \mathrm{g\ cm^{-3}}$ for $|M| \approx 0.1 M_\odot$

$|\Omega| < 10^{-7}$ (cosmological density parameter)

Previous upper bound on abundance of Ellis wormhole

Abe 2010

Microlensing effect in our galaxy

Constraint on wormhole with throat radius

$$a = 100 - 10^7\text{km}$$

Yoo+ 2013

Gravitational lensing of distant GRBs(Gamma Ray Bursts) by wormholes

$$n < 10^{-9}\text{AU}^{-3} \quad \text{for } a \approx 0.1\text{cm}$$

Magnification curve

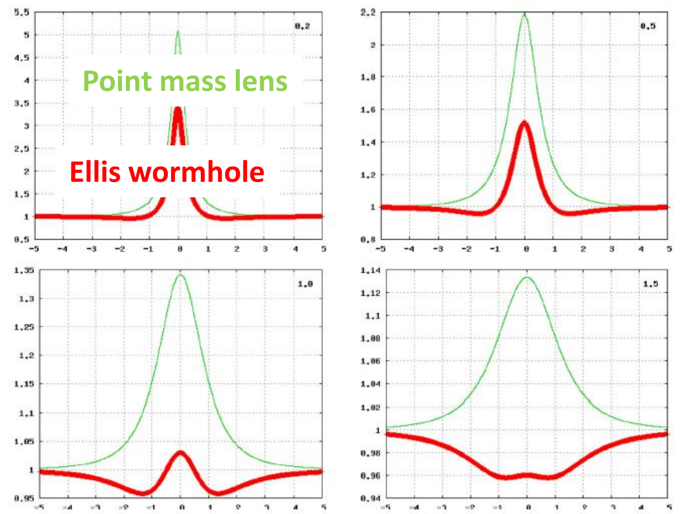

Figure 4. Light curves for $\hat{\beta}_0 = 0.2$ (top left), $\hat{\beta}_0 = 0.5$ (top right), $\hat{\beta}_0 = 1.0$ (bottom left), and $\hat{\beta}_0 = 1.5$ (bottom right). Thick red lines are the light curves for wormholes. Thin green lines are corresponding light curves for Schwarzschild lenses.
(A color version of this figure is available in the online journal.)

Observational data we used

SDSS（Sloan Digital Sky Survey）Quasar Lens Search

Largest homogeneous sample of Quasars

（Oguri+ 2006,2008,2012; Inada+ 2012）

- **# of quasars　50836**
- **redshifts　z=0.6-2.2**
- **apparent magnitude <19.1（i band）**
- **Lensed quasar systems　19　（image separations　1-20arcsec）**
- **No multiple image lensed by negative masses and Ellis wormholes**

（Oguri & Kayo, 2012, private communication）

Lensing by Negative Mass (Cramer+ 1995; Safonova+ 2001)

Negative point mass $(M < 0)$

Deflection angle is same as ordinary point mass lens, but its sign is opposite

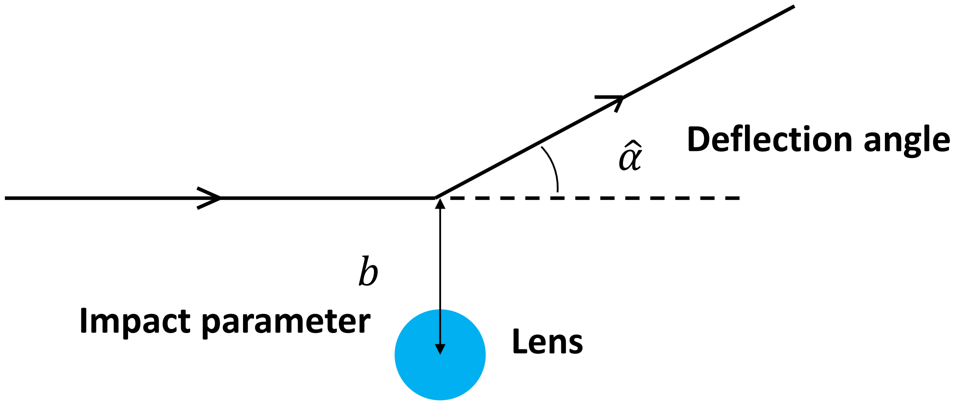

$$\hat{\alpha} = \frac{4|M|}{b}$$

of images

$\beta > 2\theta_{\mathrm{E}}$ **double images**

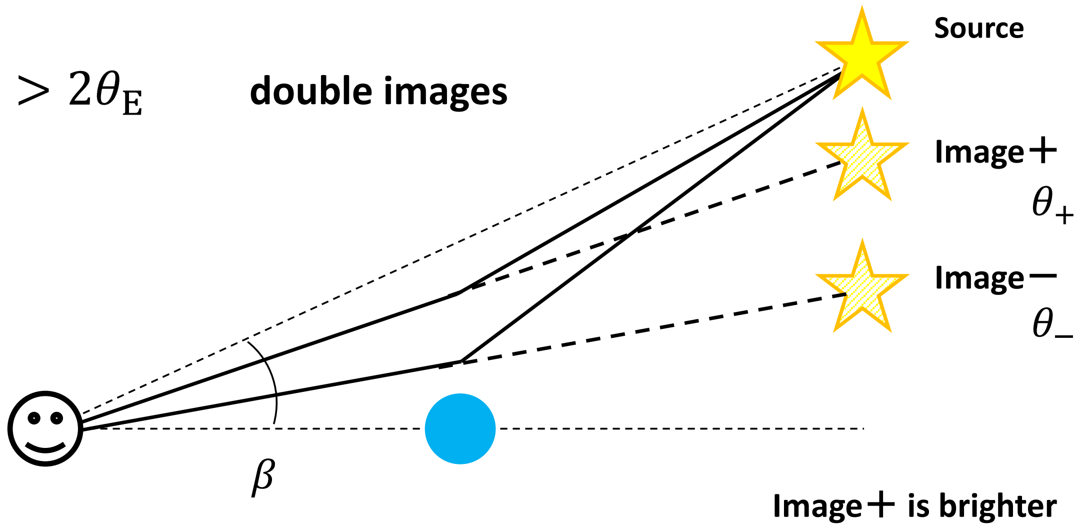

$$\theta_\pm = \frac{1}{2}\left(\beta \pm \sqrt{\beta^2 - 4\theta_{\mathrm{E}}^2}\right)$$

of images

$\beta < 2\theta_{\mathrm{E}}$ **zero image**

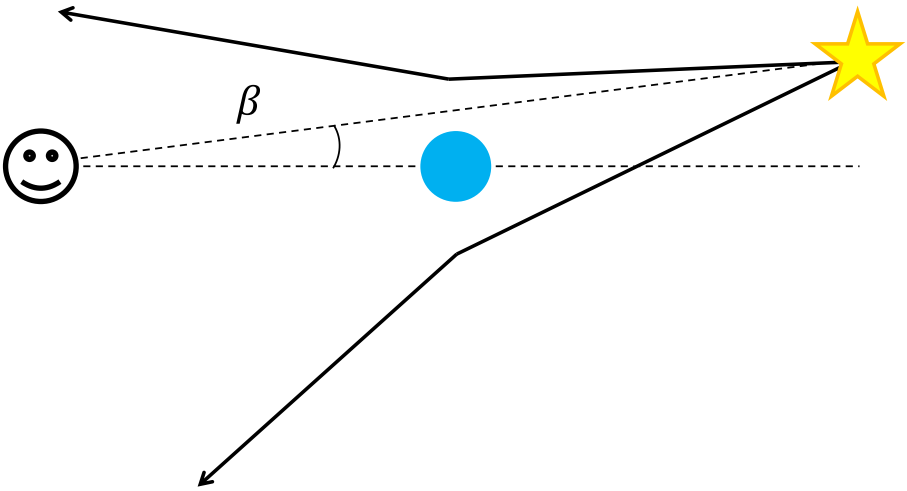

Gravitational lensing by Ellis wormhole

（Clement 1984; Dey & Sen 2008; Toki+ 2011; Nakajima & Asada 2012）

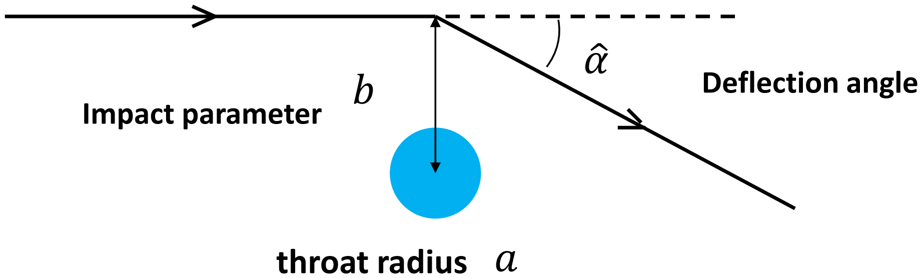

$$\boxed{\hat{\alpha} = \frac{\pi}{4}\frac{a^2}{b^2}}$$

Lens equation

$$\beta = \theta - \theta_{\mathrm{E}}^{3}\frac{\theta}{|\theta|^{3}}$$

Einstein radius

$$\theta_{\mathrm{E}}=\left(\frac{\pi a^{2}}{4}\frac{D_{LS}}{D_{L}^{2}D_{S}}\right)^{1/3}$$

Double images form

throat radius estimated from Einstein radius

$$a = 10h^{-1}\mathrm{pc}\left(\frac{\theta_{\mathrm{E}}}{1''}\right)^{3/2}\left[\frac{D_{L}D_{S}/D_{LS}}{(1h^{-1}\mathrm{Gpc})^{2}}\right]^{1/2}$$

throat radius $a = 10 - 100\mathrm{pc}$

Negative Masses & Ellis Wormholes are distributed homogeneous

Number density of lenses *n* → Lensing probability ∝ *n*

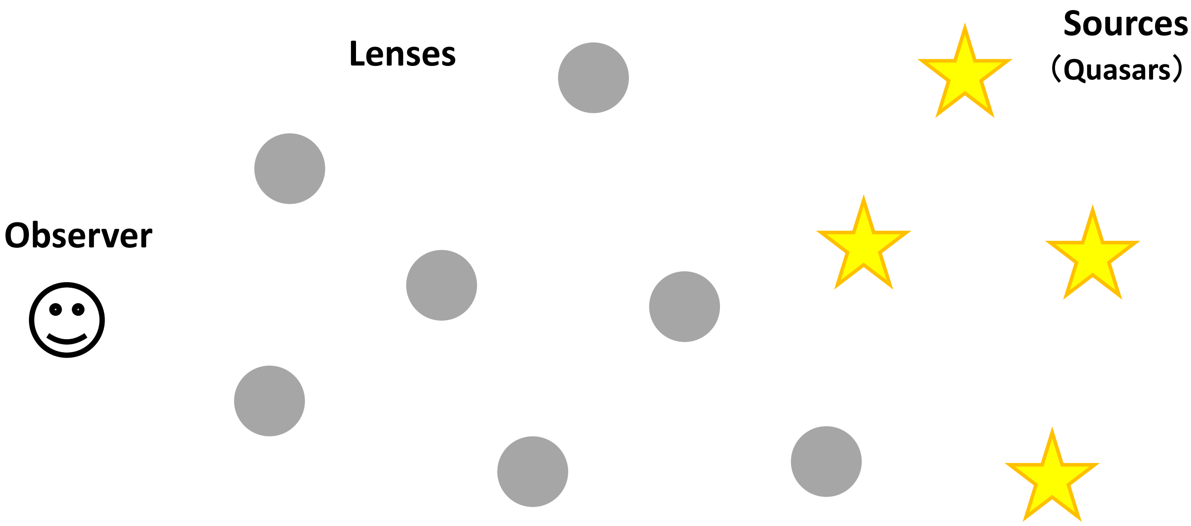

Upper Bound on Cosmological Number Density of Negative Mass

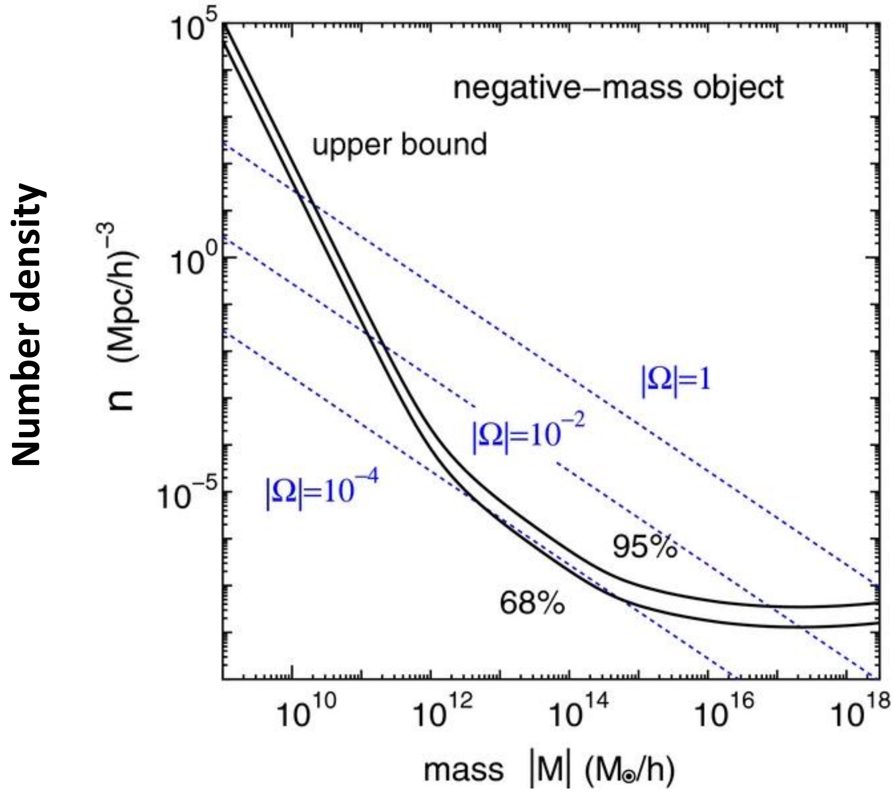

$$\Omega = \frac{Mn}{\rho_{\text{crit}}}$$

(cosmological density parameter)

Upper Bound on Cosmological Number Density of Negative Mass

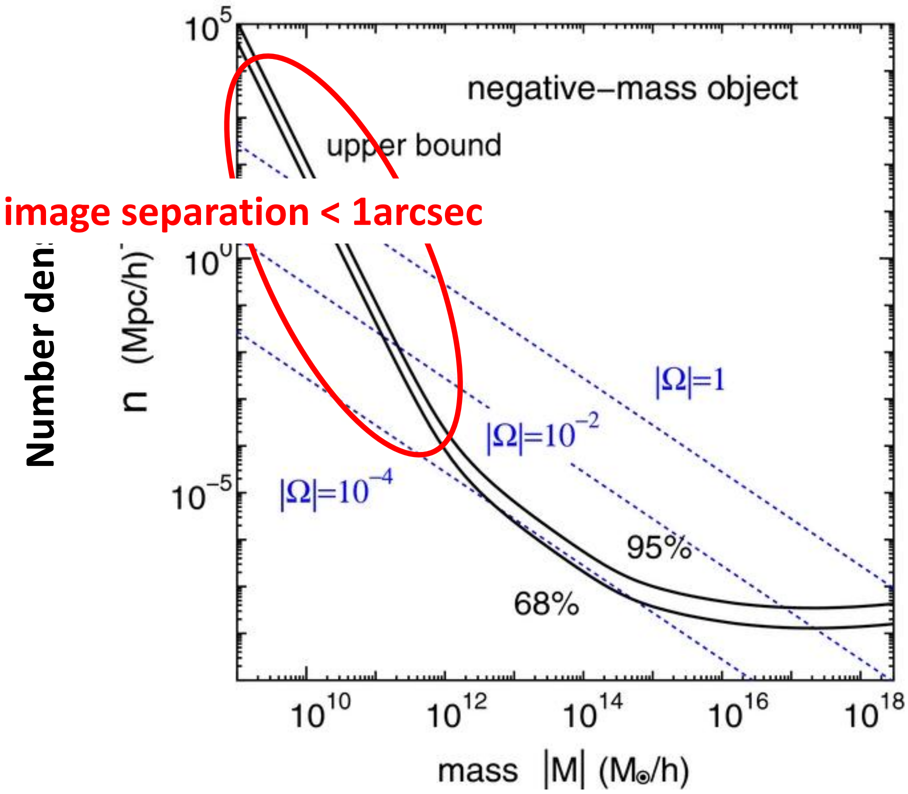

$$\Omega = \frac{Mn}{\rho_{\text{crit}}}$$

(cosmological density parameter)

Upper Bound on Cosmological Number Density of Negative Mass

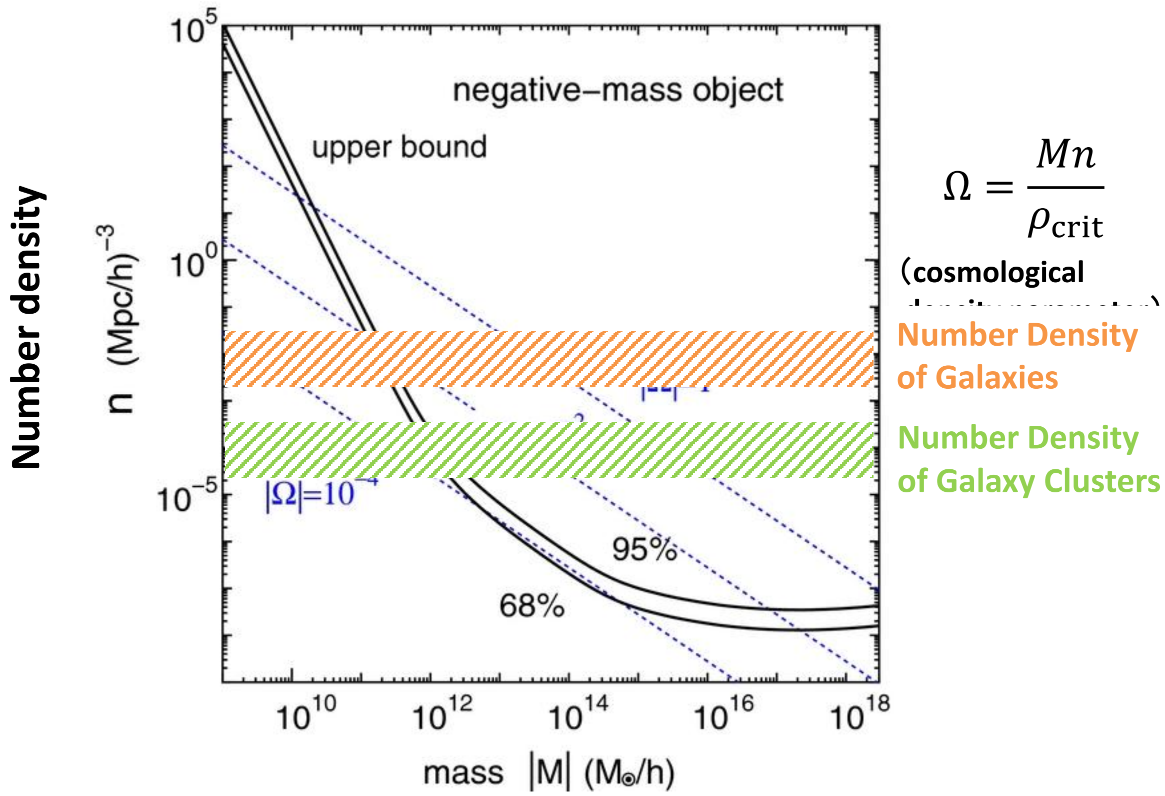

Upper Bound on Cosmological Number Density of Ellis Wormhole

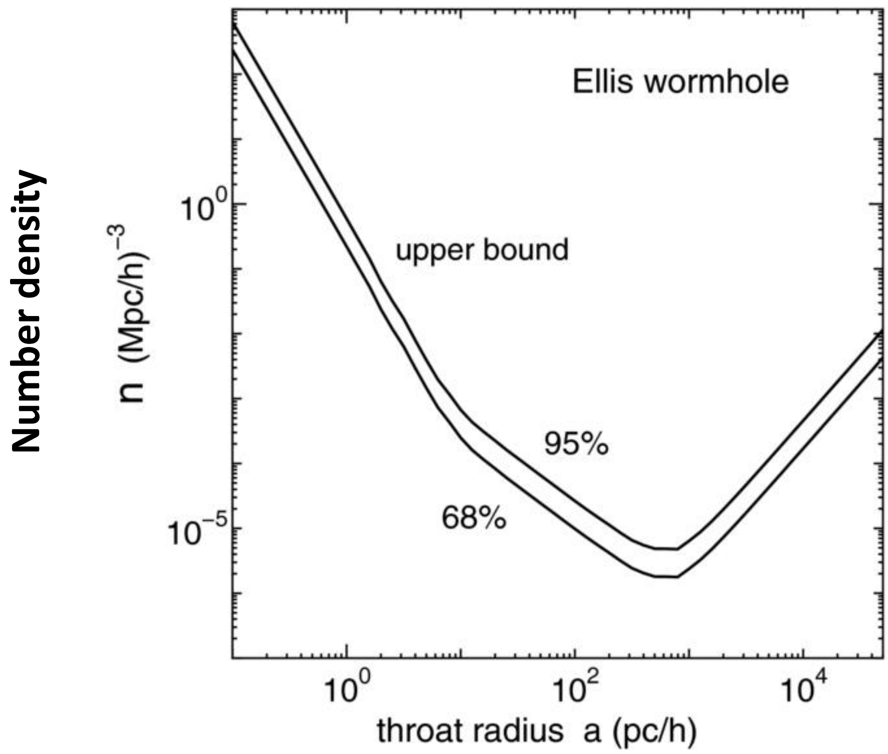

Upper Bound on Cosmological Number Density of Ellis Wormhole

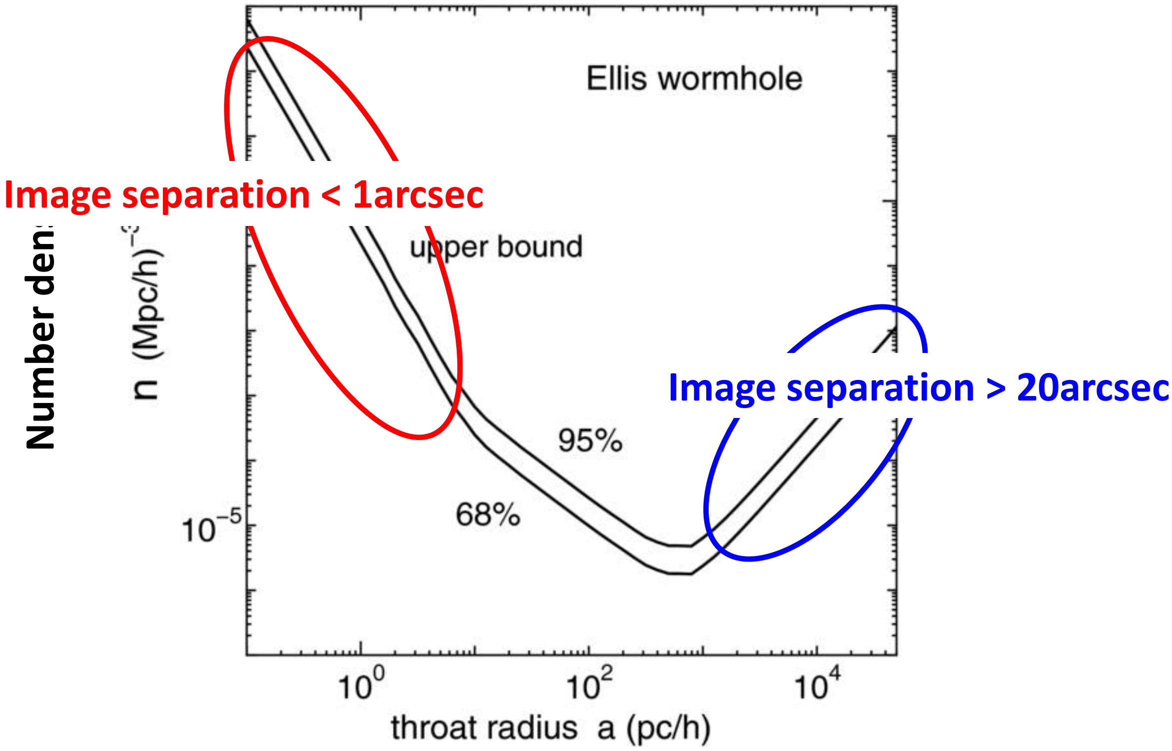

Summary

- **Negative Mass Object**

$$n < 10^{-8}(10^{-4})\ h^3\mathrm{Mpc}^{-3}$$

for mass $|M| > 10^{15}(10^{12})M_\odot$

$$|\Omega| < 10^{-4}$$ **for mass** $M = 10^{12-14}M_\odot$

- **Ellis Wormhole**

$$n < 10^{-4}\ h^3\mathrm{Mpc}^{-3}$$

for throat radius $a = 10 - 10^4\mathrm{pc}$

Thank you for your attention

Enjoy your stay in Hirosaki

“Analytic formula for the threshold

of primordial black hole formation”

by Tomohiro Harada

[JGRG23(2013)110804]

Analytic formula for the threshold of primordial black hole formation

Tomohiro Harada

Department of Physics, Rikkyo University

The 23rd JGRG meeting @ Hirosaki U, 5-8 Nov 2013

In collaboration with Yoo (Nagoya U) and Kohri (KEK)
arXiv:1309.4201; PRD88, 084051 (2013)

Outline

1. Introduction
2. Model and Maximum
3. PBH Threshold
4. Summary

Outline

1 Introduction

2 Model and Maximum

3 PBH Threshold

4 Summary

Introduction
Model and Maximum
PBH Threshold
Summary

Primordial black holes

- Primordial black holes (PBHs) may have formed from primordial fluctuations (Zeldovich & Novikov 1967, Hawking 1971).
- PBHs can be used as a probe into the early Universe. (Carr 1975).

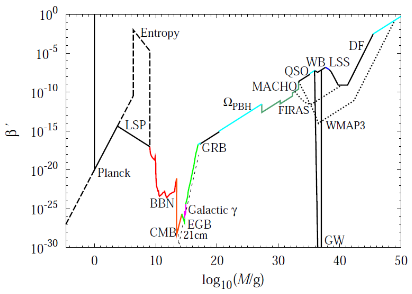

Carr et al. (2010)

T. Harada with Yoo and Kohri PBH Threshold

Condition for the PBH formation

- An analytic estimate: Carr (1975)

$$w = \delta_c < \delta_H < \delta_{\max} = 1,$$

  where the EOS is $p = w\rho c^2$ and δ_H is $\delta = (\rho - \rho_b)/\rho_b$ at the horizon crossing. $\delta_c = 1/3$ for radiation ($w = 1/3$).
- The production rate β is very sensitive to δ_c.
- Numerical relativity simulations
  - $\delta_c \simeq 0.43 - 0.47$: Musco et al. (2005), Polnarev & Musco (2009)
  - δ_c for different values of w: Musco & Miller (2012)
  - More detailed study with radiation: Nakama et al. (2013)
- $\delta_{\max}$ is not due to the separate universe condition but due to geometry: Kopp et al. (2011)

Introduction
Model and Maximum
PBH Threshold
Summary

Questions

- How good Carr's condition is in comparison with the recent numerical results?
- Can we improve Carr's condition, which was obtained 38 years ago?

T. Harada with Yoo and Kohri PBH Threshold

Outline

1 Introduction

2 Model and Maximum

3 PBH Threshold

4 Summary

Introduction
Model and Maximum
PBH Threshold
Summary

Three-zone model

- The background universe: a flat Friedmann for $r > r_b$
- The overdense region: a closed Friedmann

$$ds^2 = -c^2dt^2 + a^2(t)(d\chi^2 + \sin^2\chi d\Omega^2) \quad \text{for} \quad 0 \le \chi < \chi_a.$$

The areal radius of the overdensity is $R_a = a(t)\sin\chi_a$.

- The underdense layer compensates the overdensity.

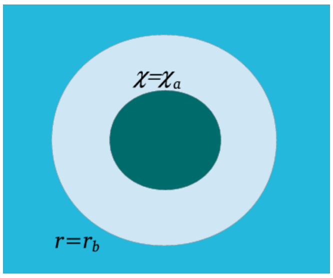

T. Harada with Yoo and Kohri PBH Threshold

Maximum amplitude

- The Friedmann equations

$$H^2 = \frac{8\pi G\rho}{3} - \frac{c^2}{a^2} \quad \text{and} \quad H_b^2 = \frac{8\pi G\rho_b}{3}$$

give

$$\delta_H = \left(\frac{H}{H_b}\right)^2 - \cos^2\chi_a,$$

at the horizon crossing $R_a = R_{H_b} \equiv cH_b^{-1}$.

- In the uniform Hubble slice, on which $H = H_b$, it follows

$$0 < \delta_H^{\mathrm{UH}} = \sin^2\chi_a \leq 1,$$

where $\delta_H^{\mathrm{UH}} = 1$ holds only for $\chi_a = \pi/2$. This is a 3-hemisphere and not the separate universe $\chi_a = \pi$.

Introduction
Model and Maximum
PBH Threshold
Summary

Trapped surfaces and apparent horizons

- The Misner-Sharp mass M for the closed Friedmann is given by

$$\frac{2GM}{c^2R} = \left[1 + \left(\frac{\dot{a}}{c}\right)^2\right]\sin^2\chi,$$

- An apparent horizon is given by a 2-sphere on which $2GM/(c^2R) = 1$.
- Therefore, if $\chi_a > \pi/2$, the region has a (future) apparent horizon immediately after the maximum expansion.

T. Harada with Yoo and Kohri PBH Threshold

Outline

1 Introduction

2 Model and Maximum

3 PBH Threshold

4 Summary

Jeans radius and Carr's threshold formula

- At the maximum expansion, the areal radius $R_{a,\max}$ of the overdense region which goes into a PBH should satisfy

$$R_J < R_{a,\max} \leq a_{\max},$$

where R_J is the Jeans radius.

- In an analogy with Jeans's analysis in Newtonian gravity, one can adopt the following choice:

$$R_J = \sqrt{w}c\frac{1}{\sqrt{8\pi G\rho_{\max}/3}} = \sqrt{w}a_{\max}.$$

After some calculation, we find

$$w < \delta_H^{\rm UH} \leq 1.$$

This is nothing but Carr's condition. However, this is clearly dependent on the choice of R_J.

Solution for the overdense region

- Defining the new variables $\tilde{a}$ and $\tilde{t}$ such that

$$\tilde{a} = a^{1+3w}, \quad d\tilde{t} = (1+3w)\tilde{a}^{3w/(1+3w)}dt,$$

the Friedmann equation can be integrated to give

$$\tilde{a} = \tilde{a}_{\max}\frac{1-\cos\eta}{2}, \quad \tilde{t} = \tilde{t}_{\max}\frac{\eta-\sin\eta}{\pi},$$

where $\tilde{t}_{\max} = (\pi/2)(\tilde{a}_{\max}/c)$.

- The line element can be rewritten in the form

$$ds^2 = \tilde{a}^{2/(1+3w)}\left[-\frac{1}{(1+3w)^2}d\eta^2 + d\chi^2 + \sin^2\chi d\Omega^2\right].$$

Introduction
Model and Maximum
PBH Threshold
Summary

Trajectory of sound waves

- The sound wave propagates in the closed Friedmann geometry according to

$$a\frac{d\chi}{dt} = \pm\sqrt{w}c \quad \text{or} \quad \frac{d\chi}{d\eta} = \pm\frac{\sqrt{w}}{1+3w}.$$

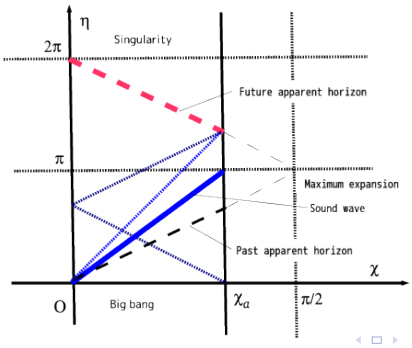

New analytic formula

- Let us adopt the following criterion:
  If and only if the overdensity reaches the maximum expansion before the sound wave crosses over the radius, it collapses to a black hole.
  Equivalently, the sound crossing time > the free-fall time
- This reduces to the following condition:

$$\chi_a > \frac{\pi\sqrt{w}}{1+3w} \quad \text{or} \quad R_J = a_{\max} \sin\left(\frac{\pi\sqrt{w}}{1+3w}\right).$$

- This leads to the following threshold value:

$$\delta_{Hc}^{\rm UH} = \sin^2\left(\frac{\pi\sqrt{w}}{1+3w}\right).$$

Density perturbation in the comoving slice

- Most of the numerical simulations of PBH formation have been implemented in the comoving slice.
- Polnarev and Musco (2007) introduce the asymptotic quasihomogeneous (AQH) solutions and use them for setting initial data.
- Defining $\tilde{\delta} = \delta_1^{\rm COM}(R_a/R_{H_b})^2$, where $\delta_1^{\rm COM}$ is δ in the comoving slice in the first-order AQH solution, we can find for the present model

$$\tilde{\delta} = \frac{3(1+w)}{5+3w}\delta_H^{\rm UH}.$$

- $\tilde{\delta}$ is used as the measure of the initial density perturbation.

Comparison with the numerical result

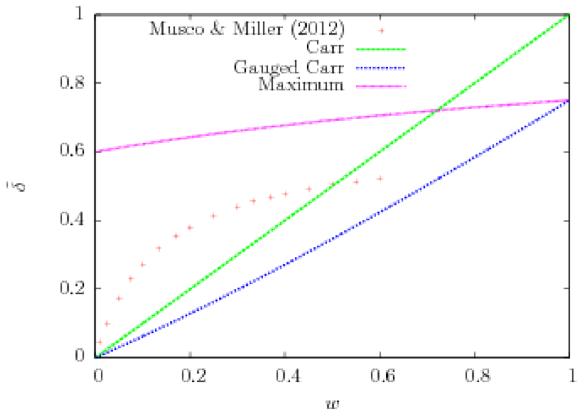

Figure: Carr's formula has a factor-of-10 error.

Introduction
Model and Maximum
PBH Threshold
Summary

Comparison with the numerical result

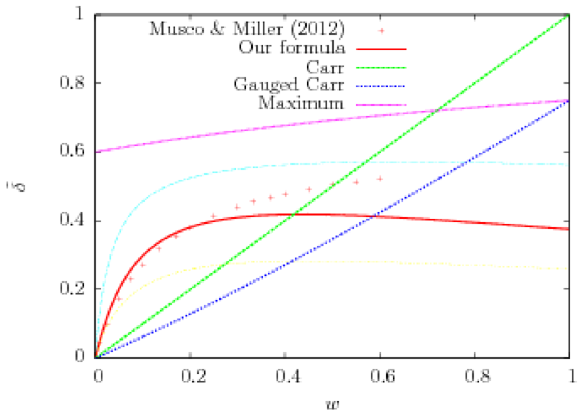

Figure: Our new formula agrees within 10-20%.

T. Harada with Yoo and Kohri PBH Threshold

Summary of our analytic formula

$$\tilde{\delta}_c = \frac{3(1+w)}{5+3w}\sin^2\left(\frac{\pi\sqrt{w}}{1+3w}\right)$$

- Shows an agreement with the numerical result within 10-20 % for $0.01 \le w \le 0.6$. This is much better than Carr's estimate both qualitatively and quantitatively.
- Special cases
  - $\tilde{\delta}_c \approx 3\pi^2 w/5$ for $w \ll 1$
  - $\tilde{\delta}_c \simeq 0.4135$ for $w = 1/3$
  - $\tilde{\delta}_c \simeq 0.4$ for $1/3 \lesssim w \lesssim 1$
  - 3/8 for $w = 1$

Introduction
Model and Maximum
PBH Threshold
Summary

Probability distribution

- Conventionally, a Gaussian distribution is assumed for δ_H:

$$\beta_0(M) = \int_{\delta_c(M)}^{\delta_{\max}(M)} \frac{2}{\sqrt{2\pi\sigma^2(M)}}\exp\left(-\frac{\delta^2}{2\sigma^2(M)}\right)d\delta.$$

  However, it has a problem in the nonlinear regime. (Recall $\delta_H = \sin^2\chi_a$.)
- Kopp et al. (2011) suggested a Gaussian distribution for a curvature fluctuation ζ:

$$\beta_0(M) = \int_{\zeta_c(k_{\rm BH})}^{\infty} \frac{2}{\sqrt{2\pi P_\zeta(k_{\rm BH})}}\exp\left(-\frac{\zeta^2}{2P_\zeta(k_{\rm BH})}\right)d\zeta$$

T. Harada with Yoo and Kohri PBH Threshold

Threshold values for curvature fluctuations

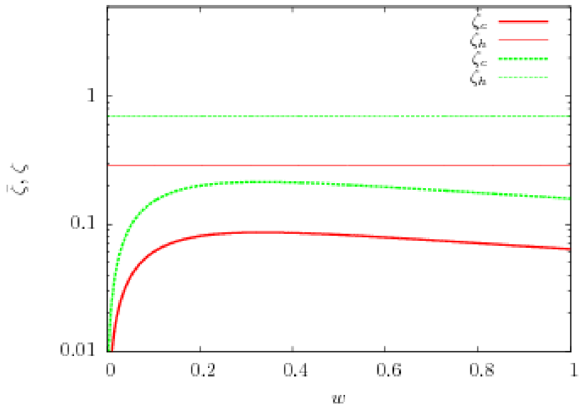

Figure: The threshold values for the averaged value $\bar{\zeta}$ (red thick line) and peak value ζ (green thick line).

Outline

1 Introduction
2 Model and Maximum
3 PBH Threshold
4 Summary

Summary

- A new analytic formula for the PBH threshold is derived.
- It shows a very good agreement with the numerical result.
- The maximum amplitude is analytically derived.
- Further analytic and numerical studies are important.

“First—Quantized Theory of Expanding Universe from Quantum Field in Mini—Superspace”

by Daisuke Ida

[JGRG23(2013)110805]

First–Quantized Theory of Expanding Universe from Quantum Fields in Mini–Superspace

Daisuke Ida, Miyuki Saito (Gakushuin Univ.)

- **mini–superspace model**
- **quantum fields in mini–superspace**
- **structure of Hilbert space**
- **pseudo–1-particle states**
- **classical–quantum correspondence**

Hamiltonian formulation of Einstein gravity

Einstein-Hilbert action:

$$S = \int d^4x\sqrt{-g}R$$

ADM decomposition:

$$g = -N^2dt^2 + h_{ij}(dx^i + N^i dt)(dx^j + N^j dt)$$

canonical variables: (h_{ij}, π^{ij})

$$\pi^{ij} = \frac{\sqrt{h}}{16\pi G}(K^{ij} - Kh^{ij})$$

extrinsic curvature of Σ_t

$$K_{ij} = N\Gamma^0_{ij} = \frac{1}{2N}(\partial_t h_{ij} - 2D_{(i}N_{j)})$$

total Hamiltonian:

$$H_T = \int_{\Sigma_t} d^3x (N\Phi^0 + N_i \Phi^i)$$

Hamiltonian constraint:

$$\Phi^0 = G_{ij,kl}\pi^{ij}\pi^{kl} - \frac{\sqrt{h}}{16\pi G}{}^{(h)}R \approx 0$$

momentum constraint:

$$\Phi^i = -2D_k \pi^{ik} \approx 0$$

superspace metric:

$$G_{ij,kl} = \frac{1}{2\sqrt{h}}(h_{ij}h_{kl} + h^{il}h^{jk} - h_{ij}h_{kl})$$

Wheeler-DeWitt quantization: $\widehat{\Phi}_\mu |\Psi\rangle = 0$

$$(-\frac{\delta}{\delta h_{ij}} G_{ij,kl} \frac{\delta}{\delta h_{kl}} - \frac{\sqrt{h}}{16\pi G}{}^{(h)}R)\Psi[h_{ij}] = 0,$$

$$D_k \frac{\delta}{\delta h_{ik}} \Psi[h_{ij}] = 0.$$

$\Rightarrow$

- *No unitary evolution.*
- *Interpretation of the wave function* $\Psi[h_{ij}]$.

Classical theory: Einstein gravity + real scalar field
(FRW background)

$$S[g, X] = \int d^4x\sqrt{-g}(R - (1/2)X_{,\mu}X^{,\mu})$$

FRW metric:

$$g = -N(t)^2dt^2 + a(t)^2\gamma_K \quad (K = 0, \pm 1)$$

Hamiltonian:

$$H_T = N\Phi_0$$

$$\Phi_0 = \frac{1}{2v}\left(-\frac{p_a^2}{12a} + \frac{p_X^2}{a^3}\right) - 6Kva \approx 0, \qquad (v = \int d^3x\sqrt{\gamma_K})$$

minisuperspace coodinates: $q^m = (a, X)$

minisuperspace metric:

$$g_S = 2v(-12ada^2 + a^3dX^2)$$

Hamiltonian is rewritten as:

$$H_T = N[(g_S)^{mn}p_mp_n + u(q^k)], \quad u(q^k) = -6Kva$$

Einstein, Klein–Gordon eqs.

$$\frac{d^2q^k}{dt^2} + \Gamma[g_S]^k_{mn}\frac{dq^m}{dt}\frac{dq^n}{dt} \approx N^{-1}\frac{dN}{dt}\frac{dq^k}{dt} - 2N^2(g_S)^{kl}\frac{du}{dq^l}$$

Conformal Transformation of Mini–Superspace:

invariance under conformal transformation (DeWitt, Misner etc.):

$$(g_S, u) \mapsto (f g_S, f^{-1} u)$$

conformal transformation ($u(q^k) \neq 0$):

$$(g_s)_{mn} = \frac{C^2}{u(q^k)}(g_C)_{mn}, \qquad (C = \text{const.})$$

reparametrization of time:

$$t(s) = \int^s ds \frac{C}{2Nu}$$

$\Rightarrow$ **geodesic eq. in mini–superspace:**

$$\frac{d^2 q^k}{ds^2} + \Gamma[g_C]^k_{mn} \frac{dq^m}{ds}\frac{dq^n}{ds} \approx 0$$

Hamiltonian constraint:

$$\Phi_0 = u \left[(g_C)_{mn} \frac{dq^m}{ds}\frac{dq^n}{ds} + 1 \right] \approx 0$$

equivalent classical system:

$$H'_T = \lambda((g_C)^{mn} p_m p_n + 1)$$

Quantization of Einstein eq. ($K=-1$ case):

Mini–superspace ($\mathscr{M}, g_C$):

$$H'_T = \lambda((g_C)^{mn} p_m p_n + 1)$$

$$g_C = A^2 e^{2T/\sqrt{3}}(-dT^2 + dX^2), \qquad (a = a_0 e^{T/2\sqrt{3}}, \quad A^2 = \frac{12v^2 a_0^4}{C^2})$$

Quantum theory: **Klein–Gordon field in $(\mathscr{M}, g_C)$,**

$$S[\phi] = \frac{1}{2}\int dTdX[(\partial_T\phi)^2 - (\partial_X\phi)^2 - A^2 m^2 e^{2T/\sqrt{3}}\phi^2]$$

mode function: $\{f(p;T,X), f^*(p;T,X)\}$

$$f(p;T,X) \propto J_{-i\sqrt{3}|p|}(\sqrt{3}Ame^{T/\sqrt{3}})e^{ipX} \to \frac{1}{\sqrt{4\pi|p|}}e^{-i|p|T}e^{ipX} \qquad (T \to -\infty)$$

quantization:

$$\phi = \int dp[a(p)f(p;T,X) + a^*(p)f(p;T,X)]$$

Fock representation w.r.t. $|\Omega\rangle$:

$$a(p)|\Omega\rangle = 0 \quad (p \in \boldsymbol{R})$$

Hamiltonian for K–G field at T:

$$H = \int dp \left[\sigma(|p|;T)a(p)a^*(p) \underbrace{+\frac{\tau(|p|;T)}{2}a(p)a(-p) + \frac{\tau^*(|p|;T)}{2}a^*(p)a^*(-p)}_{\text{off–diagonal terms}} \right]$$

$$\begin{aligned}
\sigma(|p|;T) := {} & |\Gamma(1-i\sqrt{3}|p|)|^2 \\
& \times \left[\frac{A^2m^2e^{2T/\sqrt{3}}}{8|p|} \left| J_{i\sqrt{3}|p|-1}\left(\sqrt{3}Ame^{T/\sqrt{3}}\right) - J_{i\sqrt{3}|p|+1}\left(\sqrt{3}Ame^{T/\sqrt{3}}\right) \right|^2 \right. \\
& \left. + \frac{1}{2}\left(|p| + \frac{A^2m^2e^{2T/\sqrt{3}}}{|p|}\right) \left| J_{i\sqrt{3}|p|}\left(\sqrt{3}Ame^{T/\sqrt{3}}\right) \right|^2 \right],
\end{aligned}$$

$$\begin{aligned}
\tau(|p|;T) := {} & \Gamma(1-i\sqrt{3}|p|)^2 \left(\frac{\sqrt{3}Am}{2}\right)^{i2\sqrt{3}|p|} \\
& \times \left\{ \frac{A^2m^2e^{2T/\sqrt{3}}}{8|p|} \left[J_{-i\sqrt{3}|p|-1}\left(\sqrt{3}Ame^{T/\sqrt{3}}\right) - J_{-i\sqrt{3}|p|+1}\left(\sqrt{3}Ame^{T;\sqrt{3}}\right) \right]^2 \right. \\
& \left. + \frac{1}{2}\left(|p| + \frac{A^2m^2e^{2T/\sqrt{3}}}{|p|}\right) \left[J_{-i\sqrt{3}|p|}\left(\sqrt{3}Ame^{T/\sqrt{3}}\right) \right]^2 \right\}
\end{aligned}$$

cf. standard approach (particle creation in FRW):

Bogoliubov transformation:

$$a(p;T) := a(p)\cosh\theta(p;T) + a^*(-p)e^{i\gamma(p;T)}\sinh\theta(p;T)$$

$$a(p;T) = U(T)a(p)U^*(T), \quad U(T) = \exp\frac{1}{2}\int dp\theta(e^{-i\gamma}a(p)a(-p) - e^{i\gamma}a^*(p)a^*(-p))$$

Hamiltonian is diagonalized:

$$H = \int dp\omega(|p|;T)a^*(p;T)a(p;T), \quad \omega = \sqrt{\sigma^2 - \tau\tau^*}$$

"T–vacuum":

$$a(p;T)|\Omega;T\rangle = 0 \qquad (p \in \boldsymbol{R})$$

Creation of scalar particles:

$$\langle\Omega|a^*(p;T)a(p;T)|\Omega\rangle \neq 0.$$

But "the universe should be in a 1–particle state."

Structure of Hilbert space:

1. **K–G Hamiltonian defines continuum of Fock spaces** $\mathscr{F}_T \ (T \in \boldsymbol{R})$

2. $\mathscr{F}_{T_1}$ **and** $\mathscr{F}_{T_2}$ $(T_1 \neq T_2)$ **are improperly unitarily equivalent:**
$\mathscr{F}_{T_1} \cap \mathscr{F}_{T_2} = \{\mathbf{0}\}$ **or**
finite particle state of $\mathscr{F}_{T_1}$ $\Rightarrow$ **"infinite particle state" of** $\mathscr{F}_{T_2}$

3. **K–G Hamiltonian at** $H(T) : \mathscr{F}_T \to \mathscr{F}_T$

4. **This means it immediately becomes infinite particle state:**

$$e^{-iH(T)\Delta T} : \underbrace{\mathscr{F}_T^{(1)}}_{\text{1–particle state}} \to \mathscr{F}_T^{(1)} \sim \underbrace{\mathscr{F}_{T+\Delta T}^{(\infty)}}_{\text{“infinite–particle state”}}$$

Structure of Hilbert space:

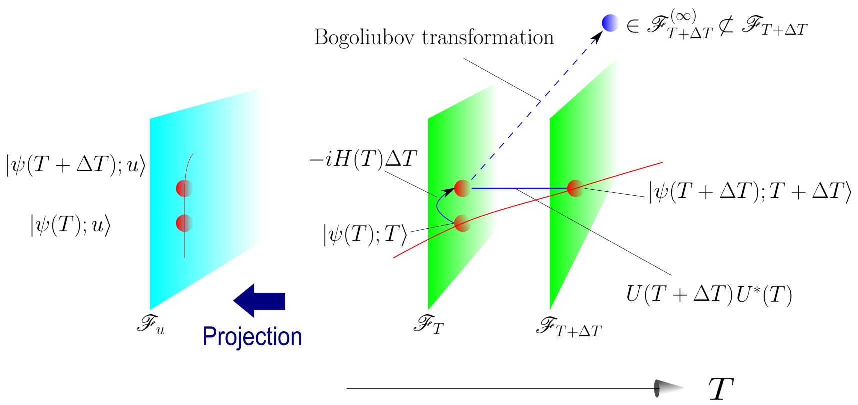

Fibre bundle structure → notion of parallel transport

Proposal: covariant unitary time evolution

- **covariant time derivative:**
$$D_T := \frac{d}{dT} + U(\partial_T U^*)$$
is anti self–adjoint operator on $\mathscr{F}_T$.
- **unitary evolution:**
$$iD_T|\psi(T);T\rangle = H(T)|\psi(T);T\rangle$$

$$\Leftrightarrow \; i\partial_T|\psi(T);u\rangle = H(T)|\psi(T);u\rangle \quad \text{(in projected Fock space } \mathscr{F}_u\text{)}$$
- **Any 1–particle state remains in the space of 1–particle states.**

Canonical observables in space of 1–particle states:

- **annihilation operator for a localized particle:**
$$\widetilde{a}(X;T) := \frac{1}{\sqrt{2\pi}} \int dp a(p;T) e^{ipX}$$
- **position operator in $\mathscr{F}_T^{(1)}$:**
$$Q(T) := \int dX \widetilde{a}^*(X;T) X \widetilde{a}(X;T)$$
- **localized 1–particle state in $\mathscr{F}_T$:**
$$|X;T\rangle := \widetilde{a}^*(X;T)|\Omega;T\rangle$$
$$\Rightarrow Q(T)|X;T\rangle = X|X;T\rangle$$
- **momentum operator in $\mathscr{F}_T^{(1)}$:**
$$P(T) := -i \int dX \widetilde{a}^*(X;T) \partial_X \widetilde{a}(X;T)$$
- **CCR–algebra:**
$$[Q(T), P(T)] = i\mathbf{1}\big|_{\mathscr{F}_T^{(1)}}$$

Schrödinger representation:

- **completeness of localized states:**

$$\int dX |X;T\rangle\langle X;T| = \mathbf{1}\Big|_{\mathscr{F}_T^{(1)}}$$

- **wave function for the 1–particle state $|\psi(T);T\rangle$:**

$$\psi(X,T) := \langle X;T|\psi(T);T\rangle$$

- **Hamiltonian at early universe ($T \to -\infty$):**

$$\langle X;T|H(T)|X';T\rangle = \frac{1}{2\pi}\int dp \left[|p| + \frac{A^2 m^2 e^{2T/\sqrt{3}}}{2|p|} + O(e^{4T/\sqrt{3}})\right] e^{ip(X'-X)}$$

- **Schrödinger eq.**

$$i\partial_T \psi(X,T) = \left[\sqrt{-\partial_X^2 + A^2 m^2 e^{2T/\sqrt{3}}} + O(e^{4T/\sqrt{3}})\right]\psi(X,T)$$

— **free from operator ordering ambiguity.**

Classical–quantum correspondence:

from quantum theory:

- **asymptotic solution to the Schrödinger eq.**

$$\psi(X,T) = \int dp\ c(p) \exp\left[-i\left(|p|T + \frac{\sqrt{3}A^2 m^2 e^{2T/\sqrt{3}}}{4|p|} + O(e^{4T/\sqrt{3}})\right)\right] e^{ipX}$$

- **group velocity of a wave packet**

$$v_g(p) = 1 - \frac{A^2 e^{2T/\sqrt{3}}}{2(p/m)^2} + O(e^{4T/\sqrt{3}})$$

from classical theory:

- **Hamiltonian constraint:**

$$p_T \approx -\sqrt{p_X^2 + A^2 e^{2T/\sqrt{3}}}$$

- **velocity:**

$$v = -\frac{p_X}{p_T} = \frac{p_X}{\sqrt{p_X^2 + A^2 e^{2T/\sqrt{3}}}} = 1 - \frac{A^2 e^{2T/\sqrt{3}}}{2p_X^2} + O(e^{4T/\sqrt{3}})$$

dynamics of a localized 1–particle state:

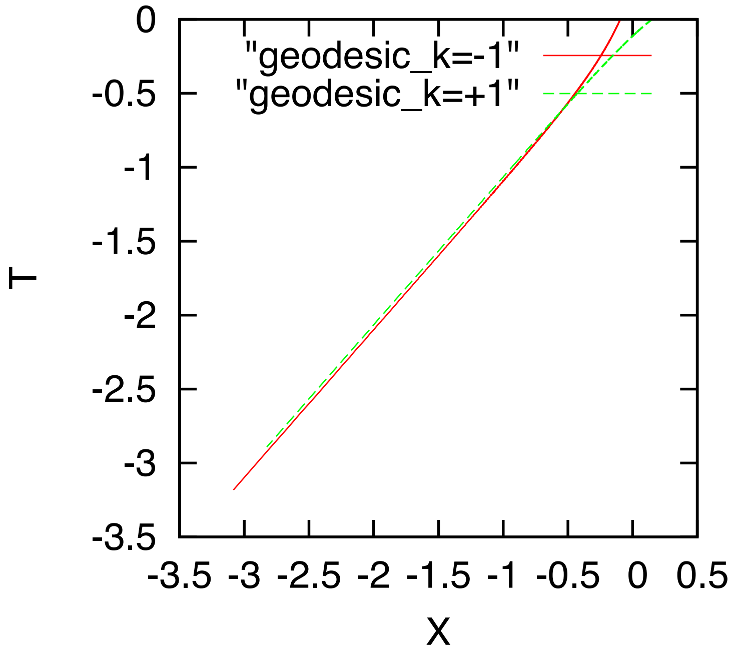

dynamics of a localized 1–particle state $(k = -1)$ **:**

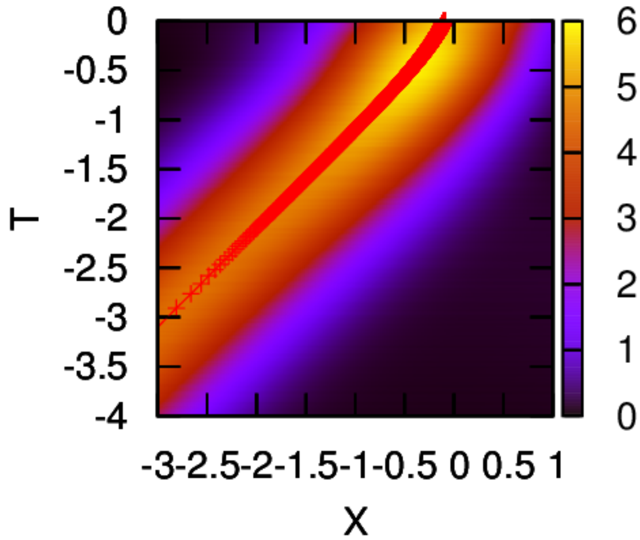

dynamics of a localized 1–particle state $(k = -1)$ **:**

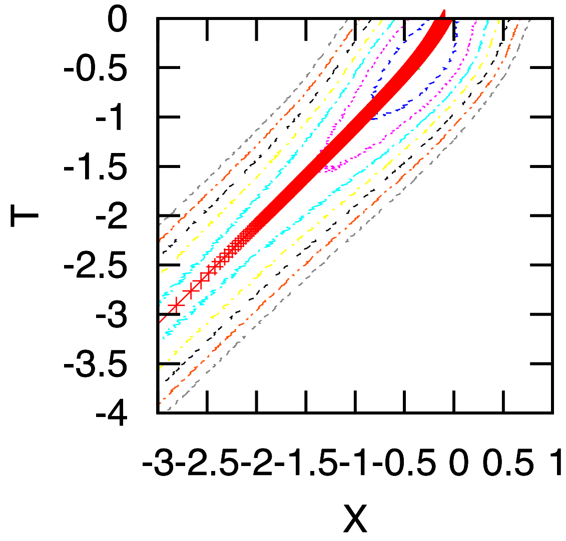

dynamics of a localized 1–particle state $(k = 1)$ **:**

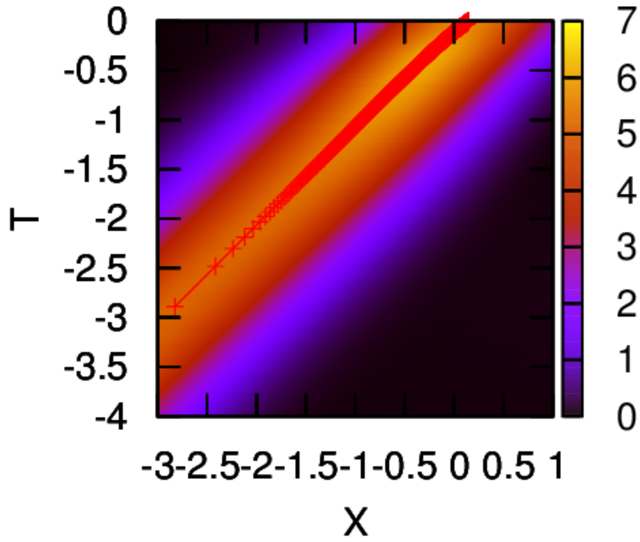

dynamics of a localized 1–particle state $(k = 1)$ **:**

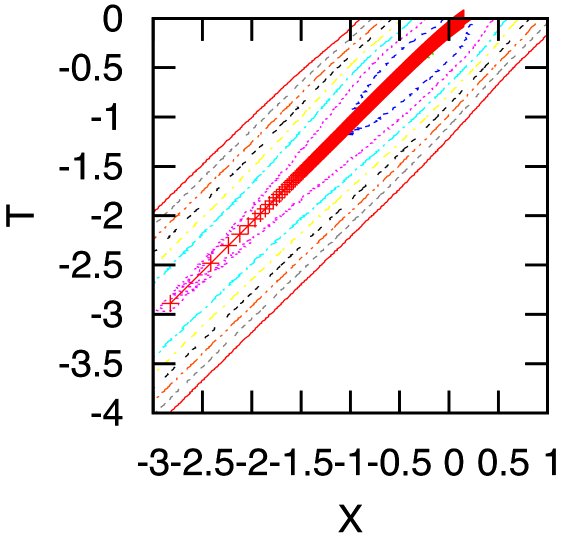

Summary

- **We consider the quantum Klein–Gordon field in the mini–superspace fixing the conformal frame s.t. Einstein eq. becomes geodesic eq.**
- **The present method can be applied to fermionic quantization in the mini–superspace.**
- **We propose a quantum theory in which the Hamiltonian gives a unitary time evolution of a 1–particle state in a separable Hilbert space.**
- **We construct the observable set subject to the CCR–algebra.**
- **This quantum system reproduces Einstein eq. as a correct classical limit.**

“Constraining the small scale perturbations in our big universe”

by Christian Byrnes (invited)

[JGRG23(2013)110806]

From very large to very small scales

- We have the "precision era" measurements on CMB and LSS scales
- These span approximately the largest 5-10 efoldings which are inside the Hubble scale today
- Lyman alpha, 21cm and spectral mu distortions in the CMB may add a similar range of scales in the (farish) future
- But inflation is believed to have lasted at least 50-60 efoldings
- So we only observe a small fraction of all scales
- Limits our ability to constrain the early universe

Probing the small scales

- Very hard to go beyond the linear scales of structure formation ~ Mpc scales
- Problem is that structure formation erases memory of the very small scales
- Two examples of a sufficiently dense probe which could survive until today
- Ultra Compact Mini Haloes (UCMHs), if DM annihilates we have a good chance to see them
- Primordial Black Holes (PBHs), only Hawking radiation can make them disappear

3

Other small scale probes

- Gravitational waves - should leave a fossil which will be preserved, but detectors not yet competitive
- Spectral distortions of the CMB blackbody spectrum - silk damping injects energy - promising future probe with Pixie/Prism
- New: lack of Sne 1a lensing dispersion weakly constrains another 4-7 efolds of inflation - Ben-Dayan & Kalaydzhyan '13

What we observe

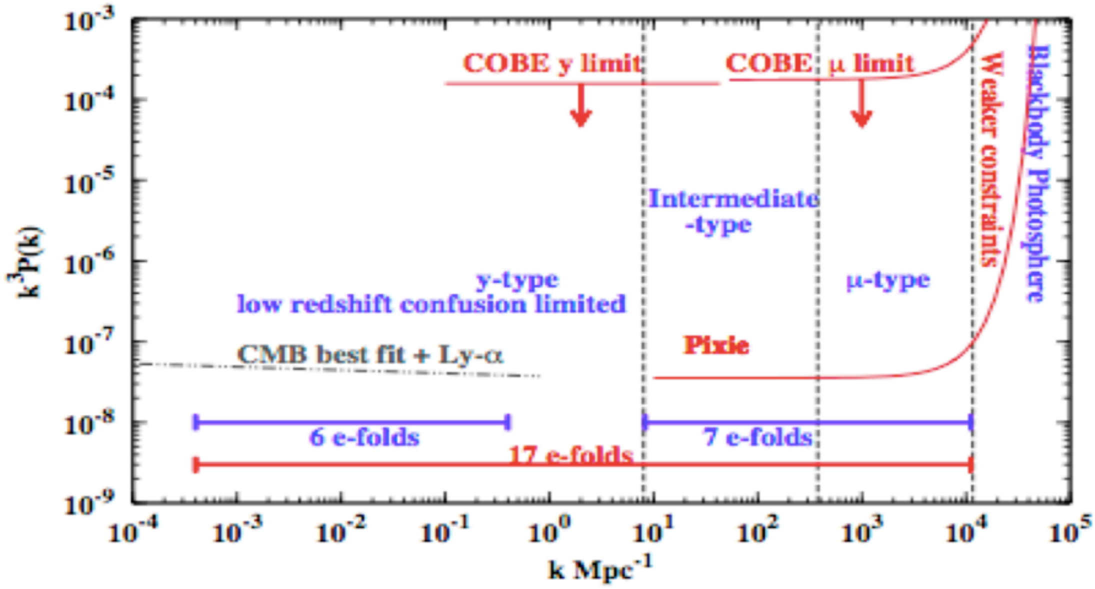

Currently about 6 efolds
With Pixie, maybe 17 efolds
Still far short of 50-60 efolds

Khatri '13

Where PBH constraints come from?

- The Hawking radiation from PBHs must not:
- stop the success of big bang nucleosynthesis
- Interfere with the CMB
- Be compatible with the observed extragalactic photon background
- PBHs must not have greater energy density than DM (but could be a DM candidate)
- Strongly scale/mass constraints in terms of beta, the fraction of the energy density of the universe in PBHs satisfies (over many scales):

$$\beta \equiv \left.\frac{\rho_{PBH}}{\rho_{tot}}\right|_{formation} \lesssim 10^{-20} - 10^{-5}$$

PBH constraints

$$\beta' = \Omega_{\rm PBH}\Big|_{\rm formation}$$

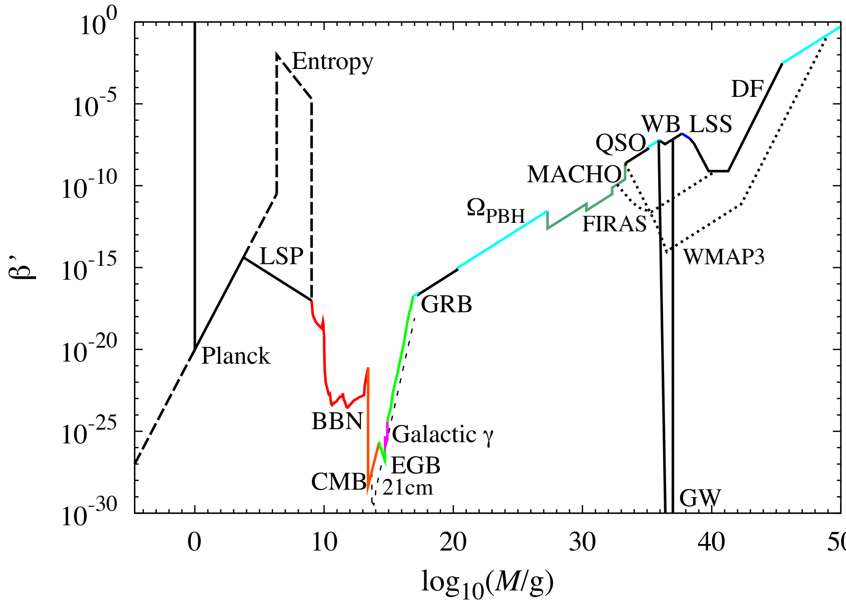

Carr et al review; 2010

The Gaussian case

People usually assume this to be a good estimate

$$P(\zeta) = \frac{1}{\sqrt{2\pi}\sigma} exp\left(-\frac{\zeta^2}{2\sigma^2}\right)$$

$$\beta \simeq \int_{\zeta_c}^{\infty} P(\zeta)d\zeta \simeq exp\left(-\frac{\zeta_c^2}{2\sigma^2}\right)$$

$$\frac{\sigma}{\zeta_c} = \sqrt{\frac{1}{2\ln(1/\beta)}} \qquad \zeta_c \simeq 1$$

Critical value is uncertain: for radiation domination Green et al ‘04, using Shibata & Sasaki ’99 found 0.7-1.2, Harada et al ’13 found 0.2. Sensitive to both equation of state and overdensity profile (2 parameters) - See Tomohiro Harada’s talk and recent papers

Result is accurate to order of 10% (compared to more involved calculation using density perturbation with window functions)

$\mathcal{P}_\zeta \lesssim 10^{-2}$ on the relevant PBH scales

Power spectrum bounds

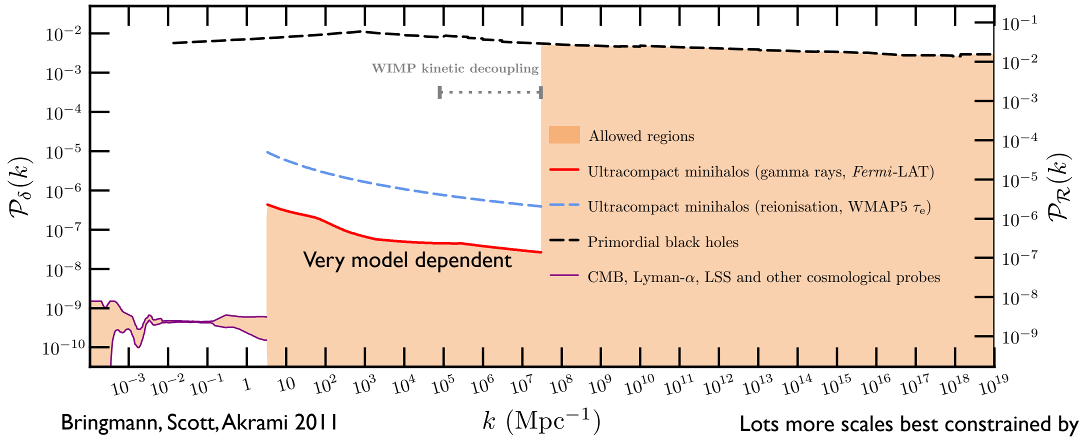

Bringmann, Scott, Akrami 2011 Lots more scales best constrained by PBHs

Amplitude of power spectrum very uncertain beyond a few 1/Mpc, huge uncertainty on much smaller scales, PBHs give the tightest constraint we have got over the biggest range
UCMH - dependent on DM model
PBH amplitude assumes a Gaussian distribution, result can be several orders of magnitude different if thats not true

9

Could the perturbations become large?

- If quasi scale invariance holds until the end of inflation, then clearly no
- But no reason to assume this - remember we observe only a small window onto inflation
- Running mass model - spectral index strongly k dependent
- Hybrid inflation: popular model in which a second stage generates much larger small scale perturbations (also highly non-Gaussian)

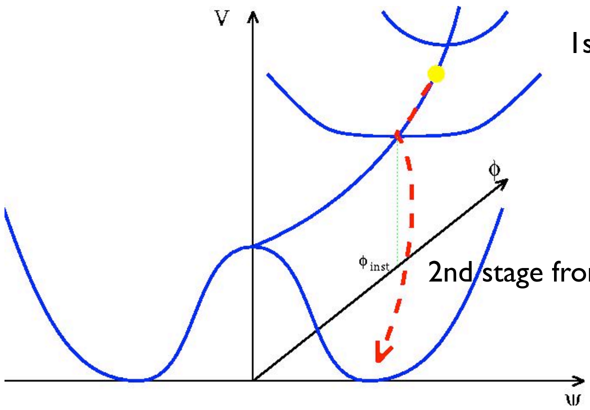

1st stage from inflaton field

2nd stage from waterfall field - tachyonic instability

10

Power spectrum constraints only sensitive to log of the observational constraints

So small changes in the amplitude of perturbations changes the PBH formation rate exponentially

We will see that even small non-Gaussianity is very important (small f_{NL} can mean a large skewness, when the amplitude of perturbations grow)

PBH formation is very rare, so we are measuring the tails of the pdf's, typically larger than 5-10 sigma deviations

So skewness/kurtosis really matters!

Lets take it into account, and see how the normal constraints on the power spectrum change

Quadratic non-Gaussianity

$$\zeta = \zeta_G + \frac{3}{5} f_{NL} \left(\zeta_G^2 - \langle \zeta_G^2 \rangle \right) + \frac{9}{25} \cancelto{0}{g_{NL}} \zeta_G^3$$

Results will depend on the sign of the non-Gaussianity, if positive its easier to form overdensities because the linear and quadratic terms act in the same direction (similarly to the speculated “too big, too early clusters” which could be explained by large and positive f_{NL})

Otherwise the two terms tend to cancel each other, and zeta is bounded from above

Large influence of small f_{NL}

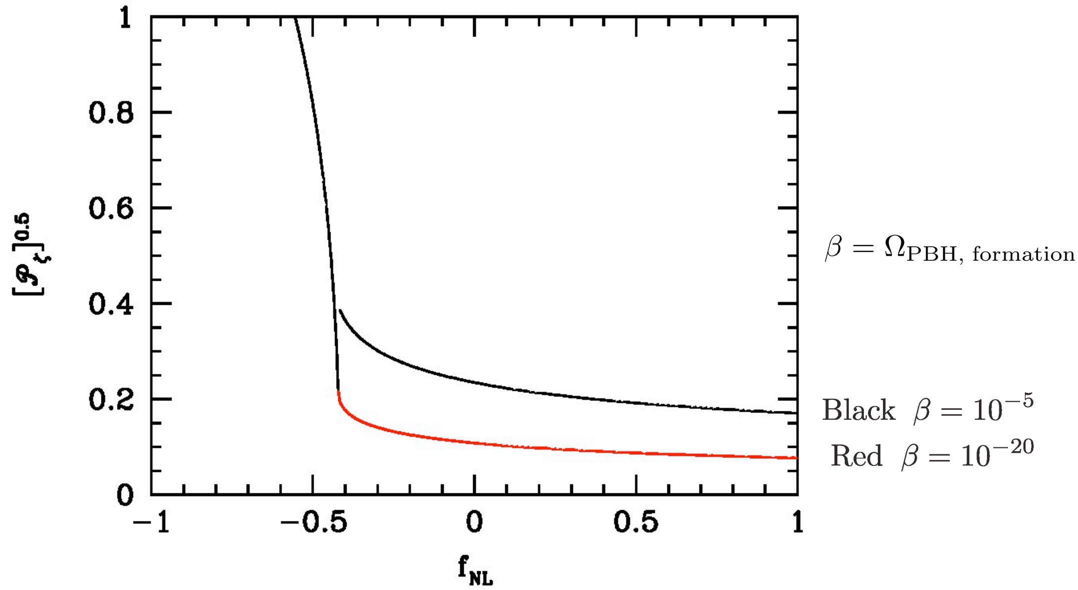

Results especially dramatic for negative f_{NL}

If PBHs are detected in the future, f_{NL}<0 (and all higher-order parameters zero) on the relevant scales is ruled out, unless it has a tiny amplitude

13

Very large and positive f_{NL}

- Results are about the square of the Gaussian case, hence much more stringent

$$\beta = 10^{-20}, \quad \underset{\text{Gaussian}}{\mathcal{P}_\zeta \simeq 10^{-2}} \rightarrow \underset{\text{Chi-squared}}{\mathcal{P}_\zeta \simeq 10^{-4}}$$

- Limit of very small and very large non-Gaussianity was previously known, we recover those results and interpolate between them CB, Copeland & Green 2012
- Very small: Seery & Hidalgo '06
- Chi squared non-Gaussianity: Avelino '05 and Lyth '12

14

Small g_{NL}, big changes again

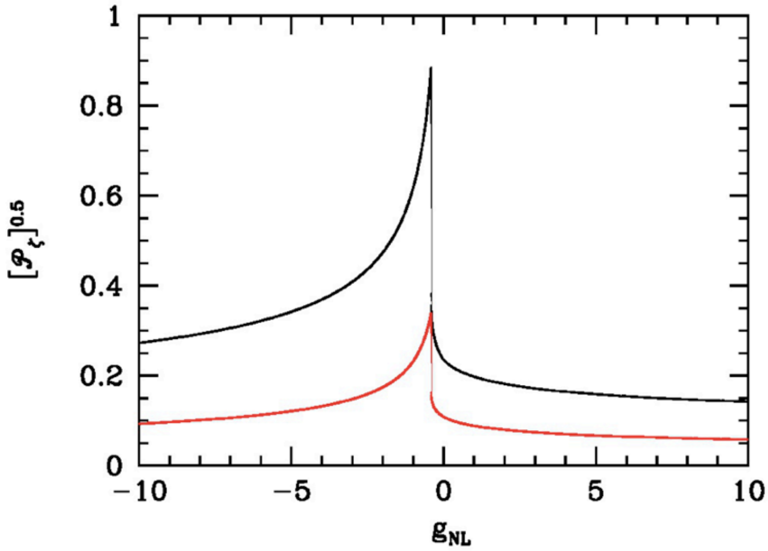

$\beta = \Omega_{\text{PBH, formation}}$

Black $\beta = 10^{-5}$

Red $\beta = 10^{-20}$

There is a symmetry as $g_{NL} \rightarrow \pm$ infinity, because the Gaussian is an even function

What happens to the pdf's?

$f_{NL} > 0$ $\quad$ $f_{NL} < 0$

$g_{NL} > 0$ $\quad$ $g_{NL} < 0$

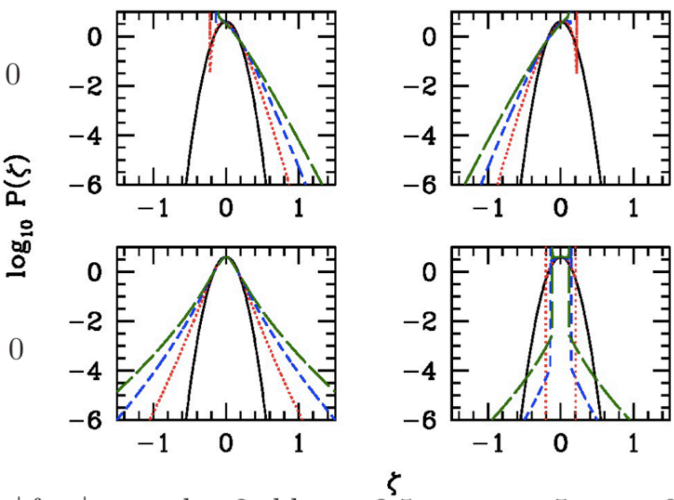

$|f_{NL}|$: red = 2, blue = 3.5, green = 5, $\sigma = 0.1$

$|g_{NL}|$: red = 10, blue = 20, green = 30, $\sigma = 0.1$

What if f_{NL} and g_{NL} are not zero?

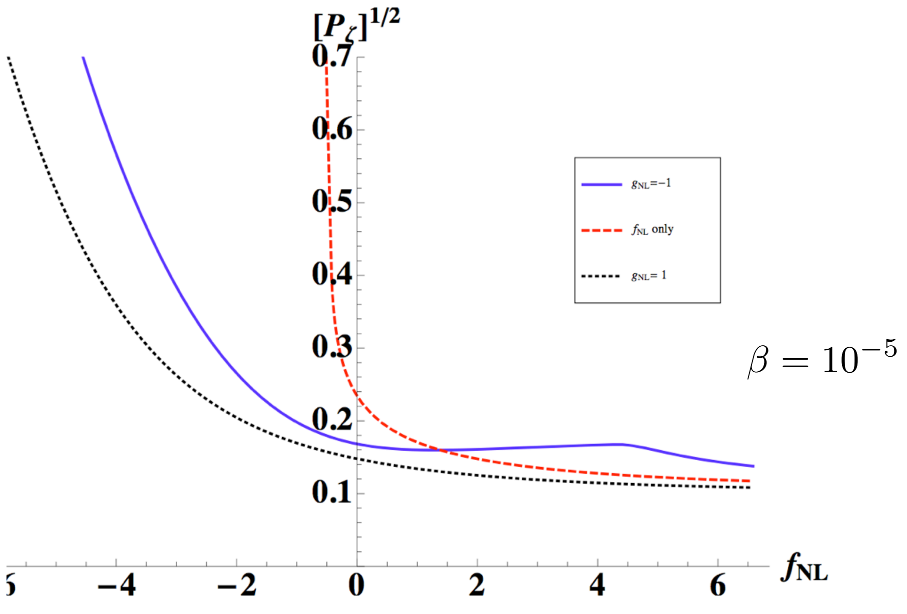

17

One parameter at a time, higher order

$$\zeta = \zeta_g + \frac{3}{5} f_{NL}\left(\zeta_g^2 - \sigma^2\right) + \frac{9}{25} g_{NL}\zeta_g^3 + \frac{27}{125} h_{NL}\left(\zeta_g^4 - 3\sigma^4\right) + \frac{81}{625} i_{NL}\zeta_g^5 + \ldots$$

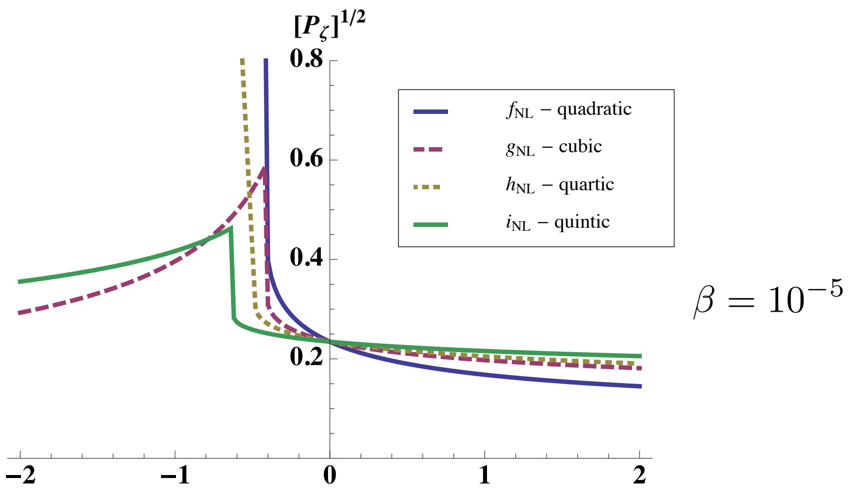

Notice the similarity between odd and even terms

18

What if all non-linearity parameters are interdependent?

- If all non-linearity parameters are positive, constraints keep getting tighter, no problem.
- If some are negative, life gets complicated!
- Result may depend on the highest order non-linearity parameter and its sign, since the perturbations are large, no certainty of convergence
- Good test bed is the quadratic curvaton scenario, the complete non-linear zeta is known (Sasaki, Valiviita & Wands '06)

Hierarchical scaling

$$\zeta \sim \zeta_g + \frac{3}{5} f_{NL} \left(\zeta_g^2 - \sigma^2 \right) + \frac{9}{25} f_{NL}^2 \zeta_g^3 + \frac{27}{125} f_{NL}^3 \left(\zeta_g^4 - 3\sigma^4 \right) + \frac{81}{625} f_{NL}^4 \zeta_g^5 + \ldots$$

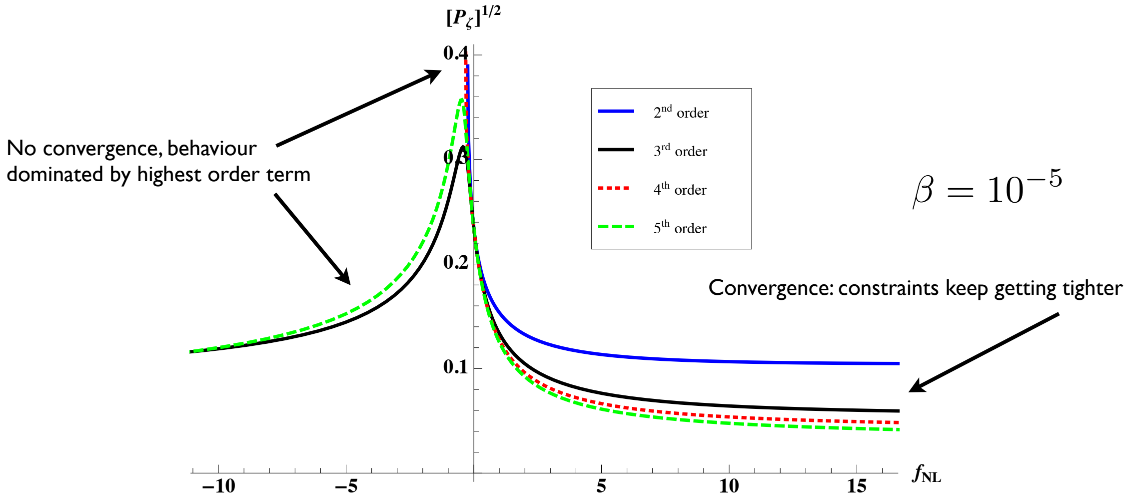

Curvaton scenario I

- Specific inflationary scenario in which perturbations are often non-Gaussian
- Assume curvaton chi has a quadratic potential, then full pdf can be calculated (does any other example exist?) - Sasaki, Valiviita & Wands 2006
- Key parameter is Ω_{chi}, energy density of curvaton at decay time. When small $f_{NL} \sim 1/\Omega_{chi}$
- For CMB constraints, all other non-linearity parameters are unimportant

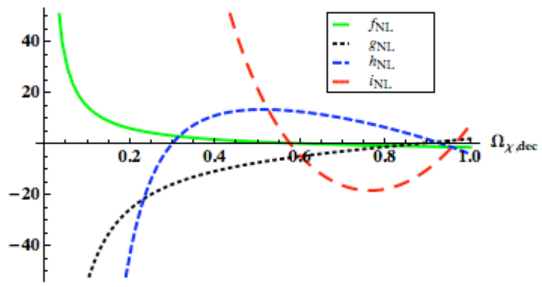

Curvaton scenario II

- For the curvaton scenario, all higher-order terms are important, approximating the pdf as Gaussian is never accurate

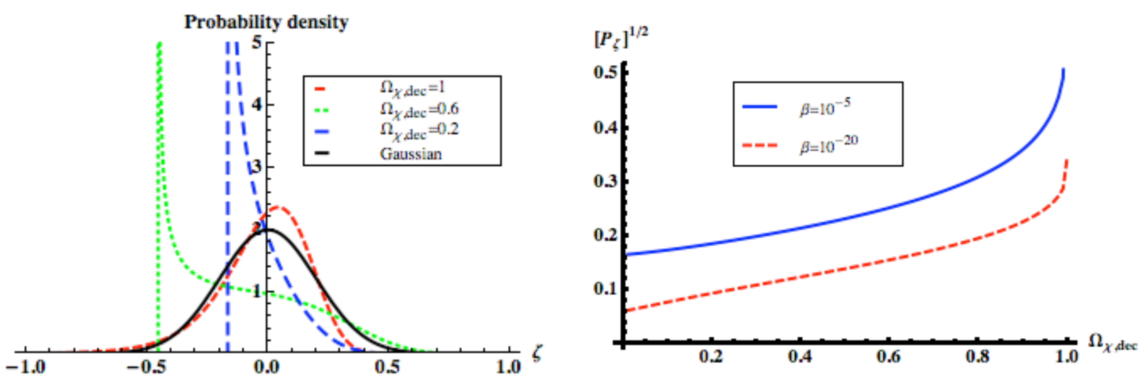

Young and CB 2013

Conclusions

- Even today, non-Gaussianity arguably remains the best window onto the early universe (and provides the tightest constraints)
- Our constraints come from a very limited range of scales, about 6 efoldings out of 60
- PBHs give us a much larger (albeit cloudier) window onto the physics of the early universe
- Constraints are weak, but the tightest which exist on small scales
- Since PBHs are rare, they measure the extreme tail of the pdf and hence are highly sensitive to non-Gaussianity
- Given a model which forms PBHs, you need to take non-Gaussianity into account, even if this is irrelevant on CMB scales
- Truncating the results at low order in the non-linearity parameters is not safe (especially if some of them are negative)

Poster Presentations

P01 Takashi Torii (Osaka Institute of Technology)
"Wormhole solutions in higher dimensional space-time and their linear stability analysis" [JGRG23(2013)P01]

P02 Takashi Tamaki (Nihon University)
"Gauged Q-balls"
[JGRG23(2013)P02]

P03 Takashi Hiramatsu (Yukawa Institute for Theoretical Physics, Kyoto University)
"Bound states of extreme Type-I cosmic strings in two-dimensional space"
[JGRG23(2013)P03]

P04 Koji Izumi (Hirosaki University)
"Gravitational lensing shear by an exotic lens object with negative convergence or negative mass" [JGRG23(2013)P04]

P05 Koki Nakajima (Hirosaki University)
"Shapiro delay by an exotic lens object with negative convergence or negative mass"
[JGRG23(2013)P05]

P06 Yasumichi Sano (Osaka University)
"Gravitational field of a rotating ring around a Schwarzschild black hole"
[JGRG23(2013)P06]

P07 Chisaki Hagiwara (Hirosaki University)
"Demagnification by an exotic lens object with negative mass"
[JGRG23(2013)P07]

P08 Naomasa Fushimi (Hirosaki University)
"Criterion for bound (or unbound) orbits in the Kottler spacetime"
[*]

P09 Hisaaki Shinkai (Osaka Institute of Technology)
"Wormholes in higher dimensional space-time: Dynamics"
[JGRG23(2013)P09]

P10 Hideyoshi Arakida (Nihon University)
"General Relativistic Sitnikov 3-Body Problem"
[JGRG23(2013)P10]

P11 Chulmoon Yoo (Nagoya University)
"Black Hole Universe with Lambda"
[JGRG23(2013)P11]

P12 Norichika Sago (Kyushu University)
"Modeling of the secular evolution of a inspiral orbit around a Kerr black hole"
[JGRG23(2013)P12]

P13 Hiroyuki Nakano (Yukawa Institute for Theoretical Physics, Kyoto University)
"Spin-Regge-Wheeler-Zerilli formalism and gravitational waves"
[JGRG23(2013)P13]

P14 Kouji Nakamura (National Astronomical Observatory of Japan)
"3+1 gauge-invariant variables for perturbations on Schwarzschild spacetime"
[JGRG23(2013)P14]

P15 Hiromi Saida (Daido University)
"How can we detect BHs ?"
[JGRG23(2013)P15]

P16 Masashi Kimura (Yukawa Institute for Theoretical Physics)
"Analysis of curvature singularity on the black hole horizon"
[*]

P17 Takuya Tsuchiya (Waseda University)
"A new numerical scheme for Einstein equations with discrete variational derivative method" [JGRG23(2013)P17]

P18 Shinya Tomizawa (Ibaraki Universtiy)
"Gravitational Faraday effect of soliton waves"
[*]

P19 Cancelled

P20 Sakine Nishi (Rikkyo University)
"Cosmological matching conditions in Horndeski's theory"
[JGRG23(2013)P20]

P21 Keisuke Taniguchi (University of Tokyo)
"Quasiequilibrium sequences of binary neutron stars in a scalar-tensor theory of gravity" [*]

P22 Cancelled

P23 Naoya Kitajima (Institute for Cosmic Ray Research, University of Tokyo)
"21cm signature of minihaloes from cosmic string wakes"
[JGRG23(2013)P23]

P24 Umpei Miyamoto (Akita Prefectural University)
"Liquid bridges and black strings in general dimensions: Stability"
[JGRG23(2013)P24]

P25 Cancelled

P26 Seiju Ohashi (KEK)
"(In-)stability of naked singularity formation in gravitational collapse"
[JGRG23(2013)P26]

P27 Shuichiro Yokoyama (Institute for Cosmic Ray Research, University of Tokyo)
"Issues on curvaton scenario with the thermal effect"
[JGRG23(2013)P27]

P28 Hiroshi Suenobu (Nagoya University)
"Monte Carlo simulation of quantum cosmology"
[JGRG23(2013)P28]

P29 Masaaki Takahashi (Aichi University of Education)
"Magnetic Penrose Process in a Black Hole Magnetosphere"
[JGRG23(2013)P29]

P30 Yoshiyuki Morisawa (Osaka University of Economics and Law)
"Irreducible Killing tensor from dimensional reduction"
[*]

P31 Kohji Yajima (Rikkyo University)
"Gravitational waves generated during slow-roll inflation in Lorentz-violating Weyl gravity" [JGRG23(2013)P31]

P32 Hiroshi Kozaki (Ishikawa National College of Technology)
"An exact solution describing a closed membrane without spherical symmetry"
[JGRG23(2013)P32]

P33 Keiju Murata (Keio University)
"On the horizon instability of an extreme Reissner-Nordstrom black hole"
[*]

“Wormhole solutions in higher dimensional space-time

and their linear stability analysis”

by Takashi Torii

[JGRG23(2013)P01]

131105-08 JGRG23

P01

Wormhole solutions in higher dimensional space-time and their linear stability analysis

Takashi TORII (Osaka Institute of Technology)
Hisa-aki Shinkai (Osaka Institute of Technology)

We derive the simplest traversable wormhole solutions in n-dimensional general relativity, assuming static and spherically symmetric spacetime with a ghost scalar field. This is the generalization of the Ellis solution (or the so-called Morris-Thorne's traversable wormhole) into a higher-dimension. We also study their stability using linear perturbation analysis. We obtain the master equation for the perturbed gauge-invariant variable and search their eigenvalues. Our analysis shows that all higher-dimensional wormholes have an unstable mode against the perturbations with which the throat radius is changed. The instability is consistent with the earlier numerical analysis in four-dimensional solution.

1

Wormhole is ...

- Wormhole is ...
  - a region of spacetime containing a "world tube" (the time evolution of a closed surface) that cannot be continuously deformed (shrunk) to a world line.
  - It has a throat which connect two asymptotic regions (which can be identified).
  - Historically, a "tunnel structure" in the Schwarzschild solution was first pointed out by Flamm in 1916, Einstein and Rosen propose a "bridge structure".
  - Morris and Thorne considered human travel through wormholes and concluded that such a wormhole solution is available if we allow "exotic matter".

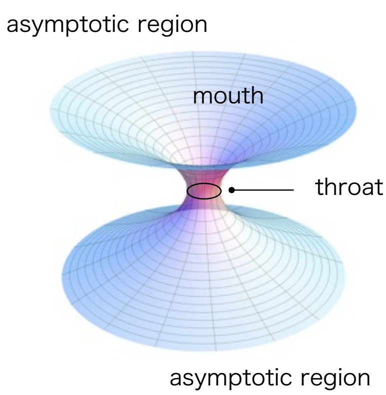

2

Wormhole is …

- Desirable wormhole is …
  - No horizon for travel through
  - Tidal gravitational forces should be small for traveler
  - Traveler should cross it in a finite and reasonably small proper time
  - Must have a physically reasonable stress-energy tensor (but some energy condisions are violated).
  - Should be perturbatively stable
  - Should be possible to assemble

- How to constract a wormhole solution (three classes)
  - wormholes genelated from exotic thin shells.
  - wormholes generated from matching an interior exotic solution to an exterior vacuum, at a junction surface.
  - wormholes generated by continuous funcamental fields with exotic properties.

We focus on this type.

3

in this poster

- We derive the higher-dimensional Ellis wormhole solutions in general relativity with a ghost scalar field.

- We study their stability using linear perturbation analysis and show that all higher-dimensional wormholes have an unstable mode.

4

Ellis wormhole

H. G. Ellis, J. Math. Phys. 14 (1973) 104

- general relativity, 4-dimentional
- massless scalar field (ghost)
- static and spherically symmetric, asymptotically flat
- exact solution
- everywhere regular, no horizon
- stability
  - stable against linear perturbation

    C. Armendariz-Picon, Phys. Rev. 65 (2002) 104010
  - dynamically unstable

    H. Shinkai & S. A. Hayward, Phys. Rev. 66 (2002) 044005

    ➡ re-analyze

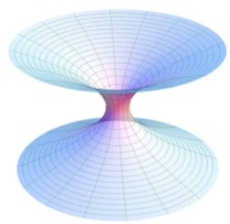

5

higher-dim Ellis wormhole

- general relativity, n-dimentional

massless scalar field (ghost)

$$S=\int d^nx\sqrt{-g}\left[\frac{1}{2\kappa_n^2}R-\frac{1}{2}\epsilon(\partial\phi)^2-\cancel{V(\phi)}\right],\qquad \epsilon=-1$$

- static and spherically symmetric, asymptotically flat

$$ds_n^2=-f(r)dt^2+f(r)^{-1}dr^2+R(r)^2\underbrace{h_{ij}dx^idx^j}_{(k=1)}$$

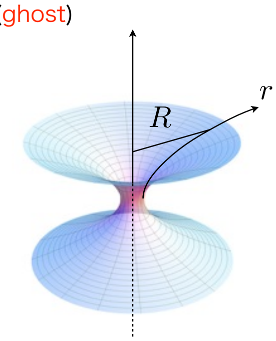

- basic equations

$$(t,t):\quad -\frac{n-2}{2}f^2\left[\frac{2R''}{R}+\frac{f'R'}{fR}+\frac{(n-3)R'^2}{R^2}\right]+\frac{(n-2)(n-3)kf}{2R^2}=\kappa_n^2f\left[\frac{1}{2}\epsilon f\phi'^2+\cancel{V(\phi)}\right],$$

$$(r,r):\quad \frac{n-2}{2}\frac{R'}{R}\left[\frac{f'}{f}+\frac{(n-3)R'}{R}\right]-\frac{(n-2)(n-3)k}{2fR^2}=\frac{\kappa_n^2}{f}\left[\frac{1}{2}\epsilon f\phi'^2-\cancel{V(\phi)}\right],$$

$$(i,j):\quad \frac{f''}{2}+(n-3)f\left(\frac{R''}{R}+\frac{f'R'}{fR}+\frac{n-4}{2}\frac{R'^2}{R^2}\right)-\frac{(n-3)(n-4)k}{2R^2}=\kappa_n^2\left[\frac{1}{2}\epsilon f\phi'^2+\cancel{V(\phi)}\right],$$

$$(KG):\quad \frac{1}{R^{n-2}}\left(R^{n-2}f\phi'\right)'=-\epsilon\cancel{\frac{dV}{d\phi}}.\qquad \Rightarrow\qquad \phi'=\frac{C}{fR^{n-2}}$$

constant

6

higher-dim Ellis wormhole

- regularity condition (+ symmetry) at the throat $r=0$

$R = a$ ←— throat radius

$R' = 0, \quad f = f_0, \quad f' = 0, \quad \phi = 0$

★ By scaling symmetry we can generically assume

$a = 1 \qquad f_0 = 1$

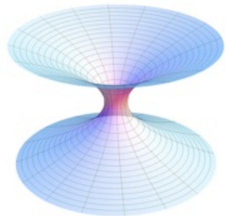

basic equation ➡ $\kappa_n^2 C^2 = (n-2)(n-3)a^{2(n-3)}$

- exact solution

$$f \equiv 1$$

$$r(R) = -mB_z\left[-m, \frac{1}{2}\right] - \frac{\sqrt{\pi}\Gamma[1-m]}{\Gamma[m(n-4)]}$$

(higher-dim Ellis解)

$$\phi = \frac{\sqrt{(n-2)(n-3)}}{\kappa_n} a^{n-3} \int \frac{1}{R(r)^{n-2}} dr$$

$$m = \frac{1}{2(n-3)}, \quad z = R^m \qquad B_z(p,q) := \int_0^z t^{p-1}(1-t)^{q-1}dt$$ 不完全ベータ関数

★ In the another metric ansatz : V. Dzhunushaliev, arXiv:1309.2448

7

higher-dim Ellis wormhole

- exact solution

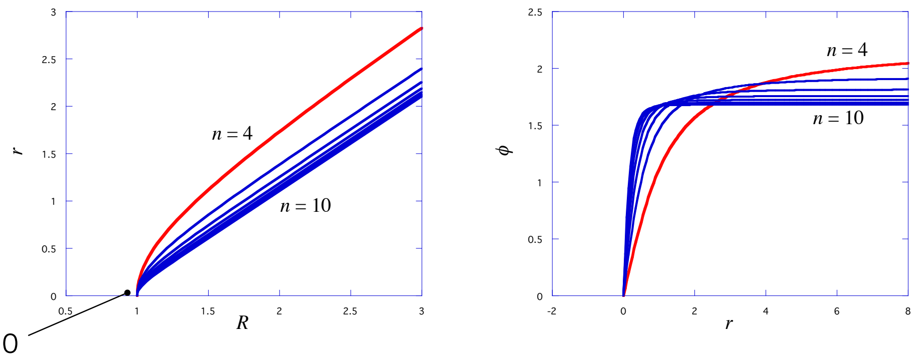

expansion is 0

trapping horizon

★ the throat of the wormhole has larger curvature and the scalar field becomes steeper as the dimension goes higher.

★ In the $n \to \infty$ limit

$$R = r + 1 \qquad \phi = 0 \ \ (r = 0) \quad \frac{\pi}{2} \ \ (r > 0)$$

8

linear perturbations

★ For the non-linear analysis, see P09 (Shinkai & Torii).

- metric ansatz

$$ds_n^2 = -f(t,r)e^{-2\delta(t,r)}dt^2 + f(t,r)^{-1}dr^2 + R(t,r)^2 h_{ij}dx^i dx^j$$

- linear perturbations

static solution

$$f = f_0(r) + f_1(r)e^{i\omega t}, \quad R = R_0(r) + R_1(r)e^{i\omega t},$$
$$\delta = \delta_0(r) + \delta_1(r)e^{i\omega t}, \quad \phi = \phi_0(r) + \phi_1(r)e^{i\omega t}.$$

- master equation

$$\boxed{\begin{aligned} &-\Psi_1'' + W(r)\Psi_1 = \omega^2\Psi_1, \\ &W(r) = -\frac{1}{4R_0^2}\left[\frac{3(n-2)^2}{R_0^{2(n-3)}} - (n-4)(n-6)\right]. \end{aligned}}$$

$$\Psi_1 = \mathcal{D}_+\psi_1 \quad \mathcal{D}_+ = \frac{d}{dr} - \frac{\bar{\psi}_1'}{\bar{\psi}_1} \quad \psi_1 = R_0^{\frac{n-2}{2}}\left(\phi_1 - \frac{\phi_0'}{R_0'}R_1\right),$$

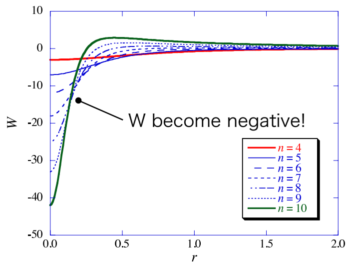

★ potential function W

★ Ψ_1 is gauge invariant under the spherically symmetric ansatz.

9

linear perturbations

- negative mode

n	ω^2
4	-1.39705243371511
5	-2.98495893027790
6	-4.68662054299460
7	-6.46258414126318
8	-8.28975936306259
9	-10.1535530451867
10	-12.0442650147438
11	-13.9552091676647
20	-31.5751101285105
50	-91.3457759137153
100	-191.283017729717

eigen-values of netive mode

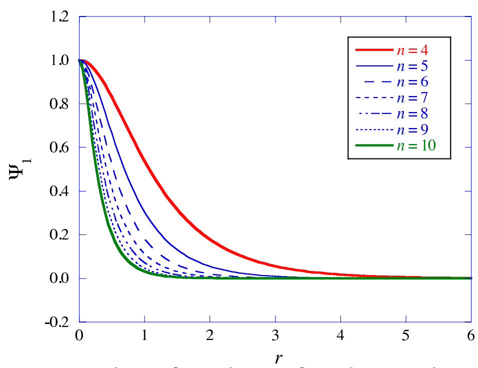

eigen-functions of netive mode

★ There is one negative mode for each dimension.

➡ The higher-dim. Ellis's wormhome is unstable.

★ We find large negative eigen-vallus for higher n, which indicates the time-scale of instability becomes shorter.

“Gauged Q-balls”

by Takashi Tamaki

[JGRG23(2013)P02]

Gauged Q-balls

Takashi Tamaki (Nihon university)
tamaki@ge.ce.nihon-u.ac.jp

collaboration: Nobuyuki Sakai (Yamaguchi university)
nsakai@yamaguchi-u.ac.jp

I. Introduction

Ordinary Q-balls
(many investigations since 1985)

Gauged Q-balls
only a few investigations

The reason:
Gauge field *kills* Q-balls !!

II. Basic eqs.

$$\mathcal{S} = \int d^4x \left[\frac{1}{4}F_{\mu\nu}F^{\mu\nu} - \frac{1}{2}\eta^{\mu\nu}D_\mu\phi_a D_\nu\phi_a - V(\phi)\right]$$

Assumptions: $\boldsymbol{\phi} = \phi(r)(\cos\omega t, \sin\omega t)$

only static electric field $A_0 = A_0(r)$

$$\frac{d^2\phi}{dr^2} + \frac{2}{r}\frac{d\phi}{dr} + \Omega^2\phi = \frac{dV}{d\phi}$$

$$\frac{d^2\Omega}{dr^2} + \frac{2}{r}\frac{d\Omega}{dr} = \Omega(q\phi)^2 \qquad \Omega := \omega + qA_0$$

Ordinary Q-balls (q=0)

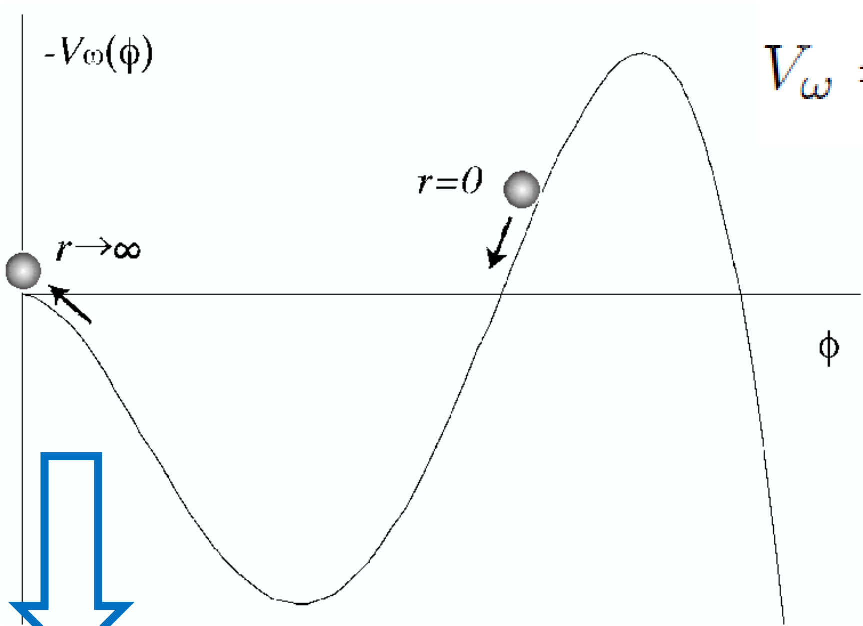

$$V_\omega = V - \frac{1}{2}\omega^2\phi^2$$

$\omega^2 < \frac{d^2V}{d\phi^2}(0)$ ⇨ with gauge field ?

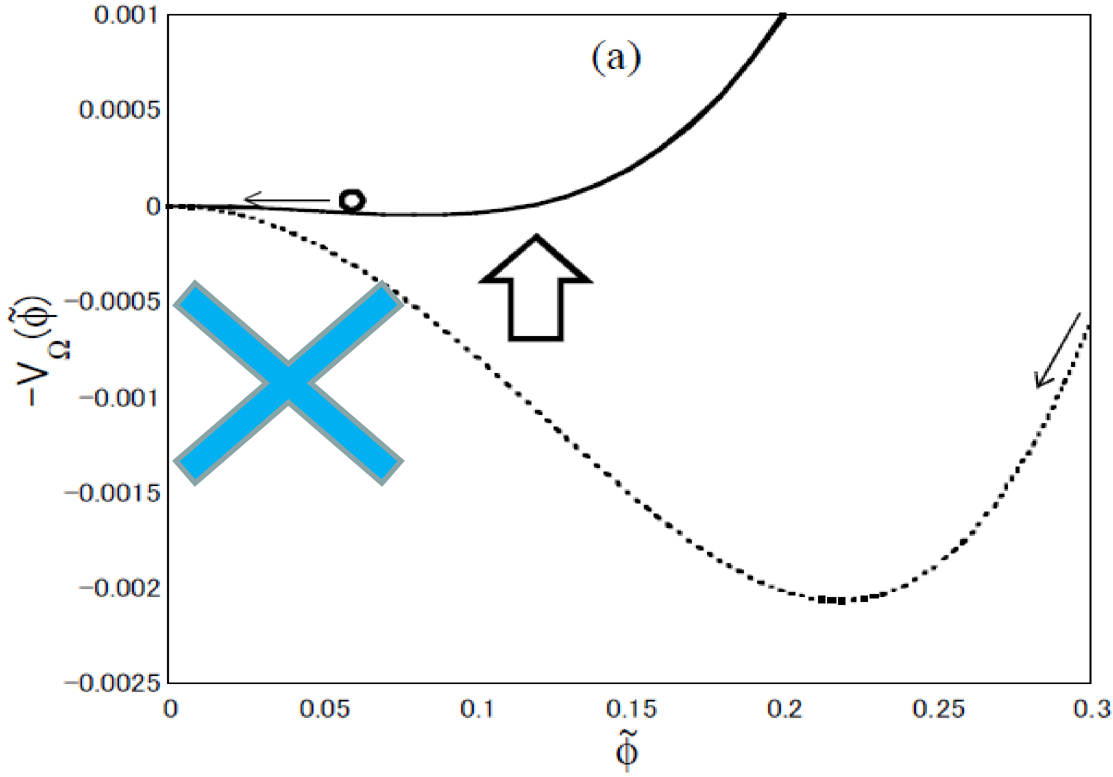

$$V_4(\phi) := \frac{m^2}{2}\phi^2 - \lambda\phi^4 + \frac{\phi^6}{M^2} \quad \text{with} \quad m^2,\ \lambda,\ M^2 > 0,$$

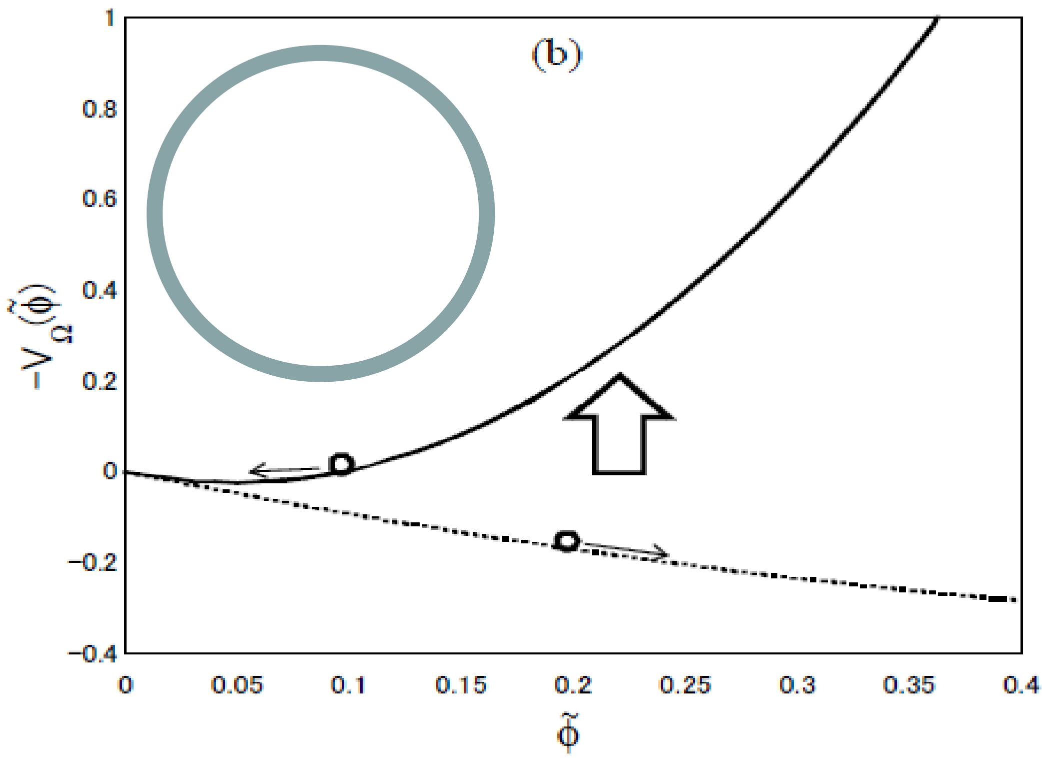

$$V_{\text{grav.}}(\phi) := \frac{m_{\text{grav.}}^2}{2}\phi^2\left[1 + K\ln\left(\frac{\phi}{M}\right)^2\right] \qquad K<0$$

III. Results

K=-0.1

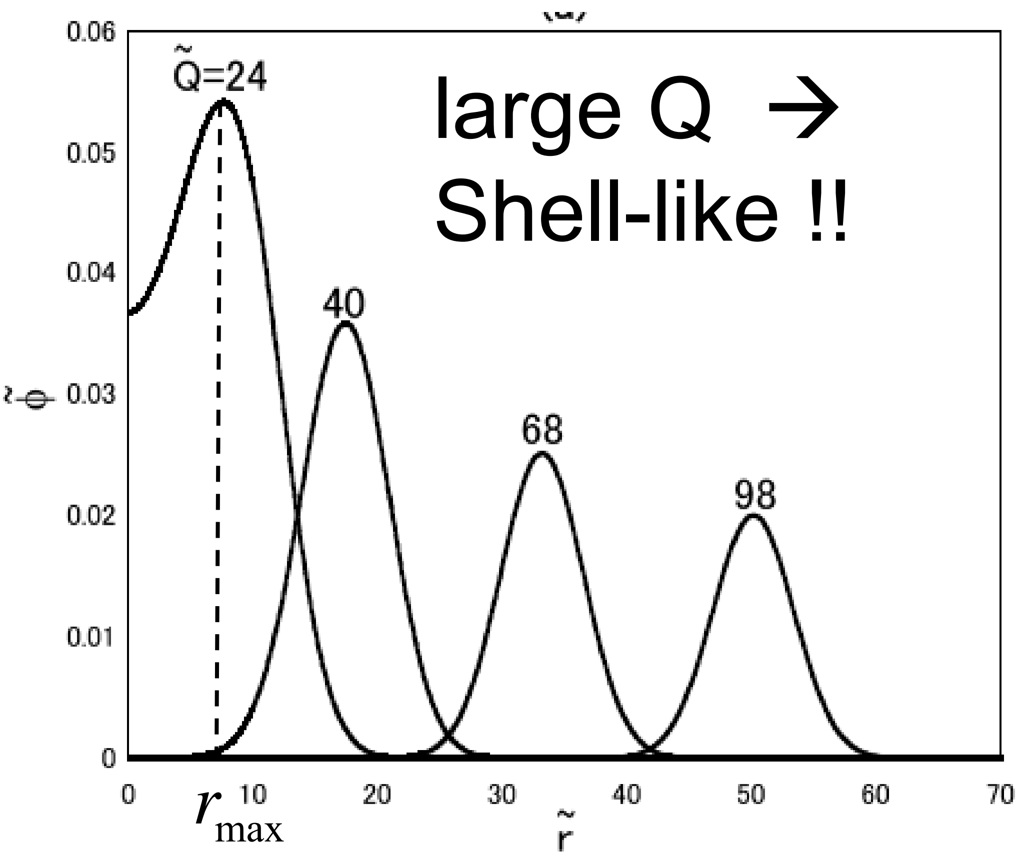

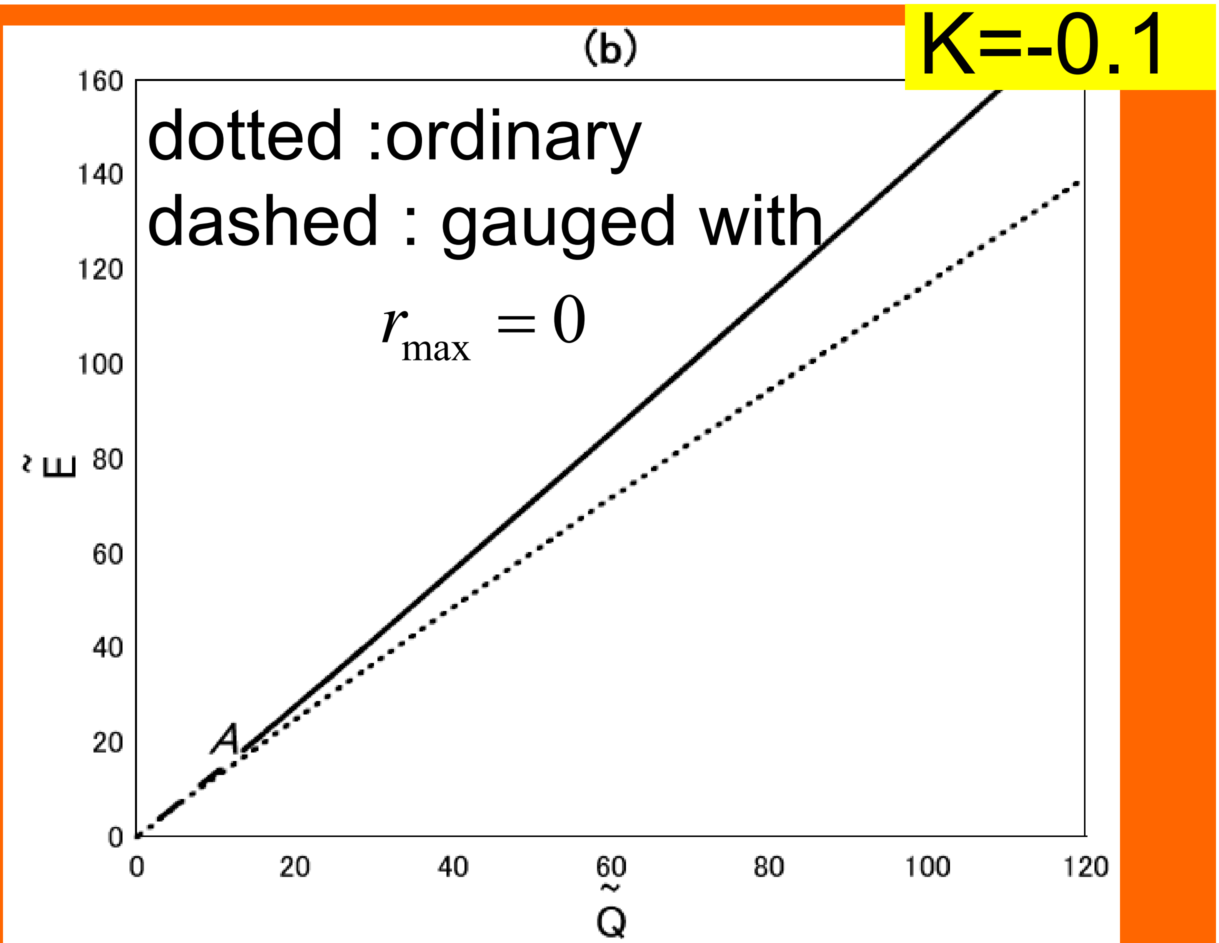

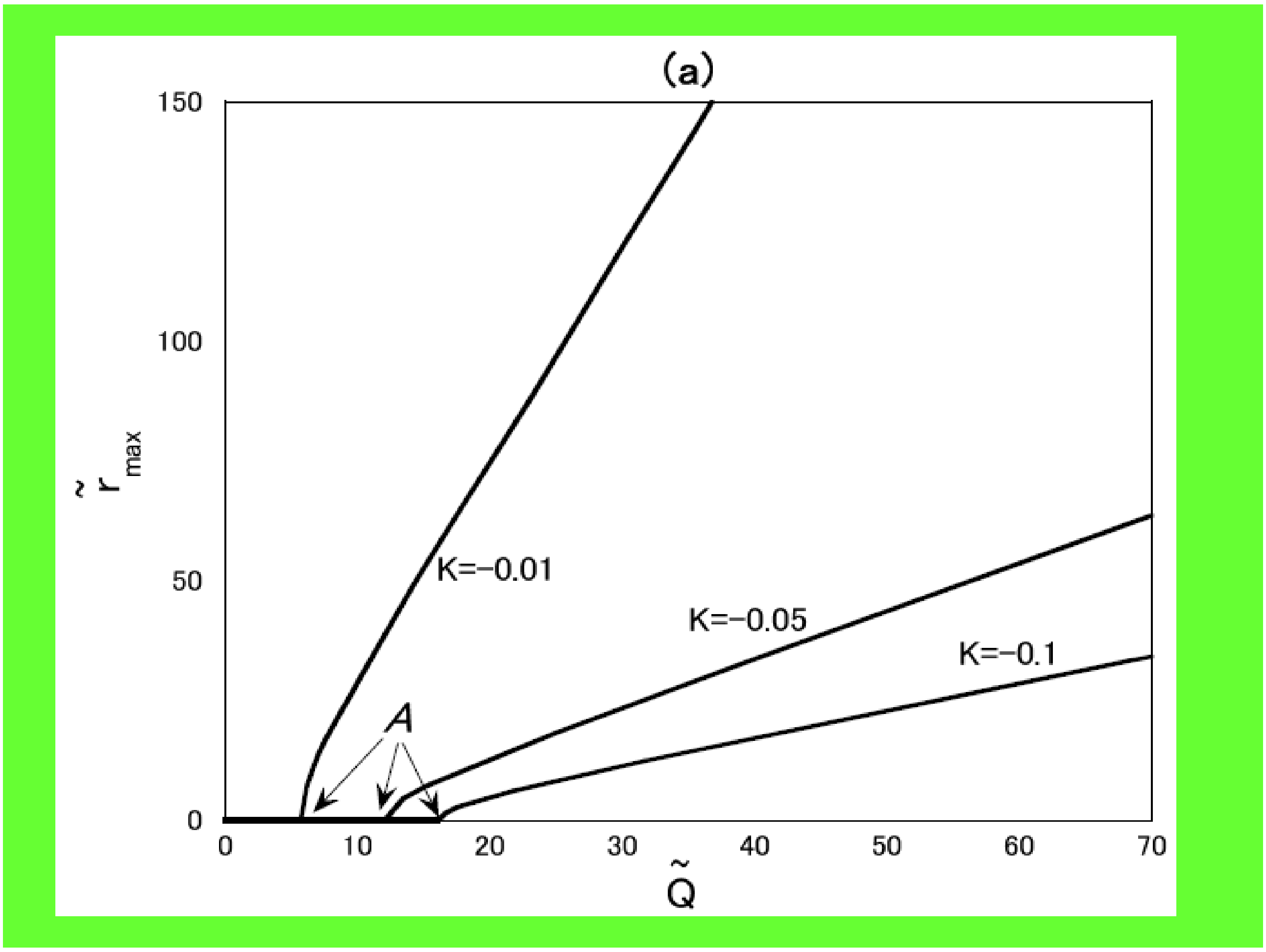
(a)
150
100
50
0
$\tilde{r}_{max}$
K=−0.01
K=−0.05
K=−0.1
A
0
10
20
30
40
50
60
70
$\tilde{Q}$

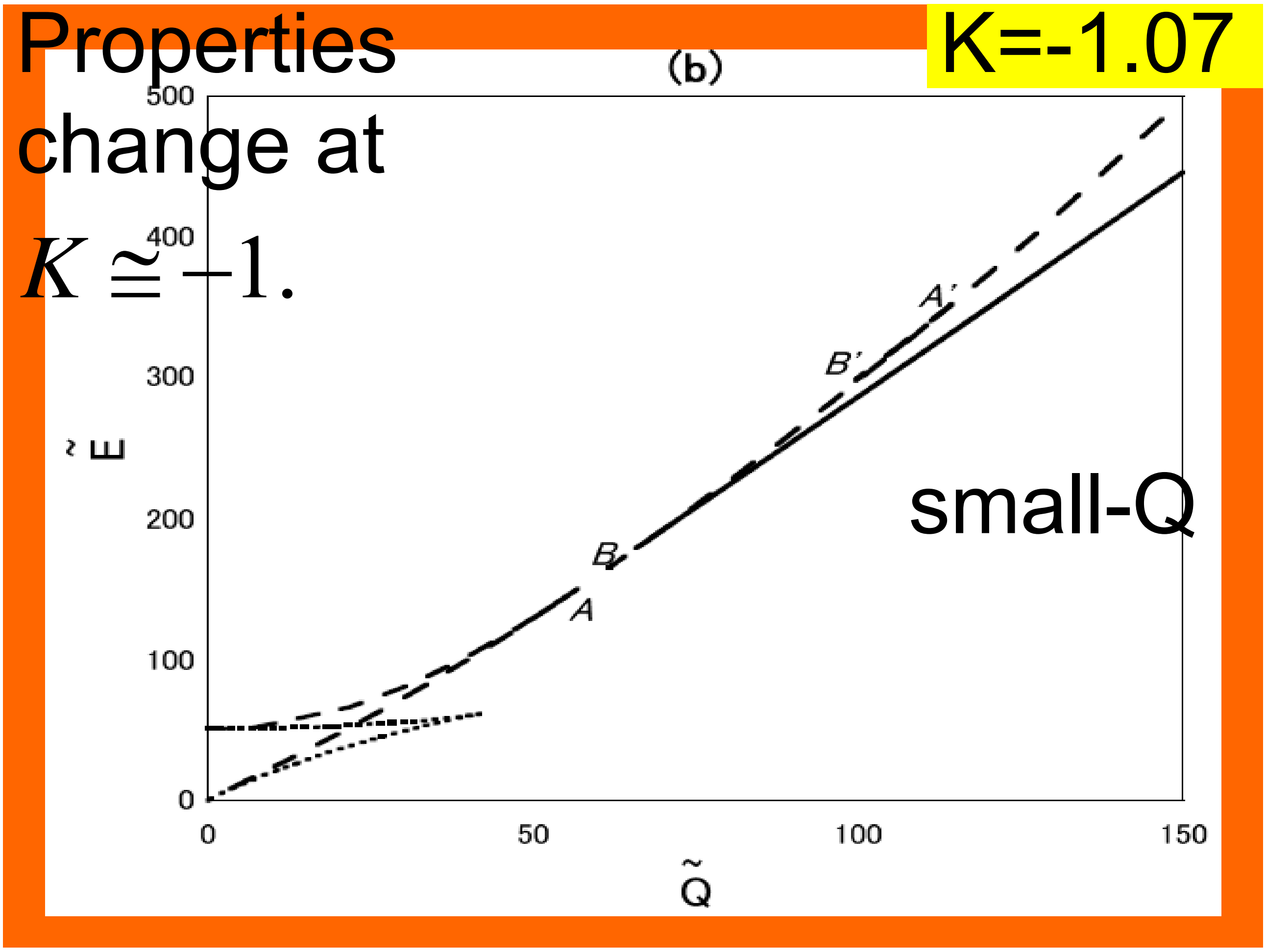
Properties change at $K \cong -1.$
K=-1.07
(b)
500
400
300
200
100
0
$\tilde{E}$
A'
B'
B
A
small-Q
0
50
100
150
$\tilde{Q}$

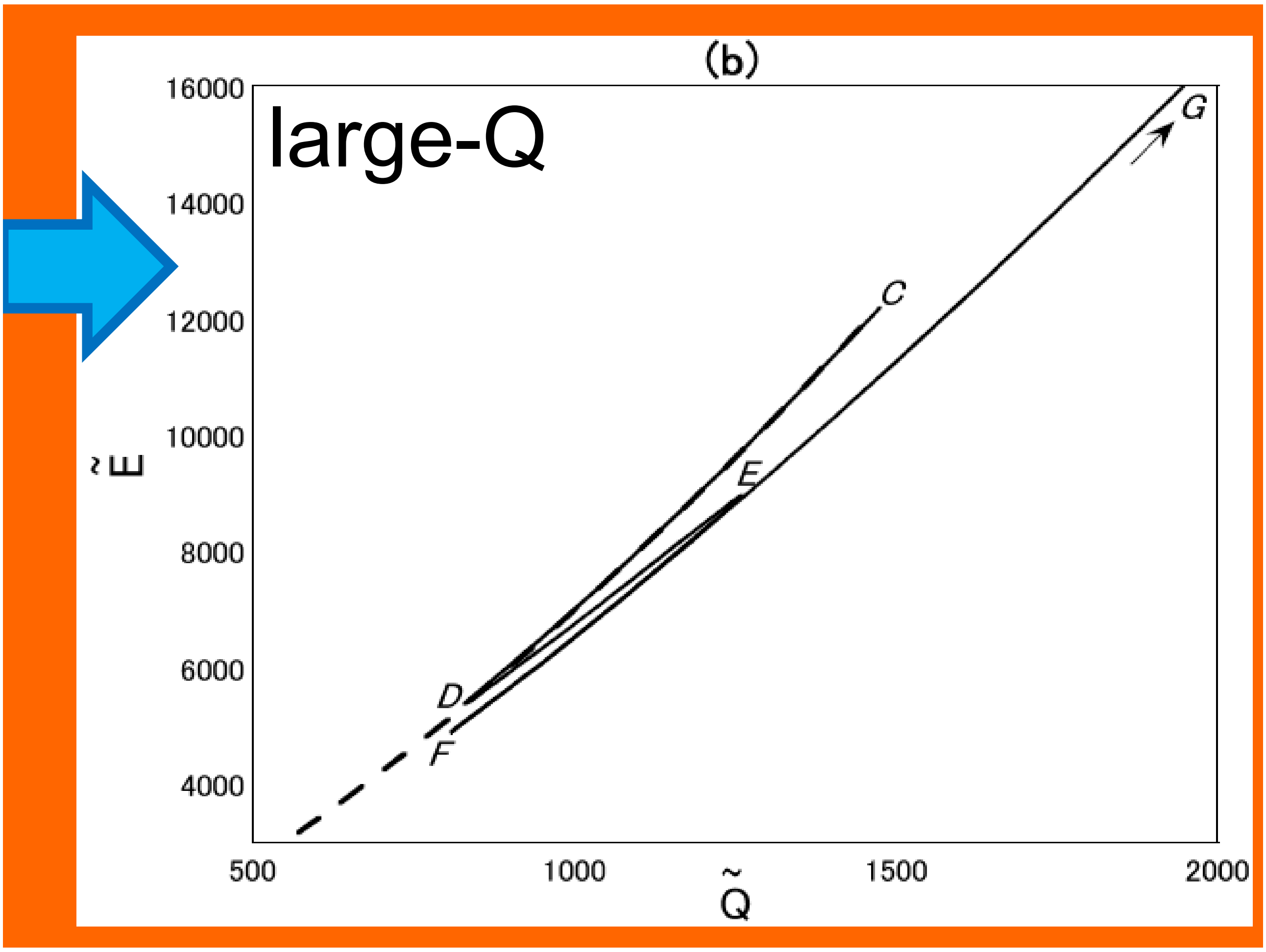

(b)
large-Q
16000
14000
12000
10000
8000
6000
4000
$\tilde{E}$
500
1000
1500
2000
$\tilde{Q}$
C
D
E
F
G

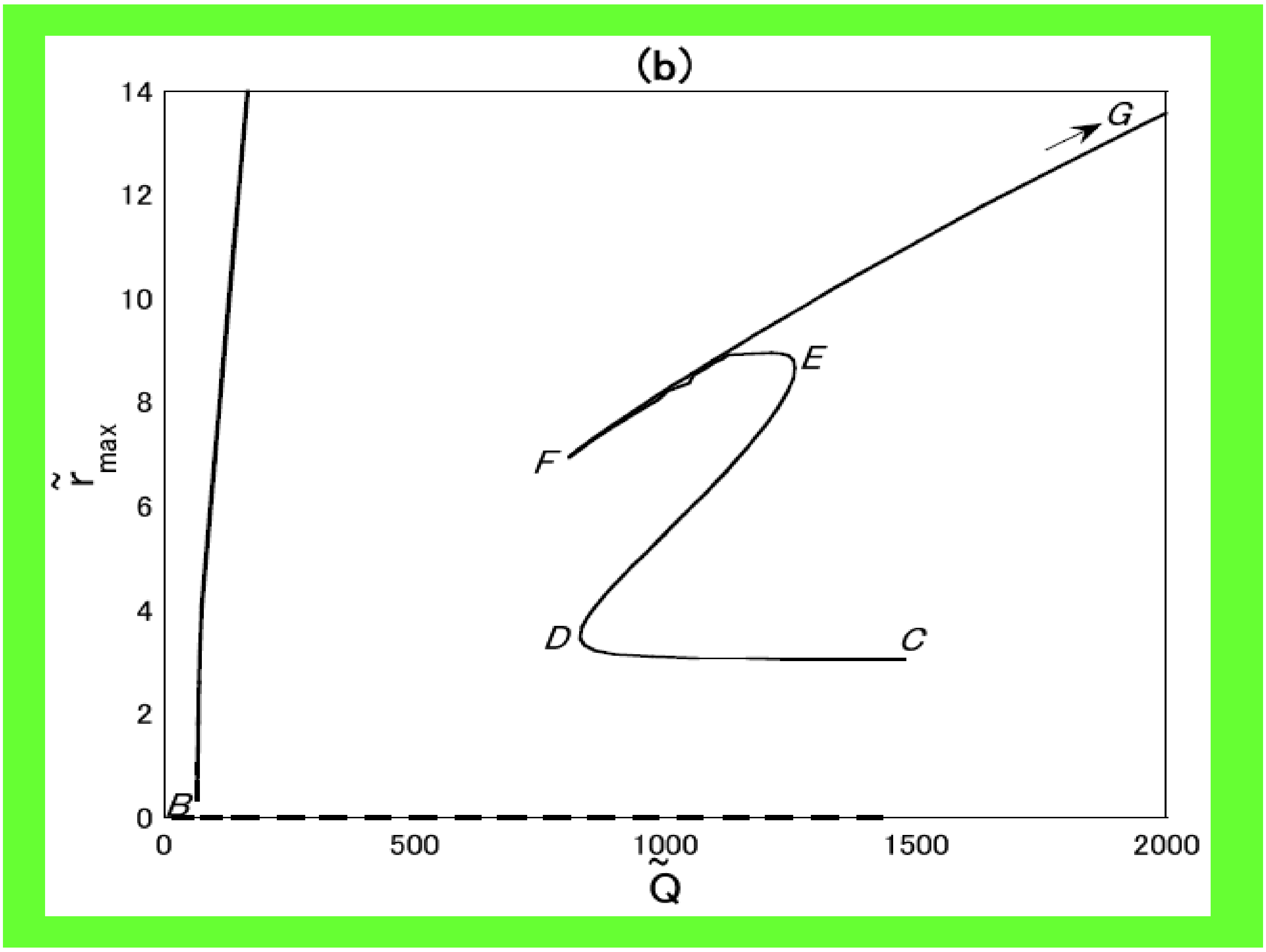

(b)
14
12
10
8
6
4
2
0
$\tilde{r}_{max}$
0
500
1000
1500
2000
$\tilde{Q}$
B
C
D
E
F
G

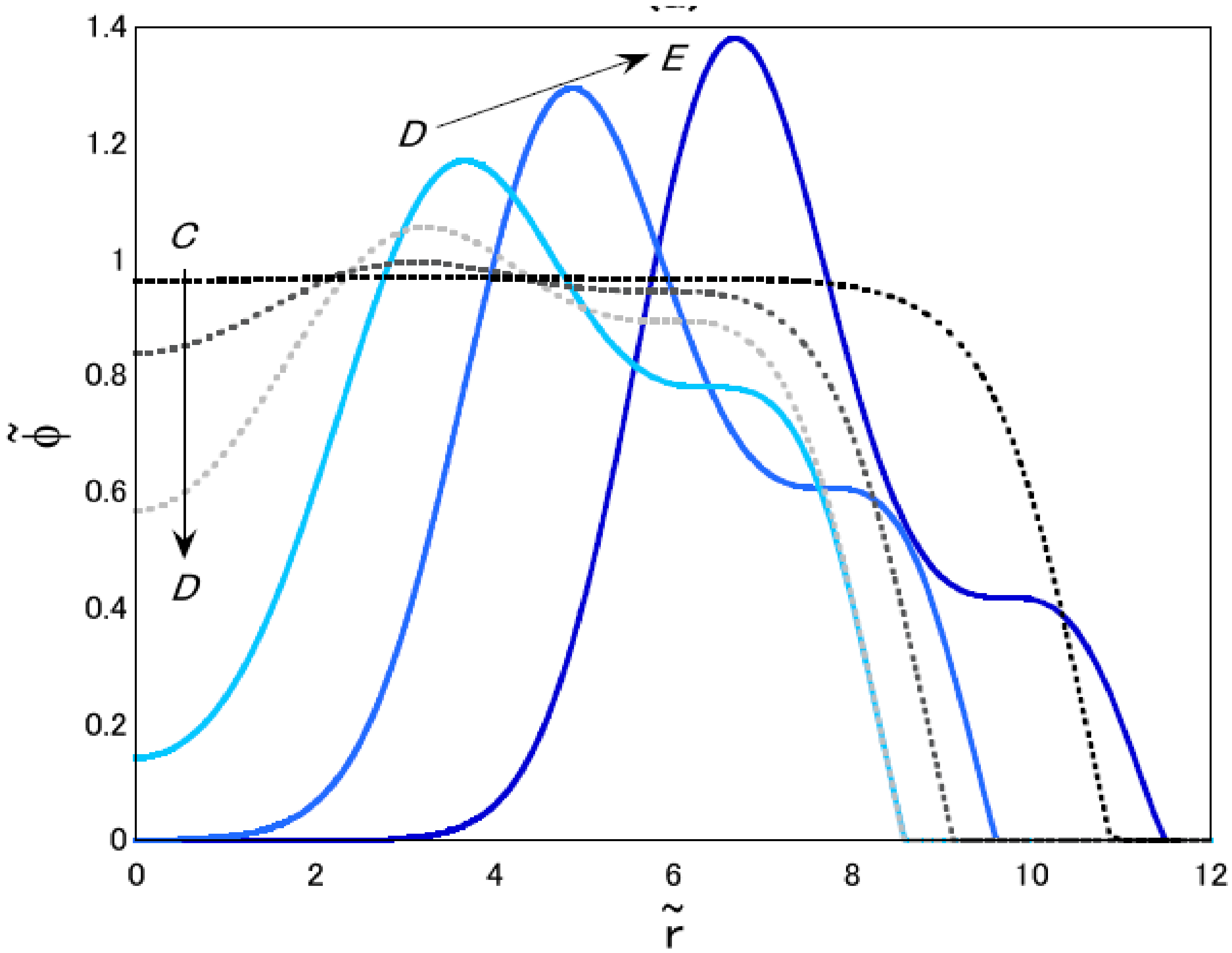

1.4
1.2
1
0.8
0.6
0.4
0.2
0
0
2
4
6
8
10
12
$\tilde{\phi}$
$\tilde{r}$
C
D
D
E

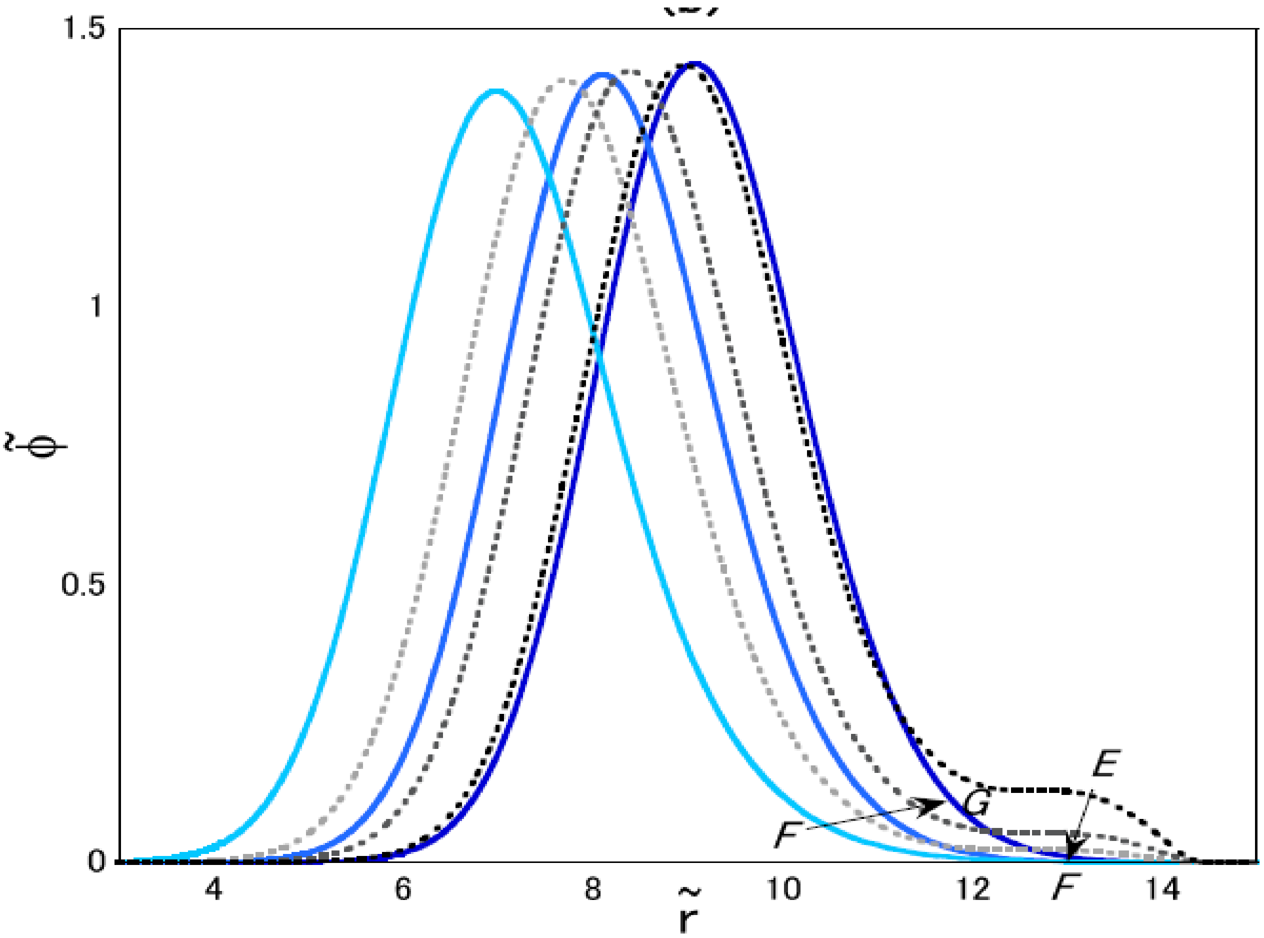

1.5
1
0.5
0
4
6
8
10
12
14
$\tilde{\phi}$
$\tilde{r}$
E
F
F
G

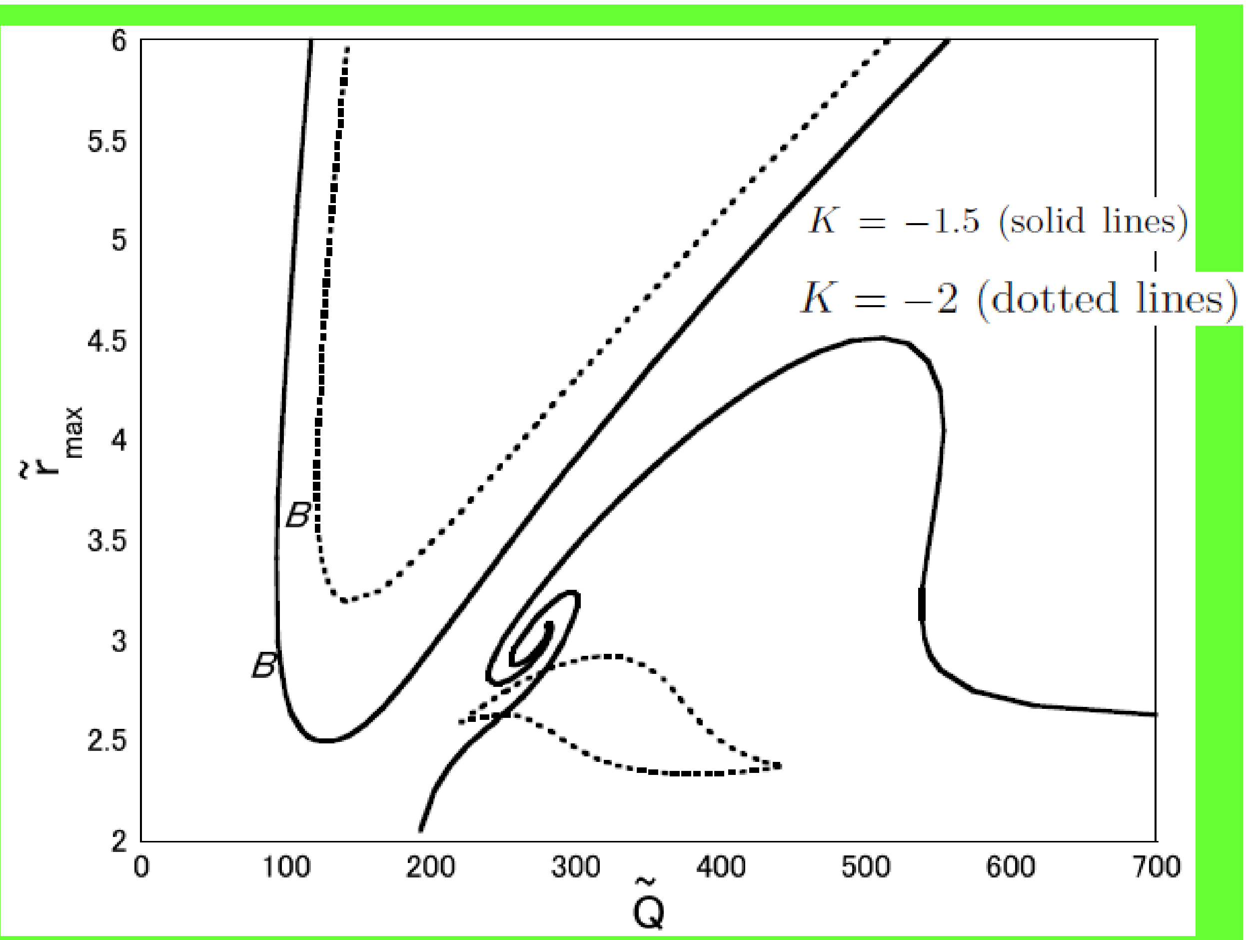

IV. Summary

Complicated structures
→exquisite balance between gauge and scalar fields!!

The branch having linear relation in Q-E would be stable.

Other branches unstable(?)

⇨ We will confirm them !!

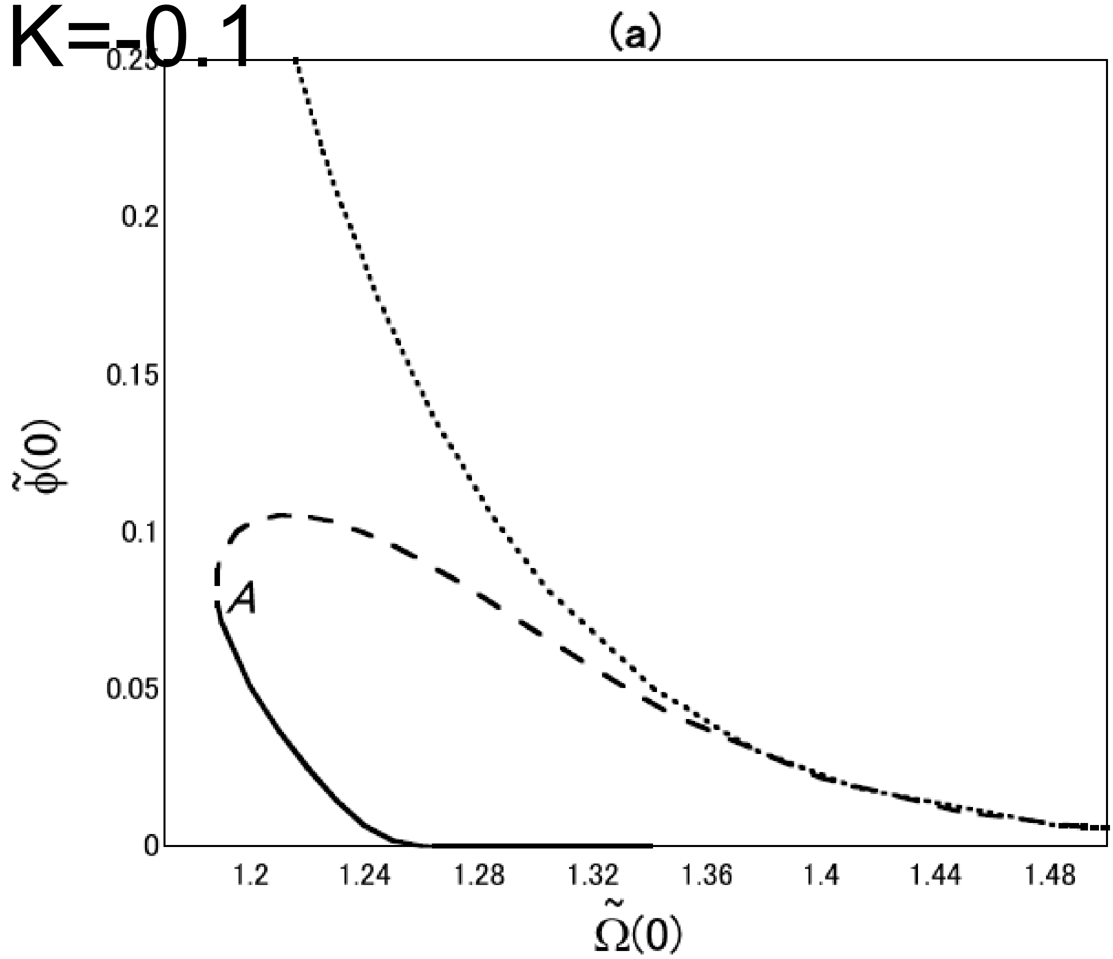
K=-0.1
(a)
0.25
0.2
0.15
0.1
0.05
0
1.2
1.24
1.28
1.32
1.36
1.4
1.44
1.48
A
$\tilde{\phi}(0)$
$\tilde{\Omega}(0)$

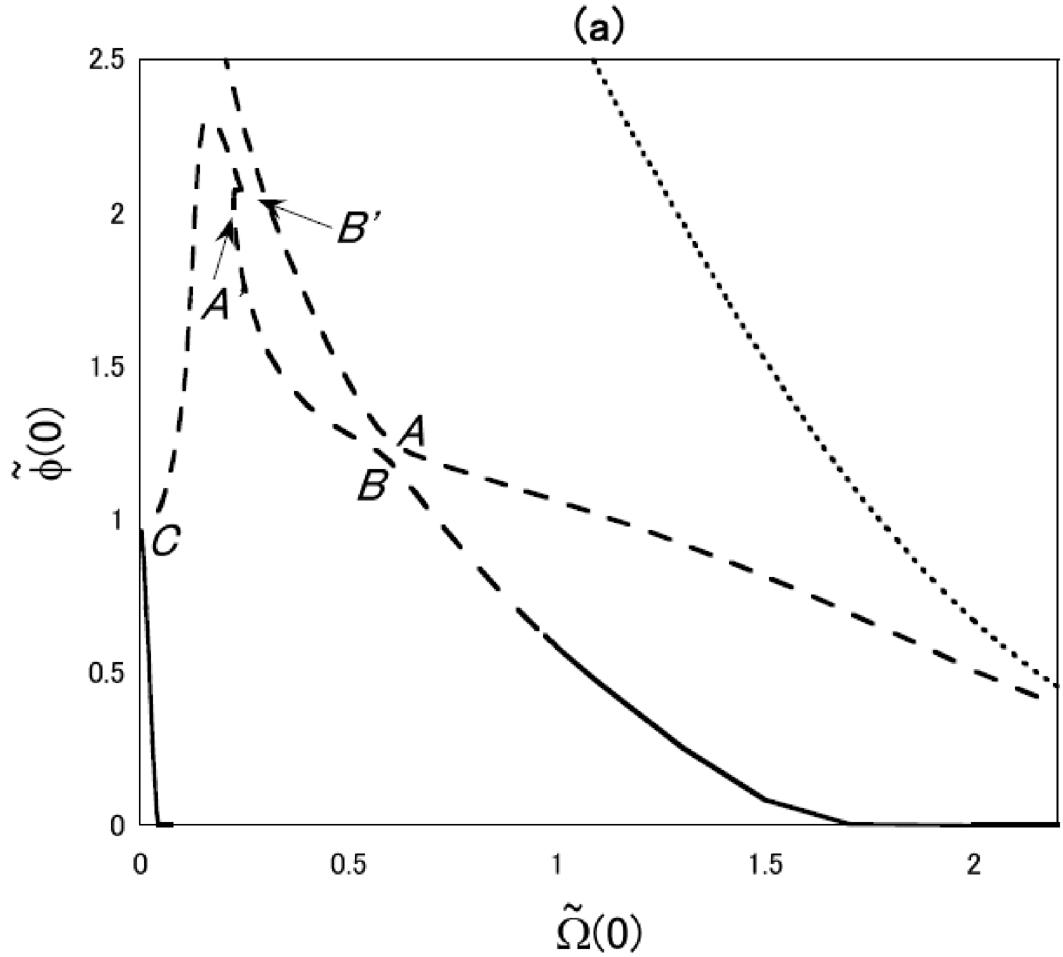
(a)
2.5
2
1.5
1
0.5
0
0.5
1
1.5
2
B'
A'
A
B
C
$\tilde{\phi}(0)$
$\tilde{\Omega}(0)$

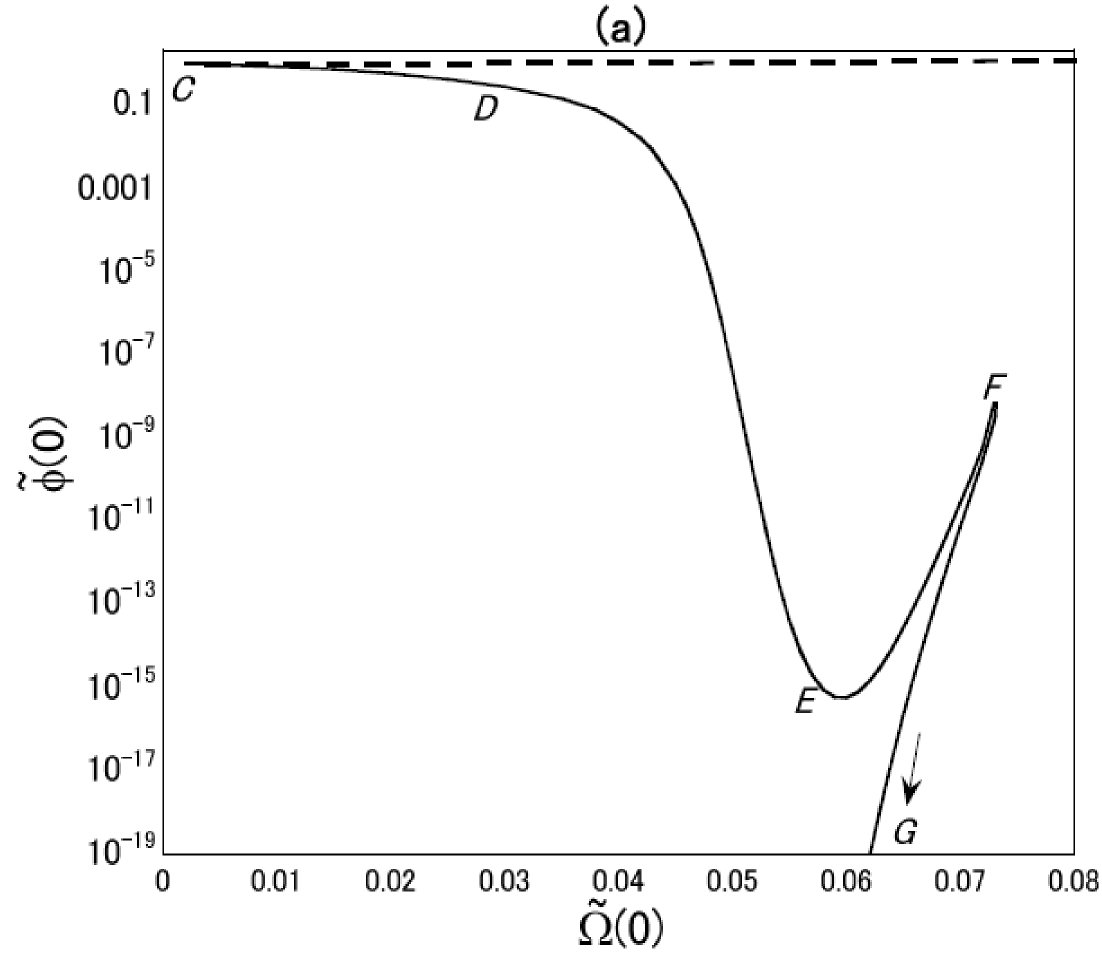

(a)
0.1
0.001
10^-5
10^-7
10^-9
10^-11
10^-13
10^-15
10^-17
10^-19
φ̃(0)
0
0.01
0.02
0.03
0.04
0.05
0.06
0.07
0.08
Ω̃(0)
C
D
E
F
G

“Bound states of extreme Type-I cosmic strings

in two-dimensional space”

by Takashi Hiramatsu

[JGRG23(2013)P03]

JGRG23, 5-8 Nov 2013 @ Hirosaki Univ.

Bound states of extreme Type-I cosmic strings in two-dimensional space

Takashi Hiramatsu

Yukawa Institute for Theoretical Physics (YITP)
Kyoto University

Collaboration with Daisuke Yamauchi (RESCEU)

Cosmic strings

Takashi Hiramatsu

- 1D (linear) topological defect associated with spontaneous symmetry breaking in high energies **Kibble, J.Phys.A9 (1976) 1387**
- Old days : ~~seeds of large scale structure~~ → Inflation
- Recent attention
  - Possibility of direct observation of superstrings
  - As a probe for high energy phenomena involving phase transition
  - As a source of gravitational waves
- Scaling property
  - Naively thinking, the string energy evolves as $\rho_{\rm str} \propto a^{-2}$.
  - Loops created through the reconnection of strings carry off the energy from long strings, which maintain the string energy as $\rho_{\rm str} \propto a^{-4}$, avoiding to overclose the Universe.

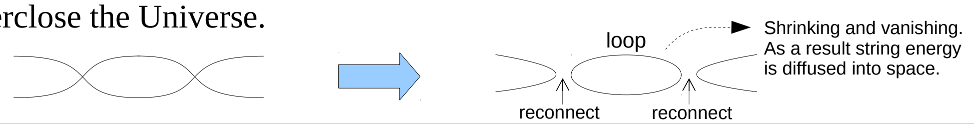

Field theoretic model

Takashi Hiramatsu

Abelian Higgs model : complex scalar + local U(1) gauge

U(1) gauge field   complex scalar field

$$S = -\int dx^4 \sqrt{-g}\left(\frac{1}{4}F_{\mu\nu}F^{\mu\nu} + (D_\mu\phi)^*(D^\mu\phi) + V(\phi;T)\right)$$

$$V(\phi;T) = \frac{\lambda}{4}(|\phi|^2 - \eta^2) + \frac{\lambda}{6}T^2|\phi|^2$$

$$D_\mu \equiv \partial_\mu - ieA_\mu$$

$$F_{\mu\nu} \equiv \partial_\mu A_\nu - \partial_\nu A_\mu$$

T : environmental temperature supported by radiation. The temperature-dependent term becomes important in the high-energy regime. When the temperature becomes Lower than the critical temperature, the U(1) symmetry breaks spontaneously.

$T \ll T_c$ $T \gg T_c$

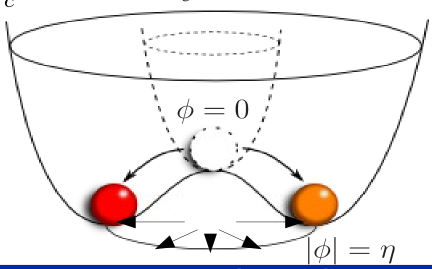

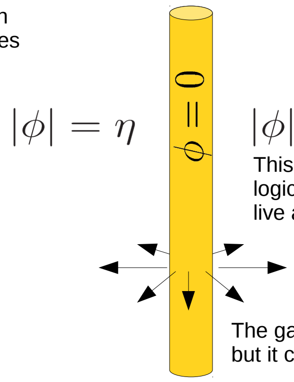

This linear shape is topo-logically stable. So strings live a long time.

The gauge field is not shown, but it clings around the string

Type-I strings

Takashi Hiramatsu

After the spontaneously breaking of U(1) symmetry, the scalar field possess its vacuum expectation value, $|\phi_{\mathrm{vac}}| = \eta$, and thus the scalar and gauge fields acquire their masses (neglecting the temperature dependence)

Scalar mass : $m_\phi = \sqrt{\lambda}\eta$

Gauge mass : $m_A = \sqrt{2}e\eta$

The physical property of a static streight string in the Minkowski background is determined by the unique parameter

$$\beta \equiv \frac{\lambda}{2e^2} = \frac{m_\phi^2}{m_A^2}$$

We focus on the case with $\beta < 1$, so-called Type-I strings. Type-I strings have not so well studied, and it has been reported that this kind of strings is associated with SSB of flat direction in MSSM. **Cui, Martin, Morrissey, Wells, PRD 77 (2008) 043528**

As a first step, we performed simulations of Type-I string network.

TH, Sendouda, Takahashi, Yamauchi, Yoo, PRD 88 (2013) 085021

Interaction of two parallel strings

Takashi Hiramatsu

Bettencourt et al., PRL 78 (1997) 2066

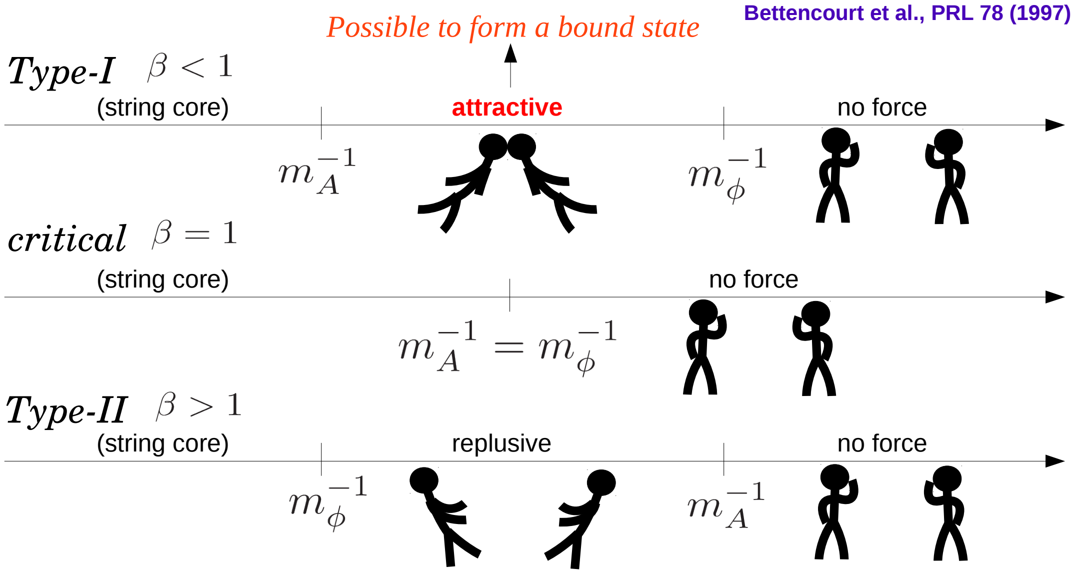

The attractive force between strings promotes to form a bound state. If the bound states are efficiently formed in the network, the late-time evolution of string networks would be changed. Besides, the networks perhaps lose the scaling property.

3D simulation for Type-I string network

Takashi Hiramatsu

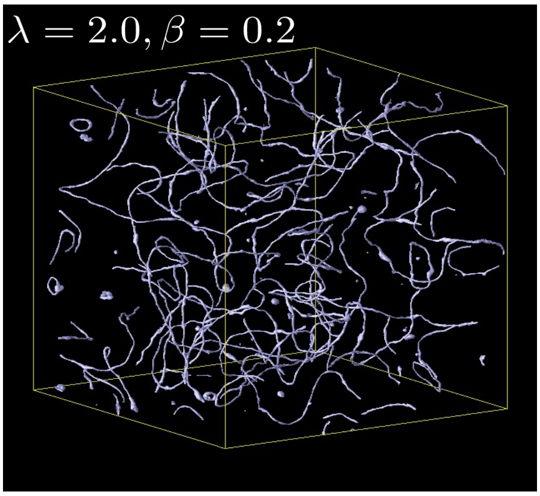

Mean number of strings in a horizon-sized box

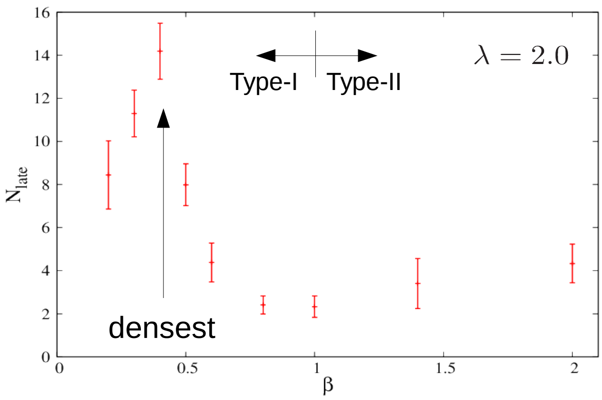

TH, Sendouda, Takahashi, Yamauchi, Yoo, PRD 88 (2013) 085021

According to our 3D simulations in recent paper, we confirmed that the networks have the scaling property even in the extreme cases, $\beta = 0.2$. Moreover, we found a peculier property that the number of strings depend on β and can be largest with a specific value of β depending on the energy scale of the phase transition ($\beta \approx 0.4$ in the above case.)

Have the bound states been formed in these simulations ... ?

404 Not found...

No bound states

at least in all our realisations whose effective volume is $(38.8H_{\mathrm{in}}^{-1})^3$

According to numerical experiments about the collision of two straight strings with low-angle (nearly parallel) and low-velocity, it has been reported that they form a bound state for $\beta = 0.36,\ 0.125$. Salmi et al., PRD 77 (2008) 041701R

Bound states are quite rare even in $\beta = 0.2$?

In more extreme cases, the bound states may be formed more.
Go further with smaller β !

2 dimensional toy model

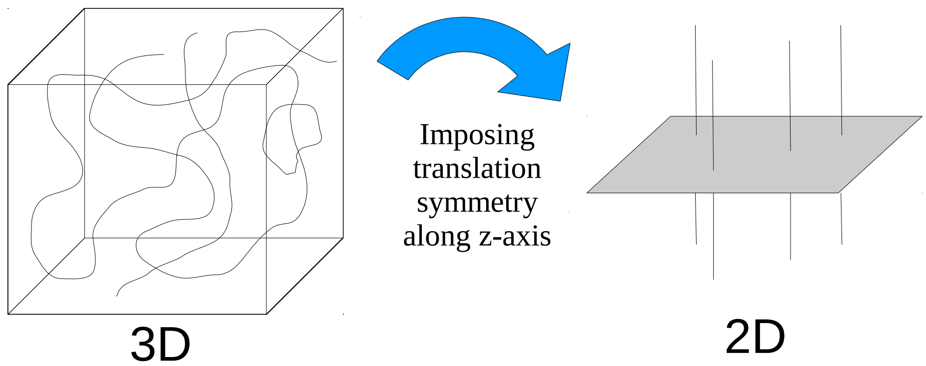

2D space strongly restricts the dynamics of strings after their formation

➡ the collision rate is expected to be larger than 3D

➡ It is expected to give an upper limit of the fraction of bound states for realistic 3D box simulations

And, of course, 2D simulations ...

- save the computational resources.
- allow a larger dynamical range and surveys in large parameter space.

Our goal / Warning !

Takashi Hiramatsu

To obtain number fraction of dynamically formed bound states in Abelian-Higgs model.

But,...

2D is not the real world.

The energy release mechanism in 3D to support the scaling property is loop production. But, there are no loops in 2D space.

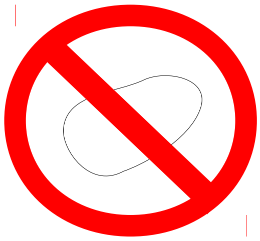

The only mechanism is pair annihilation.

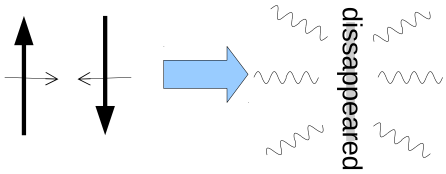

dissipates into kinetic energy in bulk

Network properties involving its long lifetime would be different from those in 3D. (cf. time evolution of correlation length.) So, taking care of the above peculiar property, we have to extract the physically meaningful results being independent to the dimension.

Simulation setup

Takashi Hiramatsu

- Computational domain
  - comoving box
  - periodic boundaries
  - radiation dominant
  - not considering gravitational backreaction

Temperature : $2T_c \to \frac{2}{9}T_c$

Box size/horizon scale : $\frac{L}{\mathcal{H}^{-1}} = 18 \to 2$

Grid : $2048^2 \sim 8192^2$

- Equations

gauge condition $A_0 = 0$

constraint $\partial_i A_i' = 2ea^2\ \mathrm{Im}(\phi^*\phi')\quad (i = x, y)$

EOM
$$\begin{cases} A_i'' - \partial_j F_{ji} = 2e\ \mathrm{Im}(\phi^*\partial_i\phi) - 2e^2 A_i|\phi|^2 \\ \phi'' + 2\mathcal{H}\phi' - \dfrac{a''}{a}\phi - D_iD_i\phi + a^2\dfrac{dV}{d\phi^*} = 0 \end{cases}$$

derivative w.r.t conformal time

$= 0$ in radiation-dominant universe

Initial conditions

Takashi Hiramatsu

The values of the complex scalar field on the grid are given as Gaussian random numbers with the power spectrum for the thermal fluctuations,

$$\langle T|\phi(\mathbf{x},\tau_{\rm in})\phi^*(\mathbf{y},\tau_{\rm in})|T\rangle = \int \frac{d^3\mathbf{k}}{(2\pi)^3\omega_k}\frac{e^{i\mathbf{k}\cdot(\mathbf{x}-\mathbf{y})}}{e^{\omega_k/T}-1}$$

$$(\omega_k = \sqrt{\mathbf{k}^2+m^2})$$

The phases, $\mathrm{Arg}\ \phi(\mathbf{x},\tau_{\rm in})$, are given as homogeneous random numbers between $0 \sim 2\pi$.

How about A_i ? Dufaux, Figueroa, Garcia-Bellido, PRD82 (2010) 083518

$A'_i(\mathbf{x},\tau_{\rm in}) \longrightarrow$ given by solving constraint equation using FFT

$$\partial_i A'_i = 2ea^2\ \mathrm{Im}(\phi^*\phi')$$

$A_i(\mathbf{x},\tau_{\rm in}) \longrightarrow$ No way to give it... So usually set

$$A_i = 0$$

(Strictly speaking, the gauge field in the thermal bath should be determined on the basis of the finite-temperature field theory. But the concrete calculation would be difficult for Type-I strings where the gauge coupling is strong.)

Snapshots of field configuration

Takashi Hiramatsu

After the phase transition, the scalar field starts to condense in the true vacuum which has a non-vanishing expectation value (blue region) , and the false vacuum, which has been left topologically, form strings (red region).

Some strings meet together and make a bound state with oscillating around each other like a binary/triple star.

$\lambda = 2.0$

$\beta = 0.1$

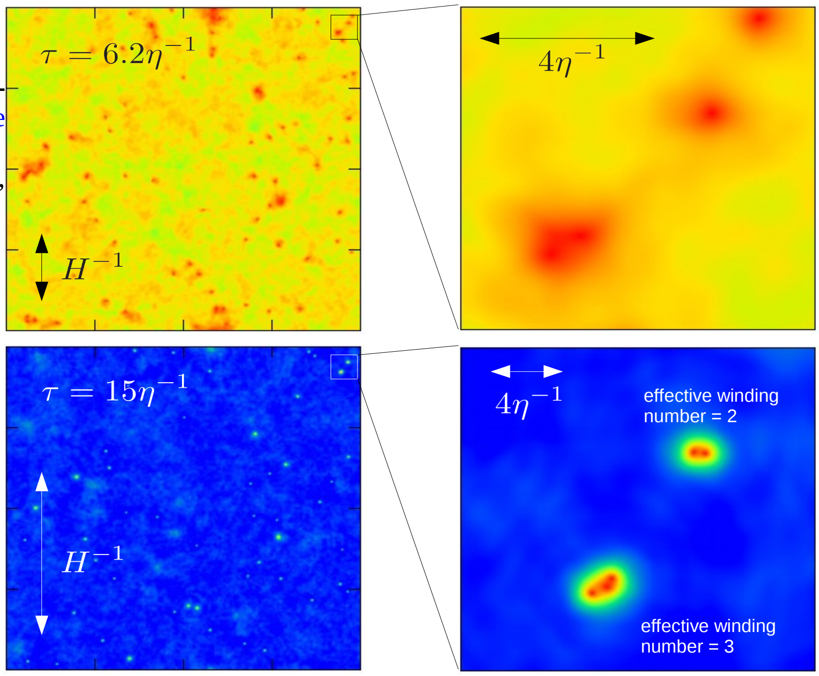

Number of strings / correlation length

Takashi Hiramatsu

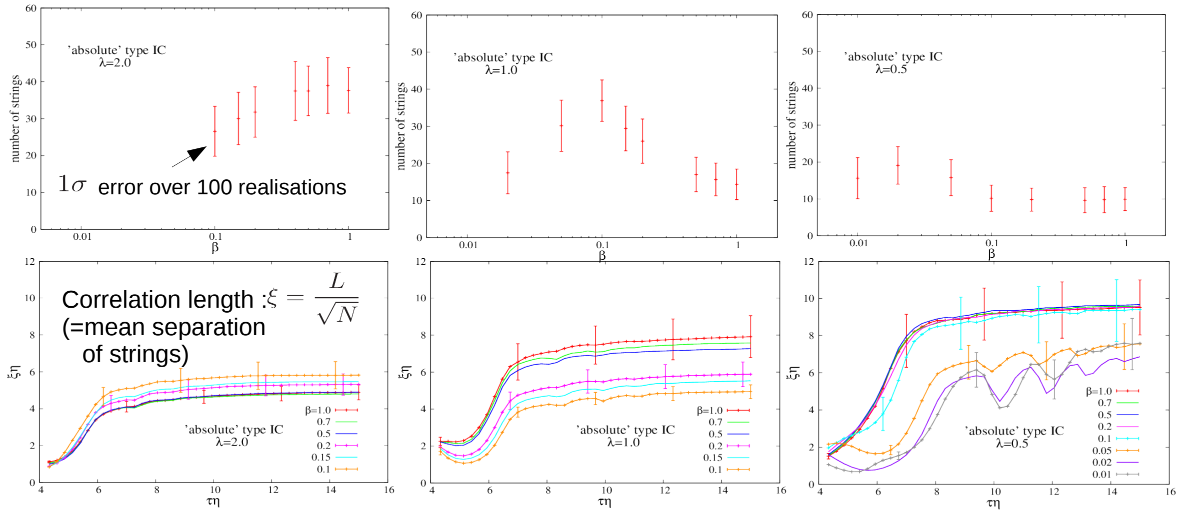

The number of strings (upper panels) depends on β and the value of β realising the largest number becomes smaller for larger λ .
The time evolution of correlation length (lower panels) is almost flat at late time, which is reflected by the limitation of the energy release mechanism. It has been reported that the correlation length evolves logarithmically in time (for global strings). **Yamaguchi, Yokoyama, Kawasaki, PTP100 (1998) 535**

Number fraction of bound states

Takashi Hiramatsu

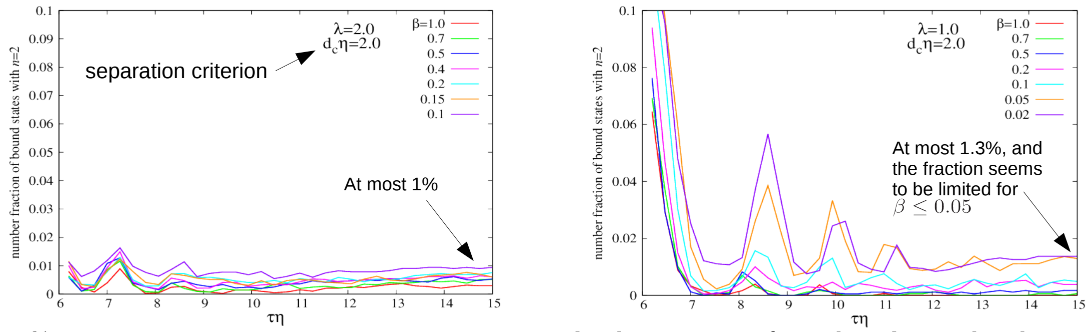

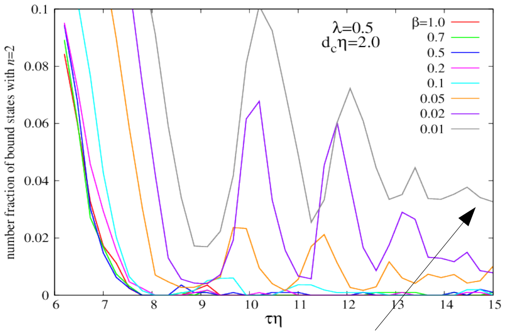

3.5%? but seems to need more simulation time.

We judge that two strings form a bound state when the separation becomes shorter than the criterion.

- The fraction is ~ 3.5% even for the best case.
- For $\lambda = 1.0$, the fraction seems to be limited even if we set smaller β . It is needed to investigate the other cases.

From these results, we expect that

- The λ dependence would be resulted from the change of the ratio H/m_ϕ controling the strength of dragging effect by the cosmic expansion against the binding energy of strings.
- The β dependence seems to be reflected by the number of the strings just after the string formation. Actually, for such an extreme case, the number of strings itself becomes smaller, according to the results in the previous page.

Gauge field prevents to form strings ?

Takashi Hiramatsu

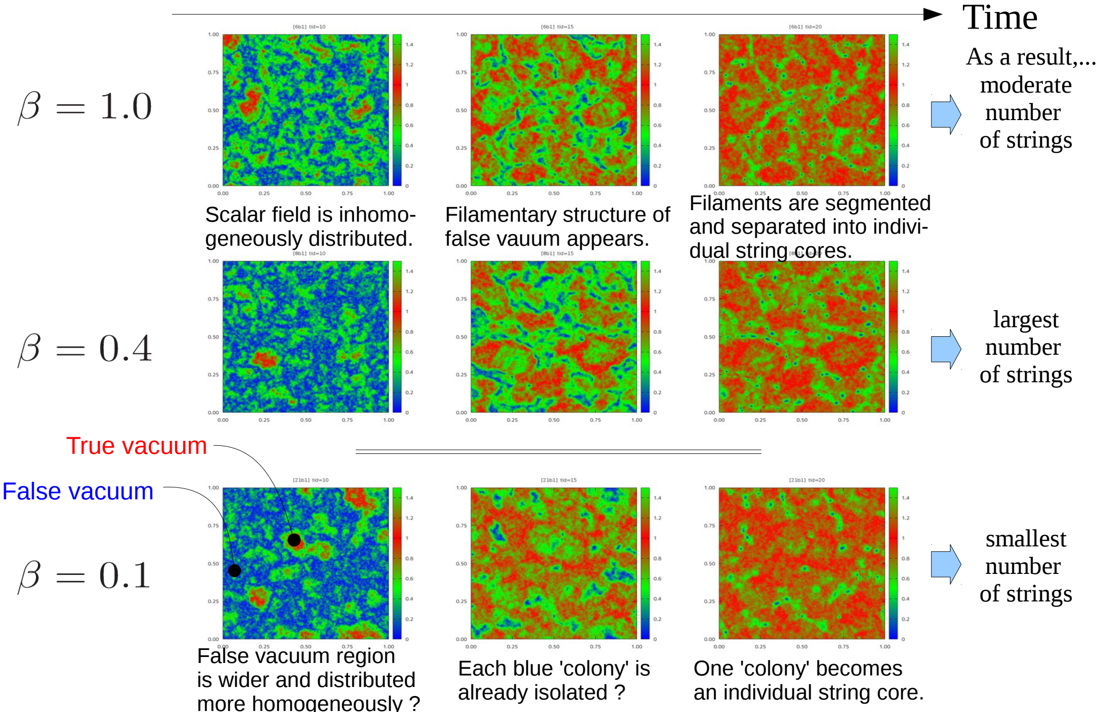

Summary

Takashi Hiramatsu

In order to study the number fraction of dynamically formed bound states in Abelian-Higgs model, we performed string 'network' simulations in the expanding 2D space.

The important parameters characterising string networks are λ and β. Varying them, we obtain

<u>number of strings</u>

- The number of strings depends on them.
- Fixing λ, there is a specific value of β realising the largest number of strings.
- The 'critical β' becomes smaller when λ is smaller, and the number becomes also smaller.

<u>number fraction of bound states</u>

- The fraction is ~ 3.5% even for the best case.
- The fraction seems to be limited even if we set smaller β.

In the 3D case, it is expected that two strings are required to collide head-on, where the collision angle is as small as possible, to form a bound state, and thus the formation rate would be reduced.

This work is in progress. But we speculate that the gauge field between strings plays an important role.

<u>Conjecture</u>

Strong gauge field plays an important role to homogenise the scalar field during the string formation and prevents to form large number of strings. The number of bound states would be determined by the competition between the binding energy contributed by the gauge field and number of strings.

“Gravitational lensing shear by an exotic lens object with negative convergence or negative mass”

by Koji Izumi

[JGRG23(2013)P04]

Gravitational lensing shear by an exotic lens object

Hirosaki University　　Koji Izumi

I ,Abstract

In recent years, concern about an exotic matter and energy is increasing. However, the behavior is not yet known well, it is difficult to detect directly. However, it is possible by being with The gravitational lens to observe the existence indirectly. By calculating the physical quantity called gravitational lensing shear, we explore the difference between ordinary lens and exotic lens. Therefore, the following metric is used[1].

$$ds^2 = -\left(1-\frac{\varepsilon_1}{r^n}\right)dt^2 + \left(1+\frac{\varepsilon_2}{r^n}\right)dr^2 + r^2(d\Theta^2 + \sin^2\Theta d\phi^2) + O(\varepsilon_1^2, \varepsilon_2^2, \varepsilon_1\varepsilon_2)$$

where r is the circumference radius and ε_1 and ε_2 are small book-keeping parameters in the following iterative calculations. Here, ε_1 and ε_2 may be either positive or negative, respectively. Negative ε_1 and ε_2 for n = 1 correspond to a negative mass (in the linearized Schwarzschild metric). The deflection angle of light is obtained at the linear order as [1]

$$\alpha = \frac{\varepsilon}{b^n}\int_0^{\frac{\pi}{2}} \cos^n \psi d\psi + O(\varepsilon^2)$$

where the integral is positive definite, b denotes the impact parameter of the light ray, and we define $\varepsilon \equiv n\varepsilon_1 + \varepsilon_2$. For $\varepsilon > 0$, the deflection angle of light is always,positive, which means the corresponding spacetime model causes the gravitational pull on light rays. For $\varepsilon > 0$, on the other hand, it is inevitably negative, which implies the gravitational repulsion on light rays like a concave lens. Thinking from how to turn at light, $\varepsilon > 0$ corresponds to ordinary lens, $\varepsilon < 0$ corresponds to exotic lens, respectively.

II ,Gravitational lensing shear

The lens equation, shear, convergence of the two types is as follows.

pull type$(\varepsilon > 0)$

$$\beta = \theta - \frac{1}{\theta^n}$$

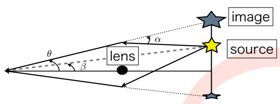

$$\lambda_+ = \frac{\hat\beta}{\hat\theta} = 1 - \frac{1}{\hat\theta^{n+1}}$$

$$\lambda_- = \frac{d\hat\beta}{d\hat\theta} = 1 + \frac{n}{\hat\theta^{n+1}}$$

$$\kappa = 1 - \frac{\lambda_+ + \lambda_-}{2} = \frac{1-n}{2}\frac{1}{\hat\theta^{n+1}}$$

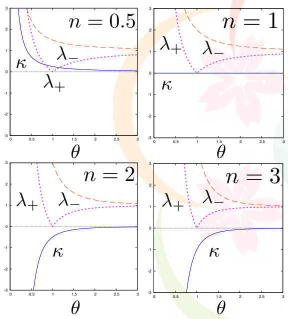

repulsio type$(\varepsilon < 0)$

$$\beta = \theta + \frac{1}{\theta^n}$$

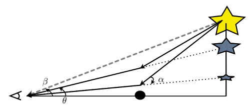

$$\lambda_+ = \frac{\hat\beta}{\hat\theta} = 1 + \frac{1}{\hat\theta^{n+1}}$$

$$\lambda_- = \frac{d\hat\beta}{d\hat\theta} = 1 - \frac{n}{\hat\theta^{n+1}}$$

$$\kappa = 1 - \frac{\lambda_+ + \lambda_-}{2} = -\frac{1-n}{2}\frac{1}{\hat\theta^{n+1}}$$

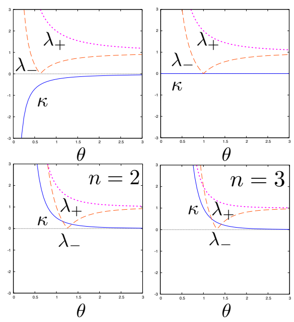

Where β denotes the angular position of the source, θ denotes the angular position of the image, λ_+ and λ_- denotes shear, κ denotes convergence.

III,Simulation

Here, In order to understand intuitively modification of the image by the gravitational lens of two types, we performed the simulation using the suitable figure. Moreover, the lens object assumes the galaxy cluster.

nomal lens　　　　exotic lens

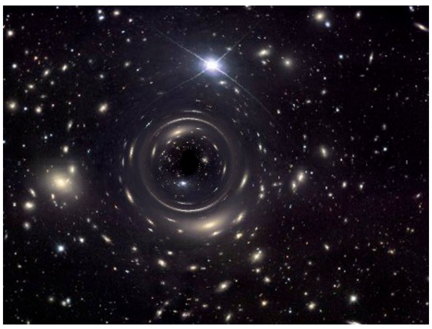

IV,Conclusion

In conclusion, It turned out that the gravitational lens by the ordinary matter differs from the gravitational lens by an exotic matter(Especially, the position and modification of an image). Moreover, from this,

Discovery of radial pair= Discovery of exotic matter or enerugy

Reference

[1]T. Kitamura, K. Nakajima, and H. Asada, Phys. Rev. D 87, 027501 (2013)
[2]K.Izumi,C.Hagiwara,K.Nakajima,T.Kitamura,and H.Asada, Phys. Rev. D 88, 024049(2013)

“Shapiro delay by an exotic lens object

with negative convergence or negative mass”

by Koki Nakajima

[JGRG23(2013)P05]

Shapiro delay by an exotic lens object with negative convergence

Koki Nakajima

Hirosaki University, Japan
with H. Asada (Hirosaki)

JGRG23 in Hirosaki Nov. 5 - 8, 2013

Abstract: We give Shapiro delay by an exotic lens object with negative convergence.

1 Introduction

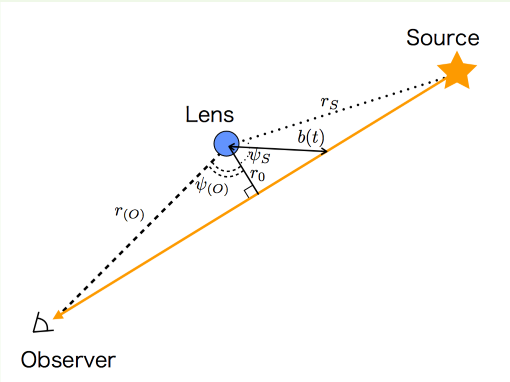

Fig 1: Image of Shapiro delay

Shapiro predicted that gravitational field delays round-trip travel time for rader signals (Shapiro delay) and it was confirmed in 1960's.[1, 2]

This is one of the tests of General rerlativity. In solar system, Shapiro delay by the Sun is about 200 micro seconds(from the Earth to Mercury). Shapiro delay is also tested with electromagnetic wave of pulsars in our Galaxy.

Our motivation is that exploreing exotic lens object in our Galaxy.

We consider Shapiro delay in modified gravity lens model[3], and use weak field approxmation.

2 Method

The line element

$$ds^2 = -\left(1-\frac{\varepsilon_1}{r^n}\right)dt^2 + \left(1+\frac{\varepsilon_2}{r^n}\right)dr^2 + r^2 d\Omega^2 + O(\varepsilon_1\varepsilon_2,\ \varepsilon_1^2,\ \varepsilon_2^2), \tag{1}$$

$$\frac{\varepsilon_1}{r^n} << 1, \frac{\varepsilon_2}{r^n} << 1, \quad d\Omega^2 = d\theta^2 + \sin^2\theta d\phi^2, n > 0$$

This metric gives the Lagrangian for a massless (light-like) particle as

$$L = -\left(1-\frac{\varepsilon_1}{r^n}\right)\dot{t}^2 + \left(1+\frac{\varepsilon_2}{r^n}\right)\dot{r}^2 + r^2(\dot{\theta}^2 + \sin^2\theta\dot{\phi}^2), \tag{2}$$

$$\text{“ $\cdot$ ”} = \frac{d}{d\lambda}, \quad \lambda: \ affine\ parameter$$

We have two constants of motion as

$$E \equiv \left(1-\frac{\varepsilon_1}{r^n}\right)\dot{t}, \quad h \equiv r^2\dot{\phi}, \tag{3}$$

$$E: \ specific\ energy, \quad h: \ specific\ angular\ momentum$$

The two constants of motion are substituted into the null condition $ds^2 = 0$ to obtain an equation for arrival time of the photon as

$$\left(\frac{dr}{dt}\right)^2 \approx \left(1-\frac{\varepsilon_1+\varepsilon_2}{r^n}\right)\left(1-\frac{r_0^2}{r^2}\left(1-\frac{\varepsilon_1}{r^n}+\frac{\varepsilon_1}{r_0^n}\right)\right) \tag{4}$$

r_0: the closest approach of the light

An integration of Eq. (4) immediately gives the Shapiro delay expressed as

$$\Delta T = 2\int_{r_S}^{r_{(O)}} \left(1-\frac{r_0^2}{r^2}\right)^{-\frac{1}{2}} \left(1-\frac{r_0^2}{r^2}\frac{\varepsilon_1}{r_0^n}\left(1-\frac{r_0^n}{r^n}\right)\left(1-\frac{r_0^2}{r^2}\right)^{-1} - \frac{\tilde{\varepsilon}}{r^n}\right)^{-\frac{1}{2}} dr \\ -2\int_{r_S}^{r_{(O)}} \left(1-\frac{r_0^2}{r^2}\right)^{-\frac{1}{2}} dr \tag{5}$$

$\tilde{\varepsilon} \equiv \varepsilon_1 + \varepsilon_2$

This is rewritten as

$$\Delta T = \frac{1}{r_0^{n-1}}\int_{\psi_S}^{\psi_{(O)}} \left(\frac{\varepsilon_1(1-\cos^n\phi)}{\sin^2\phi} + \tilde{\varepsilon}\cos^{n-2}\phi\right) d\phi \tag{6}$$

with $r = r_0/\cos\psi$

We have not carry out the integration of (6), but this corresponds Schwarzschild geometry at n=1 , $\varepsilon_1 = r_g$, and $\tilde{\varepsilon} = 2r_g$(r_g is schwarzschild radius).

3 Discussion

Shapiro delay causes relativistic frequency shift. Frequency shift y is written as

$$y \equiv \frac{d\Delta T(t)}{dt} \tag{7}$$

Let us consider for Schwarzschild geometry, frequency shift y is

$$y = 4\frac{\tilde{\varepsilon}}{b}\frac{db}{dt}, \quad b(t) = \sqrt{r_0 + v^2 t^2} \tag{8}$$

b(t) is distance of right and lens.

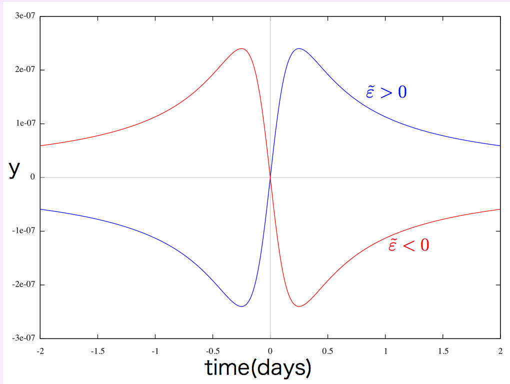

Fig 2: Dependence of frequency shift on the distance b and $\tilde{\varepsilon}$ for $n = 1$. Blue line is the Sun's Shapiro delay (around the Earth and Mercury) for $\tilde{\varepsilon} > 0$, and red one is for $\tilde{\varepsilon} < 0$.

See Fig. 2. Negative $\tilde{\varepsilon}$ may cause frequency shift but bring arrival time of radio signal forward.

4 Conclusion

- We expressed Shapiro delay by an exotic lens model with negative convergence.
- We pointed out that exotic lens may bring the arrival time of photon forward in negative $\tilde{\varepsilon}$ case.

References

[1] I. I. Shapiro, Phys. Rev. Lett, 13, 789-791 (1964).

[2] I. I. Shapiro et al. Phys. Rev. Lett, 20, 1265-1269 (1968).

[3] T. Kitamura, K. Nakajima, and H. Asada, Phys. Rev. D 87, 027501(2013).

“Gravitational field of a rotating ring around a Schwarzschild black hole”

by Yasumichi Sano

[JGRG23(2013)P06]

P06

Gravitational field of a rotating ring around a Schwarzschild black hole

[Metric reconstruction in radiation gauge]

Yasumichi SANO

Supervisor: Hideyuki TAGOSHI

Osaka University

Introduction

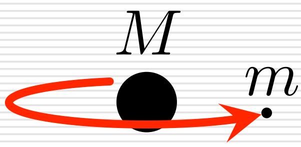

- EMRI (Extreme Mass Ratio Inspiral) is one of sources of gravitational wave.
  - We consider Black hole perturbation of Kerr spacetime (non-vacuum perturbation) $\boxed{g_{\alpha\beta} = g^{(0)}_{\alpha\beta} + h_{\alpha\beta}}$

    1st order perturbation
- We investigate the method for calculating $h_{\alpha\beta}$ using Hertz potential.
  - This method is based on Chrzanowski (1975) and Kegeles & Cohen (1979) ⋯CCK formalism
  - We discuss the problem about the lower modes $l = 0,\ 1$ of perturbation.

Setting

- Schwarzschild BH＋Rotating ring
  - Ring ··· Set of point particles on a circular geodesic

$\theta = \frac{\pi}{2}$

- Energy momentum tensor (axisymmetric & steady)

$$\boxed{T^{\alpha\beta} = \frac{m u^\alpha u^\beta}{u^t {r_0}^2}\delta(r - r_0)\delta(\cos\theta)}$$

  - Rest mass $2\pi m \ll M$
  - Radius r_0
    - Four velocity u^α is geodetic (determined by the radius r_0)
      → Angular velocity $\Omega = \sqrt{\frac{M}{{r_0}^3}}$

Teukolsky equation＋CCK formalism

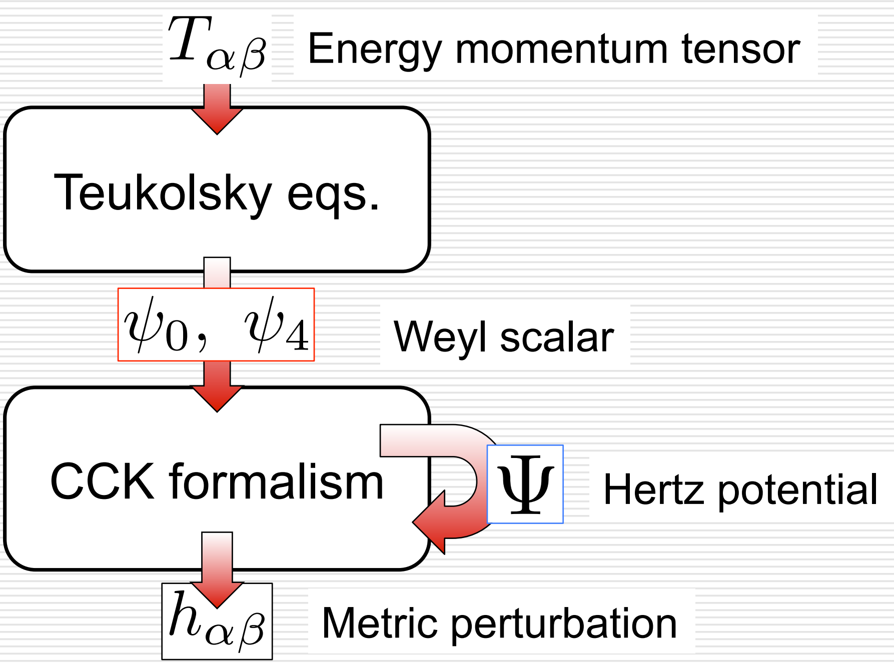

§ 1 : Teukolsky equations and $\psi_0,\ \psi_4$

Teukolsky equation

- Weyl scalar: components of Weyl tensor $\psi_0,\ \psi_1,\ \psi_2,\ \psi_3,\ \psi_4$
  - They represent the curvature at a vacuum point
- Teukolsky equation (Teukolsky 1972, 1973)
  - Perturbation equations for $\psi_0,\ \psi_4$
- We can solve ψ_0 and ψ_4 analytically

$$\boxed{\psi_0(r,\theta) = \sum_{l=2}^{\infty} R_l^{\psi_0}(r)\,{}_2Y_l(\theta)}$$

$${}_sY_l(\theta) = {}_sY_{l,m=0}(\theta,\phi)$$

$$\boxed{\psi_4(r,\theta) = \frac{1}{r^4}\sum_{l=2}^{\infty} R_l^{\psi_4}(r)\,{}_{-2}Y_l(\theta)}$$

ψ_0 and ψ_4

- Green's function for the radial function

$$\boxed{G_l(r,r') = \frac{\Theta(r'-r)h_1(r)h_2(r') + \Theta(r-r')h_1(r')h_2(r)}{W(r')}}$$

(*W*: Wronskian)

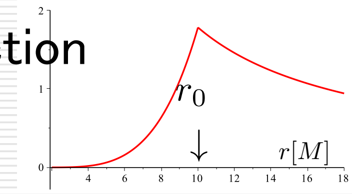

- ψ_4 is continuous and smooth at $r = r_0$

$\theta \neq \pi/2$

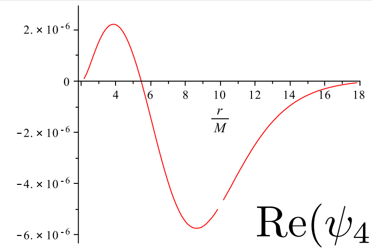

$\mathrm{Re}(\psi_4(r,\pi/4))$

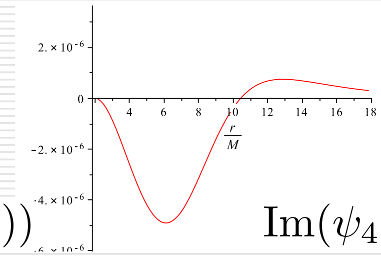

$\mathrm{Im}(\psi_4(r,\pi/4))$

- ψ_0 is smooth when $\theta \neq \pi/2$, too

§ 2 : CCK formalism and Hertz potential

CCK: Chrzanowski (1975), Kegeles & Cohen (1979)

- Hertz Potential $\boxed{\Psi}$
  - Application of Hertz potential in electromagnetism
  - Hertz potential is a vacuum solution of Teukolsky equation.
  - Metric perturbation is given by Ψ. [Radiation gauge]

$$g_{\alpha\beta} = g^{(0)}_{\alpha\beta} + h_{\alpha\beta}$$

$$h_{22} = -\frac{1}{r^2}\left(\frac{\partial}{\partial\cos\theta}\right)^2 \mathrm{Re}\left(\sin^2\theta\,\overline{\Psi}\right)$$

$$h_{23} = -\sqrt{2}\left(\partial_r - \frac{1}{r}\right)\frac{1}{r\sin\theta}\left(\frac{\partial}{\partial\cos\theta}\right)\sin^2\theta\,\overline{\Psi}$$

$$h_{33} = -\left(\partial_r + \frac{1}{r}\right)\left(\partial_r - \frac{3}{r}\right)\overline{\Psi}$$

$$h_{24} = \overline{h_{23}},\ h_{44} = \overline{h_{33}}$$

$$h_{11} = h_{12} = h_{13} = h_{14} = h_{34} = 0$$

- The problem is how to find the Hertz potential.

Weyl scalar & Hertz potential

- Weyl scalars $\psi_0,\ \psi_1,\ \psi_2,\ \psi_3,\ \psi_4$ are also given by Hertz potential Ψ

$$h_{22} = -\frac{1}{r^2}\left(\frac{\partial}{\partial\cos\theta}\right)^2 \mathrm{Re}\left(\sin^2\theta\,\overline{\Psi}\right)$$

$$h_{23} = -\sqrt{2}\left(\partial_r - \frac{1}{r}\right)\frac{1}{r\sin\theta}\left(\frac{\partial}{\partial\cos\theta}\right)\sin^2\theta\,\overline{\Psi}$$

$$h_{33} = -\left(\partial_r + \frac{1}{r}\right)\left(\partial_r - \frac{3}{r}\right)\overline{\Psi}$$

$$\psi_0 = \frac{1}{2}\left(\frac{\partial}{\partial r}\right)^4 \overline{\Psi}$$

$$\psi_4 = \frac{1}{2}\frac{1}{4r^4}\sin^2\theta\left(\frac{\partial}{\partial\cos\theta}\right)^4 \frac{1}{\sin^2\theta}\overline{\Psi}$$

- We already know ψ_0 and ψ_4 as the solutions of Teukolsky equations.

$$\psi_0(r,\theta) = \sum_{l=2}^{\infty} R_l^{\psi_0}(r)\,{}_2Y_l(\theta)$$

$$\psi_4(r,\theta) = \frac{1}{r^4}\sum_{l=2}^{\infty} R_l^{\psi_4}(r)\,{}_{-2}Y_l(\theta)$$

  - We look for Ψ which gives those solutions ψ_0 and ψ_4.

$$\psi_0 = \frac{1}{2}\left(\frac{\partial}{\partial r}\right)^4 \overline{\Psi}$$

$$\psi_4 = \frac{1}{2}\frac{1}{4r^4}\sin^2\theta\left(\frac{\partial}{\partial\cos\theta}\right)^4 \frac{1}{\sin^2\theta}\overline{\Psi}$$

§ 3 : Finding Hertz potential Ψ (Part 1)

3.1 A solution for Hertz potential

$$\psi_0 = \frac{1}{2}\left(\frac{\partial}{\partial r}\right)^4 \overline{\Psi}$$

$$\psi_0(r,\theta) = \sum_{l=2}^{\infty} R_l^{\psi_0}(r)\,{}_2Y_l(\theta)$$

$$\psi_4 = \frac{1}{2}\frac{1}{4r^4}\sin^2\theta\left(\frac{\partial}{\partial\cos\theta}\right)^4 \frac{1}{\sin^2\theta}\overline{\Psi}$$

$$\psi_4(r,\theta) = \frac{1}{r^4}\sum_{l=2}^{\infty} R_l^{\psi_4}(r)\,{}_{-2}Y_l(\theta)$$

- "A" solution $\Psi_{\rm P}$ (particular solution) is found.

$$\overline{\Psi}_{\rm P} = \sum_{l=2}^{\infty} \frac{8R_l^{\psi_4}(r)\,{}_2Y_l(\theta)}{(l+2)(l-1)(l+1)l}$$

- We used the following relations.

$$\left(\frac{\partial}{\partial r}\right)^4 \frac{R_l^{\psi_4}(r)}{(l+2)(l-1)(l+1)l} = \frac{1}{4}R_l^{\psi_0}(r)$$

(Teukolsky-Starobinsky relation)

$$\sin^2\theta\left(\frac{\partial}{\partial\cos\theta}\right)^4 \frac{1}{\sin^2\theta}\frac{{}_2Y_l(\theta)}{(l+2)(l-1)(l+1)l} = {}_{-2}Y_l(\theta)$$

(spin-weighted spherical harmonics)

Reconstruction of Weyl scalars from $\Psi_{\rm P}$

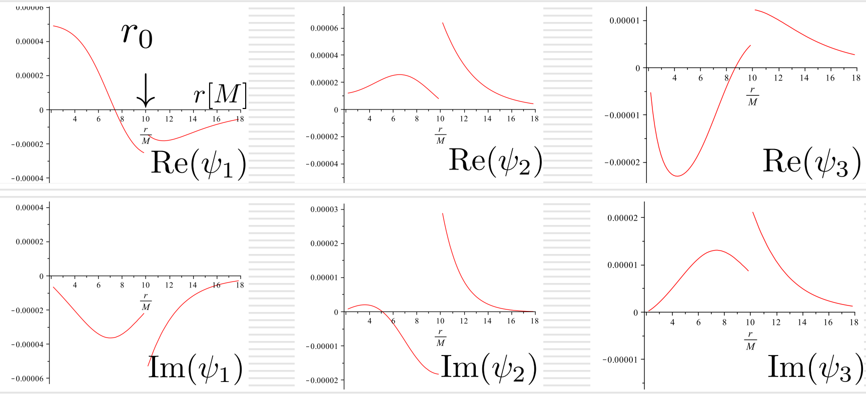

(Plotted with $\theta = \pi/4$ fixed)

- There are unphysical jumps at vacuum point $(r, \theta) \neq (r_0, \pi/2)$.

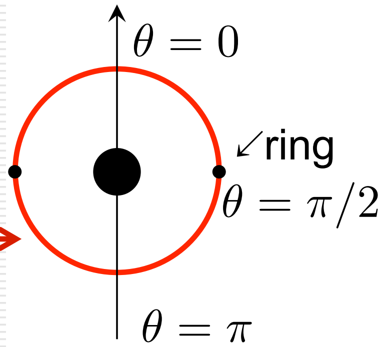

$\Psi_{\rm P}$ lacks lower modes

- $\Psi_{\rm P}$ contains only $l \geq 2$ modes
  - The lower modes $l = 0,\ 1$ is the perturbation of mass and angular momentum

$$\overline{\Psi}_{\rm P} = \sum_{l=2}^{\infty} \frac{8R_l^{\psi_4}(r)\,{}_2Y_l(\theta)}{(l+2)(l-1)(l+1)l}$$

- $\Psi_{\rm P}$ is a particular solution.
- More general solution of these equations would contain the lower modes.

$$\psi_0 = \frac{1}{2}\left(\frac{\partial}{\partial r}\right)^4 \overline{\Psi}$$

$$\psi_4 = \frac{1}{2}\frac{1}{4r^4}\sin^2\theta\left(\frac{\partial}{\partial\cos\theta}\right)^4 \frac{1}{\sin^2\theta}\overline{\Psi}$$

$$\Psi = \boxed{\Psi_{\rm P}} + \boxed{\Psi_{\rm H}}$$

- Are the unphysical jumps of Weyl scalars (and $h_{\alpha\beta}$) due to the lack of $\Psi_{\rm H}$?

3.2 General solution for Hertz potential

$\psi_0 = \frac{1}{2}\left(\frac{\partial}{\partial r}\right)^4 \overline{\Psi}$ $\psi_4 = \frac{1}{2}\frac{1}{4r^4}\sin^2\theta\left(\frac{\partial}{\partial\cos\theta}\right)^4 \frac{1}{\sin^2\theta}\overline{\Psi}$

- Since $\boxed{\Psi_{\rm P}}$ is a solution, $\Psi = \boxed{\Psi_{\rm P}} + \boxed{\Psi_{\rm H}}$ also satisfies the above equations for Hertz potential if

$$\boxed{\overline{\Psi}_{\rm H}(r,\theta) = \frac{2A}{\sin^2\theta}\left[\frac{a(r)}{6}\cos^3\theta + \frac{b(r)}{2}\cos^2\theta + c(r)\cos\theta + d(r)\right]}$$

$$a(r) = a_1 r^2(r-3M) + a_2 \qquad A = \frac{m}{r_0\sqrt{\Delta_0}}$$
$$b(r) = b_1 r^2 + (r-M)b_2$$
$$c(r) = -\frac{1}{2}a_1(r-M)(r^2+4M^2) - \frac{1}{2}a_2 + c_2(r-M) + c_1 r^2$$
$$d(r) = \frac{1}{2}b_1 r^2 + \frac{1}{2}b_2 r + d_1 r^2(r-3M) + d_2$$

  - Degrees of freedom are reduced to 8 complex parameters
    - (We used the condition that a Hertz potential is a vacuum solution of Teukolsky eq.)

Hertz potential

- Vacuum solution of Teukolsky equation can not satisfy both of $\psi_0 = \frac{1}{2}\left(\frac{\partial}{\partial r}\right)^4 \overline{\Psi}$ and $\psi_4 = \frac{1}{2}\frac{1}{4r^4}\sin^2\theta\left(\frac{\partial}{\partial\cos\theta}\right)^4 \frac{1}{\sin^2\theta}\overline{\Psi}$ because of the presenof matter (the ring).

- We look for Ψ that…
  - satisfies $\psi_0 = \frac{1}{2}\left(\frac{\partial}{\partial r}\right)^4 \overline{\Psi}$ and $\psi_4 = \frac{1}{2}\frac{1}{4r^4}\sin^2\theta\left(\frac{\partial}{\partial\cos\theta}\right)^4 \frac{1}{\sin^2\theta}\overline{\Psi}$
  - and is a vacuum solution of Teukolsky equation at $r < r_0$ and $r > r_0$.

- We try to remove jumps by considering

$$\Psi = \boxed{\Psi_{\rm P}} + \boxed{\Psi_{\rm H}\Theta(r-r_0)}$$

$$\overline{\Psi}_{\rm H}(r,\theta) = \frac{2A}{\sin^2\theta}\left[\frac{a(r)}{6}\cos^3\theta + \frac{b(r)}{2}\cos^2\theta + c(r)\cos\theta + d(r)\right]$$

$$a(r) = a_1 r^2(r-3M) + a_2$$

$$b(r) = b_1 r^2 + (r-M)b_2$$

$$c(r) = -\frac{1}{2}a_1(r-M)(r^2+4M^2) - \frac{1}{2}a_2 + c_2(r-M) + c_1 r^2$$

$$d(r) = \frac{1}{2}b_1 r^2 + \frac{1}{2}b_2 r + d_1 r^2(r-3M) + d_2$$

§ 4 : Finding Hertz potential (Part 2: Determining parameters)

Angular momentum perturbation

- It is found that $\mathrm{Im}(a_2)$ corresponds to the angular momentum perturbation. $\delta J = -A\ \mathrm{Im}(a_2)$ $\quad A = \frac{m}{r_0\sqrt{\Delta_0}}$
  - (Keidl, Friedman, and Wiseman 2007)
- We equate δJ with the angular momentum of the ring $J_{\rm ring} = 2\pi m u_\phi$ and add the associated $\boxed{\Psi_{\rm H}}$ to $\boxed{\Psi_{\rm P}}$.
- ➡ Jumps of $\mathrm{Im}(\psi_1)$, $\mathrm{Im}(\psi_2)$, and $\mathrm{Im}(\psi_3)$ vanish simultaneously! r_0

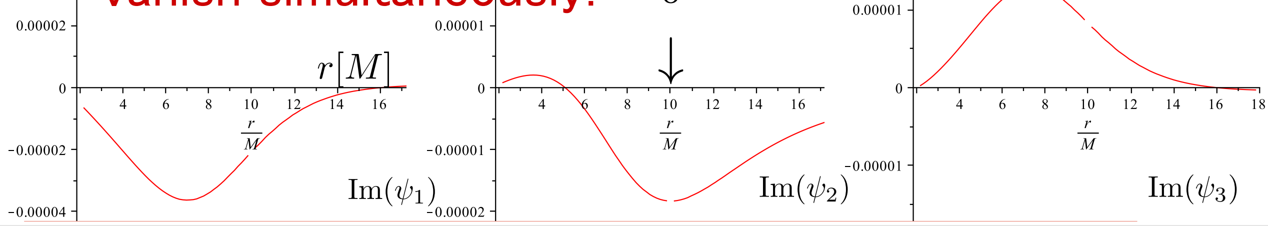

How to determine other parameters?

- It is found that $\mathrm{Re}(b_1)$ and $\mathrm{Re}(b_2)$ correspond to the mass perturbation. $\delta M = -A(3M\mathrm{Re}(b_1) + \mathrm{Re}(b_2))$
  - (Keidl, Friedman, and Wiseman 2007)
- Two conditions are needed to determine them. But we know only one.
  - δM equals to the energy of the ring $M_{\mathrm{ring}} = 2\pi m u_t$
- We expect that all the jumps vanish when the parameters are fixed properly.

➡ We fit the parameters to cancel the jumps

Cancelling the jumps in fields

- We look for parameters that fill the jumps in Weyl scalars, metric perturbation and Ψ.
- Result
  - Parameters are found if we allow a new discontinuity at the equatorial plane $(r > r_0,\ \theta = \pi/2)$.

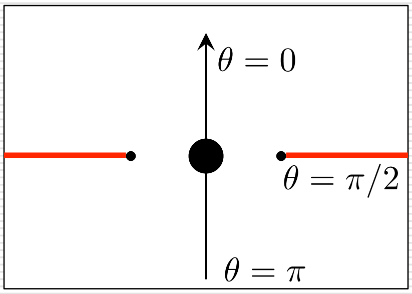

  - Each of obtained Weyl scalars, metric perturbation and Ψ is smooth at the sphere surface $(r = r_0)$.
  - Physical parameters satisfy

$$M_{\mathrm{ring}} = -A(3M\mathrm{Re}(b_1) + \mathrm{Re}(b_2)) \qquad J_{\mathrm{ring}} = -A\ \mathrm{Im}(a_2)$$

§5 Conclusion

- Perturbed metric (radiation gauge) is completed.
  - The $l \geq 2$ modes are directly calculated from $\psi_0,\ \psi_4$
    → Field has a discontinuity at the sphere $(r = r_0)$
  - The lower modes perturbation and pure gauge are added outside the sphere
    → Field becomes smooth at the sphere.
    → Discontinuity at the equatorial plane appeared.
- Future works
  - Circular-orbiting particle around a black hole
    - ... and calculate the gravitational self force (following the work by Pound, Merlin & Barack 2013)
  - More analytic determination of the lower modes

“Demagnification by an exotic lens object with negative mass”

by Chisaki Hagiwara

[JGRG23(2013)P07]

Gravitational lensing by negative mass object

Chisaki Hagiwara

Hirosaki University, Japan
with H. Asada (Hirosaki)

JGRG23 in Tohoku Nov. 5 - 8, 2013

Abstract: We have derived the lens equation and the deflection angle when the lens object with negative mass is expressed by the exterior metric of the Schwarzschild space-time. As a result, we have found that at most two images appear on the source. Also, no images are observed if the source is inside Caustics.

1 Motivation

The structure of space-time can be studied indirectly by observing the light bended by gravitational field that is caused by astronomical bodies. Recently, exotic matter or exotic energy such as dark energy which accelerates the cosmic expansion has attracted interests. While these matter and energy are difficult to be detected directly, it is expected that they can be detected by observing exotic space-time using gravitaional lensing. We discuss gravitational lensing caused by an object with negative mass which is one of the exotic matter.

2 Introduction

From the Schwarzschild metric, taking b as the impact parameter, the bending angle in the weak field approximation is[1]

$$\alpha = \frac{4GM}{bc^2}. \tag{1}$$

The lens equation derived from the relative position of the images θ_I, source object θ_S and the observer is[2]

$$\theta_S = \theta_I - \frac{\alpha_0^2}{\theta_I}, \tag{2}$$

where $\alpha_0 = \sqrt{\frac{4GMD_{LS}}{c^2 D_{OS} D_{OL}}}$ is the Einstein ring radius and D_{OS}, D_{OL}, D_{LS} are the distance from observer to the source object, from observe to the lens object, and from the lens object to the source object, respectivelly.

Solving it respet to θ_I, angular position of the images are

$$\theta_I = \theta_\pm = \frac{1}{2}\left(\theta_S \pm \sqrt{\theta_S^2 + 4\alpha_0^2}\right). \tag{3}$$

The magnification is ratio of the luminosity of the images to the source object. Taking A_+ and A_- as the magnification of the images appearing at θ_+ and θ_- respectively, the total magnification is[2]

$$A_{tot} \;=\; |A_+| + |A_-| = \frac{x^2+2}{x\sqrt{x^2+4}}, \tag{4}$$

where $x = \theta_S/\alpha_0$.

Considering the motion of the source object which performs linear motion of constan speed to the lens plane that is D_{OL} distant from the observer with the origin at the lens object, the angular position of the source object at the time t is

$$\theta_S(t) = \sqrt{t^2 + \theta_{S0}^2}, \tag{5}$$

where θ_{S0} is the nearest distance between the source object and the lens object (the distance of closest approach). It is normalized by the time at which the source object crosses the Einstein ring radius. The magnification is written as

$$A_{tot}(t) = \frac{x(t)^2+2}{x(t)\sqrt{x(t)^2+4}}. \tag{6}$$

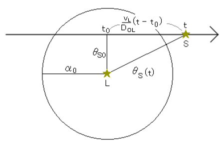

Figure 1: Relative motion of the source and lens object on the lens plane

3 The effect of gravitational lensing by lens object with negative mass

Assuming the mass of the lens object is $M_{neg} = -M (M > 0)$, from (1), the bending angle is

$$\alpha_{neg} = \frac{4GM_{neg}}{bc^2} = \frac{4G(-M)}{bc^2} = -\alpha. \tag{7}$$

Einstein ring radius is

$$\alpha_{0neg}^2 \;=\; \left(\sqrt{\frac{4GM_{neg}D_{LS}}{c^2 D_{OS} D_{OL}}}\right)^2 = \left(\sqrt{-\frac{4GMD_{LS}}{c^2 D_{OS} D_{OL}}}\right)^2 = -\alpha_0^2. \tag{8}$$

Therefore lens equation and the angular position of the images are written as

$$\theta_S \;= \theta_I - \frac{\alpha_{0neg}^2}{\theta_I} = \theta_I + \frac{\alpha_0^2}{\theta_I}, \tag{9}$$

$$\theta_I \;= \theta_{1,2} = \frac{1}{2}\left(\theta_S \pm \sqrt{\theta_S^2 - 4\alpha_0^2}\right), \tag{10}$$

taking θ_+ as θ_1 and θ_- as θ_2 for convinience. From the above, it proves that the images appear up to 2. (See also Figure2)

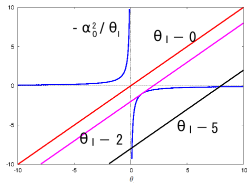

Figure 2: The solution of th lens equation of a negative mass object (blue:α^2/θ_I, red:$\theta_S = 0$, pink:$\theta_S = 2$, black:$\theta_S = 5$)

From the relative motion of the source object and the lens object on the lens plane, the total magnification derived from the equation is

$$A_{tot}(t) = \frac{x(t)^2-2}{x(t)\sqrt{x(t)^2-4}}. \tag{11}$$

4 Result

The light curve that varied θ_{S0} are substituted in the expression (11) and locus of the images are shown below. In Figure3, the horizontal axis is t normalized by the time at which the source object crosses the Einstein ring radius, and the vertical axis is the total magnification $A_{tot}(t)$. The magnification is $A(t) = 1$ at the infinit point. Besides, it is confirmed that the two images θ_1 and θ_2 appear on the source side from the graph4.

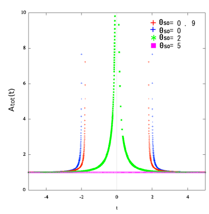

Figure 3: Light curve. blue:$\theta_{S0} = 0.9$, red:$\theta_{S0} = 0$, green:θ_{S0}=2, pink:θ_{S0}=5。

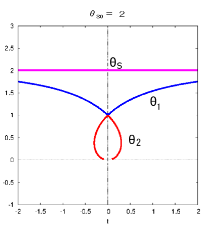

Figure 4: Locus of images(at $\theta_{S0} = 2$). blue:θ_1, red:θ_2, green:θ_S, treating the origin as the lens object.

5 Conclusion

We examined the lens equation and the deflection angle when the lens object with negative mass is expressed by the exterior metric of the Schwarzschild space-time.

- Images are magnified.
- At the most two images appears at the source side.
- No images are observed if the source is inside Caustics.

References

[1] Frittelli, T. P. Kling, and E. T. Newman, 2000, Phys. Rev. D 61, 064021

[2] P. Schneider, J. Ehlers, E. E. Falco, Gravitational Lenses

"Wormholes in higher dimensional space-time: Dynamics"

by Hisaaki Shinkai

[JGRG23(2013)P09]

poster P09

Wormhole in Higher-dim. Space-time: Dynamics

Hisaaki Shinkai & Takashi Torii (Osaka Inst. Technology, Japan)
真貝寿明 & 鳥居隆　　　(大阪工業大学)

Outline & Summary

(a) "Fate of Morris-Thorne (Ellis) wormhole" was numerically investigated in 2002. [HS & Hayward, PRD66, 044005].
The fate is either black-hole collapse or inflationary expansion, depending on the excessed energy.

(b) The higher-dimensional Ellis wormhole solutions are obtained.
Perturbation study suggests instability. [Torii & HS, PRD88 (2013), 064023]
Numerical evolutions in 4-6 dim confirm its instability. [this poster]

(c) The wormholes in 5-dim. Gauss-Bonnet gravity are numerically obtained.
Evolutions suggest that positive GB term accelerates throat inflation.

Time Machine & Science of Space-time (HS, 2011)

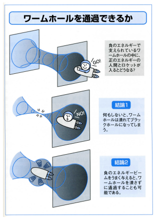

Motivations

Why wormholes?

- They make great science fiction – short cuts between otherwise distant regions. Morris & Thorne 1988, Sagan "Contact" etc
- They increase our understanding of gravity when the usual energy conditions are not satisfied, due to quantum effects (Casimir effect, Hawking radiation) or alternative gravity theories, brane-world models etc.
- They are very similar to black holes –both contain (marginally) trapped surfaces and can be defined by trapping horizons (TH).

Wormhole ≡ Hypersurface foliated by marginally trapped surfaces

- BH and WH are interconvertible?
  New duality?

[1] **How the stability changes in 5-d GR?**
[2] **How the stability changes in Gauss-Bonnet gravity?**

BH and WH are interconvertible ? (New Duality?)

S.A. Hayward, Int. J. Mod. Phys. D 8 (1999) 373

- They are very similar – both contain (marginally) trapped surfaces and can be defined by trapping horizons (TH)
- Only the causal nature of the THs differs, whether THs evolve in plus / minus density.

	Black Hole	Wormhole
Locally defined by	Achronal(spatial/null) outer TH ⇒ 1-way traversable	Temporal (timelike) outer THs ⇒ 2-way traversable
Einstein eqs.	Positive energy density normal matter (or vacuum)	Negative energy density "exotic" matter
Appearance	occur naturally	Unlikely to occur naturally. but constructible ???

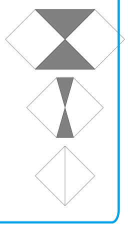

N-dim. Ellis Wormhole sol.

A Wormhole Solution (n-Dim, massless ghost scalar)

- **spherical symmetry.**

$$ds^2 = -f(t,r)e^{-2\delta(t,r)}dt^2 + f(t,r)^{-1}dr^2 + R(t,r)^2 d\Omega^2 \quad (1)$$

- **with massless ghost scalar field ϕ.**
- **static, $f \equiv 1$, and throat radius $R(0) = a$; Just solve**

$$\frac{d^2R}{dr^2} = \frac{(n-3)a^{2(n-3)}}{R^{2n-5}} \quad (2)$$

$$\frac{d\phi}{dr} = \sqrt{(n-2)(n-3)}\frac{a^{n-3}}{R^{n-2}} \quad (3)$$

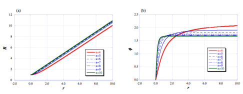

The n-dimensional wormhole solutions. The circumference radius R (a) and the scalar field ϕ (b) are plotted as a function of radial coordinate r. The cases of $n = 4$–10 are shown.

Perturbation Analysis

See the poster P01.　Torii & HS, PRD88 (2013), 064023

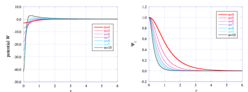

The potential function $W(r)$.　The eigenfunction Ψ_1.

n	ω^2
4	−1.397052433715108
5	−2.984958930277901
6	−4.686620542994600
7	−6.462584141263180
8	−8.289759363062593
9	−10.15355304518670
10	−12.04426501474384

Obtained negative eigenvalues of ω^2. ⟹ Unstable.

WH evolution in 4, 5, 6-dim. GR

in prep.

4d 5d 6d GR
ghost pulse (additional amp.) input

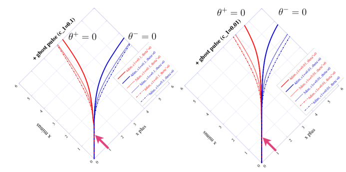

negative energy input --> throat inflates

4d 5d 6d GR
ghost pulse (subtract amp.) input

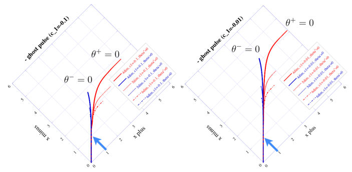

positive energy input --> BH formation

Results in 4-dim. GR

PRD66 (2002) 044005

Bifurcation of the horizons
-- go to a Black Hole or Inflationary expansion

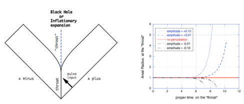

Ghost pulse input -- Bifurcation of the horizons

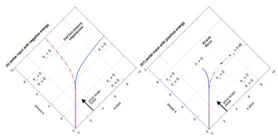

Travel through a Wormhole
-- with Maintenance Operations!

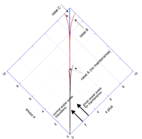

Field Eqs.

Gauss-Bonnet gravity

- **Action**

$$S = \int_{\mathcal{M}} d^{N+1}x\sqrt{-g}\Big[\frac{1}{2\kappa^2}\{\alpha_1\mathcal{R} + \alpha_2\mathcal{L}_{GB}\} + \mathcal{L}_{\text{matter}}\Big] \quad (1)$$

where $\mathcal{L}_{GB} = \mathcal{R}^2 - 4\mathcal{R}_{\mu\nu}\mathcal{R}^{\mu\nu} + \mathcal{R}_{\mu\nu\rho\sigma}\mathcal{R}^{\mu\nu\rho\sigma}$

- **Field eqs.**

$$\alpha_1 G_{\mu\nu} + \alpha_2 H_{\mu\nu} + g_{\mu\nu}\Lambda = \kappa^2 T_{\mu\nu} \quad (2)$$

where $H_{\mu\nu} = 2[\mathcal{R}\mathcal{R}_{\mu\nu} - 2\mathcal{R}_{\mu\alpha}\mathcal{R}^{\alpha}{}_{\nu} - 2\mathcal{R}^{\alpha\beta}\mathcal{R}_{\mu\alpha\nu\beta} + \mathcal{R}_{\mu}{}^{\alpha\beta\gamma}\mathcal{R}_{\nu\alpha\beta\gamma}] - \frac{1}{2}g_{\mu\nu}\mathcal{L}_{GB}$

Assumptions

☐ 5-dim. Spherical Symmetry
☐ Dual-null coordinate

$$ds^2 = -2e^{-f(x^+,x^-)}dx^+dx^- + r^2(x^+,x^-)d\Omega_3^2 \quad (3)$$

conformal factor	$\Omega = \frac{1}{r}$	(4)
expansions	$\vartheta_\pm = 3\partial_\pm r = -3\Omega^{-2}\partial_\pm\Omega$	(5)
inaffinities	$\nu_\pm = \partial_\pm f$	(6)
momenta of ϕ	$\wp_\pm = r\partial_\pm\phi = \Omega^{-1}\partial_\pm\phi$	(7)
momenta of ψ	$\pi_\pm = r\partial_\pm\psi = \Omega^{-1}\partial_\pm\psi$	(8)

☐ matter = normal field $\psi(u,v)$ and/or ghost field $\phi(u,v)$

$$T_{\mu\nu} = T^{\psi}_{\mu\nu} + T^{\phi}_{\mu\nu} \quad (9)$$
$$= \left[\psi_{,\mu}\psi_{,\nu} - g_{\mu\nu}\left(\frac{1}{2}(\nabla\psi)^2 + V_1(\psi)\right)\right] + \left[-\phi_{,\mu}\phi_{,\nu} - g_{\mu\nu}\left(-\frac{1}{2}(\nabla\phi)^2 + V_2(\phi)\right)\right]$$

Field Equations in 5-Dim. Gauss-Bonnet gravity

$$\eta = \Omega^2\left(e^{-f} + \frac{2}{9}\vartheta_+\vartheta_-\right), \quad \tilde{A} = (\alpha_1 + 4\alpha_2\eta e^f), \quad B = \kappa^2 T_{+-} + e^{-f}\Lambda$$

$\boxed{x^+\text{-direction } \partial_+}$ $\boxed{x^-\text{-direction } \partial_-}$

$$\partial_\pm\Omega = -\frac{1}{3}\vartheta_\pm\Omega^2 \quad (1)$$
$$\partial_\pm\vartheta_\pm = -\nu_\pm\vartheta_\pm - \frac{1}{\tilde{A}\Omega}\kappa^2 T_{\pm\pm} \quad (2)$$
$$\partial_\pm\vartheta_\mp = \frac{1}{\tilde{A}\Omega}(-3\alpha_1\eta + B) \quad (3)$$
$$\partial_\pm f = \nu_\pm \quad (4)$$
$$\partial_\pm\nu_\mp = \frac{\alpha_1}{\tilde{A}}\left\{\eta - \frac{4(3\alpha_1\eta - B)}{3\tilde{A}}\right\} + \frac{(\kappa^2 T_{zz}\Omega^2 - \Lambda)}{\tilde{A}e^f} + \frac{8\alpha_2}{9\tilde{A}^3}\{e^f(3\alpha_1\eta - B)^2 - \kappa^4 T_{++}T_{--}\} \quad (5)$$
$$\partial_\pm\psi = \Omega\pi_\pm \quad (6)$$
$$\partial_\pm\phi = \Omega p_\pm \quad (7)$$
$$\partial_\pm\pi_\mp = -\frac{1}{6}\Omega\vartheta_\pm\pi_\mp - \frac{1}{2}\Omega\vartheta_\mp\pi_\pm - \frac{1}{2e^f\Omega}\frac{dV_1}{d\psi} \quad (8)$$
$$\partial_\pm p_\mp = -\frac{1}{6}\Omega\vartheta_\pm p_\mp - \frac{1}{2}\Omega\vartheta_\mp p_\pm - \frac{1}{2e^f\Omega}\frac{dV_2}{d\phi} \quad (9)$$

Energy-momentum tensor

$$T_{++} = \Omega^2(\pi_+^2 - p_+^2) \quad (10)$$
$$T_{--} = \Omega^2(\pi_-^2 - p_-^2) \quad (11)$$
$$T_{+-} = -e^{-f}(V_1(\psi) + V_2(\phi)) \quad (12)$$
$$T_{zz} = e^f(\pi_+\pi_- - p_+p_-) - \frac{1}{\Omega^2}(V_1(\psi) - V_2(\phi)) \quad (13)$$

WH evolution in 5-dim. GB

in prep.

Wormholes in Gauss-Bonnet gravity (initial data on x^+)

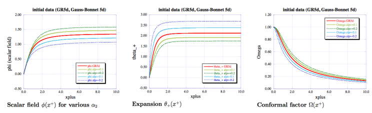

5d GR vs Gauss-Bonnet　　instability appears

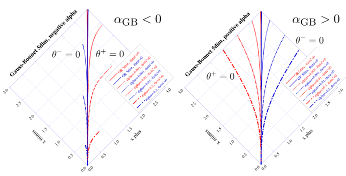

BH formation　　throat inflates

$$S = \int_{\mathcal{M}} d^{N+1}x\sqrt{-g}\Big[\frac{1}{2\kappa^2}\{\alpha_1\mathcal{R} + \alpha_2\mathcal{L}_{GB}\} + \mathcal{L}_{\text{matter}}\Big]$$

where $\mathcal{L}_{GB} = \mathcal{R}^2 - 4\mathcal{R}_{\mu\nu}\mathcal{R}^{\mu\nu} + \mathcal{R}_{\mu\nu\rho\sigma}\mathcal{R}^{\mu\nu\rho\sigma}$

shinkai@is.oit.ac.jp　　http://www.is.oit.ac.jp/~shinkai/　　@ JGRG23 workshop, Hirosaki U., 2013/11/5-8

“General Relativistic Sitnikov 3-Body Problem”

by Hideyoshi Arakida

[JGRG23(2013)P10]

P10 General Relativistic Sitnikov 3-Body Problem

Hideyoshi ARAKIDA (Nihon University)
arakida@ge.ce.nihon-u.ac.jp

1 Introduction：Sitnikov 3-Body Problem

- One of the restricted 3-body problem.
- Under the gravitational attraction due to two-equal mass primaries, third body (zero-mass test body) moves along the trajectory which is through the center of mass of primaries and perpendicular to the orbital plane of primaries.

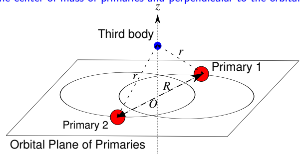

- We consider the Sitnikov 3-body problem in first-order post-Newtonian approximation.

2 Equation of Motion (EOM)

Einstein–Infeld–Hoffmann (EIH) equation: 1st post-Newtonian order $\mathcal{O}(c^{-2})$ EOM.

$$\begin{aligned}\frac{d\boldsymbol{v}_k}{dt} = &-\sum_{i\neq k}\frac{Gm_i}{r_{ki}^3}\boldsymbol{r}_{ki} + \frac{1}{c^2}\left\{\sum_{i\neq k}\frac{Gm_i}{r_{ki}^3}\boldsymbol{r}_{ki}\left[\sum_{j\neq i}\frac{Gm_j}{r_{ij}} + 4\sum_{j\neq k}\frac{Gm_j}{r_{kj}}\right.\right.\\ &\left.-\frac{1}{2}\sum_{j\neq i}\frac{Gm_j}{r_{ij}^3}(\boldsymbol{r}_{ki}\cdot\boldsymbol{r}_{ij}) + \frac{3}{2}\frac{(\boldsymbol{r}_{ki}\cdot\boldsymbol{v}_i)^2}{r_{ki}^2} - 2\boldsymbol{v}_i\cdot\boldsymbol{v}_i - \boldsymbol{v}_k\cdot\boldsymbol{v}_k + 4\boldsymbol{v}_k\cdot\boldsymbol{v}_i\right]\\ &\left.+\sum_{i\neq k}\frac{Gm_b}{r_{ki}^3}\boldsymbol{v}_{ki}[(4\boldsymbol{v}_k - 3\boldsymbol{v}_i)\cdot\boldsymbol{r}_{ki}] - \frac{7}{2}\sum_{i\neq k}\frac{Gm_i}{r_{ki}}\sum_{j\neq i}\frac{Gm_j}{r_{ij}^3}\boldsymbol{r}_{ij}\right\} + \mathcal{O}(c^{-4}),\end{aligned} \tag{1}$$

2.1 EOM of Primaries

Introducing relative coordinates: $\boldsymbol{R} = \boldsymbol{r}_1 - \boldsymbol{r}_2$, $\boldsymbol{V} = d\boldsymbol{R}/dt = \boldsymbol{v}_1 - \boldsymbol{v}_2$

$$\frac{d\boldsymbol{V}}{dt} = -\frac{GM}{R^3}\boldsymbol{R} + \frac{GM}{c^2R^3}\left\{\left[\frac{GM}{R}(4+2\nu) + \frac{3}{2}\nu\frac{(\boldsymbol{R}\cdot\boldsymbol{V})^2}{R^2} - (1+3\nu)(\boldsymbol{V}\cdot\boldsymbol{V})\right]\boldsymbol{R} + (4-2\nu)(\boldsymbol{R}\cdot\boldsymbol{V})\boldsymbol{V}\right\} \tag{2}$$

$R = |\boldsymbol{R}|, M = m_1 + m_2, \nu = m_1m_2/M^2$

2.2 EOM of third body

$m_1 = m_2 = m$, $m_3 = 0$,

$$\frac{dv_z}{dt} = -2\frac{Gm}{r^3}z + \frac{Gm}{c^2r^3}\left\{\left[\frac{5}{2}\frac{Gm}{R} + 16\frac{Gm}{r} + \frac{3}{16}\frac{(\boldsymbol{R}\cdot\boldsymbol{V})^2}{r^2} - \boldsymbol{V}\cdot\boldsymbol{V} + 6v_z^2\right]z + \frac{3}{2}(\boldsymbol{R}\cdot\boldsymbol{V})v_z\right\}, \quad \frac{dv_x}{dt} = \frac{dv_y}{dt} = 0, \tag{3}$$

$$r = |\boldsymbol{r}_{31}| = |\boldsymbol{r}_{32}| = \sqrt{\left(\frac{R}{2}\right)^2 + z^2}, \quad \boldsymbol{r}_1 = -\boldsymbol{r}_2 = \frac{1}{2}\boldsymbol{R}, \quad \boldsymbol{R} = (X, Y, 0), \quad \boldsymbol{v}_1 = -\boldsymbol{v}_2 = \frac{1}{2}\boldsymbol{V}, \quad \boldsymbol{V} = (V_X, V_Y, 0).$$

2.3 Transforming into dimensionless variables

Introducing a dimensionless gravitational radius λ: Characterized by semi-major axis a and mass M of primaries.

$$\lambda = \frac{2Gm}{c^2a} \tag{4}$$

2.3.1 Primaries

$$\frac{d\bar{\boldsymbol{V}}}{dT} = -\frac{\bar{\boldsymbol{R}}}{\bar{R}^3} + \frac{\lambda}{\bar{R}^3}\left\{\left[\frac{9}{2}\frac{1}{\bar{R}} + \frac{3}{8}\frac{(\bar{\boldsymbol{R}}\cdot\bar{\boldsymbol{V}})^2}{\bar{R}^2} - \frac{7}{4}(\bar{\boldsymbol{V}}\cdot\bar{\boldsymbol{V}})\right]\bar{\boldsymbol{R}} + \frac{7}{2}(\bar{\boldsymbol{R}}\cdot\bar{\boldsymbol{V}})\bar{\boldsymbol{V}}\right\}. \tag{5}$$

$$t = \frac{1}{n}T, \quad \boldsymbol{R} = a\bar{\boldsymbol{R}}, \quad R = a\bar{R}, \quad \boldsymbol{V} = na\bar{\boldsymbol{V}}, \quad \bar{\boldsymbol{V}} = \frac{d\bar{\boldsymbol{R}}}{dT}, \quad n = \sqrt{\frac{2Gm}{a^3}}, \tag{6}$$

2.3.2 Third body

$$\frac{d\bar{v}_z}{dT} = -\frac{\bar{z}}{\bar{r}^3} + \frac{\lambda}{\bar{r}^3}\left\{\left[\frac{5}{8}\frac{1}{\bar{R}} + \frac{4}{\bar{r}} + \frac{3}{32}\frac{(\bar{\boldsymbol{R}}\cdot\bar{\boldsymbol{V}})^2}{\bar{r}^2} - \frac{1}{2}(\bar{\boldsymbol{V}}\cdot\bar{\boldsymbol{V}}) + 3\bar{v}_z^2\right]\bar{z} + \frac{3}{4}(\bar{\boldsymbol{R}}\cdot\bar{\boldsymbol{V}})\bar{v}_z\right\}, \quad \frac{d\bar{v}_x}{dT} = \frac{d\bar{v}_y}{dT} = 0. \tag{7}$$

$$z = a\bar{z}, \quad r = a\bar{r}, \quad \bar{r} = \sqrt{\left(\frac{\bar{R}}{2}\right)^2 + \bar{z}^2}, \quad v_z = na\bar{v}_z, \quad \bar{v}_z = \frac{d\bar{z}}{dT}, \tag{8}$$

3 Numerical Experiments

Initial value of third body	$0 \leq \bar{z}_0 \leq 6,\ \delta\bar{z} = 0.05,\ \dot{\bar{z}}_0 = 0$ (Free fall from $\bar{z}_0$)
Initial value of primaries	$\bar{X} = 1 - e,\ \bar{Y} = 0,\ \dot{\bar{X}} = 0,\ \dot{\bar{Y}} = \sqrt{1-e^2}/(1-e)$ (Starting from periastron)
Range of dimensionless gravitational radius	$0 \leq \lambda \leq 0.035,\ \delta\lambda = 0.0005$
Range of Eccentricity of primaries	$0 \leq e \leq 0.9,\ \delta e = 0.1$
Integration method	Gragg's Extrapolation method based on Aitken–Neville algorithm
Integration time	1000 Kepler Periods of primaries (Maximum)
Judgment condition for unstable orbit	Kepler energy $E_K \geq 0$

Initial value dependent of stable/unstable orbits　　Escape time　　Escape velocity

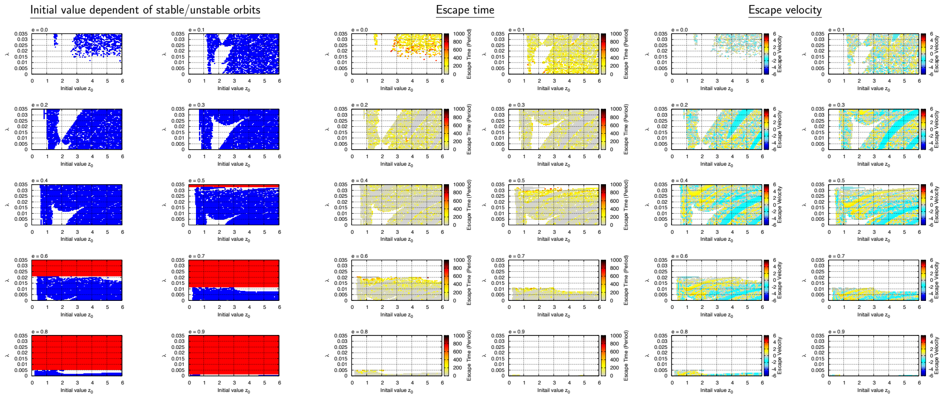

White □：In stable, Blue ■:Third body in unstable, Red ■:Primaries in unstable

$r:\ R/2$ ratio when escape　　Acceleration when escape　　Rate of surviving particles

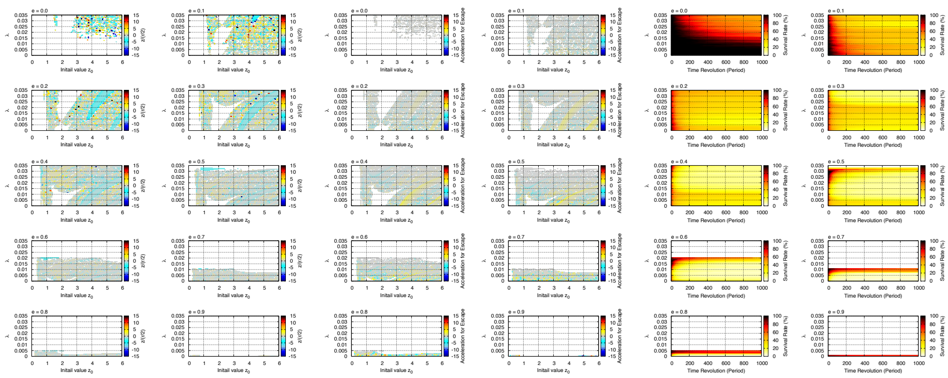

“Black Hole Universe with Lambda”

by Chulmoon Yoo

[JGRG23(2013)P11]

Black Hole Universe with Λ

Chul-Moon Yoo

Graduate School of Science, Nagoya University

△Introduction

◎BH Universe vs Dust Universe

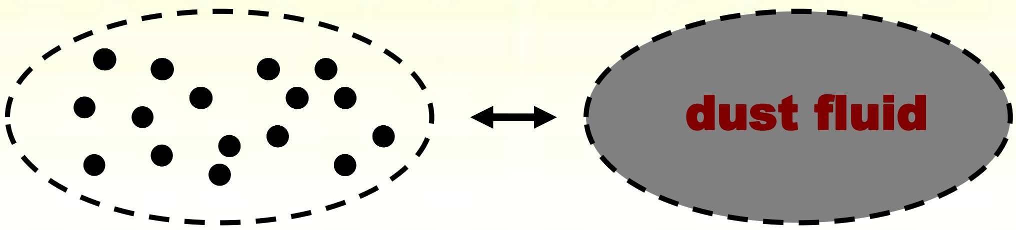

- Can global aspects of the BH universe be approximated by those of a dust universe? →Yes (see 1306.1389)
- What about with Λ?

◎What we want to do

- Construction of initial data for the BH universe with Λ
- Comparing it with a dust universe with Λ

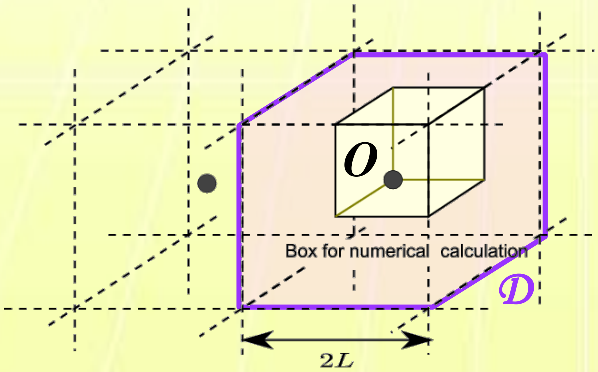

- Expanding Universe with periodically aligned BHs
- BH at the center of a cubic domain $\mathcal{D}$

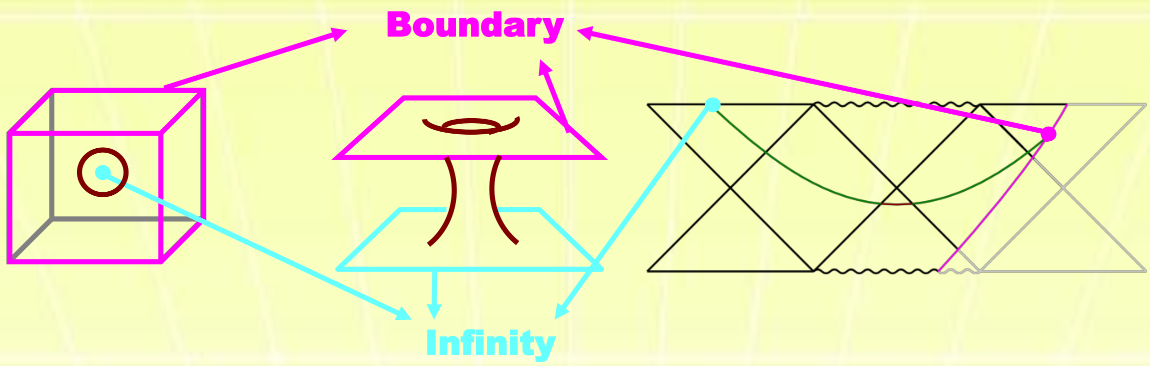

△Construction of Initial Data

◎Constraint Equations

- **Conformally flat, no TT-part of the extrinsic curvature**

$$\gamma_{ij} = \Psi^4 \delta_{ij}\ ,\quad K^{ij} = \Psi^{-10}\left[\partial^i X^j + \partial^j X^i - \frac{2}{3}\delta^{ij}\partial_k X^k\right] + \frac{1}{3}\Psi^{-4}\delta^{ij}K$$

- **Hamiltonian constraint**

$$\Delta\Psi + \frac{1}{8}(LX)_{ij}(LX)^{ij}\Psi^{-7} - \frac{1}{12}K^2\Psi^5 + \frac{1}{4}\Lambda\Psi^5 = 0$$

- **Momentum constraint**

$$\Delta X^i + \frac{1}{3}\partial^i\partial_j X^j - \frac{2}{3}\Psi^6\partial^i K = 0$$

One component is enough because of the discrete sym.

- **Form of K...?**

◎CMC slice in Kottler(Sch-dS) sol.

- **Line element**

$$\mathrm{d}s^2 = -f(r)\mathrm{d}t^2 + \frac{1}{f(r)}\mathrm{d}r^2 + r^2\mathrm{d}\Omega^2,\ f(r) = 1 - \frac{2M}{r} - \frac{\Lambda r^2}{3}$$

- **Normal vector to $t = h(r)$**

$$n^\mu = \frac{1}{\sqrt{f^{-1} - f\,h'^2}}\left(f^{-1}, fh', 0, 0\right)$$

- **constant mean curvature condition**

$$\nabla_\mu n^\mu = -K$$

- **Induced metric**

$$dl^2 = F(r;M,K)dr^2 + r^2 d\Omega^2, \quad F(r;M,K) = \left(1 - \frac{2M}{r} - \frac{1}{3}\Lambda r^2 + \frac{1}{9}K^2 r^2\right)^{-1}$$

- **Isotropic coordinate**

$$dl^2 = \Psi^4\left(dR^2 + R^2 d\Omega^2\right)$$

$$R = C\exp\left[\pm\int_{r_{min}}^{r} dr\sqrt{F(r;M,K)}\,/r\right]$$

$$\Psi = \sqrt{r/R}$$

- **Puncture structure requires**

$R = 0$ for $r \to \infty \Rightarrow K^2 = 3\Lambda$

$$\Leftrightarrow F(r;M,K) = \left(1 - \frac{2M}{r}\right)^{-1} \Rightarrow \Psi = 1 + \frac{M}{2R}$$

◎Form of K and sol. near the center

$K(\vec{x}) = K_c + (K_b - K_c)W(R)$, **where** $K_c = -\sqrt{3\Lambda}$

$$W(R) = \begin{cases} 0 & \text{for } 0 \le R \le \ell \\ \sigma^{-36}\left[(R-\sigma-\ell)^6 - \sigma^6\right]^6 & \text{for } \ell \le R \le \ell + \sigma \\ 1 & \text{for } \ell + \sigma \le R \end{cases}$$

⇒**sol. near the center** $X^i \simeq 0, \Psi \simeq 1 + \frac{M}{2R}$

- **New regular variable** ψ

$$\psi := \Psi - \frac{M}{2R}[1 - W(R)]$$

- **Hamiltonian constraint**

$$\boxed{\Delta\psi = \Delta\left(\frac{M}{2R}W(R)\right) - \frac{1}{8}(LX)_{ij}(LX)^{ij}\Psi^{-7} + \frac{1}{12}(K^2 - K_c^2)\Psi^5}$$

◎Integrability condition (integral of Hamiltonian constraint)

$$2\pi M + \frac{1}{8}\int (LX)_{ij}(LX)^{ij}\Psi^{-7}dx^3 - \frac{1}{12}\left(V_1 K_b^2 + 2V_2 K_c K_b - V_3 K_c^2\right) = 0$$

where $V_1 = \int W^2\Psi^5 dx^3$, $V_2 = \int (1-W)W\Psi^5 dx^3$, $V_3 = V_1 + 2V_2$

→**determines the value of** K_b

◎Momentum constraints

$$\boxed{\Delta Z = \frac{1}{2}\partial_i(\Psi^6 \partial^i K), \text{ where } Z = \partial_i X^i}$$

$$\boxed{\Delta X^i = -\frac{1}{3}\partial^i Z + \frac{2}{3}\Psi^6 \partial^i K}$$

△Marginal Surfaces in Initial Data

CH : cosmological horizon
BH : black hole horizon
WH: white hole horizon

I- : inner -
O- : outer -

◎Possible configurations(for $\Lambda < 1/9\mathrm{M}^{-2}$)

(a) ICH + IWH + OWH

(b) ICH + IWH + OWH + OCH

(c) ICH + IBH + OBH

(d) ICH + IBH + OBH + OCH (expected final config.)

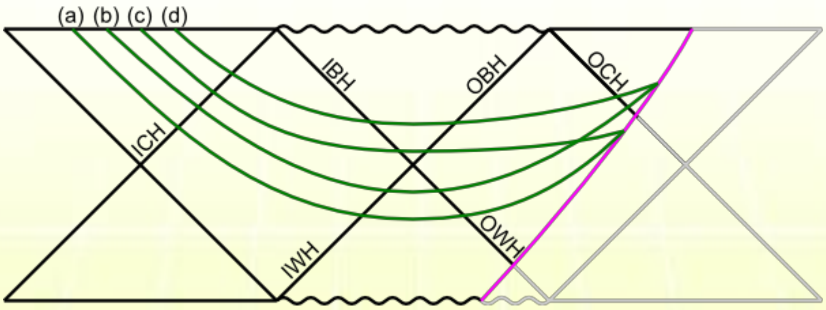

◎Equations

- null expansions

$\Theta_{\pm} = (\gamma^{ij} - s^i s^j)(\pm D_i s_j - K_{ij})$

s^i: **outgoing unit vector normal to the 2-surface**

- marginal surfaces ($r = h(\vartheta, \varphi)$)

$\Theta_+ = 0$ **for ICH, IWH, OBH ($+45°$ lines in the diagram)**

$\Theta_- = 0$ **for IBH,OWH, OCH ($-45°$ lines in the diagram)**

- **elliptic equations in polar coord.**

$$\frac{\partial^2 h}{\partial \vartheta^2} + \cot\vartheta \frac{\partial h}{\partial \vartheta} + \frac{1}{\sin^2\vartheta}\frac{\partial^2 h}{\partial \varphi^2} - (2-\eta)h = \eta h + S_{\pm}(h)$$

$S_{\pm}$**: complicated function of** h

$\eta = 1$ **for WHs and BHs,** $\eta = 3$ **for CHs**

◎Typical examples

- $\Lambda = 0.1M^{-2}, L = 2.6M$ **(case (b))**

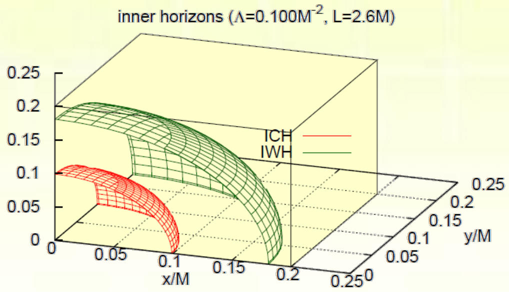

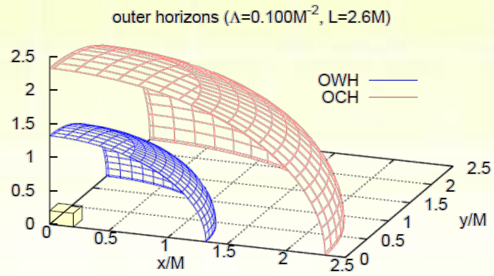

- $\Lambda = 0.111M^{-2}, L = 2.6M$ **(case (b))**

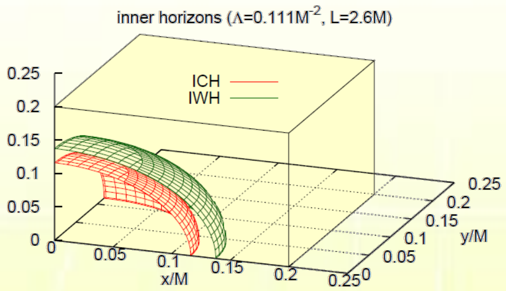

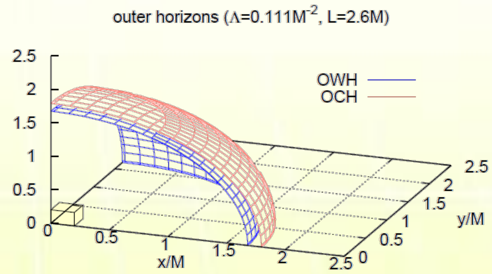

- **horizons disappear for larger** Λ **(**$\Lambda M^2 > 1/9$**)**

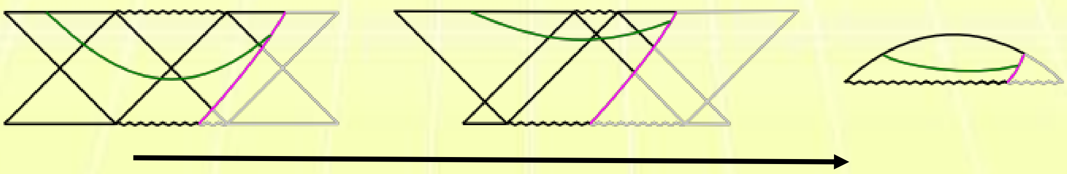

large Λ

△Time evolution

◎Gauge conditions(BSSN formalism)

- **Lapse condition**

$$\left(\frac{\partial}{\partial t} - \beta^i \frac{\partial}{\partial x^i}\right) N = -2N(K - K_\mathrm{v})$$

K_v: K **at the vertex of the box**

- **Shift condition : hyperbolic Gamma driver**

◎Transition of horizon configuration

- **Appearance of OCH: (a) → (b) ($\Lambda = 0.1M^{-2}, L = 2M$)**

initial time : (a)

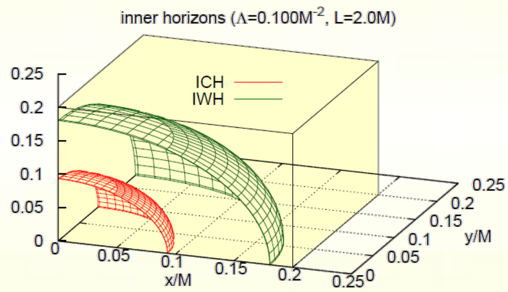

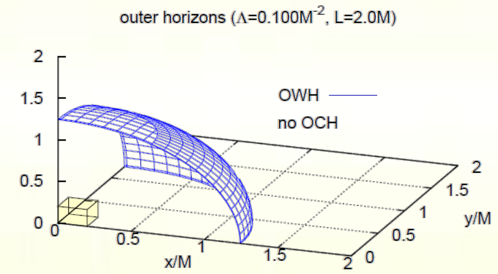

$t = 0.2M$: (b)

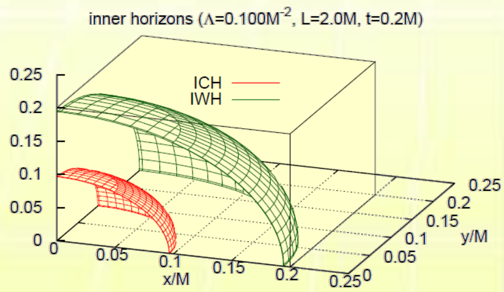

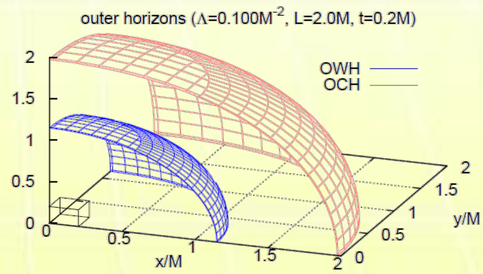

- **Bifurcation surface cross: (a) → (c) ($\Lambda = 10^{-3}M^{-2}, L = 2M$)**

initial time : (a) ⟶ $t = 0.16M$: (c)

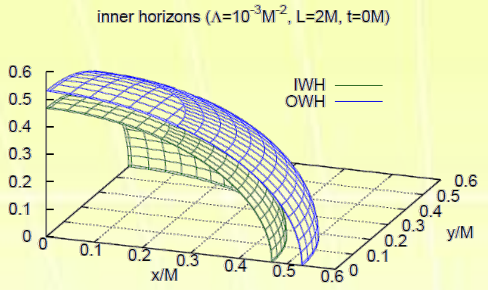

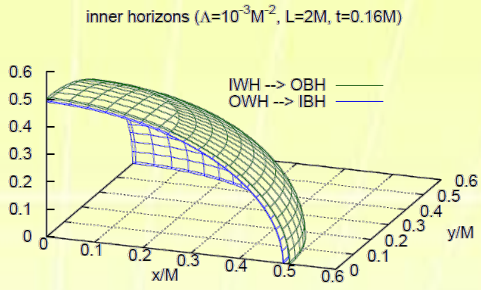

◎Cosmic expansion

- **Effective scale factor:** $a_A := \sqrt{A(\tau)}$

  τ: proper time

  $A(\tau)$: area of a face on const. proper time slice

- **Fiducial scale factor:** a_{FLRW} **(flat dust+Λ)**

$$a_{\mathrm{FLRW}} = a_{\mathrm{f}} \left[\frac{\left(1-\exp\left[\sqrt{3\Lambda}(\tau+\tau_{\mathrm{f}})\right]\right)^2}{\left(1+\exp\left[\sqrt{3\Lambda}(\tau+\tau_{\mathrm{f}})\right]\right)^2 - \left(1-\exp\left[\sqrt{3\Lambda}(\tau+\tau_{\mathrm{f}})\right]\right)^2} \right]^{1/3}$$

2 free parameters(a_{f} and τ_{f})

- **Comparison with fitting**

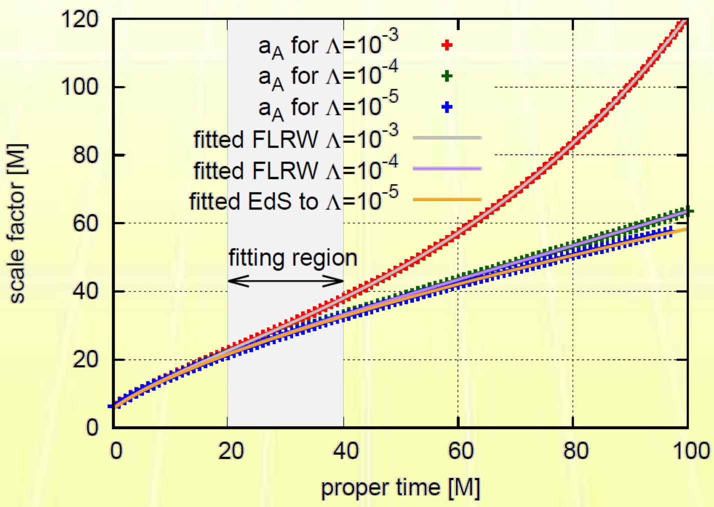

△Summary

- Black hole lattice universe with Λ is simulated
- The vacuum Einstein equations in a cubic box with a black hole at the origin, periodic boundary
- Configuration of marginal surfaces is analyzed
- Comparison between effective scale factor a_A and a_{FLRW}

◎**Behavior of the effective scale factor is well approximated by that in the FLRW universe even with Λ**

“Modeling of the secular evolution of a inspiral orbit around a Kerr black hole”

by Norichika Sago

[JGRG23(2013)P12]

Modeling of the secular evolution of an inspiral orbit around a Kerr black hole

Kyushu University
Norichika Sago

with S. Isoyama, T. Tanaka, R. Fujita, H. Nakano

九州大学
KYUSHU UNIVERSITY

JGRG23 at Hirosaki University
5-8 November 2013

KYUSHU UNIVERSITY 2011
100th Anniversary

Introduction

- Extreme Mass Ratio Inspiral (EMRI) is a candidate of GW targets.
- GW analysis requires accurate prediction of the dynamics and GW waveforms.
- Self-force picture in BH perturbation theory can describe EMRI well.
- Currently, calculations of the instantaneous SF are developed.
- Still, there are several issues to incorporate the SF effect to the long term orbital evolution and GW waveform.

Aiming to solve the issues, we study a new formulation to describe and solve the equation of motion of a particle in Kerr geometry based on Hamiltonian mechanics.

Kerr spacetime

Kerr metric in the Boyer-Lindquist coordinate

$$g^{(0)}_{\mu\nu}dx^\mu dx^\nu = -\left(1-\frac{2Mr}{\Sigma}\right)dt^2 - \frac{4Mar\sin^2\theta}{\Sigma}dtd\phi + \frac{\Sigma}{\Delta}dr^2 + \Sigma d\theta^2 + \left(r^2+a^2+\frac{2Ma^2r}{\Sigma}\sin^2\theta\right)\sin^2\theta d\phi^2$$

$$\Sigma \equiv r^2 + a^2\cos^2\theta$$
$$\Delta \equiv r^2 - 2Mr + a^2$$

Kinnersley null tetrad

$$l^\mu = \frac{1}{\Delta}(r^2+a^2, \Delta, 0, a),$$

$$n^\mu = \frac{1}{2\Sigma}(r^2+a^2, -\Delta, 0, a),$$

$$m^\mu = \frac{1}{\sqrt{2}(r+ia\cos\theta)}\left(ia\sin\theta, 0, 1, \frac{i}{\sin\theta}\right)$$

Killing vector/tensor

$$\xi^\mu_{(t)} = (1,0,0,0),$$

$$\xi^\mu_{(\phi)} = (0,0,0,1),$$

$$K_{\mu\nu} = 2\Sigma l_{(\mu}n_{\nu)} + r^2 g^{(0)}_{\mu\nu}$$

3

Bound geodesics in Kerr geometry

Hamiltonian for a test particle in Kerr spacetime

$$H_{(0)}\left(x^\mu, p^{(0)}_\mu\right) = \frac{1}{2m} g^{\alpha\beta}_{(0)}(x^\rho) p^{(0)}_\alpha p^{(0)}_\beta$$

Constants of motion

mass : m

energy : $E^{(0)} = -p^{(0)}_\alpha \xi^\alpha_{(t)}$

angular momentum : $L^{(0)}_z = p^{(0)}_\alpha \xi^\alpha_{(\phi)}$

Carter constant : $C^{(0)} = K^{\alpha\beta}p^{(0)}_\alpha p^{(0)}_\beta - (aE^{(0)} - L^{(0)}_z)^2$

For simplicity, label these constants

$$P_0 = -\frac{m^2}{2}, \qquad P_1 = E^{(0)}, \qquad P_2 = L^{(0)}_z, \qquad P_3 = C^{(0)}$$

4

Action variables (unperturbed case)

Introduce an action variables J_μ [Schmidt (2002)]:

$$J_t = -E^{(0)}, \quad J_\phi = L_z^{(0)}, \quad J_r = \frac{1}{2\pi}\oint \frac{\sqrt{R(r)}}{\Delta} dr, \quad J_\theta = \frac{1}{2\pi}\oint \sqrt{\Theta(\theta)} d\theta$$

$$R(r) = \left\{(r^2+a^2)E^{(0)} - aL_z^{(0)}\right\}^2 - \Delta\left\{m^2 r^2 + \left(L_z^{(0)} - aE^{(0)}\right)^2 + C^{(0)}\right\}$$

$$\Theta(\theta) = C^{(0)} - \left\{(m^2 - E^{(0)2})a^2 + \frac{L_z^{(0)2}}{\sin^2\theta}\right\}\cos^2\theta$$

These variables can be expressed as functions of constants of motion:

$$J_\mu = f_\mu(P_\alpha) \qquad (f \text{ is bijective and } C^\infty)$$

The corresponding coordinates (action angle variables) are given by

$$q^\mu = \frac{\partial W(x^\nu, P_\alpha)}{\partial J_\mu} = \frac{\partial W(x^\nu, f_\alpha^{-1}(J_\nu))}{\partial J_\mu}$$

where the generating function is given by [Carter (1968)] :

$$W(x^\mu, P_\alpha) = -E^{(0)}t + L_z^{(0)}\phi + \int^r \frac{\sqrt{R(r')}}{\Delta} dr' + \int^\theta \sqrt{\Theta(\theta')} d\theta'$$

Perturbed orbits in Kerr geometry

Perturbed orbits can be expressed by the geodesics for the effective metric [Mino-Sasaki-Tanaka(1997), Detweiler-Whiting (2003)]:

$$g_{\alpha\beta}[x^\mu;\gamma] = g_{\alpha\beta}^{(0)}(x^\mu) + h_{\alpha\beta}^{(R)}[x^\mu;\gamma]$$

$h_{\alpha\beta}^{(R)}$: regularized metric perturbation
γ : trajectory of the particle

The effective Hamiltonian for a point mass is given by

$$H_{\rm eff}[x^\mu, p_\mu; \gamma] = \frac{1}{2m} g^{\alpha\beta}[x^\mu;\gamma] p_\alpha p_\beta$$
$$= \underbrace{H_{(0)}(x^\mu, p_\mu)}_{\text{background}} + \underbrace{H_{\rm int}[x^\mu, p_\mu; \gamma]}_{\text{interaction}}$$

$$H_{(0)}(x^\mu, p_\mu) \equiv \frac{1}{2m} g_{(0)}^{\alpha\beta}(x^\mu) p_\alpha p_\beta \qquad H_{\rm int}[x^\mu, p_\mu;\gamma] \equiv -\frac{1}{2m} h_{(R)}^{\alpha\beta}[x^\rho;\gamma] p_\alpha p_\beta$$

"Action variables" (perturbed case)

Introduce the generating function

$$W(x^\mu, P_\alpha) = -\mathcal{E}t + \mathcal{L}_z\phi + \int^r \frac{\sqrt{R(r')}}{\Delta}dr' + \int^\theta \sqrt{\Theta(\theta')}d\theta'$$

$$R(r) = \{(r^2+a^2)\mathcal{E} - a\mathcal{L}_z\}^2 - \Delta\{\mu^2 r^2 + (\mathcal{L}_z - a\mathcal{E})^2 + C\}$$

$$\Theta(\theta) = C - \left\{(\mu^2 - \mathcal{E}^2)a^2 + \frac{\mathcal{L}_z^2}{\sin^2\theta}\right\}\cos^2\theta$$

with the following variables

$$P_0 = -\frac{\mu^2}{2}, \qquad P_1 = \mathcal{E}, \qquad P_2 = \mathcal{L}_z, \qquad P_3 = C$$

Define "action variables" by the relation in unperturbed case:

$$J_\mu = f_\mu(P_\alpha)$$

Then the other associated phase space variables are given by

$$p_\mu = \frac{\partial W\,(x^\nu, P_\alpha)}{\partial x^\mu}, \qquad q^\mu = \frac{\partial W\,(x^\nu, P_\beta)}{\partial J_\mu} = \frac{\partial W\,(x^\nu, f_\alpha^{-1}(J_\nu))}{\partial J_\mu}$$

EOM in Hamiltonian mechanics

Rewrite the Hamiltonian in (x^μ, J_μ) : $H(x^\sigma, J_\sigma) \equiv H(x^\sigma, p_\sigma(x^\nu, J_\nu))$

Hamiltonian equation for J_μ

$$\frac{dJ_\mu}{d\tau} = -\left(\frac{\partial H(x^\sigma, J_\sigma)}{\partial q^\mu}\right)_{J_\sigma} = -\left(\frac{\partial x^\nu}{\partial q^\mu}\frac{\partial H(x^\sigma, J_\sigma)}{\partial x^\nu}\right)_{J_\sigma} = -\left(\frac{\partial J_\mu}{\partial p_\nu}\right)_{x^\sigma}\left(\frac{\partial H_{\text{int}}(x^\sigma, J_\sigma)}{\partial x^\nu}\right)_{J_\sigma}$$

using the following relation

$$\left(\frac{\partial p_\nu}{\partial J_\mu}\right)_{x^\sigma} = \frac{\partial W(x^\sigma, J_\sigma)}{\partial x^\nu \partial J_\mu} = \left(\frac{\partial q^\mu}{\partial x^\nu}\right)_{J_\sigma}$$

$$H(x^\sigma, J_\sigma) = H_{(0)}(x^\sigma, J_\sigma) + H_{\text{int}}(x^\sigma, J_\sigma)$$

$$H_{(0)}(x^\sigma, J_\sigma) = -\frac{\mu^2}{2} = P_0 = f_0^{-1}(J_\sigma)$$

This expression coincides with that in the previous work [NS et al. (2005)].

Hamiltonian equation for q^μ

$$\frac{dq^\mu}{d\tau} = -\left(\frac{\partial H(x^\sigma, J_\sigma)}{\partial J_\mu}\right)_{J_\sigma} = \Omega^\mu(J_\sigma) + \left(\frac{\partial H_{\text{int}}(x^\sigma, J_\sigma)}{\partial J_\mu}\right)_{J_\sigma} \qquad \Omega^\mu(J_\sigma) \equiv \frac{\partial H_{(0)}}{\partial J_\mu}$$

Interaction Hamiltonian H_{int} is important to determine the dynamics.

Radiative and symmetric pieces

The interaction Hamiltonian is expressed as

$$H_{\rm int}[x^\mu, p_\mu; \gamma] = \frac{m}{2}\int_{-\infty}^{\infty} d\tau' G^{(R)\alpha\beta}_{\rho'\sigma'}[x, z(\tau')] p_\alpha p_\beta u^{\rho'} u^{\sigma'}$$

The regularized Green function can be divided into the radiative and symmetric pieces:

$$\begin{aligned} G^{(R)}(x,x') &= G^{(\rm ret)}(x,x') - G^{(\rm S)}(x,x') \\ &= G^{(\rm rad)}(x,x') + G^{(\rm sym-S)}(x,x') \end{aligned}$$

$$G^{(\rm rad)} = \frac{G^{(\rm ret)} - G^{(\rm adv)}}{2}, \quad G^{(\rm sym-S)} = \frac{G^{(\rm ret)} + G^{(\rm adv)}}{2} - G^{(\rm S)}$$

Following this splitting,

$$H_{\rm int}[x^\mu, p_\mu; \gamma] = H^{(\rm rad)}_{\rm int}[x^\mu, p_\mu; \gamma] + H^{(\rm sym-S)}_{\rm int}[x^\mu, p_\mu; \gamma]$$

Radiative piece
- including the dissipative effect
- regular at the particle's position

Symmetric piece
- only conservative effect
- need regularization

Secular approximation of Hamiltonian eqs.

Introduce a slow time variable: $\tilde{\tau} \equiv \epsilon\tau \quad (\epsilon \ll 1)$

Divide (q, J) into the secular and oscillatory parts:

$$\begin{aligned} q^\mu(\tau,\epsilon) &= \bar{q}^\mu(\tilde{\tau}) + \epsilon q^\mu_{(1)}(\Psi^\nu, \tilde{\tau}) + O(\epsilon^2) \\ J_\mu(\tau,\epsilon) &= \bar{J}_\mu(\tilde{\tau}) + \epsilon J^{(1)}_\mu(\Psi^\nu, \tilde{\tau}) + O(\epsilon^2) \end{aligned}$$

Ψ^ν: phase variables
($\Psi^\nu = \bar{q}^\mu(\tilde{\tau})$ at 0th order)

Secular term
(contains all order of ϵ)

Oscillatory term (no secular growth)
The leading term is at $O(\epsilon)$.

Then, the Hamiltonian eqs. can be divided into the corresponding parts:

$$\frac{d\bar{q}^\mu}{d\tilde{\tau}} = \Omega^\mu[\bar{J}_\nu(\tilde{\tau})] + \left\langle \frac{\partial H^{(R)}_{\rm int}[q^\nu, J_\nu]}{\partial J_\mu} \right\rangle_\tau$$

$$\frac{d\bar{J}_\mu}{d\tilde{\tau}} = \left\langle \frac{\partial H^{(R)}_{\rm int}[q^\nu, J_\nu]}{\partial q^\mu} \right\rangle_\tau$$

$$\frac{dq^\mu_{(1)}}{d\tilde{\tau}} = \frac{\partial \Omega^\mu[\bar{J}_\nu(\tilde{\tau})]}{\partial J_\sigma} J^{(1)}_\sigma + \left(\frac{\partial H^{(R)}_{\rm int}[q^\nu, J_\nu]}{\partial J_\mu} - \left\langle \frac{\partial H^{(R)}_{\rm int}[q^\nu, J_\nu]}{\partial J_\mu} \right\rangle_\tau \right)$$

$$\frac{dJ^{(1)}_\mu}{d\tilde{\tau}} = \frac{\partial H^{(R)}_{\rm int}[q^\nu, J_\nu]}{\partial q^\mu} - \left\langle \frac{\partial H^{(R)}_{\rm int}[q^\nu, J_\nu]}{\partial q^\mu} \right\rangle_\tau$$

Since $(q^\mu_{(1)}, J^{(1)}_\mu)$ give only the higher order contribution,
(q^ν, J_ν) can be replaced with $(\bar{q}^\mu, \bar{J}_\mu)$ at the leading order.

Osculating geodesic approximation

Replace the secular terms with the geodesics approximately:

$$\begin{aligned} \bar{q}^{\mu}(\tau) &= \boxed{q^{\mu}_{(\mathrm{osc})}(\tau;\tau_0)} + \boxed{\Delta\bar{q}^{\mu}(\tau;\tau_0)} \\ \bar{J}_{\mu}(\tilde{\tau}) &= \boxed{J^{(\mathrm{osc})}_{\mu}(\tau_0)} + \boxed{\Delta\bar{J}_{\mu}(\tau;\tau_0)} \end{aligned}$$

errors

Bound geodesic with the initial value, $\{\bar{q}^{\mu}(\tau_0),\ \bar{J}_{\mu}(\tau_0)\}$ at $\tau = \tau_0$

Parity for the transformation $(t,r,\theta,\phi) \to (-t,r,\theta,-\phi)$

q^{μ}, $H^{(\mathrm{rad})}_{\mathrm{int}}$: odd parity $\qquad$ J_{μ}, $H^{(\mathrm{sym-S})}_{\mathrm{int}}$: even parity

Using these properties, the secular EOM can be expressed by:

$$\frac{d\bar{q}^{\mu}}{d\tilde{\tau}} = \Omega^{\mu}[\bar{J}_{\nu}(\tilde{\tau})] + \left\langle \frac{\partial H^{(\mathrm{sym-S})}_{\mathrm{int}}[q^{\nu}_{(\mathrm{osc})}, J^{(\mathrm{osc})}_{\nu}]}{\partial J_{\mu}} \right\rangle_{\tau}, \qquad \frac{d\bar{J}_{\mu}}{d\tilde{\tau}} = \left\langle \frac{\partial H^{(\mathrm{rad})}_{\mathrm{int}}[q^{\nu}_{(\mathrm{osc})}, J^{(\mathrm{osc})}_{\nu}]}{\partial q^{\mu}} \right\rangle_{\tau}$$

$\bar{q}^{\mu}$ is determined by averaged $H^{(\mathrm{sym-S})}_{\mathrm{int}}$, while $\bar{J}_{\mu}$ by averaged $H^{(\mathrm{rad})}_{\mathrm{int}}$.

11

Gauge invariance of averaged H_{int}

Physically acceptable gauge transformation

$$h^{(\mathrm{new})}_{\mu\nu} = h^{(\mathrm{old})}_{\mu\nu} + \nabla_{\mu}\xi_{\nu} + \nabla_{\nu}\xi_{\mu}$$

where $\xi^{\mu}[z^{\alpha}(\lambda)]$ has no secular growth.

This gauge transformation does not break the perturbation scheme.

Under this gauge transformation,

$$H^{(\mathrm{new})}_{\mathrm{int}}[x^{\mu}, p_{\mu}; \bar{\zeta}^{I}_{(\mathrm{osc})}] = H^{(\mathrm{old})}_{\mathrm{int}}[x^{\mu}, p_{\mu}; \bar{\zeta}^{I}_{(\mathrm{osc})}] + \Sigma \frac{d}{d\lambda}(\xi^{\mu} p_{\mu})$$

Taking the long term average, the gauge-dependent term vanishes:

$$\boxed{\left\langle H^{(\mathrm{new})}_{\mathrm{int}}[x^{\mu}, p_{\mu}; \bar{\zeta}^{I}_{(\mathrm{osc})}] \right\rangle_{\tau} = \left\langle H^{(\mathrm{old})}_{\mathrm{int}}[x^{\mu}, p_{\mu}; \bar{\zeta}^{I}_{(\mathrm{osc})}] \right\rangle_{\tau}}$$

12

Summary

- Formulate the orbital evolution of a point mass in Kerr geometry in Hamiltonian mechanics.
- The secular evolution can be expressed by the averaged interaction Hamiltonian in a gauge invariant manner.

$\bar{q}^{\mu}$ is determined by averaged $H_{\rm int}^{\rm (sym-S)}$.
$\bar{J}_{\mu}$ is determined by averaged $H_{\rm int}^{\rm (rad)}$.

Toward the post-adiabatic order:

- Evaluate the error of the osculating approximation
- Estimate 2nd order effects (including oscillatory parts)
- The oscillatory parts become more important in resonance case.

“Spin-Regge-Wheeler-Zerilli formalism and gravitational waves”

by Hiroyuki Nakano

[JGRG23(2013)P13]

Spin-Regge-Wheeler-Zerilli Formalism and Gravitational Waves

Hiroyuki Nakano

Y. Zlochower, C. O. Lousto, M. Campanelli

YITP, Kyoto University
CCRG, Rochester Institute of Technology

JGRG23, Hirosaki University, November 5-8, 2013

Intermediate-mass-ratio binary black holes

Mass ratio: $1/10 \geq q \geq 1/100$ for binary black holes (BBHs)

"Full numerical simulations" (NR):

Challenge in the exploration of the extremes of BBH parameter space

"Analytic treatments" (AR): Which is a better description?

Post-Newtonian (PN) approach

Effective One Body approach

Gravitational self-force [See (P12) by Norichika Sago] in Black Hole Perturbation (BHP) and so on.

Simple as possible : We use

- Regge-Wheeler-Zerilli formalism (BHP) + remnant BH's spin
- TaylorT4 orbital phase evolution (PN) + fitting parameters

Final remnant of BBH mergers

Final remnant black hole's spin after BBH merger in NR,

Mass ratio	$q = 1/10$	$q = 1/15$	$q = 1/100$
Non-dim. spin	0.261 ± 0.002	0.189 ± 0.006	0.0332 ± 0.0001

Lousto *et al.*, Phys. Rev. D82, 104057 (2010).

- We want to introduce the spin effect into the black hole perturbation approach.
- The background BH has mass ($M = m_1 + m_2$) and a particle ($\mu = m_1 m_2 / M$) orbits around the BH.

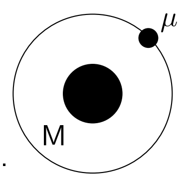

Analytic, perturbative approach

Spin-Regge-Wheeler-Zerilli (SRWZ) formalism

Lousto *et al.*, Phys. Rev. D82, 104057 (2010).

- Extension of the RWZ for Schwarzschild perturbations.
- We include a term linear in the remnant BH's spin perturbatively.
- Coupling between linear waves and the spin is discussed in 2nd order perturbations.

$$\Psi_{\ell m}(t,r) = \Psi^{(1)}_{\ell m}(t,r) + \Psi^{(2)}_{\ell m}(t,r) \,,$$
$$\Psi^{(\mathrm{o})}_{\ell m} = \Psi^{(\mathrm{o},1)}_{\ell m}(t,r) + 2 \int dt\, \Psi^{(\mathrm{o,Z},2)}_{\ell m}(t,r) \,,$$

$\Psi^{(1)}_{\ell m}$, $\Psi^{(2)}_{\ell m}$: Even parity Zerilli function

$\Psi^{(\mathrm{o},1)}_{\ell m}$: Odd parity Regge-Wheeler function

$\Psi^{(\mathrm{o,Z},2)}_{\ell m}$: Odd parity Zerilli function

The SRWZ formalism

Example (even parity wave equation)

$$-\frac{\partial^2}{\partial t^2}\Psi_{\ell m}(t,r)+\frac{\partial^2}{\partial r^{*2}}\Psi_{\ell m}(t,r)-V_\ell^{(\mathrm{even})}(r)\Psi_{\ell m}(t,r)+i\,m\,\chi\,\hat{P}_\ell^{(\mathrm{even})}\Psi_{\ell m}(t,r)$$
$$=S_{\ell m}^{(\mathrm{even})}(t,r;r_p(t),\phi_p(t))\,,$$

$(t,\,r,\,\theta,\,\phi)$:	Background Schwarzschild coordinates $r^*=r+2M\ln[r/(2M)-1]$
$(\ell,\,m)$:	Harmonic decomposition for $(\theta,\,\phi)$
χ:	Nondimensional spin parameter
$V_\ell^{(\mathrm{even})}$:	Potential
$\hat{P}_\ell^{(\mathrm{even})}$:	Differential operator
$S_{\ell m}^{(\mathrm{even})}$:	Source term (with 2nd order effects, including the mode couplings)

- It is noted that the SRWZ formalism gives a reasonable result for $-0.3<\chi<0.3$ (from the analysis of quasinormal modes).
- We need the particle's trajectory $(r_p(t),\phi_p(t))$.

Check: Quasinormal modes

Quasinormal mode frequencies for various χ

- Considering only the dominant harmonics, $\ell=2$, $m=2$, i.e., ignoring the mode couplings.
- The second and third columns are shown as $\rho=-i\omega_{\mathrm{QNM}}$.
- Numerical analysis in the third column by [Glampedakis and Andersson (2003)].
- Note that the even and odd parity equations become same via "Chandrasekhar transformation".

χ	$m=2$ (SRWZ)	$m=2$ (Numerical)	$\mathrm{Err}_{\Re}$	$\mathrm{Err}_{\Im}$
−0.5	−0.176825 − 0.643379 i	−0.178062 − 0.648614 i	−0.006947	0.008071
−0.4	−0.177466 − 0.661283 i	−0.178262 − 0.664916 i	−0.004465	0.005463
−0.3	−0.177930 − 0.680440 i	−0.178368 − 0.682666 i	−0.002455	0.003260
−0.2	−0.178181 − 0.701019 i	−0.178364 − 0.702106 i	−0.001025	0.001548
−0.1	−0.178186 − 0.723233 i	−0.178228 − 0.723536 i	−0.000235	0.000418
0.0	−0.177923 − 0.747340 i	−0.177924 − 0.747344 i	−0.000005	0.000005
0.1	−0.177398 − 0.773654 i	−0.177412 − 0.774036 i	−0.000078	0.000493
0.2	−0.176662 − 0.802534 i	−0.176622 − 0.804290 i	0.000226	0.002183
0.3	−0.175836 − 0.834372 i	−0.175458 − 0.839054 i	0.002154	0.005580
0.4	−0.175116 − 0.869549 i	−0.173764 − 0.879684 i	0.007780	0.011521
0.5	−0.174747 − 0.908398 i	−0.171278 − 0.928246 i	0.020253	0.021382

Trajectory: Orbital frequency Ω evolution

Time evolution of the orbital frequency:

Based on TaylorT4 evolution [Boyle *et al.* (2007)]

$$\frac{d\Omega}{dt} = \frac{96}{5}\,\Omega^{11/3} M^{5/3} \eta \left(1 + B\,(\Omega/\Omega_0)^{\beta/3}\right)^{-1} \Bigg[1 + \left(-\frac{743}{336} - \frac{11}{4}\,\eta\right)(M\Omega)^{2/3} + 4\,\pi\,M\Omega$$
$$+ \left(\frac{34103}{18144} + \frac{13661}{2016}\,\eta + \frac{59}{18}\,\eta^2\right)(M\Omega)^{4/3} + \left(-\frac{4159}{672}\,\pi - \frac{189}{8}\,\eta\,\pi\right)(M\Omega)^{5/3}$$
$$+ \left(\frac{16447322263}{139708800} + \frac{16}{3}\,\pi^2 - \frac{1712}{105}\,\gamma - \frac{1712}{315}\,\ln(64\,M\Omega) - \frac{56198689}{217728}\,\eta + \frac{451}{48}\,\eta\,\pi^2 + \frac{541}{896}\,\eta^2\right.$$
$$\left. - \frac{5605}{2592}\,\eta^3\right)(M\Omega)^2 + \left(-\frac{4415}{4032}\,\pi + \frac{358675}{6048}\,\eta\,\pi + \frac{91495}{1512}\,\eta^2\pi\right)(M\Omega)^{7/3} + A\,(\Omega/\Omega_0)^{\alpha/3}\Bigg],$$

$$\Omega = \frac{d\phi}{dt}, \quad M = m_1 + m_2\,, \quad \eta = \frac{m_1 m_2}{M^2}\,,$$

- We introduce A, α, B and β: **Fitting parameters**
- $M\Omega_0 = (1/3)^{3/2} \sim 0.19$ at $R_{\rm Sch} = 3M$ for circular orbit.
- $\alpha > 7$ and $\beta > 7$ to be consistent with the 3.5PN formula.

Trajectory: Orbital radius

Orbital radius:

Based on the ADM (Arnowitt, Deser and Misner)-TT PN
(NR coordinates $\sim$ ADM-TT
$\sim$ "trumpet" stationary $1 +$ log slice of Schwarzschild)

$$R = \frac{M}{(M\Omega)^{2/3}} \Bigg[1 + \left(-1 + \frac{1}{3}\,\eta\right)(M\Omega)^{2/3} + \left(-\frac{1}{4} + \frac{9}{8}\,\eta + \frac{1}{9}\,\eta^2\right)(M\Omega)^{4/3}$$
$$+ \left(-\frac{1}{4} - \frac{1625}{144}\,\eta + \frac{167}{192}\,\eta\,\pi^2 - \frac{3}{2}\,\eta^2 + \frac{2}{81}\,\eta^3\right)(M\Omega)^2\Bigg] / \left(1 + a_0(\Omega/\Omega_0)^{a_1}\right) + C\,,$$

- R and Ω: in the NR coordinates
- a_0, a_1, C: **Fitting parameters**
- $M\Omega_0 = (1/3)^{3/2} \sim 0.19$
- $a_1 > 2$ to be consistent with the 3PN calculation.

C (looks like 1PN)

Inconsistent with the ADM-TT PN formula. → But, we need!

Trajectory: Fitting for orbital frequency and radius

Fitting parameters:

- For the orbital frequency

Mass-ratio	A	α	B	β
$q = 1/10$	17.0500	7.21975 (> 7)	8.18920	12.5197 (> 7)
$q = 1/15$	26.0150	7.54047 (> 7)	8.65525	13.6168 (> 7)
$q = 1/100$	93.0650	4.32071 (< 7)	5.42457	14.9711 (> 7)

- For the orbital radius

Mass-ratio	C	a_0	a_1
$q = 1/10$	0.216953 $(\neq 0)$	0.513214	4.68472 (> 2)
$q = 1/15$	0.237427 $(\neq 0)$	0.600321	4.57899 (> 2)
$q = 1/100$	0.198137 $(\neq 0)$	0.923360	5.29681 (> 2)

Nakano *et al.*, Phys. Rev. D84, 124006 (2011).

Wave calculation in the SRWZ formalism

1. Radial transformation to remove the offset C between the NR and the "trumpet" coordinates by assuming $T_{\rm NR} = T_{\rm Log}$,

$$R_{\rm NR} \to R_{\rm Log} = R_{\rm NR} - C\,.$$

2. Coordinate transformation to the standard Schwarzschild coordinates

$$(T_{\rm Log},\, R_{\rm Log}) \to (T_{\rm Sch},\, R_{\rm Sch})\,,$$

Final plunge trajectory:

Plunging (Schwarzschild) orbit from a matching radius $R_{\rm M} \sim 3M$ to the horizon $R = 2M$: Geodesic without the radiation reaction.

The SRWZ waveforms at a sufficiently distant location $R_{\rm Obs}$:

$$\frac{R_{\rm Obs}}{M}\,(h_+ - i\,h_\times) = \sum_{\ell m} \frac{\sqrt{(\ell-1)\ell(\ell+1)(\ell+2)}}{2M} \left(\Psi_{\ell m}^{\rm (even)} - i\,\Psi_{\ell m}^{\rm (odd)}\right) {}_{-2}Y_{\ell m}\,.$$

Short summary for wave calculation

Extended TaylorT4 (Trajectory)
$+$
SRWZ formalism (Wave generation)

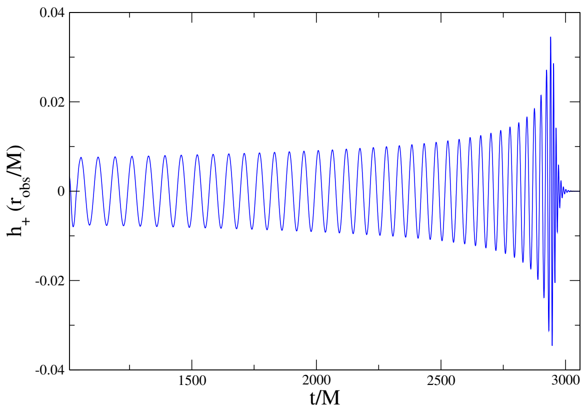

Wave extrapolation for NR waveforms

Relation between the Weyl scalar ψ_4 and the wave strain h:

$$h = h_+ - ih_\times = \int_{-\infty}^{t} dt' \int_{-\infty}^{t'} dt'' \psi_4 \,.$$

- In NR, ψ_4 is typically extracted at a finite radius ($r_{\rm Ext}$).
- To extrapolate $\psi_4^{\ell m}(r = r_{\rm Ext}, t)$ to $r \to \infty$, we may use a **perturbative formula** as

$$\lim_{r\to\infty} [r\,\psi_4^{\ell m}(r,t)] = \left[r\,\psi_4^{\ell m}(r,t) - \frac{(\ell-1)(\ell+2)}{2} \int_0^t dt\, \psi_4^{\ell m}(r,t) \right]_{r=r_{\rm Ext}} + O(r_{\rm Ext}^{-2}) \,.$$

- This formula gives reliable extrapolations for $r_{\rm Ext} \gtrsim 100M$. (from numerical study by [Babiuc *et al.* (2011)])
- For $\psi_4 \to h$, PYGWANALYSIS code [Reisswig and Pollney (2011)] in EINSTEINTOOLKIT

Results: Gravitational wave phase ($q = 1/10$)

NR vs. SRWZ waveforms

$q = 1/10$, $\phi = 0$ at $t = -830M$.

$(\ell = 2,\ m = 2)$

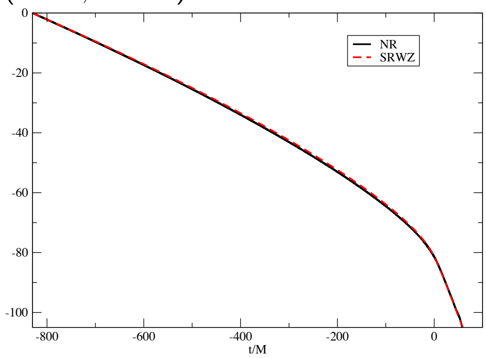

$(\ell = 2,\ m = 1)$

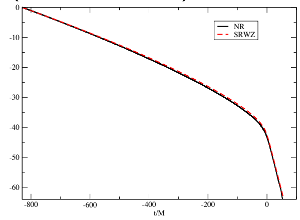

$(\ell = 3,\ m = 3)$

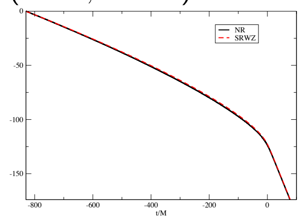

Results: Gravitational wave phase ($q = 1/15$)

NR vs. SRWZ waveforms

$q = 1/15$, $\phi = 0$ at $t = -600M$.

$(\ell = 2,\ m = 2)$

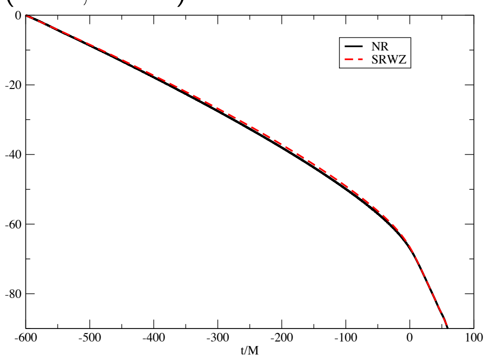

$(\ell = 2,\ m = 1)$

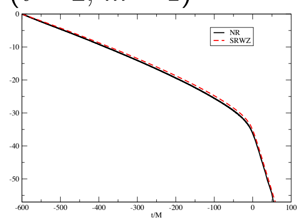

$(\ell = 3,\ m = 3)$

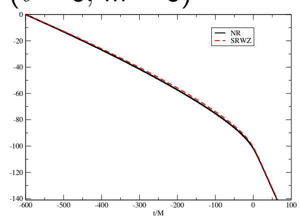

Results: Gravitational wave phase ($q = 1/100$)

NR vs. SRWZ waveforms

$q = 1/100$, $\phi = 0$ at $t = -85M$.

$(\ell = 2,\ m = 2)$

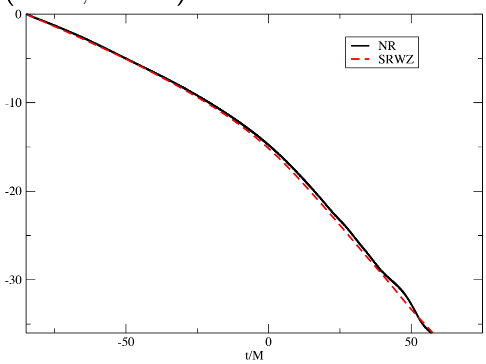

$(\ell = 2,\ m = 1)$

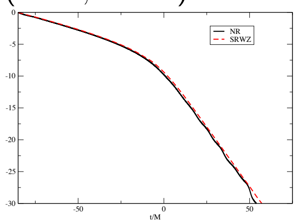

$(\ell = 3,\ m = 3)$

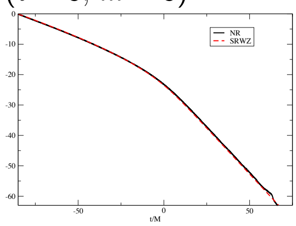

Matching and Summary

Match between the NR and SRWZ $(\ell = 2,\ m = 2)$ GWs in aLIGO (Zero Det, High Power). (Integration from $f_{\rm low} \sim 10$Hz.)

	$q = 1/10$	$q = 1/15$	$q = 1/100$
Range ($M\Omega_{22}$)	≥ 0.075	≥ 0.09	≥ 0.15
Total mass ($M_\odot$)	242	290	484
$\mathcal{M}_{22}$	0.994669	0.996039	0.995477

- Currently, we have only one approach, the effective-one-body approach (calibrated numerically) to treat gravitational waves from intermediate-mass-ratio BBHs.
- The SRWZ formalism is an alternative (and fast for calculating various GW modes).
- **Next plan** : Using longer NR simulations for various q cases, $\rightarrow$ Fitting parameters in fitting functions for the trajectory

$$(A,\ \alpha,\ B,\ \beta,\ a_0,\ a_1,\ C) = c_0 \eta^{c_1} \,.$$

“3+1 gauge-invariant variables for perturbations on Schwarzschild spacetime”

by Kouji Nakamura

[JGRG23(2013)P14]

3+1 gauge-invariant variables for the perturbations on Schwarzschild spacetime

Kouji Nakamura (NAOJ)

References :
K.N. Prog. Theor. Phys., **110** (2003), 723. (arXiv : gr-qc/0303039).
K.N. Prog. Theor. Phys., **113** (2005), 413. (arXiv : gr-qc/0410024).
K.N. Adv. in Astron. **2010** (2010), 576273. (arXiv : 1001.2621[gr-qc]).
K.N. CQG **28** (2011), 122001. (arXiv : 1011.5272 [gr-qc]).
K.N. Int. J. Mod. Phys. D **21** (2012), 1242004. (arXiv : 1203.6448 [gr-qc]).
K.N. Prog. Theor. Exp. Phys., **2013** (2013), 043E02. (arXiv : 1105.4007 [gr-qc]).
K.N. in progress

1

I. Introduction

- **The higher order perturbation theory in general relativity has very wide physical motivation.**
  - **Cosmological perturbation theory**
    - Expansion law of inhomogeneous universe (ΛCDM v.s. inhomogeneous cosmology)
    - Non-Gaussianity in CMB (beyond WMAP)
  - **Black hole perturbations**
    - Radiation reaction effects due to the gravitational wave emission.
  - **Perturbation of a star (Neutron star)**
    - Rotation – pulsation coupling (Kojima 1997)

There are many physical situations to which higher order perturbation theory should be applied.

2

However, general relativistic perturbation theory requires very delicate treatments of "gauges".

It is worthwhile to formulate the higher-order gauge-invariant perturbation theory from general point of view.

- According to this motivation, we have been formulating the general relativistic second-order perturbation theory in a gauge-invariant manner.
  - **General formulation :**
    - Framework of higher-order gauge-invariant perturbations :
      - K.N. PTP**110** (2003), 723; *ibid.* **113** (2005), 413.
    - Construction of gauge-invariant variables for the linear order metric perturbation :
      - K.N. CQG**28** (2011), 122001;
      - K.N. PTEP**2013** (2013), 043E02;
      - K.N. IJMPD**21** (2012), 1242004.
    - The nth-order extension of the definitions of gauge-invariant variables :
      - K.N. in progress. (I am trying to resolve this issue.)
  - **Application to cosmological perturbation theory** :
    - Einstein equations : K.N. PRD**74** (2006), 101301R; PTP**117** (2007), 17.
    - Equations of motion for matter fields : K.N. PRD**80** (2009), 124021.
    - Consistency of the 2nd order Einstein equations : K.N. PTP**121** (2009), 1321.
    - Summary of current status of this formulation : K.N. Adv. in Astron. **2010** (2010), 576273.
    - Comparison with a different formulation : A.J. Christopherson, et al., CQG**28** (2011), 225024.

3

Our general framework of the higher-order gauge-invariant perturbation theory is based on a single assumption for linear-order metric perturbation.

- metric perturbation : metric on PS : $\bar{g}_{ab}$, metric on BGS : g_{ab}

  metric expansion : $\bar{g}_{ab} = g_{ab} + \epsilon h_{ab} + O(\epsilon^2)$

- **Decomposition conjecture :**

When we have the gauge-transformation rule ${}_{\mathcal{Y}}h_{ab} - {}_{\mathcal{X}}h_{ab} = \pounds_{\xi} g_{ab}$ under the gauge-transformation $\Phi_\epsilon = \mathcal{X}_\epsilon^{-1} \circ \mathcal{Y}_\epsilon$, we can always decomposed the linear-order metric perturbation h_{ab} as

$$\boxed{h_{ab} = \mathcal{H}_{ab} + \pounds_X g_{ab}} \, ,$$

where the variables $\mathcal{H}_{ab}$ and X^a are the gauge-invariant and the gauge-variant parts of h_{ab}, respectively. These variables are transformed as ${}_{\mathcal{Y}}\mathcal{H}_{ab} - {}_{\mathcal{X}}\mathcal{H}_{ab} = 0$, ${}_{\mathcal{Y}}X^a - {}_{\mathcal{X}}X^a = \xi^a$ under the gauge transformation Φ_ϵ .

This conjecture is almost proved but is still a conjecture due to the "zero-mode problem" !!

[K.N. CQG **28** (2011), 122001; PTEP**2013** (2013) 043E02; IJMPD **21** (2012), 1242004.]

4

In Ref. [K.N. CQG**28** (2011), 122001.], an outline of a proof of the decomposition conjecture is shown through the ADM decomposition of the background metric: $\mathcal{M}_0 = \mathbb{R} \times \Sigma$, $\dim(\Sigma) = n$

$$g_{ab} = -(dt)_a(dt)_b + q_{ij}(dx^i)_a(dx^j)_b, \quad \mathrm{sign}(q_{ij}) = (+, \cdots, +).$$

- We assume the existence of Green functions of the elliptic derivative operators ($D_i q_{jk} = 0$, $R_j{}^l$: Ricci curv. of q_{ij}.) :

$$\Delta := D^i D_i, \quad \mathcal{D}_j{}^l := q_j^l \Delta + \left(1 - \frac{2}{n}\right) D_j D^l + R_j{}^l,$$

----> **zero-mode problem arise!!!**

- This outline is generalized to the background metric :

$$g_{ab} = -\alpha^2(dt)_a(dt)_b + q_{ij}(dx^i + \beta^i dt)_a(dx^j + \beta^j dt)_b$$

in Ref. [K.N. PTEP**2013** (2013), 043E02.].

- As a by-product, we defined gauge-invariant variables on an arbitrary background spacetime, which corresponds to the longitudinal gauge in cosmological perturbations.

To resolve the zero-mode problem, it is necessary to clarify the appearance of this problem in some specific background spacetimes.

- We are trying to apply our arguments to the Schwarzschild spacetime.

This poster presentation is a progress report of this attempt.

5

II. Construction of n+1 gauge-invariant variables for linear metric perturbations on an arbitrary background spacetime

[K.N. CQG **28** (2011), 122001; PTEP**2013** (2013) 043E02; IJMPD **21** (2012), 1242004.]

- ADM decomposition of BGS : $\mathcal{M}_0 = \mathbb{R} \times \Sigma$, $\dim(\Sigma) = n$

$$g_{ab} = -\alpha^2(dt)_a(dt)_b + q_{ij}(dx^i + \beta^i dt)_a(dx^j + \beta^j dt)_b, \quad \mathrm{sign}(q_{ij}) = (+, \cdots, +).$$

- Gauge-transformation for the linear metric perturbation h_{ab}

$$\boxed{{}_{\mathcal{Y}}h_{ab} - {}_{\mathcal{X}}h_{ab} = \pounds_\xi g_{ab}} \qquad \xi_a = \xi_t(dt)_a + \xi_i(dx^i)_a$$

$$h_{ab} = h_{tt}(dt)_a(dt)_b + 2h_{ti}(dt)_{(a}(dx^i)_{b)} + h_{ij}(dx^i)_a(dx^j)_b.$$

$$\begin{aligned}
{}_{\mathcal{Y}}h_{tt} - {}_{\mathcal{X}}h_{tt} &= 2\partial_t\xi_t - \frac{2}{\alpha}\left(\partial_t\alpha + \beta^i D_i\alpha - \beta^j\beta^i K_{ij}\right)\xi_t \\
&\quad - \frac{2}{\alpha}\Big(\beta^i\beta^k\beta^j K_{kj} - \beta^i\partial_t\alpha + \alpha q^{ij}\partial_t\beta_j \\
&\qquad + \alpha^2 D^i\alpha - \alpha\beta^k D^i\beta_k - \beta^i\beta^j D_j\alpha\Big)\xi_i, \\
{}_{\mathcal{Y}}h_{ti} - {}_{\mathcal{X}}h_{ti} &= \partial_t\xi_i + D_i\xi_t - \frac{2}{\alpha}\left(D_i\alpha - \beta^j K_{ij}\right)\xi_t - \frac{2}{\alpha}M_i{}^j\xi_j, \\
{}_{\mathcal{Y}}h_{ij} - {}_{\mathcal{X}}h_{ij} &= 2D_{(i}\xi_{j)} + \frac{2}{\alpha}K_{ij}\xi_t - \frac{2}{\alpha}\beta^k K_{ij}\xi_k, \\
M_i{}^j &:= -\alpha^2 K^j{}_i + \beta^j\beta^k K_{ki} - \beta^j D_i\alpha + \alpha D_i\beta^j.
\end{aligned}$$

covariant derivative: $D_i q_{jk} = 0$ extrinsic curvature: $K^j{}_i := q^{jk}K_{ki}$

6

Inspecting these gauge-transformation rules, we can derive the following decomposition of the components h_{ti} and h_{ij} [K.N. CQG**28** (2011), 122001; arXiv:1105.4007[gr-qc]; arXiv:1203.6448[gr-qc].] :

$$\begin{aligned}
h_{ti} &= D_i h_{(VL)} + h_{(V)i} - \frac{2}{\alpha}\left(D_i\alpha - \beta^j K_{ij}\right)\left\{h_{(VL)} - \Delta^{-1}D^k\partial_t h_{(TV)k}\right\} - \frac{2}{\alpha}M_i{}^k h_{(TV)k}, \\
h_{ij} &= \frac{1}{n}q_{ij}h_{(L)} + h_{(T)ij} + \frac{2}{\alpha}K_{ij}\left\{h_{(VL)} - \Delta^{-1}D^k\partial_t h_{(TV)k}\right\} - \frac{2}{\alpha}\beta^k K_{ij}h_{(TV)k}, \\
h_{(T)ij} &= D_i h_{(TV)j} + D_j h_{(TV)i} - \frac{2}{n}q_{ij}D^l h_{(TV)l} + h_{(TT)ij}, \\
D^i h_{(V)i} &= 0, \quad q^{ij}h_{(TT)ij} = 0, \quad D^i h_{(TT)ij} = 0.
\end{aligned}$$

The inverse relations of these decompositions are guaranteed by the existence of Green functions of elliptic derivative operators

$$\Delta := D^i D_i, \quad \mathcal{F} := \Delta - \frac{2}{\alpha}\left(D_i\alpha - \beta^j K_{ij}\right)D^i - 2D^i\left\{\frac{1}{\alpha}\left(D_i\alpha - \beta^j K_{ij}\right)\right\},$$

and the existence and the uniqueness of the integro-differential equation for a vector field A_k,

$$\mathcal{D}_j{}^k A_k + D^m\left[\frac{2}{\alpha}\tilde{K}_{mj}\left\{\mathcal{F}^{-1}D^k\left(\frac{2}{\alpha}M_k{}^l A_l - \partial_t A_k - \beta^k A_k\right)\right\}\right] = L_j, \qquad \tilde{K}_{ij} := K_{ij} - \frac{1}{n}q_{ij}K.$$

$$\Delta := D^i D_i, \quad \mathcal{D}_j{}^l := q_j^l\Delta + \left(1 - \frac{2}{n}\right)D_j D^l + R_j{}^l$$

$R_j{}^l$: Ricci curvature on Σ.

- We can derive gauge-transformation rules for variables as

$$\begin{aligned}
{}_{\mathcal{Y}}h_{tt} - {}_{\mathcal{X}}h_{tt} &= 2\partial_t\xi_t - \frac{2}{\alpha}\left(\partial_t\alpha + \beta^i D_i\alpha - \beta^j\beta^i K_{ij}\right)\xi_t \\
&\quad - \frac{2}{\alpha}\Big(\beta^i\beta^k\beta^j K_{kj} - \beta^i\partial_t\alpha + \alpha q^{ij}\partial_t\beta_j + \alpha^2 D^i\alpha \\
&\qquad - \alpha\beta^k D^i\beta_k - \beta^i\beta^j D_j\alpha\Big)\xi_i, \\
{}_{\mathcal{Y}}h_{(VL)} - {}_{\mathcal{X}}h_{(VL)} &= \xi_t + \Delta^{-1}D^k\partial_t\xi_k, \\
{}_{\mathcal{Y}}h_{(V)i} - {}_{\mathcal{X}}h_{(V)i} &= \partial_t\xi_i - D_i\Delta^{-1}D^k\partial_t\xi_k, \\
{}_{\mathcal{Y}}h_{(L)} - {}_{\mathcal{X}}h_{(L)} &= 2D^i\xi_i, \\
{}_{\mathcal{Y}}h_{(TV)i} - {}_{\mathcal{X}}h_{(TV)i} &= \xi_i, \\
{}_{\mathcal{Y}}h_{(TT)ij} - {}_{\mathcal{X}}h_{(TT)ij} &= 0.
\end{aligned}$$

- Gauge-variant variables : ${}_{\mathcal{Y}}X_t - {}_{\mathcal{X}}X_t = \xi_t, \quad {}_{\mathcal{Y}}X_i - {}_{\mathcal{X}}X_i = \xi_i.$

$$\boxed{X_t := h_{(VL)} - \Delta^{-1}D^k\partial_t h_{(TV)k}, \quad X_i := h_{(TV)i}.}$$

Gauge-invariant variables :

$$
\begin{aligned}
-2\Phi &:= h_{tt} - 2\partial_t X_t + \frac{2}{\alpha}\left(\partial_t\alpha + \beta^i D_i\alpha - \beta^j\beta^i K_{ij}\right) X_t \\
&\quad + \frac{2}{\alpha}\left(\beta^i\beta^k\beta^j K_{kj} - \beta^i\partial_t\alpha + \alpha q^{ij}\partial_t\beta_j + \alpha^2 D^i\alpha - \alpha\beta^k D^i\beta_k - \beta^i\beta^j D_j\alpha\right) X_i, \\
-2n\Psi &:= h_{(L)} - 2D^i X_i = h_{(L)} - 2D^i h_{(TV)i}, \\
\nu_i &:= h_{(V)i} - \partial_t h_{(TV)i} + D_i\Delta^{-1}D^k\partial_t h_{(TV)k}, \\
\chi_{ij} &:= h_{(TT)ij}.
\end{aligned}
$$

$$
D^i\nu_i = 0, \quad q^{ij}\chi_{ij} = 0, \quad D^i\chi_{ij} = 0, \quad \chi_{ij} = \chi_{ji}.
$$

Definitions of gauge-invariant and gauge-variant parts :

$$
\mathcal{H}_{ab} := -2\Phi(dt)_a(dt)_b + 2\nu_i(dt)_{(a}(dx^i)_{b)} + \left(-2\Psi q_{ij} + \chi_{ij}\right)(dx^i)_{(a}(dx^j)_{b)},
$$

$$
X_a := X_t(dt)_a + X_i(dx^i)_a.
$$

In terms of these variables, the original components h_{tt}, h_{ti}, and h_{ij} of the linear metric perturbation h_{ab} are summarized in the covariant form :

$$
\boxed{h_{ab} = \mathcal{H}_{ab} + \pounds_X g_{ab}}
$$

III. 3+1 gauge-invariant variables on the Schwarzschild background spacetime

Schwarzschild metric : $\alpha^2 = 1 - \dfrac{2M}{r}$, $\beta^i = 0$, $K_{ij} = 0$,

$$
q_{ab} = \frac{1}{\alpha^2}(dr)_a(dr)_b + r^2\gamma_{pq}(dx^p)_a(dx^q)_b \quad , \quad \gamma_{pq} : \text{metric on } S^2.
$$

linear metric perturbation : h_{ab}

$$
h_{ab} = h_{tt}(dt)_a(dt)_b + 2h_{ti}(dt)_{(a}(dx^i)_{b)} + h_{ij}(dx^i)_a(dx^j)_b.
$$

$$
\begin{aligned}
h_{ti} &= D_i h_{(VL)} + h_{(V)i} - \frac{2}{\alpha}D_i\alpha\left\{h_{(VL)} - \Delta^{-1}D^k\partial_t h_{(TV)k}\right\}, \\
h_{ij} &= \frac{1}{n}q_{ij}h_{(L)} + h_{(T)ij}, \\
h_{(T)ij} &= D_i h_{(TV)j} + D_j h_{(TV)i} - \frac{2}{n}q_{ij}D^l h_{(TV)l} + h_{(TT)ij}, \\
D^i h_{(V)i} &= 0, \quad q^{ij}h_{(TT)ij} = 0, \quad D^i h_{(TT)ij} = 0.
\end{aligned}
$$

The inverse relations of these decompositions are guaranteed by the existence of Green functions of elliptic derivative operators

$$
\Delta := D^i D_i, \ \mathcal{F} := \Delta - \frac{2}{\alpha}D_i\alpha D^i - 2D^i\left\{\frac{1}{\alpha}D_i\alpha\right\}, \quad \mathcal{D}_j{}^l := q_j^l\Delta + \frac{1}{3}D_j D^l + R_j{}^l
$$

$R_j{}^l$: Ricci curv. of q_{ij}.

----> **zero-mode problem arise!!!**

- Gauge-variant variables : ${}_{\mathcal{Y}}X_t - {}_{\mathcal{X}}X_t = \xi_t, \quad {}_{\mathcal{Y}}X_i - {}_{\mathcal{X}}X_i = \xi_i.$

$$\boxed{X_t := h_{(VL)} - \Delta^{-1} D^k \partial_t h_{(TV)k}, \quad X_i := h_{(TV)i}.}$$

- Gauge-invariant variables :

$$\begin{array}{rcl} -2\Phi & := & h_{tt} - 2\partial_t X_t + 2\alpha D^i \alpha X_i, \\ -6\Psi & := & h_{(L)} - 2D^i X_i = h_{(L)} - 2D^i h_{(TV)i}, \\ \nu_i & := & h_{(V)i} - \partial_t h_{(TV)i} + D_i \Delta^{-1} D^k \partial_t h_{(TV)k}, \\ \chi_{ij} & := & h_{(TT)ij}. \end{array}$$
$$D^i \nu_i = 0, \quad q^{ij}\chi_{ij} = 0, \quad D^i \chi_{ij} = 0, \quad \chi_{ij} = \chi_{ji}.$$

- Definitions of gauge-invariant and gauge-variant parts :

$$\mathcal{H}_{ab} := -2\Phi(dt)_a(dt)_b + 2\nu_i(dt)_{(a}(dx^i)_{b)} + \left(-2\Psi q_{ij} + \chi_{ij}\right)(dx^i)_{(a}(dx^j)_{b)},$$
$$X_a := X_t(dt)_a + X_i(dx^i)_a.$$

----> $\boxed{h_{ab} = \mathcal{H}_{ab} + \pounds_X g_{ab}}$

- Vacuum Einstein equations :
  - Background Einstein equations : $\Delta\alpha = 0, \quad {}^{(3)}R_{ij} = \dfrac{1}{\alpha} D_i D_j \alpha.$
  - Linearized vacuum Einstein equations :

Hamiltonian constraint : $\Delta\Psi - \dfrac{1}{4\alpha} D_k D_l \alpha \chi^{lk} = 0,$

Momentum constraint :

$$-4\alpha\partial_t D_i \Psi + 4D_i\alpha\partial_t\Psi + \alpha\Delta\nu_i + D_i D_j \alpha \nu^j - 2D^j\alpha D_{(i}\nu_{j)} + D^j\alpha\partial_t\chi_{ji} = 0,$$

Spatial components :

$$\begin{aligned} & -D_i D_j \Phi + \frac{2}{\alpha} D_i D_j \alpha \Phi - \frac{2}{\alpha^2} D_i \alpha D_j \alpha \Phi + \frac{2}{\alpha} D_{(i}\alpha D_{j)}\Phi + \alpha^2 D_i D_j \Psi - 2\alpha D_{(i}\alpha D_{j)}\Psi \\ & \qquad + q_{ij}\left[\Delta\Phi + \frac{2}{\alpha^2} D^k\alpha D_k \alpha \Phi - \frac{2}{\alpha} D^k \alpha D_k \Phi + 2\partial_t^2 \Psi - \alpha^2 \Delta\Psi\right] \\ & -\partial_t D_{(i}\nu_{j)} \\ & + \frac{1}{2}\partial_t^2 \chi_{ij} - \frac{3}{2}\alpha q_{ij} D^l D^k \alpha \chi_{lk} - \frac{1}{2}\alpha^2 \Delta\chi_{ij} + 3\alpha D^k D_{(i}\alpha\chi_{j)k} + \alpha D^k \alpha D_{(i}\chi_{j)k} - \frac{1}{2}\alpha D^k \alpha D_k \chi_{ij} \\ & = 0, \end{aligned}$$

IV. 2+2 formulation for perturbations on spherically symmetric background

One of most popular formulations for perturbations with the Schwarzschild background is **2+2 formulation.**

- Schwarzschild metric : $g_{ab} = y_{ab} + r^2\gamma_{pq}(dx^p)_a(dx^q)_b$

$$y_{ab} = y_{AB}(dx^A)_a(dx^B)_b = -\alpha^2(dt)_a(dt)_b + \frac{1}{\alpha^2}(dr)_a(dr)_b, \quad \alpha^2 = 1 - \frac{2M}{r}$$

- linear metric perturbation :

$$h_{ab} = h_{AB}(dx^A)_a(dx^B)_b + h_{pq}(dx^p)_a(dx^q)_b.$$

$$\begin{aligned}
h_{AB} &= \int \tilde{h}_{AB}S, \\
h_{Ap} &= r\hat{D}_p\int \tilde{h}_{(e)A}S + r\epsilon_{pq}\hat{D}^p\int \tilde{h}_{(o)A}S, \\
h_{pq} &= \frac{r^2}{2}\gamma_{pq}\int \tilde{h}_{e0}S + r^2\left(\hat{D}_p\hat{D}_q - \frac{1}{2}\gamma_{pq}\hat{D}^s\hat{D}_s\right)\int \tilde{h}_{(e1)}S + 2r^2\epsilon_{s(p}\hat{D}_{q)}\hat{D}^s\int \tilde{h}_{o1}S, \\
\hat{D}_s\gamma_{pq} &= 0, \quad \epsilon_{pq} = \epsilon_{[pq]}, \quad S = Y_{lm}, \quad \int = \sum_{l,m}.
\end{aligned}$$

13

- Inverse relations :

$$\int \tilde{h}_{AB}S = h_{AB}, \qquad \hat{\Delta} := \hat{D}^p\hat{D}_p$$

$$\int \tilde{h}_{(e)A}S = \frac{1}{r}\hat{\Delta}^{-1}\hat{D}^q h_{Aq}, \qquad \int \tilde{h}_{(o)A}S = \frac{1}{r}\hat{\Delta}^{-1}\hat{D}_p\left(\epsilon^{pq}h_{Aq}\right),$$

$$\int \tilde{h}_{e0}S = \frac{1}{r^2}\gamma^{pq}h_{pq},$$

$$\int \tilde{h}_{(e1)}S = \frac{2}{r^2}\left[\hat{\Delta}+2\right]^{-1}\hat{\Delta}^{-1}\hat{D}^q\hat{D}^p\left[h_{pq} - \frac{1}{2}\gamma_{pq}\gamma^{su}h_{su}\right],$$

$$\int \tilde{h}_{(o1)}S = \frac{1}{r^2}\left[\hat{\Delta}+2\right]^{-1}\hat{\Delta}^{-1}\epsilon^{qs}\hat{D}_s\hat{D}^p\left[h_{pq} - \frac{1}{2}\gamma_{pq}\gamma^{uv}h_{uv}\right].$$

In this inverse relations, we used the Green functions for the derivative operators $\hat{\Delta}$ and $\hat{\Delta}+2$, respectively.

----> **zero-mode problem arise!!!**

Zero-modes are kernel modes of the operators $\hat{\Delta}$ or $\hat{\Delta}+2$.

---> **l=0,1 mode ($\hat{\Delta}Y_{lm} = -l(l+1)Y_{lm}$) are zero-modes.**

14

Gauge-transformation rules : ${}_{\mathcal{Y}}h_{ab} - {}_{\mathcal{X}}h_{ab} = \pounds_{\xi} g_{ab}, \quad \bar{D}_A y_{BC} = 0,$

$$\boxed{\begin{aligned}
{}_{\mathcal{Y}}h_{AB} - {}_{\mathcal{X}}h_{AB} &= \nabla_A \xi_B + \nabla_B \xi_A = \bar{D}_A \xi_B + \bar{D}_B \xi_A, \\
{}_{\mathcal{Y}}h_{Ap} - {}_{\mathcal{X}}h_{Ap} &= \nabla_A \xi_p + \nabla_p \xi_A = \bar{D}_A \xi_p + \hat{D}_p \xi_A - \frac{2}{r} \bar{D}_A r \xi_p, \\
{}_{\mathcal{Y}}h_{pq} - {}_{\mathcal{X}}h_{pq} &= \nabla_p \xi_q + \nabla_q \xi_p = \hat{D}_p \xi_q + \hat{D}_q \xi_p + 2r \bar{D}^A r \gamma_{pq} \xi_A.
\end{aligned}}$$

$$\xi_a = \xi_A (dx^A)_a + \xi_p (dx^p)_a, \qquad \xi_A =: \int \zeta_A S, \quad \xi_p =: r\hat{D}_p \int \zeta_{(e)} S + r\epsilon_{pq} \hat{D}^q \int \zeta_{(o)} S,$$

$$\boxed{\begin{aligned}
&\left.\begin{aligned}
{}_{\mathcal{Y}}\tilde{h}_{(o)A} - {}_{\mathcal{X}}\tilde{h}_{(o)A} &= \bar{D}_A \zeta_{(o)} - \frac{1}{r} \bar{D}_A r \zeta_{(o)}, \\
{}_{\mathcal{Y}}\tilde{h}_{(o1)} - {}_{\mathcal{X}}\tilde{h}_{(o1)} &= -\frac{1}{r} \zeta_{(o)},
\end{aligned}\right\} \text{(Odd mode)} \\
&\left.\begin{aligned}
{}_{\mathcal{Y}}\tilde{h}_{AB} - {}_{\mathcal{X}}\tilde{h}_{AB} &= 2\bar{D}_{(A} \zeta_{B)}, \\
{}_{\mathcal{Y}}\tilde{h}_{(e)A} - {}_{\mathcal{X}}\tilde{h}_{(e)A} &= \bar{D}_A \zeta_{(e)} - \frac{1}{r} \bar{D}_A r \zeta_{(e)} + \frac{1}{r} \zeta_A, \\
{}_{\mathcal{Y}}\tilde{h}_{(e0)} - {}_{\mathcal{X}}\tilde{h}_{(e0)} &= \frac{4}{r} \zeta_A \bar{D}^A r - \frac{2}{r} \zeta_{(e)} l(l+1), \\
{}_{\mathcal{Y}}\tilde{h}_{(e1)} - {}_{\mathcal{X}}\tilde{h}_{(e1)} &= \frac{2}{r} \zeta_{(e)}.
\end{aligned}\right\} \text{(Even mode)}
\end{aligned}}$$

15

Gauge-variant variables :

$$\tilde{Y}_A := r\tilde{h}_{(e)A} - \frac{r^2}{2} \bar{D}_A \tilde{h}_{(e1)}, \qquad \tilde{Y}_{(e)} := \frac{r^2}{2} \tilde{h}_{(e1)}, \qquad \tilde{Y}_{(o)} := -r^2 \tilde{h}_{(o1)},$$

$${}_{\mathcal{Y}}\tilde{Y}_A - {}_{\mathcal{X}}\tilde{Y}_A = \zeta_A, \quad {}_{\mathcal{Y}}\tilde{Y}_{(o)} - {}_{\mathcal{X}}\tilde{Y}_{(o)} = r\zeta_{(o)}, \quad {}_{\mathcal{Y}}\tilde{Y}_{(e)} - {}_{\mathcal{X}}\tilde{Y}_{(e)} = r\zeta_{(e)}.$$

$$\boxed{Y_a := \int \tilde{Y}_A S (dx^A)_a + \left(\hat{D}_p \int \tilde{Y}_{(e)} S + \epsilon_{pq} \hat{D}^q \int \tilde{Y}_{(o)} S \right) (dx^p)_a.}$$

----> $\boxed{{}_{\mathcal{Y}}Y_a - {}_{\mathcal{X}}Y_a = \xi_a,}$

Gauge-invariant variables :

$$\tilde{F}_A := \tilde{h}_{(o)A} + r\bar{D}_A \tilde{h}_{(o1)}, \qquad \text{(Odd mode)}$$

$$\left.\begin{aligned}
\tilde{F} &:= \tilde{h}_{(e0)} - \frac{4}{r} \tilde{Y}_A \bar{D}^A r + \tilde{h}_{(e1)} \Lambda, \\
\tilde{F}_{AB} &:= \tilde{h}_{AB} - 2\bar{D}_{(A} \tilde{Y}_{B)},
\end{aligned}\right\} \text{(Even mode)}$$

$$\boxed{F_{AB} := \int \tilde{F}_{AB} S, \quad F_{Ap} := \epsilon_{pq} \hat{D}^q \int \tilde{F}_A S, \quad F := \int \tilde{F} S,}$$

Original metric perturbation ---> $\boxed{h_{ab} = \mathcal{F}_{ab} + \pounds_Y g_{ab},}$

$$\mathcal{F}_{AB} := F_{AB}, \quad \mathcal{F}_{Ap} := rF_{Ap}, \quad \mathcal{F}_{pq} := \frac{1}{2} \gamma_{pq} r^2 F.$$

16

V. To derive the relation between 3+1 and 2+2 formulations

To derive the relation between 3+1 and 2+2 formulations,
We fix the gauge choice so that $h_{ab} = \mathcal{H}_{ab} = \mathcal{F}_{ab} + \pounds_Y g_{ab}$.
This relation yields the correspondence between the variables :

$$
\begin{aligned}
\nu_r &= F_{tr} + \partial_t Y_r + \partial_r Y_t - \frac{2}{\alpha}\partial_r \alpha Y_t, \\
\nu_p &= rF_{tp} + \hat{D}_p Y_t + \partial_t Y_p, \\
\chi_{rr} &= \frac{2}{3}F_{rr} - \frac{1}{3\alpha^2}F + \frac{4}{3}\partial_r Y_r + \frac{4}{3\alpha}\partial_r \alpha Y_r - \frac{4}{3r}Y_r - \frac{2}{3r^2\alpha^2}\hat{D}^p Y_p, \\
\chi_{rp} &= rF_{rp} + \hat{D}_p Y_r + \partial_r Y_p - \frac{2}{r}Y_p, \\
\chi_{pq} &= -\frac{1}{3}\gamma_{pq} r^2 \alpha^2 F_{rr} + \frac{1}{6}\gamma_{pq} r^2 F - \frac{2}{3}r^2\alpha^2\gamma_{pq}\partial_r Y_r - \frac{2}{3}r^2\alpha\partial_r\alpha\gamma_{pq}Y_r + \frac{2}{3}r\alpha^2\gamma_{pq}Y_r \\
&\quad + \hat{D}_p Y_q + \hat{D}_q Y_p - \frac{2}{3}\gamma_{pq}\hat{D}^s Y_s.
\end{aligned}
$$

To determine the variable Y_a, we have to evaluate the properties

$$D^i \nu_i = 0 = D^i \chi_{ij}.$$

The properties $D^i \nu_i = 0 = D^i \chi_{ij}$ yields equations for the components of Y_a as follows :

$$
\begin{aligned}
&\partial_r^2 Y_t + \frac{2r^2 - 9Mr + 6M^3}{r^2(r-2M)}\partial_r Y_t + \frac{2M^2(5r-6M)}{r^3(r-2M)^2}Y_t + \frac{1}{r^2}\hat{D}^p\hat{D}_p Y_t \\
&\quad + \partial_r\partial_t Y_r + \frac{2r-3M}{r^2}\partial_t Y_r + \frac{1}{r^2}\partial_t \hat{D}^p Y_p \\
&= -\left(1 - \frac{2M}{r}\right)\partial_r F_{tr} - \frac{2r-3M}{r^2}F_{tr},
\end{aligned}
$$

$$
\begin{aligned}
&\partial_r^2 Y_r + \frac{2r-M}{(r-2M)r}\partial_r Y_r - \frac{2r-3M}{r^2(r-2M)}Y_r + \frac{3}{4r(r-2M)}\hat{D}^p\hat{D}_p Y_r \\
&\quad + \frac{1}{4r(r-2M)}\left(\partial_r \hat{D}^p Y_p - \frac{8}{r}\hat{D}^p Y_p\right) \\
&= -\frac{1}{2}\partial_r F_{rr} - \frac{3r-4M}{2(r-2M)r}F_{rr} + \frac{r}{4(r-2M)}\left(\partial_r F + \frac{3}{r}F\right),
\end{aligned}
$$

$$
\begin{aligned}
&\partial_r^2 Y_p + \frac{M}{r(r-2M)}\partial_r Y_p - \frac{1}{r^2}Y_p + \frac{1}{r(r-2M)}\left(\hat{D}^s\hat{D}_s Y_p + \frac{1}{3}\hat{D}_p\hat{D}^s Y_s\right) \\
&\quad + \frac{1}{3}\partial_r \hat{D}_p Y_r - \frac{15M-8r}{3(r-2M)r}\hat{D}_p Y_r \\
&= -r\partial_r F_{rp} + \frac{3r-5M}{r-2M}F_{rp} + \frac{1}{3}\hat{D}_p\left(F_{rr} - \frac{r}{2(r-2M)}F\right).
\end{aligned}
$$

If we have solutions to these equations, we can derive the relation between 3+1 and 2+2 gauge-invariant variables.

IV. Summary

We have shown that the 3+1 gauge-invariant variables which corresponds to the longitudinal gauge in perturbations on Minkowski spacetime is possible even in perturbations on the Schwarzschild background spacetimes.

We have to note that the zero-mode problem appears due to the construction of the 3+1 gauge-invariant variables.

We pointed out that the zero-mode problem is also exists even in the popular 2+2 formulation for perturbations on the Schwarzschild background spacetime, which is the famous l=0,1 problem.

We also derived the vacuum the Einstein equations, equations to clarify the relation between the popular 2+2 formulation for the perturbations on the Schwarzschild spacetime.

Since the 3+1 gauge-invariant variables proposed here have the similar form to the post-Newtonian expansion, it might be useful when we discuss the physical interpretation of perturbations in terms of post-Newtonian words.

"How can we detect BHs ?"

by Hiromi Saida

[JGRG23(2013)P15]

How can we detect BHs ?

Detect BH's strong gravitational lens effect by Time Delay Self-interferometry for radio observation

---

Hiromi Saida (Daido Univ.) / saida@daido-it.ac.jp

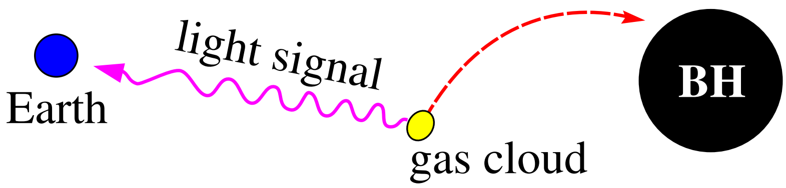

JGRG23, 2013.11.5–8 at Hirosaki Univ.

1. Intro. : I want to see the black hole.

- What is the meaning of "seeing BH (direct detection of BH)" ?

  - To verify the existence of BH horizon by detecting GR effects of BH
  - To measure the mass and angular momentum (and charge) via GR effects

- We search for **Strong Gravitational Lensing (SGL)** by BH horizon

→ What can we read from SGL ?

◇ Spatial information — viewing image

→ ex. BH Shadow

◇ Temporal information — time series of radio oscillation

→ **Time Delay Self-interferometry** · · · Topic of this presentation

∗ To make use of the phase of wave (light),

we assume radio observation at present technology.

2. Direct detection of BH with astronomical method

• Situation : $\begin{cases} \text{Observe rays emitted by a source at the same time near BH} \\ \text{Palse-like (a few wave length) emission with the same intensity.} \end{cases}$

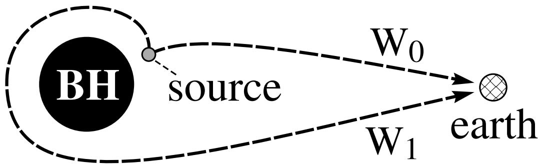

Compare two rays $\begin{cases} W_0 \text{ : } \textbf{direct ray} \\ W_1 \text{ : } \textbf{a ray winding around BH once ,} \end{cases}$

the difference of $\begin{cases} \textbf{arrival time} \\ \textbf{amplitude} \end{cases}$ **will let us detect BH directly.**

• How do the rays (waves) W_0 and W_1 appear in one telescope ?

◇ **Case 1:** Sinusoidal emission by the source

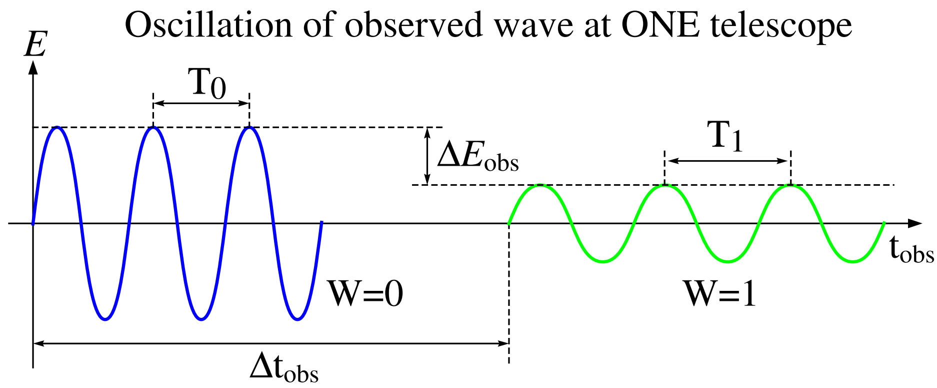

$$\rightarrow \begin{cases} \Delta t_{obs} & \text{: due to Strong Grav. Lensing by BH} \\ \Delta E_{obs} & \text{: due to Strong Grav. Lensing by BH} \\ T_0 \neq T_1 & \text{: due to Kinematic Doppler Effect by source's velocity} \end{cases}$$

∗ Exactly, Δt_{obs} and ΔE_{obs} depend on distance, BH $\leftrightarrow$ source.

◇ **Case 2:** Gaussian emission (in time) by the source

→ **Wave form changes from W_0 to W_1 !!** ⋯ **Gouy phase shift**

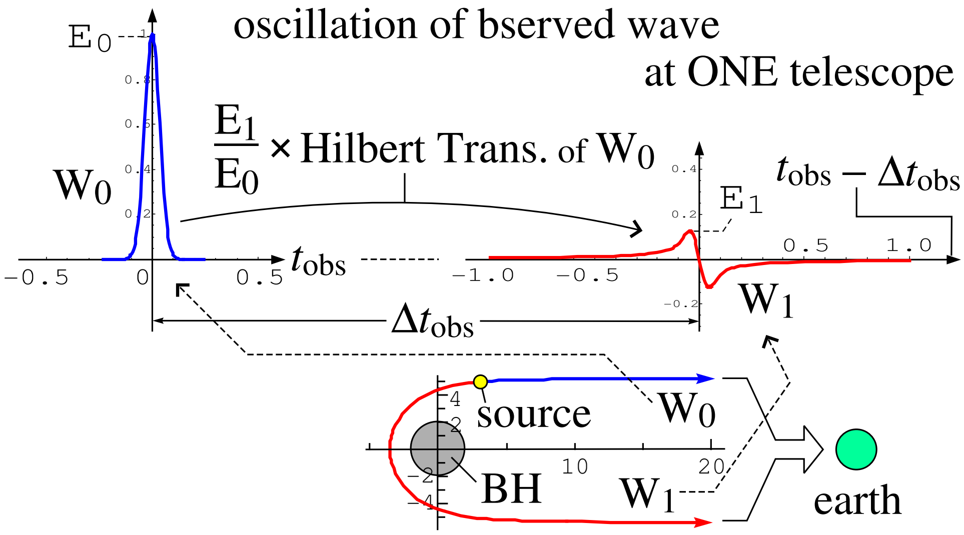

Figure reproduces the wave forms

simulated in [Zenginoglu and Galley, PRD86(2012)064030]

→ Wave form changes by Gouy Phase Shift known in Wave Optics

∘ When a ray passes one Caustic,

$$\begin{cases} + \text{ freq. component : Phase shift by } -\dfrac{\pi}{2} \\ - \text{ freq. component : Phase shift by } +\dfrac{\pi}{2} \end{cases} \quad \rightarrow \quad \text{Hilbert transformation}$$

$$\circ \begin{cases} f(t) & : \text{ Time variation } \underline{\text{before}} \text{ passing a caustic} \\ H[f](t) & : \text{ Time variation } \underline{\text{after}} \text{ passing a caustic} \end{cases}$$

$$\text{Hilbert trans. :} \quad H[f](t) \ \propto \ \mathrm{Re} \int_{-\infty}^{\infty} \mathrm{d}z \, \frac{f(z)}{z-t}$$

$$* \begin{cases} \text{Mathematics: Analytically continue } f(t)\text{, then extract the real part} \\ \text{Technology : Hilbert trans. of real time series data is already possible} \end{cases}$$

∘ Example of Hilbert trans.

∗ Case: $f(t) = \sin(\omega t) \quad \Rightarrow \quad H[f](t) = \mathrm{sign}(\omega)\, \pi\, \cos(\omega t)$

∗ Case: $f(t) = \exp\left(-\dfrac{t^2}{\sigma^2}\right)$

$$\Rightarrow \quad H[f](t) = -\pi \exp\left(-\frac{t^2}{\sigma^2}\right) \mathrm{erfi}\left(\frac{t}{\sigma}\right)$$

$$\text{where} \quad \mathrm{erfi}(x) = -i\, \mathrm{erf}(ix) = -i \int_0^{ix} \mathrm{d}z \exp\left(-t^2\right)$$

∘ **Attention** :

Gouy phase shift (Hilbert trans.) changes the wave form, but NOT the spectrum.

→ Spectrum changes due to Kinematic Doppler effect between the source and rays (W_0 , W_1)

• How can we find W_0 and W_1 in time series data ?

→ W_0 and W_1, emitted by the same source at the same time, should be coherent.

→ **Time Delay Self-interferometry , TDS** ($\neq$ Tokyo Disney Sea)

step 1 : Create two copies of time series data (A, B)

step 2 : On data B, $\begin{cases} \text{operate Hilbert trans.,} \\ \text{multiply a const. } (E_1/E_0), \\ \text{modulate for Doppler effect.} \end{cases}$

step 3 : Search for coherent part between original data A and modulated data B.

→ W_0 and W_1 are found in data A, then Δt_{obs} , E_1/E_0 , T_1/T_0 are measured.

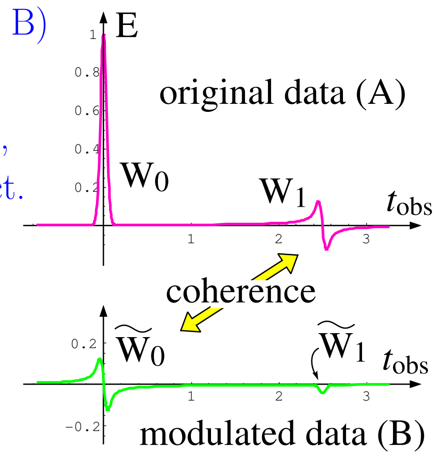

- A trial calculation : $\Delta t_{\rm obs}$, E_1/E_0 and T_0/T_1 for given M, J and source

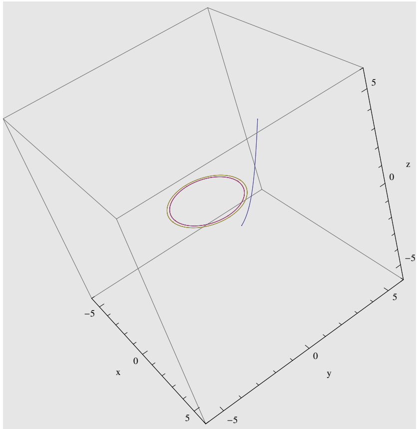

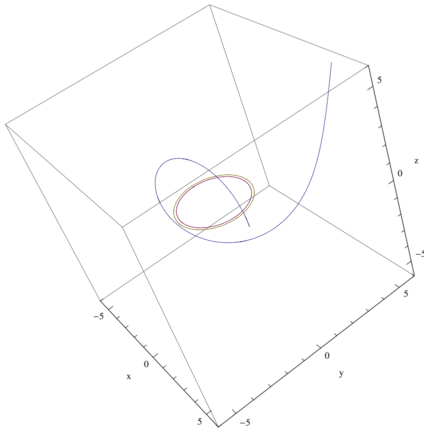

winding angle about z-axis : $0.06 \times 2\pi$ (ray W_0) $\qquad -0.94 \times 2\pi$ (ray W_1)

$$* \begin{cases} \text{Parameters} & : \; M = 1 \,,\; (\text{with } c = 1 \,,\; G = 1\,) \\ \text{BH spin} & : \; J = (1/2)(GM^2/c) \\ \text{emission at} & : \; \big(0\,,\, 3\,(GM/c^2)\,,\, \pi/2\,,\, 0\big) \text{ in Boyer-Lindquist coord.} \\ \text{source vel.} & : \; \big(1.70\,,\, 0\,,\, 0\,,\, 0.0603\big) \;\to\; u_{(\phi)}/u_{(\mathrm{t})} \simeq 0.03 \text{ (ZAMO)} \end{cases}$$

$$* \text{ The other parameters : } \begin{cases} \text{Observer's position} & : \left[\begin{array}{l} r = 3.65 \times 10^7\,(GM/c^2) \\ \theta = 0.300 \text{ rad } (17^\circ) \\ \phi = 0.405 \text{ rad} \end{array}\right. \\ \text{Freq. at emission} & : \; \omega_{\rm source} = \dfrac{2\pi}{10} \quad \text{(trial value)} \end{cases}$$

$$* \text{ Results : } \begin{cases} \Delta t_{\rm obs} \simeq 30\,\dfrac{GM}{c^3} \;\to\; \left[\begin{array}{ll} \text{Sgr.A*} & : \text{ about 10 min.} \\ \text{Cyg.X-1} & : \text{ about 0.001 sec.} \end{array}\right. \\ \left(\dfrac{E_1}{E_0}\right)^2 = \dfrac{[\text{intensity of } \mathrm{W}_1]}{[\text{intensity of } \mathrm{W}_0]} \simeq 0.00868 \;\sim\; O(10^{-2}) \\ \dfrac{T_0}{T_1} = \dfrac{[\text{doppler shift of } \mathrm{W}_1]}{[\text{doppler shift of } \mathrm{W}_0]} \simeq 0.956871 \end{cases}$$

$\to$ Formulas of these values $\cdots$ under construction (present task)

3. Does BH's Strong Grav. Lens denote BH directly ?

- Obvious relation : BH's SGL = UCON ($\neq$ ISCO)

$\rightarrow$ It is not sure : BH's SGL = BH horizon $\cdots$???

$\rightarrow$ A task for GR : To what extent does the UCON imply existence of BH ?

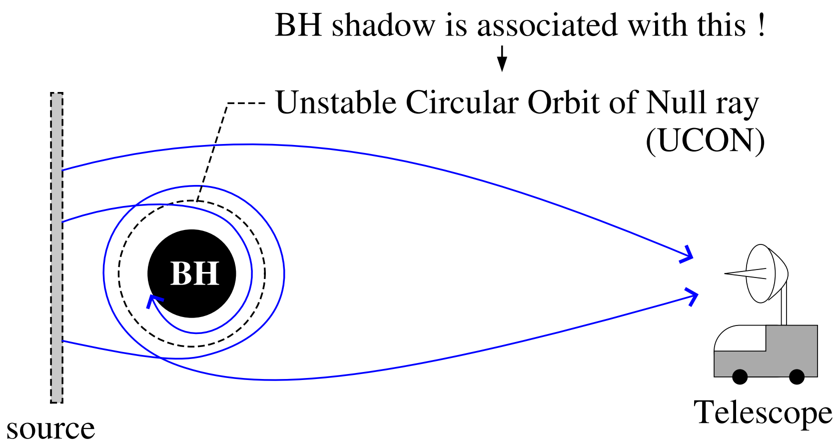

4. Summary

- Direct detection of BH is to **measure M and J via GR effects.**

  $\rightarrow$ we search for BH's Strong Grav. Lens effect:

$$\begin{cases} \text{Viewing image: BH shadow} \\ \text{Time series} \quad : \textbf{Time Delay Self-interferometry} \end{cases}$$

- Under construction: Formulae $\begin{cases} M(\Delta t_{\rm obs}\,,\ E_1/E_0\,,\ T_0/T_1) \\ J(\Delta t_{\rm obs}\,,\ E_1/E_0\,,\ T_0/T_1) \end{cases}$

- Typical band width of radio receiver: $\Delta f_{\rm rec} = \dfrac{1}{\Delta T_{\rm obs}} \sim 2$ GHz

  $\rightarrow$ Target of TDS : Source's motion giving $\Delta f_{\rm obs} \sim 2$ GHz

- GR's problem : To what extent does the UCON imply existence of BH ?

“A new numerical scheme for Einstein equations

with discrete variational derivative method”

by Takuya Tsuchiya

[JGRG23(2013)P17]

A new numerical scheme for Einstein equations with discrete variational derivative method

Takuya Tsuchiya[1] and Gen Yoneda[1]
[1]Department of Mathematics, Waseda University, Japan
email: t-tsuchiya@aoni.waseda.jp

Motivations

- What is the best way to make a discretized equations for Numerical Relativity (NR)?
- In NR, the Crank-Nicolson (CN) scheme and Runge-Kutta scheme (RK) are often used.
- However, these schemes were not proposed for NR.
- For accuracy simulations, we need to use a numerical scheme that is built for NR.

Method

- The Discrete Variational Derivative Method (DVDM) is one of the numerical scheme.
- The DVDM was proposed and extended by Furihata, Mori and Matsuo (D. Furihata and T. Matsuo, *Discrete Variational Derivative Method*, (CRC press, 2010)).
- The DVDM is considered as a discrete version of the variational principle.
- To make a discretized equations using the DVDM scheme, the Lagrangian or the Hamiltonian is necessary.
- With the DVDM scheme, we can make a discretized equations with preserving constraints and diffusion characters in the continuous system.

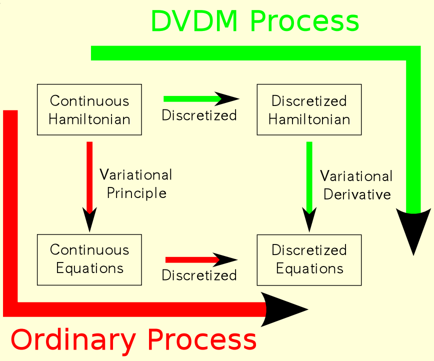

The diagram of making the discretized equations from the continuous equations. In general, the equations are derived from the Hamiltonian by the variational principle, and the discretized equations using numerical schemes such as the CN scheme or the RK scheme (red line process). On the other hand, by the DVDM scheme, we first make a discrete Hamiltonian, and derive the discretized equations (green line process).

Application to Einstein Equations

We apply the DVDM scheme to the canonical formalism of the Einstein equations. A discrete Hamiltonian density of the Einstein equations can be written as

$$\begin{aligned}\mathcal{H}^{\mathrm{GR}(n)}_{(k)} = & -\alpha^{(n)}_{(k)}\sqrt{\gamma}^{(n)}_{(k)}R^{(n)}_{(k)} - \alpha^{(n)}_{(k)}(\pi^{(n)}_{(k)})^2/(2\sqrt{\gamma}^{(n)}_{(k)}) + \alpha^{(n)}_{(k)}\pi^{ab(n)}_{(k)}\pi_{ab}{}^{(n)}_{(k)}/\sqrt{\gamma}^{(n)}_{(k)} \\ & - 2\beta_{a}{}^{(n)}_{(k)}(\widehat{\delta}^{\langle 1\rangle}_{b}\pi^{ab(n)}_{(k)}) - 2\beta^{c(n)}_{(k)}\pi^{ab(n)}_{(k)}\Gamma^{\langle 1\rangle}{}_{cab}{}^{(n)}_{(k)},\end{aligned} \tag{1}$$

then the discretized ADM formulation is calculated as

$$\mathcal{H}^{\mathrm{ADM}(n)}_{(k)} \equiv \sqrt{\gamma}^{(n)}_{(k)}R^{(n)}_{(k)} + (\pi^{(n)}_{(k)})^2/(2\sqrt{\gamma}^{(n)}_{(k)}) - \pi^{ij(n)}_{(k)}\pi_{ij}{}^{(n)}_{(k)}/\sqrt{\gamma}^{(n)}_{(k)}, \tag{2}$$

$$\mathcal{M}^{\mathrm{ADM}(n)}_{\ell\,(k)} \equiv -2\gamma_{\ell i}{}^{(n)}_{(k)}(\widehat{\delta}^{\langle 1\rangle}_{j}\pi^{ij(n)}_{(k)}) - 2\pi^{ij(n)}_{(k)}\Gamma^{\langle 1\rangle}{}_{\ell ij}{}^{(n)}_{(k)}, \tag{3}$$

$$\frac{\gamma_{ij}{}^{(n+1)}_{(k)} - \gamma_{ij}{}^{(n)}_{(k)}}{\Delta t} = \cdots, \tag{4}$$

$$\frac{\pi^{ij(n+1)}_{(k)} - \pi^{ij(n)}_{(k)}}{\Delta t} = \cdots. \tag{5}$$

Numerical Tests

Following the proposal of the Apples-with-Apples, We show damping of constraint in numerical evolutions using polarized Gowdy wave evolution, which is one of the standard tests for comparisons of formulations in numerical relativity as is known to the Apples-with-Apples testbeds (Class. Quantum Grav. 21 (2004) 589).
The metric of polarized Gowdy wave is

$$ds^2 = t^{-1/2}\mathrm{e}^{\lambda/2}(-dt^2 + dx^2) + t(\mathrm{e}^{P}dy^2 + \mathrm{e}^{-P}dz^2), \tag{6}$$

where P and λ are functions of x and t. The time coordinate t is chosen such that time increases as the universe expands, this metric is singular at $t = 0$ which corresponds to the cosmological singularity.

- Convergences

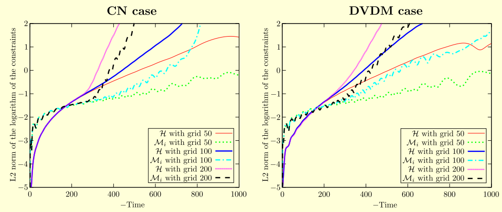

Left panel is using CN scheme, Right panel is using DVDM scheme. These values of the cases of 50 plot and 200 plot are rescaled by 1/4 and 4 times, respectively. Both of the convergences are satisfied until $t = -200$.

- Comparison of CN scheme with DVDM scheme

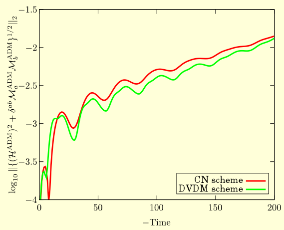

The violations of the constraints, $\{(\mathcal{H}^{\mathrm{ADM}})^2 + \delta^{ab}\mathcal{M}^{\mathrm{ADM}}_a\mathcal{M}^{\mathrm{ADM}}_b\}^{1/2}$, of the DVDM scheme (blue line) is lower than that of the CN scheme (red line).

Summary

- We proposed a discretized ADM formulation using the DVDM scheme.
- We performed some simulations using the DVDM scheme and CN scheme, and the violations of the DVDM scheme are lower than that of the CN scheme.

“Cosmological matching conditions in Horndeski's theory”

by Sakine Nishi

[JGRG23(2013)P20]

Cosmological matching conditions in Horndeski's theory

Sakine Nishi (西 咲音), Rikkyo University

Collaborators : T.Kobayashi (Rikkyo Univ.), N.Tanahashi (Cambridge Univ.), M.Yamaguchi (TITech)

Kobayashi, SN, Tanahashi, Yamaguchi, in preparation

I. Introduction

* Horndeski's theory is the most general 2nd-order scalar-tensor theory.
* This theory has a solution violating null energy condition (NEC) stably called Genesis.
* Boundary term and matching conditions are different between GR and Horndeski's theory.

The action of Horndeski's theory

$$S_{\rm Hor} = \int \mathrm{d}^4x\sqrt{-g}\Big\{G_2(\phi,X) - G_3(\phi,X)\Box\phi + G_4(\phi,X)R + G_{4X}\left[(\Box\phi)^2 - (\nabla_\mu\nabla_\nu\phi)^2\right] + G_5(\phi,X)G^{\mu\nu}\nabla_\mu\nabla_\nu\phi - \frac{1}{6}G_{5X}\left[(\Box\phi)^3 - 3\Box\phi(\nabla_\mu\nabla_\nu\phi)^2 + 2(\nabla_\mu\nabla_\nu\phi)^3\right]\Big\}$$

$$X := -g^{\mu\nu}\partial_\mu\phi\partial_\nu\phi/2$$

Phase1 $\xrightarrow{}$ Phase2

The matching condition
Boundary term in GR : K

In Horndeski's theory ··· ?

II. Surface terms

In Horndeski's theory, the action of surface term is changed as follows.

$$S = S_{\rm Hor} + S_{\rm m} + S_{\rm B}$$

General relativity		Horndeski's
$S_\Sigma = \int\sqrt{-\gamma}K\mathrm{d}^3x$	→	$S_{\rm B} = B_3 + B_4 + B_5$

$$\begin{cases} B_3 = \int_{\Sigma_\pm}\mathrm{d}^3x\sqrt{\gamma}F_3 \\ B_4 = 2\int_{\Sigma_\pm}\mathrm{d}^3x\sqrt{\gamma}\left(G_4K - F_{4Y}D^2\phi\right) \\ B_5 = \int_{\Sigma_\pm}\mathrm{d}^3x\sqrt{\gamma}\Big\{\frac{1}{2}G_5\left(K^2 - K_{\mu\nu}K^{\mu\nu}\right)n^\lambda\nabla_\lambda\phi - G_5\left(KD^2\phi - K^{\mu\nu}D_\mu D_\nu\phi\right) + \frac{1}{2}F_5R^{(3)} + \frac{1}{2}F_{5Y}\left[(D^2\phi)^2 - D_\mu D_\nu\phi D^\mu D^\nu\phi\right]\Big\} \end{cases}$$

$$F_i(\phi,X_0,Y) := \int_0^{X_0}\frac{\mathrm{d}u}{\sqrt{2u}}G_i(\phi,u+Y)$$

[A.Padilla and V.Sivanesan, JHEP **1208**, 122 (2012)]

III. Applying to Cosmology

The phase transition occurs on a hypersurface, q=const.
We take a gauge: $\delta q \to \widetilde{\delta q} = \delta q - \dot{q}\xi^0 = 0$

The perturbed metric :

$$\mathrm{d}s^2 = -(1+2A)\mathrm{d}t^2 + 2B_i\mathrm{d}t\mathrm{d}x^i + a^2\left[(1-2\psi)\delta_{ij} + 2E_{ij} + h_{ij}\right]\mathrm{d}x^i\mathrm{d}x^j$$

$$\widetilde{\delta\mathcal{J}}_i{}^j = \left[-\left(\mathcal{G}_T\dot{\tilde{\psi}} + \Theta\tilde{A}\right) + \frac{\Theta - H\mathcal{G}_T}{\dot\phi}\dot{\widetilde{\delta\phi}} + \frac{1}{3}\frac{\partial\overline{\mathcal{J}}}{\partial\phi}\widetilde{\delta\phi}\right]\delta_i{}^j + \frac{1}{2a^2}\left(\partial_i\partial^j - \delta_i{}^j\partial^2\right)\left[-\mathcal{G}_T\tilde\sigma - 2W\widetilde{\delta\phi} + f_5\tilde\psi\right]$$

$$\widetilde{\delta\mathcal{J}}^\phi = -\frac{2}{\dot\phi}\left[3\left(\Theta - H\mathcal{G}_T\right)\dot{\tilde\psi} - (\Sigma + 3H\Theta)\tilde{A} - \frac{\Theta - H\mathcal{G}_T}{a^2}\partial^2\tilde\sigma\right] + \frac{\partial\overline{\mathcal{J}}^\phi}{\partial\phi}\widetilde{\delta\phi} - \frac{\Sigma + 6H\Theta - 3H^2\mathcal{G}_T}{X}\dot{\widetilde{\delta\phi}} + \frac{Z}{a^2}\partial^2\widetilde{\delta\phi} - \frac{4W}{a^2}\partial^2\tilde\psi,$$

$$\mathcal{G}_T := 2\left[G_4 - 2XG_4 - X\left(H\dot\phi G_{5X} - G_{5\phi}\right)\right]$$
$$\mathcal{G}_S = \mathcal{G}_S(G_2,G_3,G_4,G_5)$$
$$f_i(\phi,X) := \int_0^X\sqrt{2u}G_{iu}(\phi,u)\mathrm{d}u$$
$$\Theta = \Theta(G_2,G_3,G_4,G_5)$$
$$\Sigma = \Sigma(G_2,G_3,G_4,G_5)$$

[T.Kobayashi M.Yamaguchi and J.Yokoyama, PTP **126** (2011) 511]

1) Homogeneous background

$$\frac{1}{3}\overline{\mathcal{J}}(\phi,\dot\phi,H) = -\frac{1}{2}f_3 + 2G_4H - 4HXG_{4X} + \dot\phi G_{4\phi} - H^2X\dot\phi G_{5X} + 2HXG_{5\phi},$$
$$-\overline{\mathcal{J}}^\phi(\phi,\dot\phi,H) = J + f_{3\phi} - 6HG_{4\phi}$$

Background	Scalar field
$[a]^+_- = 0$	$[\phi]^+_- = 0$
$[\overline{\mathcal{J}}]^+_- = 0$	$[\overline{\mathcal{J}}^\phi]^+_- = 0$

2) Perturbation

Scalar

$$[\tilde\psi]^+_- = 0,\quad [\tilde{E}]^+_- = 0,\quad [\widetilde{\delta\phi}]^+_- = 0$$

$$\left[\psi + H\frac{\delta\rho}{\dot\rho}\right]^+_- = 0,\quad \left[\delta\phi - \dot\phi\frac{\delta\rho}{\dot\rho}\right]^+_- = 0,\quad \left[\sigma - \frac{\delta\rho}{\dot\rho}\right]^+_- = 0$$

$$\left[\mathcal{G}_T\dot\psi + \Theta A - \frac{\Theta - H\mathcal{G}_T}{\dot\phi}\delta\dot\phi + \left(\mathcal{G}_T\dot{H} + \frac{\Theta - H\mathcal{G}_T}{\dot\phi}\ddot\phi\right)\frac{\delta\rho}{\dot\rho}\right]^+_- = 0$$

Vector

$$[E_i^{\rm V}]^+_- = 0$$
$$\left[\mathcal{G}_T\left(\frac{B_i^{\rm V}}{a^2} - \dot{E}_i^{\rm V}\right)\right]^+_- = 0$$

Tensor

$$[h_{ij}]^+_- = 0$$
$$\left[\mathcal{G}_T\dot{h}_{ij} + \frac{f_5}{a^2}\partial^2h_{ij}\right]^+_- = 0$$

* Example

$$q(t,\mathbf{x}) = \phi(t,\mathbf{x}) - \phi_*$$

$$\downarrow\ \delta\phi = 0$$

The matching condition

$$\left[\mathcal{G}_S\dot{\mathcal{R}} - \frac{1}{a^2}\left(\frac{\mathcal{G}_T^2}{\Theta} + f_5\right)\partial^2\mathcal{R}\right]^+_- = 0$$

R: Curvature perturbation in $\delta\phi = 0$ gauge

IV. Example : Generalization of genesis scenario

[P.Creminelli, A.Nicolis and E.Trincherini, JCAP **1011**,021(2010)]

We choose G2 ~ G5 as follows.

$$G_2 = e^{4\lambda\phi}g_2(Y),\quad G_3 = e^{2\lambda\phi}g_3(Y),$$
$$G_4 = \frac{M_{\rm Pl}^2}{2} + e^{2\lambda\phi}g_4(Y),\quad G_5 = e^{-2\lambda\phi}g_5(Y),$$
$$Y := e^{-2\lambda\phi}X$$

$$\hat\rho(Y) := 2Yg_2' - g_2 - 4\lambda Y\left(g_3 - Yg_3'\right)$$
$$\hat{p}(Y) := g_2 - 4\lambda Yg_3 + 24\lambda^2Y\left(g_4 - Yg_4'\right)$$
$$\mathcal{G}(Y) := M_{\rm Pl}^2 - 4\lambda Y\left(g_5 + Yg_5'\right)$$

In genesis scenario, we seek for the solution Y satisfying :

$$e^{\lambda\phi} \simeq \frac{1}{\lambda\sqrt{2Y_0}}\frac{1}{(-t)},\quad H \simeq \frac{h_0}{(-t)^3}\quad (-\infty < t < 0)$$

$\hat{p}(Y) = 0$ gives the solution Y_0 .
We get the stable NEC violating solution .

NEC violation
$\hat{p}(Y_0) < 0$

Stability of background
$\hat\rho'(Y_0) > 0$

$$\left.\left(\frac{Y\mathcal{G}}{\hat{p}}\right)'\right|_{Y_0} > 0$$

Considering the transition.

(Phase1) Genesis → (Phase2) Radiation dominant (Expanding)

The matching condition : $-g_2 - 2\lambda Y_0g_3(Y_0) + 3\lambda\sqrt{Y_0}\int_0^{Y_0}\frac{g_3(y)}{\sqrt{y}}\mathrm{d}y > 0$

When the transition occurs at t*, we get these equations.

Tensor perturbation

$$h_{ij} = C_g^- - \frac{C_d^-}{\mathcal{G}(Y_0)}\int_t^{t_*}\frac{\mathrm{d}t'}{a^3(t')}\quad (t < t_*)$$
$$h_{ij} = C_g^+ + \frac{C_d^+}{M_{\rm Pl}^2}\int_{t_*}^t\frac{\mathrm{d}t'}{a^3(t')}\quad (t > t_*)$$

Curvature perturbation

$$\mathcal{R} = C^- - \frac{D^-}{\mathcal{A}(Y_0)}\int_t^{t^*}\frac{\mathrm{d}t'}{(-t')^2a^3(t')}\quad (t < t_*)$$
$$\mathcal{R} = C^+ + \frac{D^+}{\mathcal{G}_S^+}\int_{t_*}^t\frac{\mathrm{d}t'}{a^3(t')}\quad (t > t_*)$$

Matching condition ; $C_g^+ = C_g^-,\quad C_d^+ = C_d^-,\quad C^+ = C^-,\quad D^+ = D^-.$

V. Summary

* From the surface terms in Horndeski's theory, we derived the cosmological matching conditions for the background and perturbations.

* We applied the matching conditions to the model in which the standard radiation-dominant phase is joined to the NEC violating phase.

“21cm signature of minihaloes from cosmic string wakes”

by Naoya Kitajima

[JGRG23(2013)P23]

21cm signature of minihaloes from cosmic string wakes

Naoya Kitajima

Institute for Cosmic Ray Research (ICRR),
University of Tokyo

Collaborators:
Daisuke Yamauchi & Masahiro Kawasaki

JGRG23 in Hirosaki University

1. Introduction : Cosmic string

http://www.damtp.cam.ac.uk/research/gr/public/cs_top.html

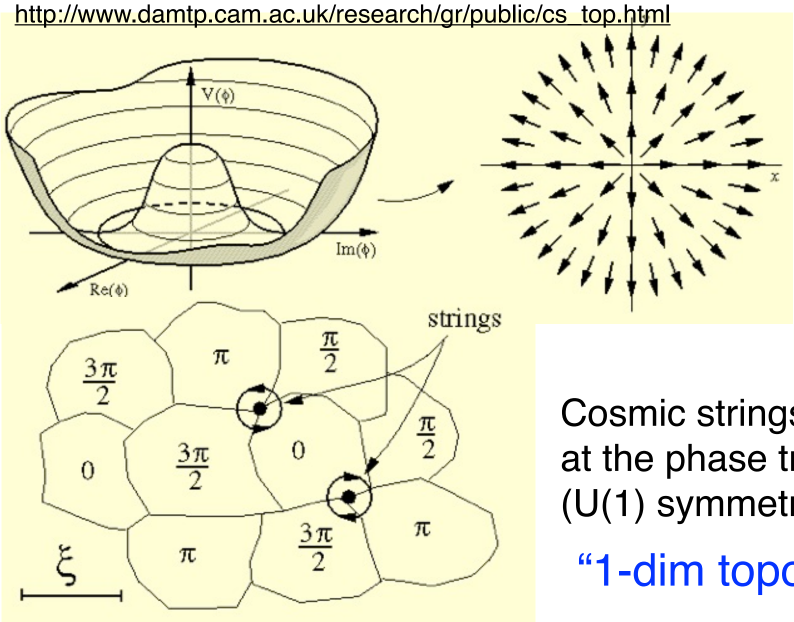

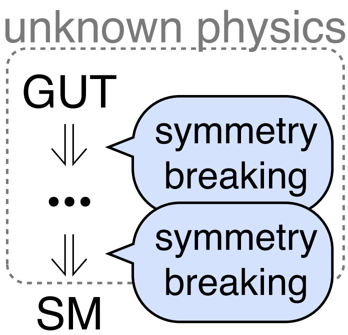

Cosmic strings (CSs) may be formed at the phase transition (U(1) symmetry breaking)

"1-dim topological defect"

- ❖ Cosmic string is characterized by the "tension" $G\mu$
- ❖ Tension is related to the symmetry breaking scale

Cosmic string detection ≈ Probe of high energy physics

Cosmic string "wake"

Moving strings change the geometry behind them!

long(infinite)

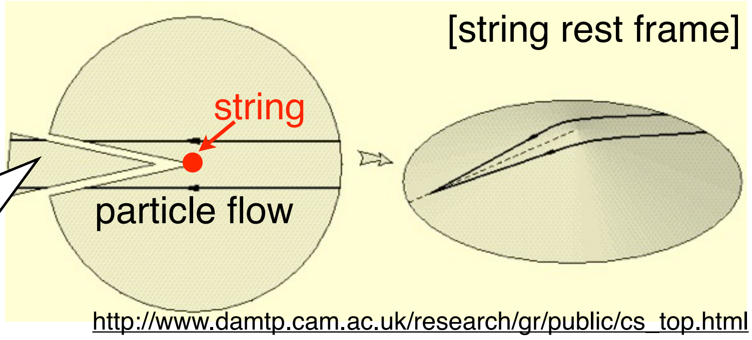

http://www.damtp.cam.ac.uk/research/gr/public/cs_top.html

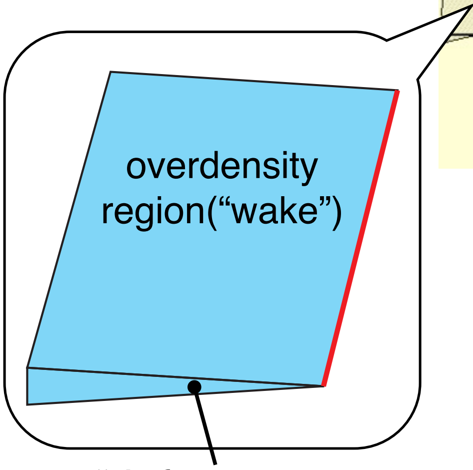

"deficit angle"

$$\Delta\theta = 8\pi G\mu$$

☑ energy density inside the wale
≈ 2×background energy density

☑ More and more particles
accrete on the wake

☛ Early structure formation!

21cm Cosmology –probe of the DARK AGE–

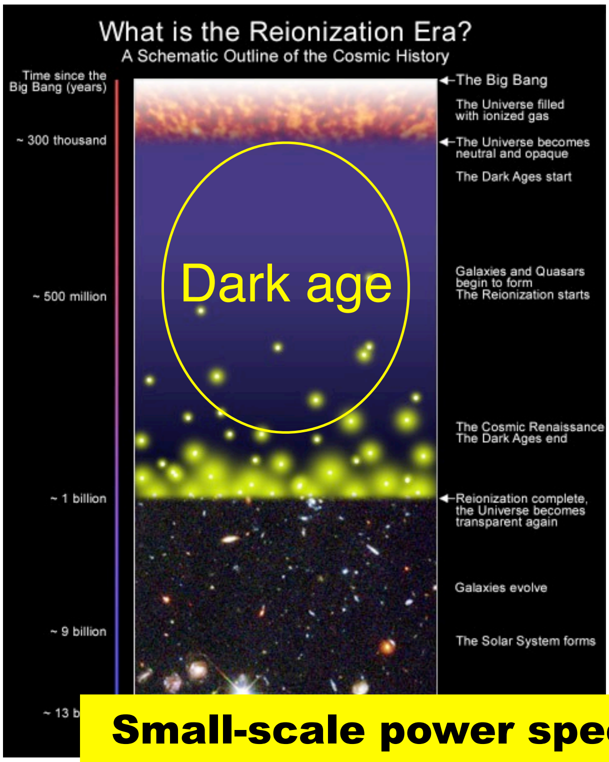

✭ After recombination
until reionization is completed

✭ The universe is filled with
the neutral hydrogen

What is interesting in dark age?

CDM & baryon can collapse

▶ Minihaloes can be formed

◆ Small mass $(M \lesssim 10^6\ M_\odot)$

◆ Atomic cooling cannot occur
$(T \lesssim 10^4\ \mathrm{K})$

Small-scale power spectrum may be imprinted on the minihalo abundance!

Q. How can we probe the dark age?

A. Redshifted 21cm emission/absorption signal due to the neutral hydrogen

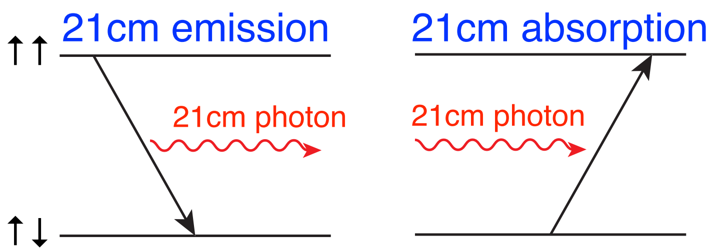

Cold IGM ➟ absorption signal

Minihaloes ➟ emission signal

Cosmic string ➟ ????????

Related works: Khatri &Wandelt (2008)
Brandenberger et al(2010)
Tashiro(2013), Tashiro, Sekiguchi & Silk(2013)

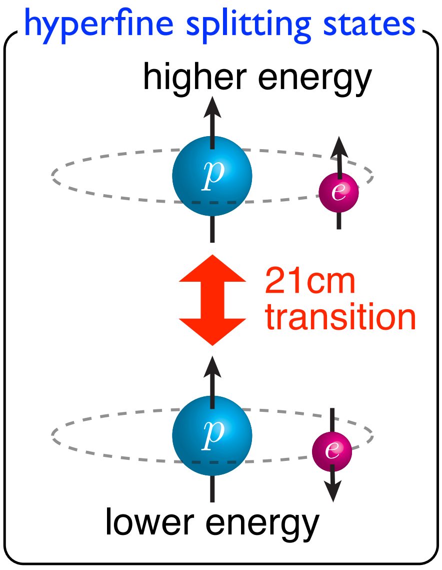

2. Structure formation from cosmic string wakes

Sheet-like structure is unstable & must collapse!

sheet ▶▶ filament ▶▶ “bead” (halo)

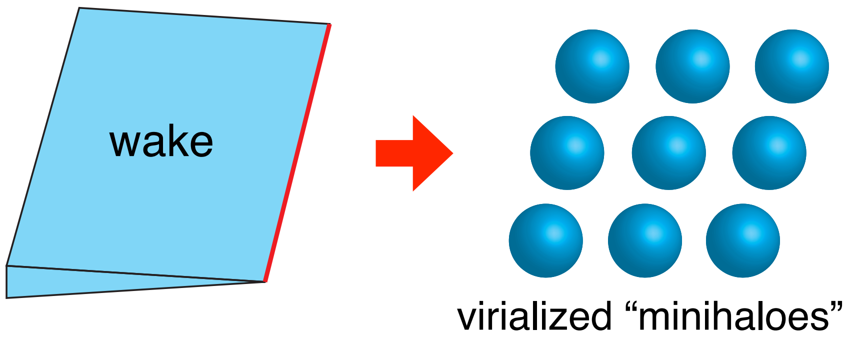

Halo mass?
Halo number density?

Equation of motion for nearby particles

✲ Distance from the center of the wake : $r = a(t)(x + \psi)$

Hubble flow perturbation

✲ Particles around the wake get an velocity kick: $u_i = 4\pi G\mu v_s \gamma_s$
(initial velocity)

Equation of motion ▶ $\ddot{\psi} + \frac{4}{3t}\dot{\psi} - \frac{2}{3t^2}\psi = 0,$

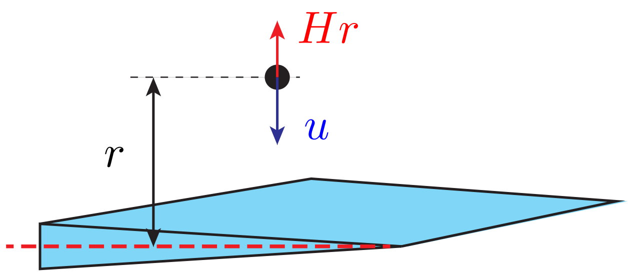

Solution for EOM : $$\psi(t) = -\frac{3}{5}\mathrm{sgn}(x)u_i t_i\left[\left(\frac{t}{t_i}\right)^{2/3} - \left(\frac{t}{t_i}\right)^{-1}\right]$$

$$\dot{\psi}(t) = -\frac{3}{5}\mathrm{sgn}(x)u_i\left[\frac{2}{3}\left(\frac{t}{t_i}\right)^{-1/3} + \left(\frac{t}{t_i}\right)^{-2}\right]$$

✦ Perturbation grows like : $\psi \propto a$

✦ When perturbation overcomes the Hubble flow, particles turn around

▶ Turnaround surface is determined via $\dot{r}_{\rm turn} = 0$

✦ After turnaround, the region is collapsed

▶ The thickness of the wake: $d_w = 2 \times \frac{1}{2} r_{\rm turn}$
(collapsed region)

analogy with the spherical collapse

MInihalo formation from cosmic string wakes

halo volume is determined
by the wake thickness: $V_h = c_h d_w^3$

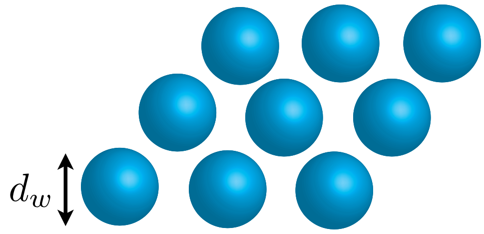

Halo mass is determined
at turnaround: $M_h = \rho_w c_h d_w^3\big|_{\rm turn}$

where $\rho_w = 2\bar{\rho}$ (background)

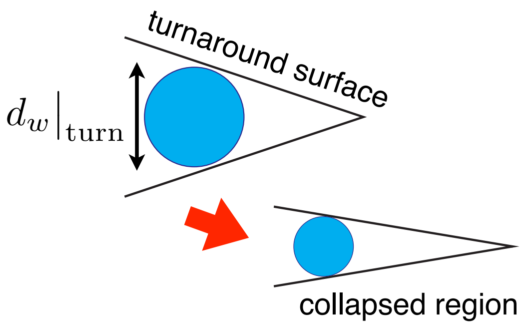

✻ number of minihaloes originated from one wake

$$\nu_h(z, z_i) = \frac{l_w(z) w_w(z) d_w(z)}{c_h d_w^3(z)}$$

wake formation

length of string: $l_w = \gamma t$ with $\gamma \sim 1$

width of wake: $w_w = v_s \gamma_s t$

✻ number density of wake: $n_{\rm wake}(z_i) = \tilde{N} H^3(z_i) a^3(z_i)$

number density of halo: $n_h(z, z_i) = \nu_h n_{\rm wake}(z_i)$

☞ We can calculate the mass function: $\dfrac{dn_h}{d\ln M_h}$

Mass function of minihaloes:
cosmic string vs primordial perturbation

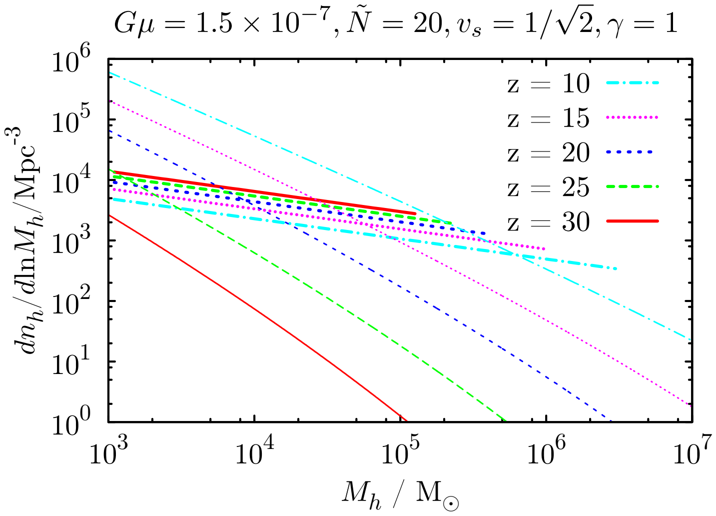

Maximum mass of minihalo ☞ $z_i = z_{\rm eq} \sim 3000$

Wake-induced minihaloes dominate for z>15

3. 21cm signature from wake-induced minihaloes

✳ Can we detect the wake-induced minihaloes by future obs.?

✳ Can we constrain the string tension?

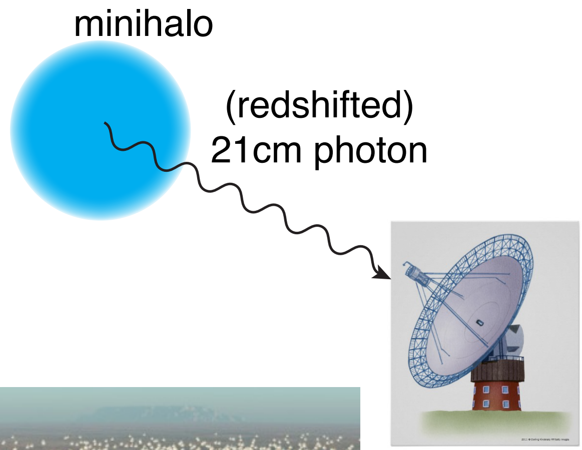

Density & temperature profile of minihalo (TIS model)

Spin temperature: $\frac{n_1}{n_0} = 3\exp\left(-\frac{T_*}{T_s}\right)$ energy splitting: $T_* = 0.068$ K

21cm brightness temperature

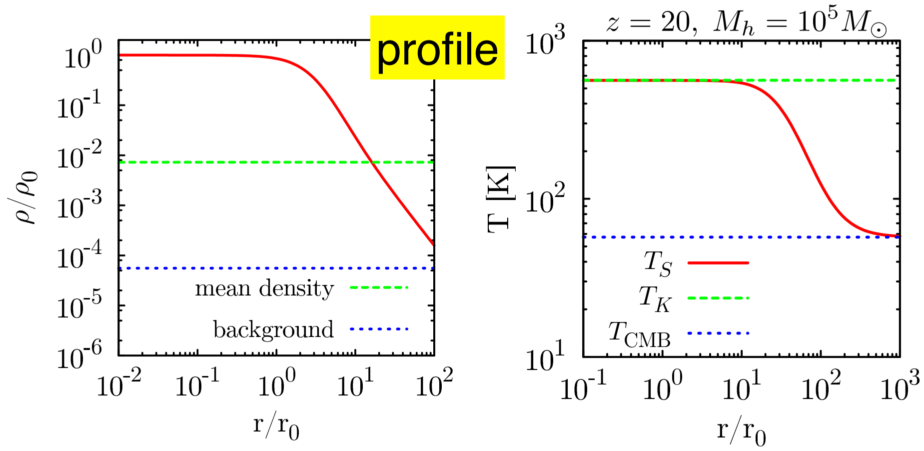

minihalo contribution ➢ $T_S \gg T_{\rm CMB}$ ➢ emission signal!

✻ Brightness temperature:

$$T_b(\nu,\alpha) = T_{\rm CMB}e^{-\tau(\nu)} + \int_{-\infty}^{\infty} T_S(R,\alpha)e^{-\tau(\nu,R)}\frac{\partial\tau}{\partial R}dR$$

✻ Differential brightness temperature: $\delta T_b = \frac{\langle T_b\rangle}{1+z} - T_{\rm CMB}(0)$

averaged over halo mass

$G\mu = 1.5\times 10^{-7}, \tilde{N} = 20, v_s = 1/\sqrt{2}, \gamma = 1$

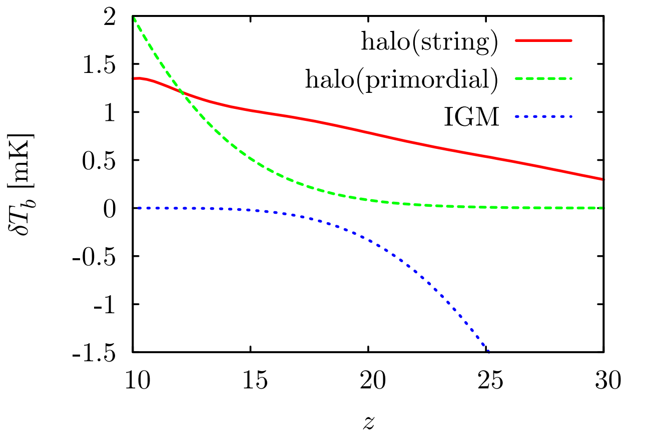

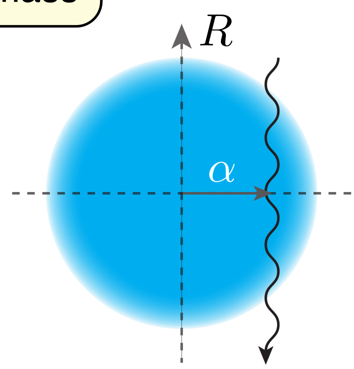

✣ RMS of the differential brightness temperature fluctuation

$$\langle \delta T_b^2 \rangle^{1/2} = q\sigma_p(\Delta\theta_{\rm beam}, \Delta\nu)\beta(z)\overline{\delta T}_b$$

rms of density perturbation smoothed over obs. cylinder

flux averaged bias

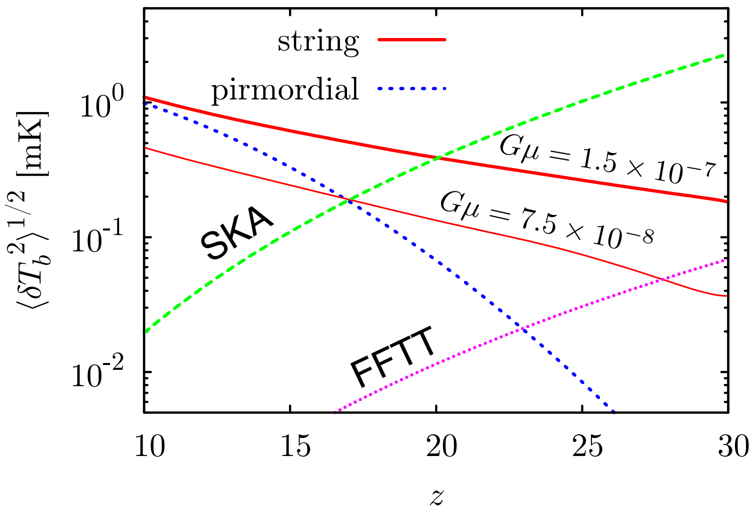

$\Delta\nu = 0.01$ MHz

$\Delta\theta_{\rm beam} = 10$ arcmin

Wake-induced halo signal can be detectable by SKA!!

Conclusions

♠ We reinvestigated the early structure formation from cosmic string wakes.

♣ The overdense planar regions induced by the cosmic string wakes collapse into the virialized minihaloes.

♥ The number density of such wake-induced minihaloes can exceed those from the primordial perturbaiton

♦ 21cm emission signal from such wake-induced minihaloes can be observed by the future radio telescopes such as SKA.

“Liquid bridges and black strings in general dimensions: Stability”

by Umpei Miyamoto

[JGRG23(2013)P24]

Liquid bridges and black strings in general dimensions: **Stability (of non-uniform bridges)**

1

Umpei **MIYAMOTO**
(Akita Prefectural Univ)
&
Miyuki **KOISO**
(Kyushu Univ)

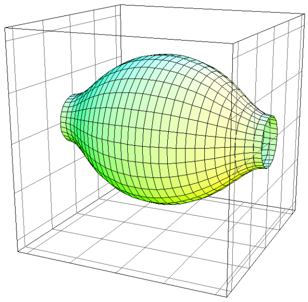

21st JGRG
Hirosaki Univ
2013.11.5-8

Abstract

2

Phase diagrams of black strings in Kaluza-Klein spacetimes and liquid bridges between parallel plates are known to exhibit startling similarities in general dimensions.

The stability of liquid bridges might tell us much about the stability of Kaluza-Klein black strings, which has not been confirmed in every mass regime.

In this study, we clarify **the stability of non-uniform liquid bridges in all dimensions and in all parameter regimes,** while formulating the problem as **a variational problem**.

3

Introduction (1):
Gregory-Laflamme instability [1993]

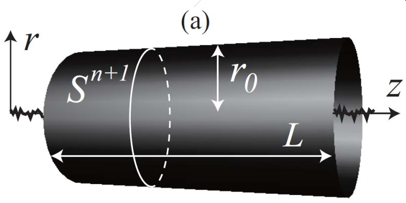

Schwarzschild black string

$$ds^2 = -f(r)d(ct)^2 + f(r)^{-1}dr^2 + r^2 d\Omega^2_{(n+1)} + dz^2$$

$$f(r) = 1 - \left(\frac{r_0}{r}\right)^n$$

$$g_{ab} \to g_{ab} + \delta g_{ab}$$

$$\delta g_{ab} \sim e^{-i\omega t + ikz} f_{ab}(r)$$

Solve the perturbed Einstein eq.

$$\delta G_{ab} = 0$$

Growth rate (dispersion relation)

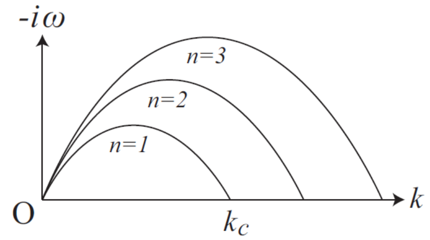

$$k_c \simeq \sqrt{n}/r_0$$

4

Introduction (2):
Rayleigh-Plateau instability [Plateau 1873; Rayleigh 1878]

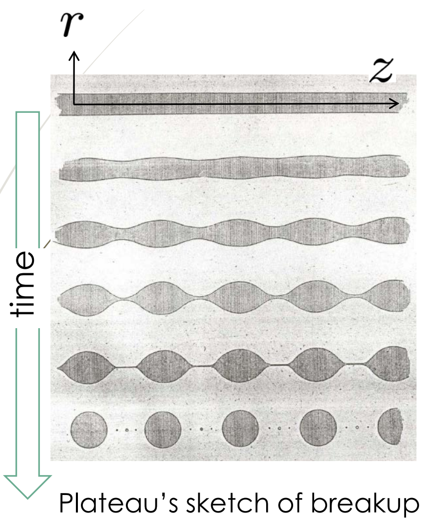

Plateau's sketch of breakup of an oil tube suspended in a mixture of alcohol and water

- Cylindrical fluid tube supported by *surface tension* is unstable if

$$(\text{length}) > 2\pi(\text{radius})$$

Pressure perturbation

$$\delta p = e^{\Omega t + ikz} f(r)$$

Solve the perturbed Euler eq.

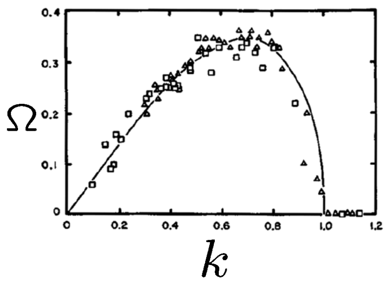

5

Introduction (3): Phase diagram of fluid lumps in $R^{n+1} \times S^1$: **critical dimension** [Miyamoto-Maeda 2008]

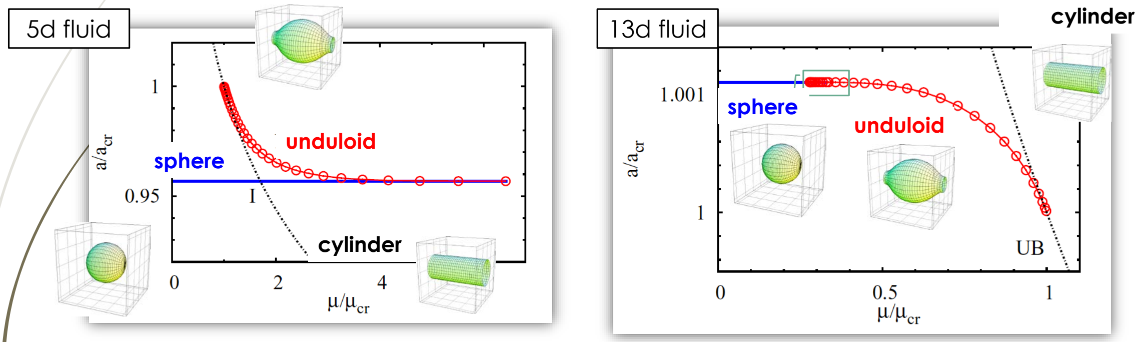

$\mu := \frac{V}{L^{n+2}}$ reduced volume (L: circumference of S^1) $a := \frac{A}{V^{(n+1)/(n+2)}}$ reduced area

6

Question/Motivation

- There exists **a critical dimension (~12)** for the fluid between two parallel plates where the phase structure drastically changes.
- The existence of **a similar critical dimension (~13)** has been reported in Kaluza-Klein BHs [Sorkin 2004]. But the stability, especially that of the non-uniform strings, has not been known [cf: Figueras-Murata-Reall 2012].
- **Let's examine the stability of the *unduloid* (non-uniform bridge) [Delaunay 1941] in all parameter (dimension and non-uniformity) regimes.**

7

Formulation as a variational problem

[Koiso-Miyamoto 2013, in preparation]

Surface area and bulk volume of fluid lump in $\mathbf{R}^{n+1}\times S^1$

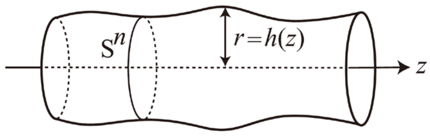

$$A[h]=s_n\int_{z_1}^{z_2}h^n\sqrt{1+h_z^2}dz$$

s_n :volume of unit n-sphere

$$V[z]=b_{n+1}\int_{z_1}^{z_2}h^{n+1}dz$$

b_{n+1} :volume of unit (n+1)-ball

8

1st variation: equilibrium state (critical point in math)

Variation of the generating curve $h(z)\to h(z)+\epsilon\phi(z)$

1st variations of area and volume

$$\begin{aligned}\delta A &:= \frac{d}{d\epsilon}|_{\epsilon=0}A[h+\epsilon\phi]\\ &= -s_n\int_{z_1}^{z_2}(n+1)Hh^n\phi dz+s_n[h_zh(1+h_z^2)^{-1/2}\phi]_{z_1}^{z_2}\\ \delta V &:= \frac{d}{d\epsilon}|_{\epsilon=0}V[h+\epsilon\phi]\\ &= s_n\int_{z_1}^{z_2}h^n\phi dz\end{aligned}$$

Mean curvature of the surface

$$H=\frac{1}{n+1}[(1+h_z^2)^{-3/2}h_{zz}-nh^{-1}(1+h_z^2)^{-1/2}]$$

- An equilibrium state is defined as the critical point of the surface area (delta_A=0) for the volume-preserving (delta_V=0) variations.
- From the above expressions, one finds that the surface is a critical point of the area for volume-preserving variations iff **H=constant** and **h_z =0 at the bdrys**.

9

2^{nd} variation: stability ⇔ eigenvalue problem

For the volume-preserving variations of the H=constant surface, the 2^{nd} variation of the area is given by

$$\begin{aligned} \delta^2 A &:= \frac{d^2}{d\epsilon^2}|_{\epsilon=0} A[h+\epsilon\phi+O(\epsilon^2)] \\ &= -s_n \int_{z_1}^{z_2} \phi L[\phi] dz + s_n [\phi\sigma\phi_z]_{z_1}^{z_2} \end{aligned}$$

$$\begin{aligned} L[\phi] &:= (\sigma\phi_z)_z + n h^{n-2}(1+h_z^2)^{-1/2}\phi \\ \sigma &:= (1+h_z^2)^{-3/2} h^n \end{aligned}$$

- The critical point is said to be **stable** if the above 2^{nd} variation is **non-negative (delta^2_A>=0)** for all volume-preserving variations.
- The problem reduces to solve the following eigenvalue problem [cf: Koiso 2002]

$$L[\phi] = -\lambda\phi, \quad \phi_z(z_1) = \phi_z(z_2) = 0$$

10

Results (1): 1=<n=<6

- Unduloids (non-uniform bridges) are **unstable** in all volume region [see Vogel 1987 and Athanassennas 1987 for n=1].
  - The phase transition from the cylinder to sphere is of 1^{st} order.

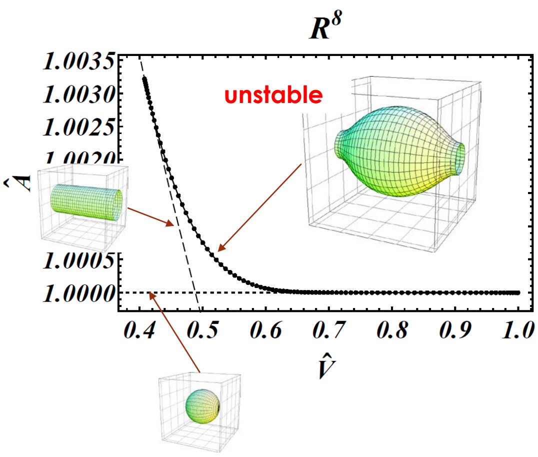

11

Results (2): n=7,8,9

- Unduloids (non-uniform bridges) close to either the sphere or cylinder are **unstable.**
- There are **stable** unduloids! [cf: Pedrosa-Ritore 1999]

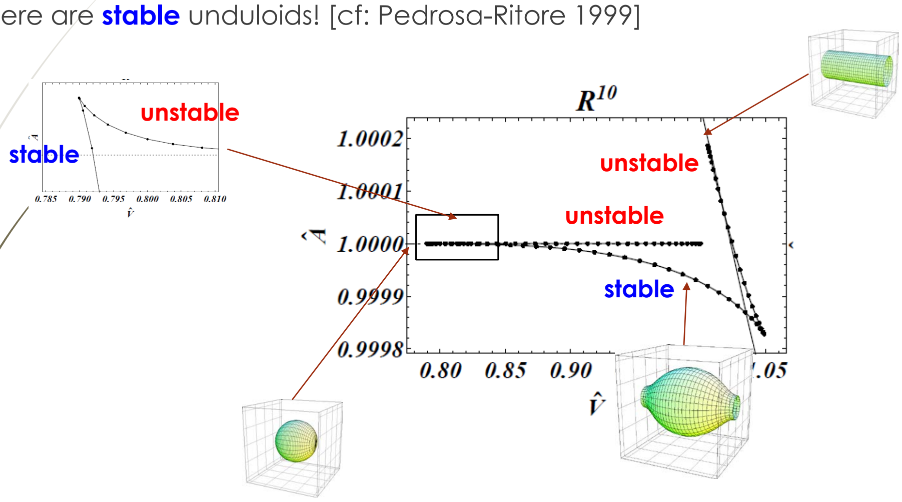

12

Results (3): n>=10

- Unduloids (non-uniform bridges) except those quite close to the sphere are **stable!**
  - The phase transition from the cylinder to sphere is of 2nd order or higher.

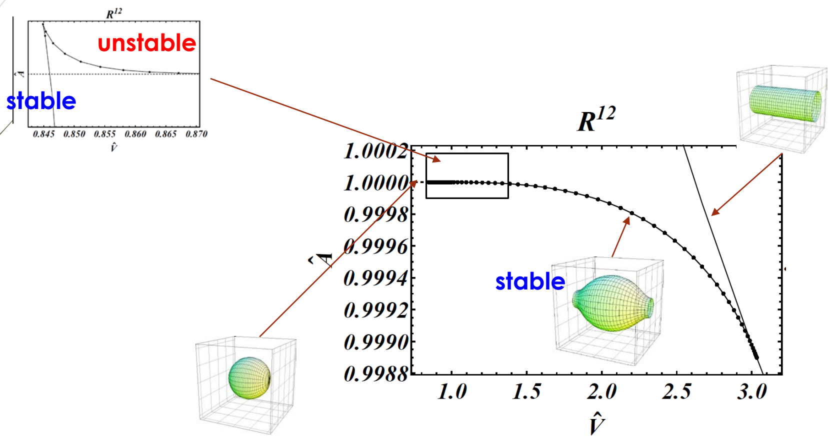

13

Conclusion

- **Summary: Stability of unduloids (non-uniform liquid bridges) in R^{n+1} x S^1 has been clarified in all dimensions (n>=1) and all parameter volume regimes.**
  - 1=<n=<6: all unduloids are unstable
  - n=7,8,9: unduloids close to either the cylinder or sphere are unstable; the rests are **stable**
  - n>=10: unduloids close to the sphere are unstable; the rests are **stable**
  - Note: all spheres are stable; thin cylinders (radius<($n^{1/2}$ /2 pi)* length) are unstable
- **Future prospect:**
  - Interpret the results in terms of **thermodynamic** quantities: e.g. S=S(U) or F=F(T)
  - Interpret the above thermodynamic results from the **holographic** viewpoint [Aharony-Minwalla-Wiseman 2006].
  - Compare our results with the stability analysis of non-uniform black strings with the **local Penrose inequality** [Figueras-Murata-Reall 2012]

“(In-)stability of naked singularity formation

in gravitational collapse”

by Seiju Ohashi

[JGRG23(2013)P26]

(In)-stability of naked singularity formation in gravitational collapse

Seiju Ohashi
KEK

Contents

1. Introduction

2. Perturbation Analysis

3. Summary

1. INTRODUCTION

1.1 Cosmic Censorship Conjecture

<Cosmic Censorship Conjecture>
No naked singularity form during the gravitational collapse

- ✓ At the singularity, gravitational theory breaks down.
- ✓ We cannot predict anything from singularity.
- ✓ It is important to study whether cosmic censorship conjecture holds .

1.2 Counter-example？

- Counter-example to CCC

4 dimension	Higher dimension
✓ Dust collapse	✓ Dust collapse
✓ Null dust collapse	✓ Null dust collapse
✓ Perfect fluid etc……	✓ Perfect fluid collapse
	✓ Collapse in Gauss-Bonnet, Lovelock gravitational theory.

- So far we have many counter-example to CCC. But are they serious counter-examples to CCC ?
- They are ***highly symmetric***, e.g. spherical symmetry, cylindrical symmetry etc.

⇨ Does naked singularity form without such a symmetry ?

1.3 Stability of NS formation

- Does naked singularity stably form under small perturbation ?

  If unstable, they are not serious counter-example to CCC

- Here we consider the stability of naked singularity formation.

  We assume that the background spacetime is

  ✓ Arbitrary dimension (D=n+2 dim)
  ✓ Spherical collapse of null dust
  （&inhomogeneous dust）
  ✓ Self-similar

2. PERTURBATION ANALYSIS

2.1 Background spacetime (null dust collapse)

- Matter (null dust)

$$T_{\mu\nu} = \underbrace{\rho}_{\text{energy density}} l_\mu l_\nu \qquad l^2 = 0$$

- Metric of spacetime

$$\boxed{ds^2 = -\left(1 - \frac{2m(v)}{r^{n-1}}\right) dv^2 + 2dvdr + r^2 d\Omega_n}$$

$$\xrightarrow[\text{Self-similarity}]{} \quad m(v) = \lambda v^{n-1}$$

✓ In other coordinate, $z = \frac{v}{r}$ $\quad x = \log r$

$$\boxed{ds^2 = e^{2x}\left[-(1-2\lambda z^{n-1})dz^2 + 2(1-z+2\lambda z^n)dzdx + z(2-z+2\lambda z^n)dx^2 + d\Omega_n\right]}$$

2.2 Perturbation

- We perform perturbation analysis on the spherical background.

$$ds^2 = g_{\mu\nu}dx^\mu dx^\nu = \underbrace{g_{AB}dx^A dx^B}_{M^2} + \underbrace{r^2\gamma_{ij}dx^i dx^j}_{S^n}$$

✓ Metric perturbation $\quad g_{\mu\nu} = g^B_{\mu\nu} + h_{\mu\nu}$

✓ Matter perturbation $\quad T_{\mu\nu} = T^B_{\mu\nu} + \delta T_{\mu\nu}$

$$\delta G_{\mu\nu} = 8\pi\delta T_{\mu\nu}$$

- There are three types of perturbation, i.e. scalar, vector and tensor.

Here we consider the ***tensor*** (vector) type perturbation.

2.3 Tensor Perturbation

- Tensor perturbations for the metric and matter.

$$\boxed{\begin{array}{lll} h_{ij} = h^T_{ij} & h_{Ai} = 0 & h_{AB} = 0 \\ \delta T_{ij} = T^T_{ij} & \delta T_{Ai} = 0 & \delta T_{AB} = 0 \end{array}}$$

with
$$\begin{array}{ll} D^i h^T_{ij} = 0 & D^i T^T_{ij} = 0 \\ h^{T\,i}_{\ \ i} = 0 & T^{T\,i}_{\ \ i} = 0 \end{array}$$

- Master equations for tensor perturbation.

$$\delta G_{\mu\nu} = 8\pi\delta T_{\mu\nu} \quad \Rightarrow \quad \boxed{\frac{1}{r^{n-2}}\left(r^n \Pi^{|A}\right)_{|A} - m_T\Pi = -8\pi T_T}$$

where
$$\begin{array}{ll} h^T_{ij} = 2r^2\Pi\mathcal{T}_{ij} & \mathcal{T}_{ij} \text{ : tensor harmonics} \\ T^T_{ij} = T_T\mathcal{T}_{ij} & m_T = l(l+n-1) \end{array}$$

2.4 Master equations

➢ Concrete form of the master equation.

Partial differential equations for perturbative quantity Φ with second order

$$\boxed{\alpha\ddot{\Phi}+2\beta\dot{\Phi}'+\gamma\Phi''+(\dot{\alpha}+\beta(n-2\kappa))\dot{\Phi}+(\dot{\beta}+\gamma(n-2\kappa))\Phi'-(\kappa(\dot{\beta}+\gamma(n-\kappa))+m_T)\Phi=0}$$

where

$$\begin{aligned} G &= \frac{1}{2}-\lambda z^{n-1} & \beta &= 1-2zG \\ \alpha &= -2z(1-zG) & \gamma &= 2G \end{aligned}$$

$$\Pi := e^{\kappa x}\Phi$$

➢ How Φ behaves on the Cauchy horizons ?

We need to judge whether Φ diverges or not on the Cauchy horizon.

2.5 Sketch of Analysis

➢ Introduce the "**norm**" of perturbation

$$E_2[\Phi](z) = \int_{\mathcal{R}} \left(-\underline{\alpha}\dot{\Phi}^2 + \underline{\gamma}\Phi'^2 + \underline{D}\Phi^2\right) dx$$

All coefficients are positive

➢ Take the derivative of the norm with respect to z.

$$\frac{dE_2}{dz} \underset{\text{By using the EoM}}{=} \int_{\mathcal{R}} \left[(\dot{\alpha}+2\beta(n-2\kappa))\,\dot{\Phi}^2 + 2\left(\dot{\beta}+\gamma(n-2\kappa)\right)\dot{\Phi}\Phi' + \dot{\gamma}\Phi'^2 + \dot{D}\Phi^2 \right] dx$$

➢ We can prove that norm is **finite**.

$$\frac{dE_2}{dz} \le CE_2 \quad \Rightarrow \quad E_2(z) \le e^{C(z-z_E)}E_2(z_E)$$

C is constant

2.6 Results

Naked singularity formation is stable under tensor type perturbation.

- We can also prove that NS formation is stable under vector type perturbation.
- The same procedure works for time-like dust collapse (LTB) for vector, tensor type of perturbations.

3. SUMMARY

3.1 Summary

- We consider the stability of naked singularity formation under small perturbation.

✓ They are ***stable*** under ***vector*** and ***tensor*** types of perturbations in the null dust and time-like dust collapse.

- At this stage, they seem to be stable under perturbations. But the scalar perturbation analysis is needed in order to have definite conclusion.

◆ It is interesting to consider the perfect fluid collapse.

◆ It is also interesting to analyze the case without self-similarity.

3.2 Table of the results

mode \ model	Dust	Null dust	Perfect fluid
Scalar	?	?	?
Vector	Stable	Stable	?
Tensor	Stable	Stable	?

“Issues on curvaton scenario with the thermal effect”

by Shuichiro Yokoyama

[JGRG23(2013)P27]

Issues on curvaton scenario with thermal effect

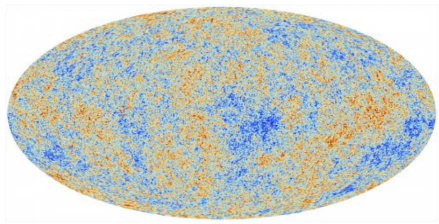

Shuichiro Yokoyama (ICRR, Univ. of Tokyo)

with Naoya Kitajima, Tomohiro Takesako, Tomo Takahashi

Introduction I

- Planck data release in March 2013

➔ Precise information about the physics of the early Universe

e.g., constraint on single-field inflation models

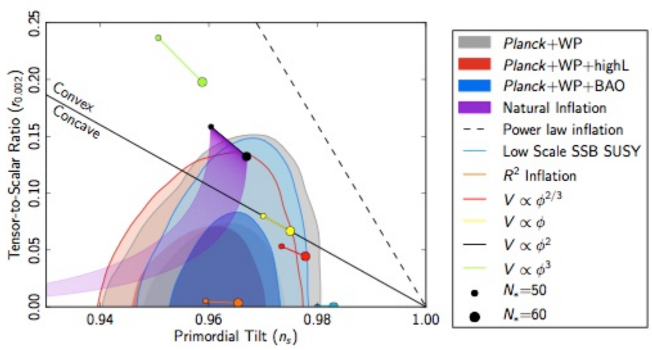

arXiv:1303.5082

constraint on non-Gaussian models

SMICA	KSW	Binned	Modal
Local	**2.7 ± 5.8**	2.2 ± 5.9	1.6 ± 6.0
Equilateral	**−42 ± 75**	−25 ± 73	−20 ± 77
Orthogonal	**−25 ± 39**	−17 ± 41	−14 ± 42

Flattened model (Eq. number)	Raw f_{NL}	Clean f_{NL}	Δf_{NL}
Flat model (13)	70	37	77
Non-Bunch-Davies (NBD)	178	155	78
Single-field NBD1 flattened (14)	31	19	13
Single-field NBD2 squeezed (14)	0.8	0.2	0.4
Non-canonical NBD3 (15)	13	9.6	9.7
Vector model $L = 1$ (19)	−18	−4.6	47
Vector model $L = 2$ (19)	2.8	−0.4	2.9

arXiv:1303.5084

make us discuss a variety of models in more detail..

Introduction II

• Curvaton scenario

Lyth and Wands, Moroi and Takahashi,
Enqvist and Sloth (2002)

A mechanism of generating primordial adiabatic perturbations through the decay of a scalar field (curvaton) other than inflaton

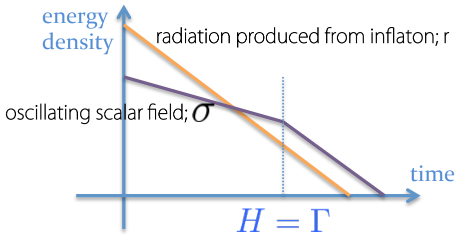

background dynamics

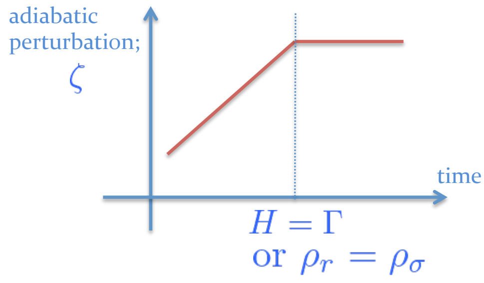

Γ ; decay rate of curvaton
(constant in time in simple standard case)

m; mass of curvaton

$$\boxed{\zeta = \frac{r_{\rm dec}}{3}\frac{\delta\rho_\sigma}{\rho_\sigma}\bigg|_{H=m}}$$

$$r_{\rm dec} := \frac{3\rho_\sigma}{3\rho_\sigma + 4\rho_r}\bigg|_{H=\Gamma}$$

neglecting the contribution from the inflaton fluctuations

Introduction III

• Thermal effects?

curvaton should decay into the radiation
➔ curvaton has the coupling to the radiation (plasma)
➔ It is expected to give some thermal effects..

e.g., $\mathcal{L}_{\rm int} = -M\sigma\chi^2 - \lambda\chi\xi^2,$

$\mathcal{L}_{\rm int} = -y\sigma\bar{\psi}\psi - gA_\mu\bar{\psi}\gamma^\mu\psi$

For background dynamics of the curvaton decay,

e.g., temperature-dependent mass/decay rate

- modulation of the evolution of the curvaton energy density $\rho_\sigma \propto a^{-3}$?
- life time of the curvaton (related to the decay rate)

There are several works
about the dynamics of oscillating scalar field in thermal bath;

We focus on the effect of the temperature dependent decay rate on the primordial adiabatic fluctuations in the curvaton scenario.

Simple model

- Temperature dependent decay rate

$$\Gamma = \Gamma(T) = \Gamma_0 \left[1 + C \left(\frac{T}{m} \right)^n \right]$$

Background dynamics

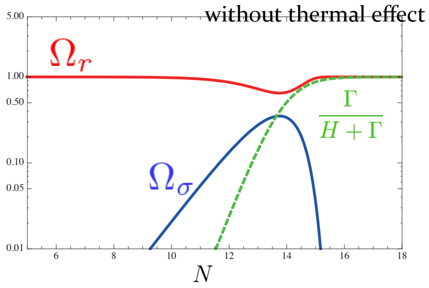

$\Gamma = \Gamma_0 = 10^{-12} m$

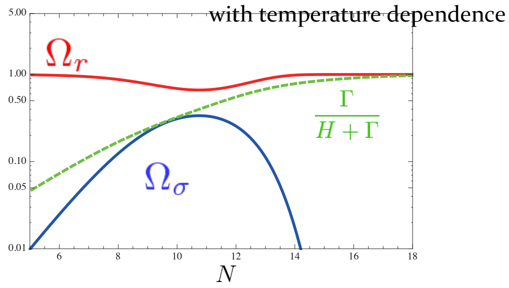

$\Gamma_0 = 10^{-14} m$

$n = 1.5,\ C = 1.0$

Little difference can be seen...

Enhancement of primordial adiabatic fluctuations? I

- sudden decay approximation

In case with the temperature-dependent decay rate,

decay hypersurface $H = \Gamma$ $\neq$ constant Hubble hypersurface $H = \text{const.}$

$$\boxed{\zeta = \frac{r_{\rm dec}}{3} \frac{\delta\rho_\sigma}{\rho_\sigma}\bigg|_{H=m} - \frac{r_{\rm dec}}{6} \frac{\delta\Gamma}{\Gamma}\bigg|_{H=\Gamma}}$$

cf. modulated decay of the curvaton

Langlois and Takahashi (2013)

Assadullahi et al. (2013)

$$\frac{\delta\Gamma}{\Gamma}\bigg|_{H=\Gamma} = -\frac{\frac{r_{\rm dec}}{3}\tilde{\Gamma}'}{1 - \left(\frac{r_{\rm dec}}{6} + \frac{1}{2}\right)\tilde{\Gamma}'} \times \underline{\frac{\delta\rho_\sigma}{\rho_\sigma}}\bigg|_{H=m}$$

iso-curvature fluctuations

cf. In the reheating era (inflaton decay), because of no iso-curvature fluctuation, the enhancement does not occur..

Ref. e.g., Weinberg (2004)

Enhancement of primordial adiabatic fluctuations? II

- amplitude, fNL by sudden decay approx.

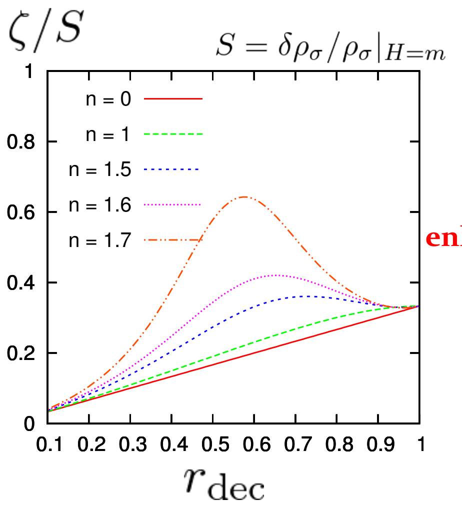

enhancement ??

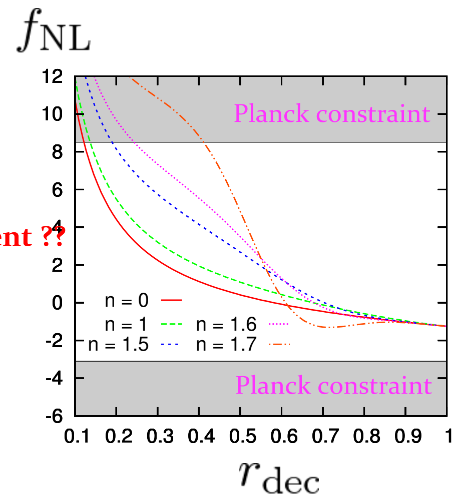

$$C = 1$$
$$\sigma_i = 10^{-1} M_{\rm P} \qquad m_\sigma = 10^{-10} M_{\rm P}$$

* Changing Γ_0 corresponds to changing $r_{\rm dec}$

Numerical analysis by delta N I

- Appropriate parameter; r $\qquad \Gamma = \text{constant}$

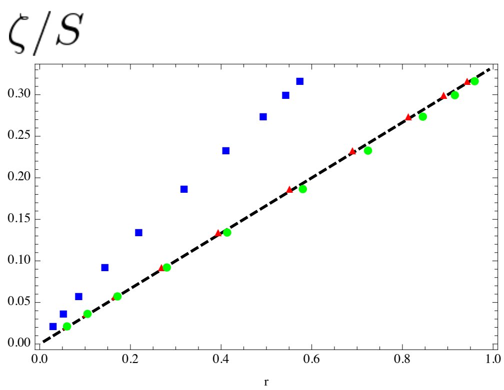

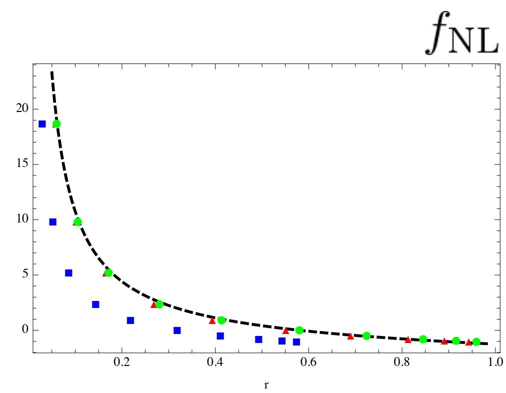

black dashed; $r/3$ $\qquad$ black dashed; $\dfrac{5}{4r} - \dfrac{5}{3} - \dfrac{5r}{6}$

blue box; numerically evaluated $r_{\rm dec}$

red triangle; Gupta et al. (2004) fitting formula $r(p) = 1 - (1 + \frac{0.924}{1.24}p)^{-1.24}$ with $p = \left(\Omega_\sigma \sqrt{\frac{H}{\Gamma}}\right)_{H=m}$

green circle; entropy production rate (we newly introduce) $\quad r_s(q) = 1 - (1 + \frac{3}{4}q)^{-1}$ with $q = \left(\dfrac{\mathcal{S}_f}{\mathcal{S}_i}\right)^{4/3} - 1$

Numerical analysis by delta N II

- r-parameter related with entropy production rate

$$r_s(q) = 1 - (1 + \frac{3}{4}q)^{-1} \text{ with } q = \left(\frac{\mathcal{S}_f}{\mathcal{S}_i}\right)^{4/3} - 1$$

$\mathcal{S}_i$; initial entropy

$\mathcal{S}_f$; total entropy after the complete curvaton decay

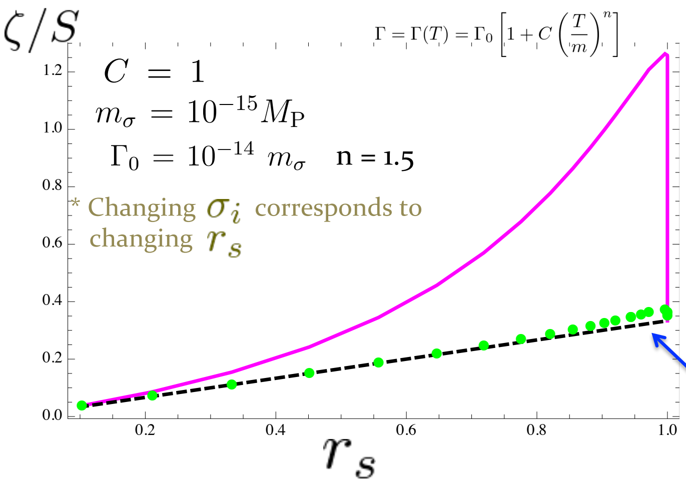

magenta; sudden decay formula

green; numerical result

black dashed; $r/3$

➔ sudden decay approximation does not work well..

thermal effect is not so large

small deviation appear around r~1 ?

Numerical analysis by delta N III

- n-dependence $\Gamma = \Gamma(T) = \Gamma_0 \left[1 + C\left(\frac{T}{m}\right)^n\right]$

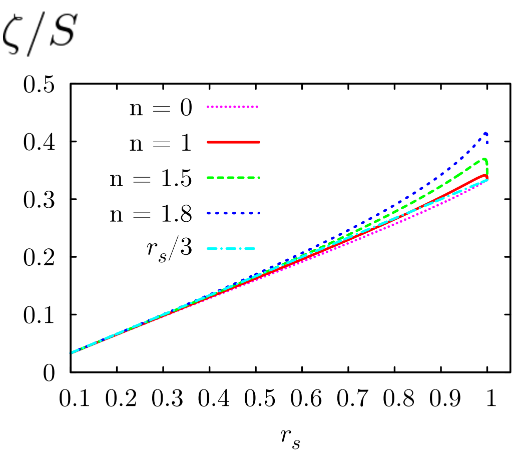

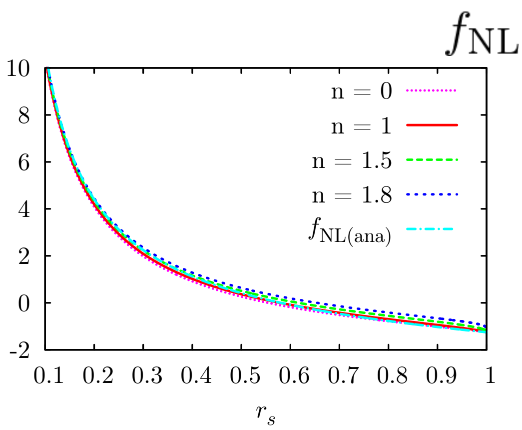

Deviation depends on the value of n.

We have also checked the result by using standard perturbation theory, and both are consistent.

It really comes from $\delta\Gamma$ or other effects??

δΓ obtained numerically

- δΓ @ H = Γ surface

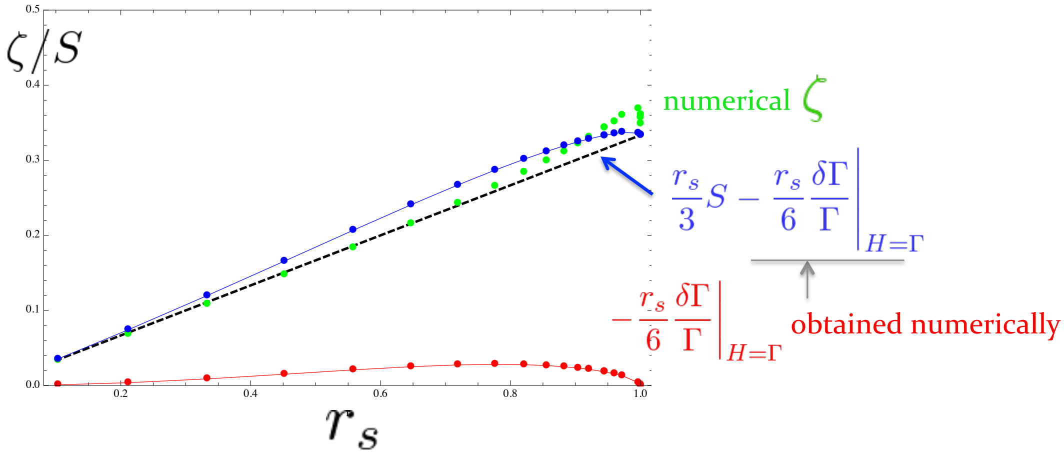

difficult to explain the numerical result only by introducing the effect of δΓ.
but numerical δΓ seems to be suppressed compared to the sudden decay approx..

- Overestimate the iso-curvature fluctuations at decay hypersurface
- overestimate the density of matter-like curvaton component

Dilution gas effect before H=Γ?

radiation component produced from curvaton decay

- negative n model (n=-5) $\sigma_i = 5 \times 10^{-3} M_{\rm Pl}$ $m_\sigma = 10^{-8} M_{\rm Pl}$ $C = 10^5$

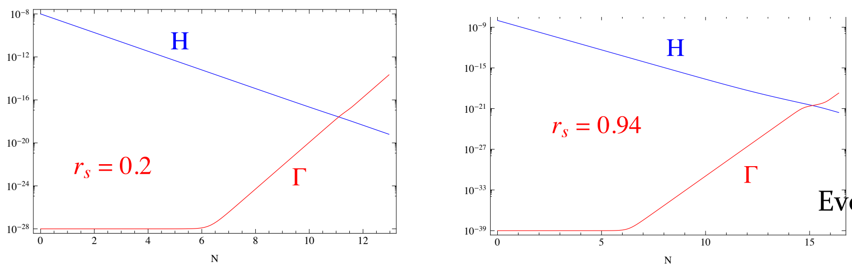

Evolution of H, Γ

For this case, due to the smallness of the decay rate, dilution gas effect before H = Γ might be small.

δΓ effect seems to be able to explain the numerical result for r<0.9..

small deviation around r~1
↔ dilution gas effect??

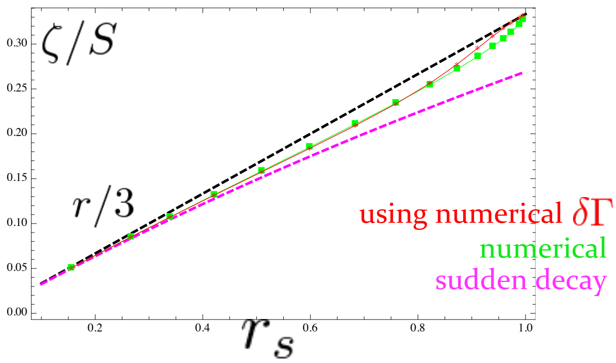

Discussion

- Thermal effect really appears in primordial curvature perturbations?

First, r_s seems to be a good parameter to describe the curvature perturbations, even in the case with temperature-dependent decay rate.

By using simple sudden decay approximation, large thermal effect seems to appear.

But, in the numerical result obtained by using delta N formalism, such large effect does not appear, but there seems to be small deviation from the result in Γ = constant case.

This deviation might be expected to come from not only the fluctuation of the decay rate at H=Γ hypersurface but also dilution gas effect before H=Γ..

How to quantify this effect?

Still need more investigation..
Anyway, the thermal effect from the temperature-dependent decay rate for the curvature perturbations could be expected to be small.

Dilution gas effect before H=Γ?

radiation component produced from curvaton decay

- negative n model (n=-5)

+ decay rate depends only on the radiation component originated from inflaton (toy model)

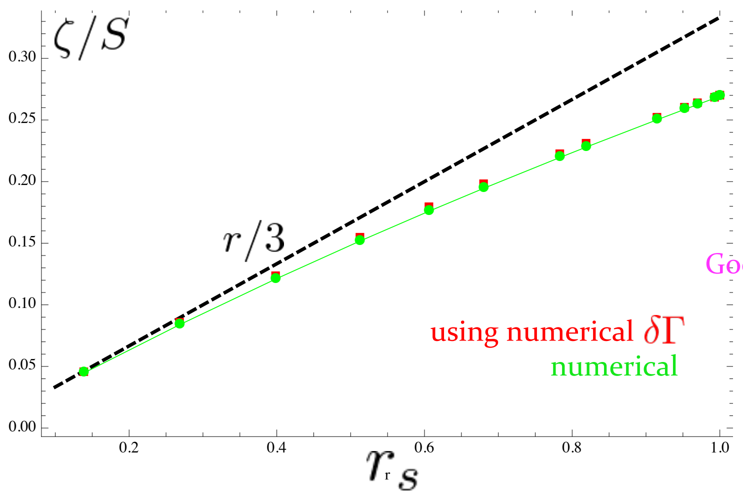

Good agreement??

“Monte Carlo simulation of quantum cosmology”

by Hiroshi Suenobu

[JGRG23(2013)P28]

Monte Carlo Simulation of Quantum Cosmology

Nagoya University Hiroshi Suenobu, Yasusada Nambu
Daidou University Hiromi Saida

Quantum Cosmology

- To investigate a quantum property of the universe especially in the very early period.
- It can be understood through the wave function of the universe.
- The wave function have been obtained exactly in a simple model, not for more complicated models so far.

Our research purpose

- Evaluating the wave-function of the universe by using the Monte Carlo method.
- Applying that method to more complicated models.

1. Quantization of the universe

Einstein-Hilbert action : $S_g = \int d^4x\sqrt{-g}(R-2\lambda)$

Quantization

Wheeler-De Witt equation : $\hat{H}_g \Psi = 0$

→ Ψ is a wave function of the universe

Path-integral representation of Ψ

$$\Psi \equiv \int \mathcal{D}g_{\mu\nu} \exp\left(iS[g_{\mu\nu}]\right)$$

Wick rotation : $t \to it_E$, $iS \equiv -S_E$

The wave function can be evaluated as the partition function.

$$Z_\lambda \equiv \int \mathcal{D}g_{\mu\nu} \exp\left(-S_E\right)$$

Probability distribution : $P(g_{\mu\nu}) \propto \exp\left(-S_E\right)$

2. Monte Carlo method

<u>We use the Monte Carlo method with probability $P(g_{\mu\nu})$ to evaluate some physical quantities and the partition function.</u>

① Generate many samples of space-time configuration by move.

move : A method to generate sample configuration from given initial configuration according to probability distribution $P(g_{\mu\nu})$.

② Obtain a physical quantity A as expectation value of samples.

$$\langle A \rangle = \sum_{sample} A_{sample}$$

③ To evaluate the partition function with Monte Carlo method

Introduce inverse temperature β as external parameter.

$$e^{-S_E} \to e^{-\beta S_E}$$

Evaluate each expectation value of the action in the interval [β:β_0] and integrate them.

Partition function : $Z[\beta] = Z(\beta_0)\exp\left(-\int_{\beta_0}^{\beta} d\beta' \langle S_E \rangle_{\beta'}\right)$

3. Our model

・Mini-supersapce model

Metric in the homogeneous and isotropic universe

$$ds^2 = \frac{N^2}{q(t)}dt^2 + q(t)d\,\Omega_3^2 \quad \text{with gauge fix } \dot{N} = 0$$

Einstein-Hilbert type action

$$S[N,q] = \int dt\left[\frac{c_1\dot{q}^2}{N} + N(c_2 - \lambda q)\right]$$

This has a classical solution with boundary condition q(0)=0, $q(t_f)$=0.

$$q(t) = \frac{\lambda N^2}{4c_1}(-t^2 + t_f t)$$

→ The Euclidean de Sitter universe

This model have been investigated by several authors. And its path-integral could be performed exactly e.g. [J. Halliwell et.al. PRD39 (1989)] ,however, over all sign of the action is opposite to ours.

In our research, we attempt to evaluate the path-integral by using the Monte Carlo method. Then, we apply that method to more complicated model, for example including inflaton, connected to Lorentian universe etc…

・Simulation details

Discrete version of the action

$$S = \sum_{i=0}^{T}\left[c_1\frac{(q_{i+1}-q_i)^2}{4N} + N\left(c_2 - \lambda\frac{(q_{i+1}+q_i)}{2}\right)\right]$$

- Consider T sites in 1-dimension (time direction).
- Distribute Q particles on the sites according to probability e^{-S} (value of Q is able to vary).
- Number of particles q_i at i-th site corresponds to spatial volume at time i.
- We obtain an equilibrium distribution by move of q_i.

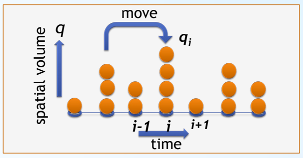

Fig.1

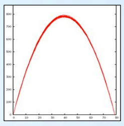

Fig.2 obtain a configuration around the classical solution (T=80, thermalized at 3×10⁶ step)

For fixed space-time volume $Q \equiv \int dt q(t) = const$, this process is regarded as a 1-dimensional effective model for the Causal Dynamical Triangulation (CDT), which is a typical quantum gravity theory with using the Monte Carlo method. L. Bogacz et. al. PRD**86**, 104015 (2012)

・Partition function and integration of lapse

Partition function with fixed N : $Z_N[N] \equiv \int \mathcal{D}q \exp\left(-S[N,q]\right)$

Partition function : $Z_\lambda = \int dN Z_N[N]$

The N integral does not converge usually.

Analytic continuation of N

$$N \to N = N_R + iN_I$$

Choose a conversing integration contour on the complex N plane (→ fig.3).

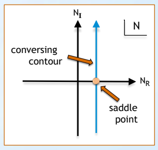

Fig.3 conversing contour on complex N palane

・Result in our simulation

We have estimated the value of Z_N by move of q.

$$Z_N \sim e^{\lambda^2} \quad (\to \text{fig.4})$$

The action evaluated with the classical solution.

$$S[N] = -\frac{\lambda^2 t_f^3 N^3}{48c_1} + c_2 t_f N$$

We have evaluated Z_λ from the S[N] by move of N on the contour in fig.3 .

$$Z_\lambda \sim e^{-\frac{1}{\lambda}} \quad (\to \text{fig.5})$$

Z_N and Z_λ are consistent with Halliwell (1989).

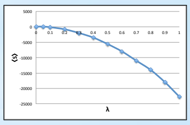

Fig.4 evaluated <S> by moveof q (T=80, simulation step 10^7)

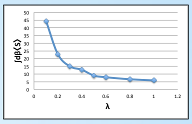

Fig.5 evaluated ∫dβ<S> by move of N (T=80, simulation step 10^7)

4. Summary and Discussion

- We could evaluate the partition function about q and N separately by using the Monte Carlo method.
- In order to evaluate the wave function automatically, we have to find the way of combining q move and N move.
- Then, extend this method to models including inflaton, or connected to the Lorentzian universe.

“Magnetic Penrose Process in a Black Hole Magnetosphere”

by Masaaki Takahashi

[JGRG23(2013)P29]

P29 JGRG23 2013 Nov. 5-8@Hirosaki Univ.

Magnetic Penrose Process in a Black Hole Magnetosphere

Masaaki Takahashi
Aichi Univ. Edu.

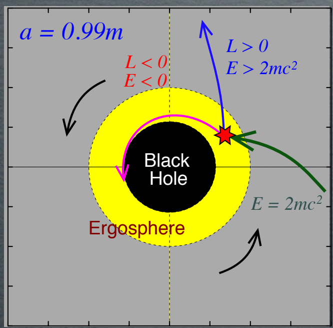

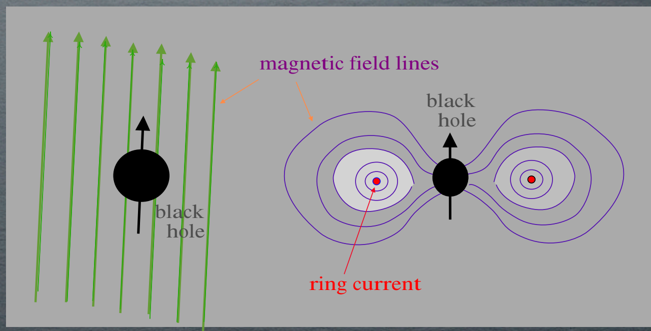

2013年12月7日土曜日

Ergosphere

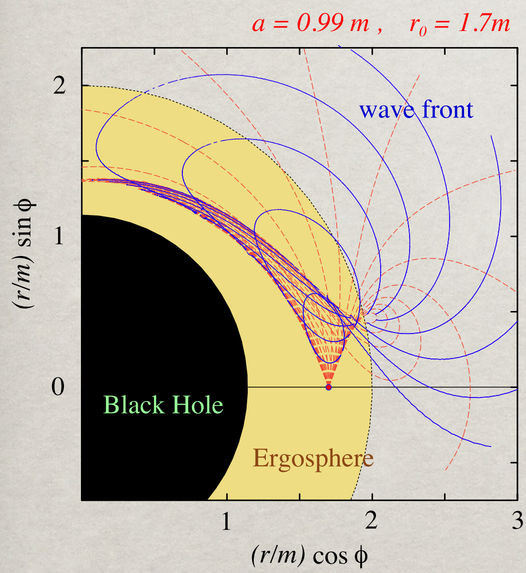

Space-time dragging effect by rotating black hole

Negative potential region

→ "Penrose process"

Magnetic field lines are also dragged near the horizon.

Energy extraction due to magnetic torque:

"Blandford-Znajek process "

2013年12月7日土曜日

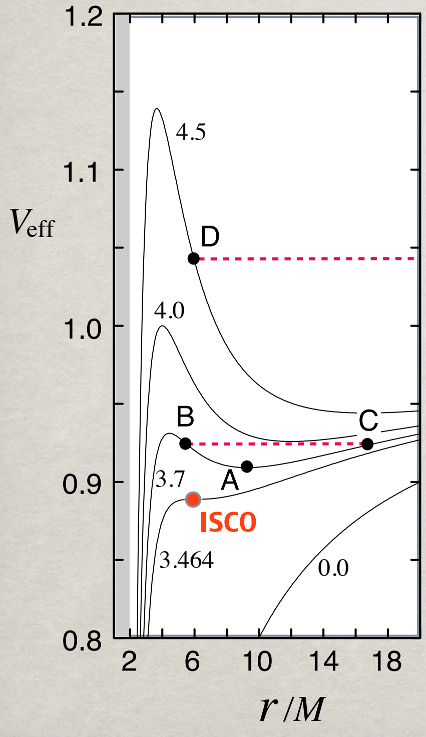

Effective Potential

シュバルツシルド・ブラックホール

動径方向の運動方程式より

$$m^2\dot{r}^2 = E^2 - V(r)$$

$$V(r) \equiv \left(1 - \frac{2M}{r}\right)\left(m^2 + \frac{L^2}{r^2}\right)$$

A ：円軌道

B-C：楕円的軌道

D- ：放物的軌道

ISCO：inner most stable circular orbit

Effective Potential

カー・ブラックホール

順回転の粒子

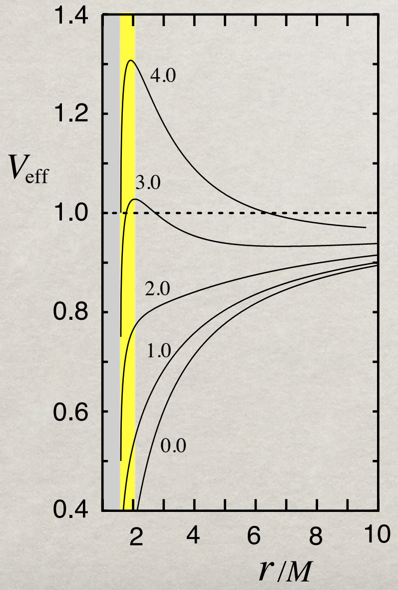

逆回転の粒子

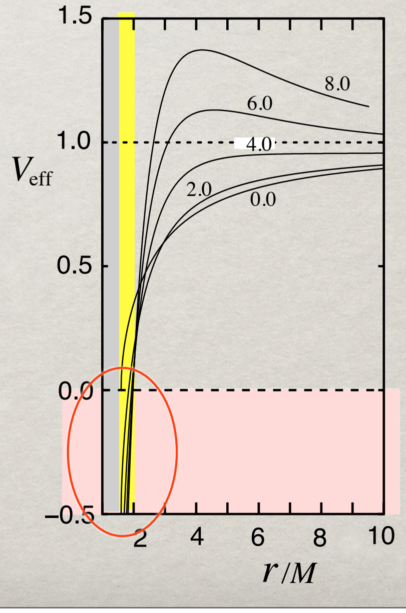

Effective Potential

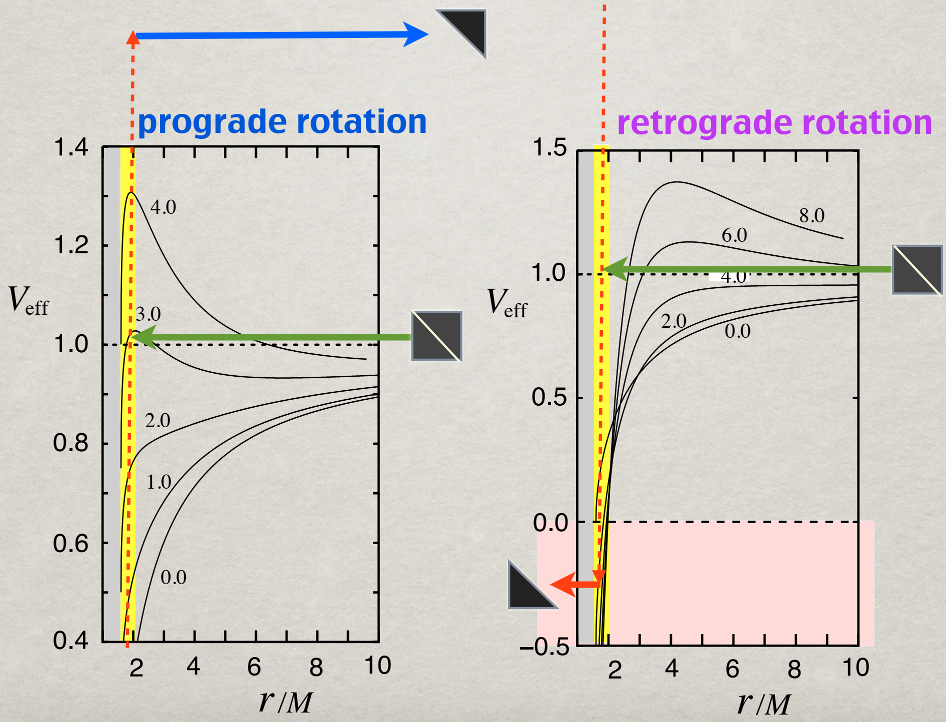

Penrose Process

Accretion of negative energy particles

Outgoing particle can release higher than incident energy.

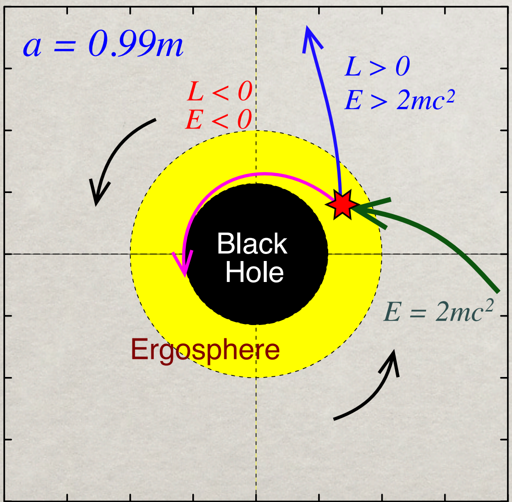

There is a **restriction** that the relative velocity of two particles exceeds c/2.

The Penrose process is not realistic when a star is destroyed by the tidal force ?

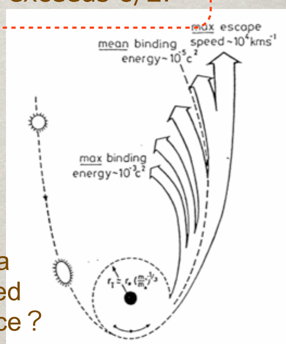

Restriction on Penrose-Process

Wagh & Dadhich(1989)

Inertial frame of particle 1 : $e^i_{(t)} = U^i_1\ ,\quad e^i_{(a)}\ (a=1,2,3)$

Energy of particle 1 :

$$E_1 = U^\mu_1 k_\mu = U^{(\alpha)}_1 k_{(\alpha)} = k_{(t)} \qquad U^{(\alpha)}_1 = (1,0,0,0)$$

Energy of particle 2 (after devision) :

$$E_2 = U^\mu_2 k_\mu = U^{(\alpha)}_2 k_{(\alpha)} = \gamma k_{(t)} + \gamma v^{(\alpha)} k_{(\alpha)} = \gamma k_{(t)} + \gamma|\boldsymbol{v}||\boldsymbol{k}|\cos\theta$$

$$U^{(\alpha)}_2 = (\gamma, \gamma\boldsymbol{v}) \qquad \gamma = (1-|\boldsymbol{v}|^2)^{-1/2}$$

relative velocity

$$\left(\begin{array}{l} k^\mu k_\mu = k^{(\alpha)}k_{(\alpha)} = k_{(t)}k^{(t)} + k_{(a)}k^{(a)} = E_1^2 - |\boldsymbol{k}|^2 \\ k^\mu k_\mu = g_{tt} \end{array}\right.$$

$$|\boldsymbol{k}| = (E_1^2 - g_{tt})^{1/2} \qquad -1 \le \cos\theta \le 1$$

2013年12月7日土曜日

Restriction on Penrose-Process (2)

Wagh & Dadhich(1989)

$$\gamma\left[E_1 - |\boldsymbol{v}|(E_1^2 - g_{tt})^{1/2}\right] \le E_2 \le \gamma\left[E_1 + |\boldsymbol{v}|(E_1^2 - g_{tt})^{1/2}\right]$$

for Penrose Process $E_2 < 0$

$$|\boldsymbol{v}| \ge \frac{E_1}{\sqrt{E_1^2 - g_{tt}}}$$

$$|\boldsymbol{v}| \ge \frac{1}{2}c$$

strict condition !

Estimate of the velocity of the lower limit

$a = M$

$E_1 \ge 1/\sqrt{3}$ (**ISCO**)

$g_{tt}(r_H) \ge -1$

near the Event Horizon

2013年12月7日土曜日

Restriction on Penrose-Process (3)

Wagh & Dadhich(1989)

Electrostatic potential $\Phi\ (= A_t)$ in Kerr spacetime

$$\gamma\left[E_1 - |\boldsymbol{v}|(E_1^2 - g_{tt})^{1/2}\right] - e_2\Phi \le E_2 \le \gamma\left[E_1 + |\boldsymbol{v}|(E_1^2 - g_{tt})^{1/2}\right] - e_2\Phi$$

$$\gamma\left[E_1 - |\boldsymbol{v}|(E_1^2 - g_{tt})^{1/2}\right] \le e_2\Phi \longleftarrow E_2 < 0$$

for Magnetic Penrose Process

$0 < e_2\Phi < E_1$ $|\boldsymbol{v}| < 1/2$ is possible

$E_1 < e_2\Phi$ **no-restrictions !**

2013年12月7日土曜日

When electromagnetic field exist、

the restriction of the limitation on Penrose process is relaxed.

What is the Extracted energy ?

Rotational energy of a Black Hole

Electrostatic potential energy

due to the dragging effects of Kerr space-time

2013年12月7日土曜日

Magnetic Field ?

Black Hole Magnetosphere with a thin disk
(vacuum solution)

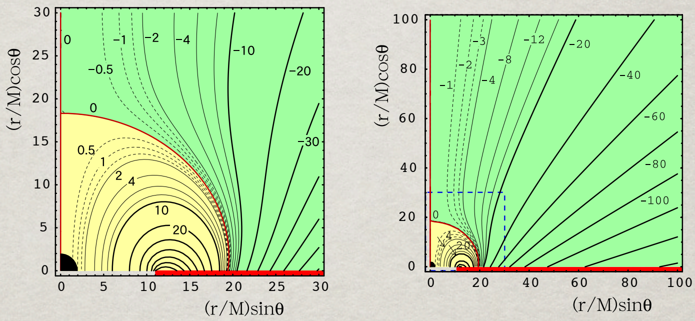

Here, we consider test magnetic fields.

- ＊ **Uniform field**
- ＊ **Loop field**
- ＊ **Dipole field**

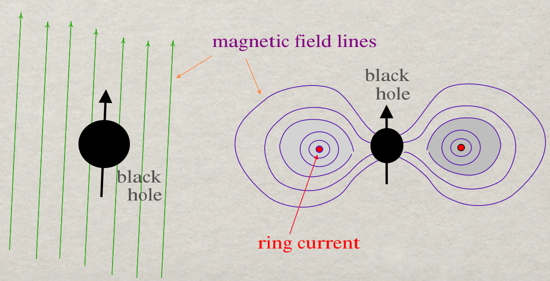

2013年12月7日土曜日

Effective Potential

$$E \equiv mu_t + eA_t \;=\; \text{constant}$$
$$-L \equiv mu_\phi + eA_\phi \;=\; \text{constant}$$

Charged Particle in Stationary and Axisymmetric Magnetic Fields

$$g^{tt}E_0^2 - 2g^{t\phi}E_0(L + qA_\phi) + g^{\phi\phi}(L + qA_\phi)^2 - m^2 = 0$$

$$V_{\rm eff} = \frac{E_0}{m} = \frac{q}{m}A_t - \frac{g_{t\phi}}{g_{\phi\phi}}\left(\frac{L}{m} + \frac{q}{m}A_\phi\right) - \frac{1}{g_{\phi\phi}}\left\{\rho_w^2\left[\left(\frac{L}{m} + \frac{q}{m}A_\phi\right)^2 - g_{\phi\phi}\right]\right\}^{1/2}$$

Dipole Magnetic Fields in Kerr Geometry

$$A_t = \frac{-3a\mu}{2\gamma^2\Sigma}\left\{\left[r(r-M) + (a^2 - Mr)\cos^2\theta\right]\frac{1}{2\gamma}\ln\left(\frac{r-r_-}{r-r_+}\right) - (r - M\cos^2\theta)\right\} \;,$$

$$A_\phi = \frac{-3\mu\sin^2\theta}{4\gamma^2\Sigma}\left\{(r-M)a^2\cos^2\theta + r(r^2 + Mr + 2a^2)\right.$$
$$\left. - \left[r(r^3 - 2Ma^2 + a^2 r) + \Delta a^2\cos^2\theta\right]\frac{1}{2\gamma}\ln\left(\frac{r-r_-}{r-r_+}\right)\right\}$$

$$\gamma \equiv (M^2 - a^2)^{1/2}$$

$$r_\pm = M \pm \gamma$$

2013年12月7日土曜日

Black Hole-Dipole Magnetosphere
Effective Potential

$$a = 0.98M, \quad V_{\rm min} = -2.0m, \quad V_{\rm max} = 2.0m$$

(blue line) = negative potential region

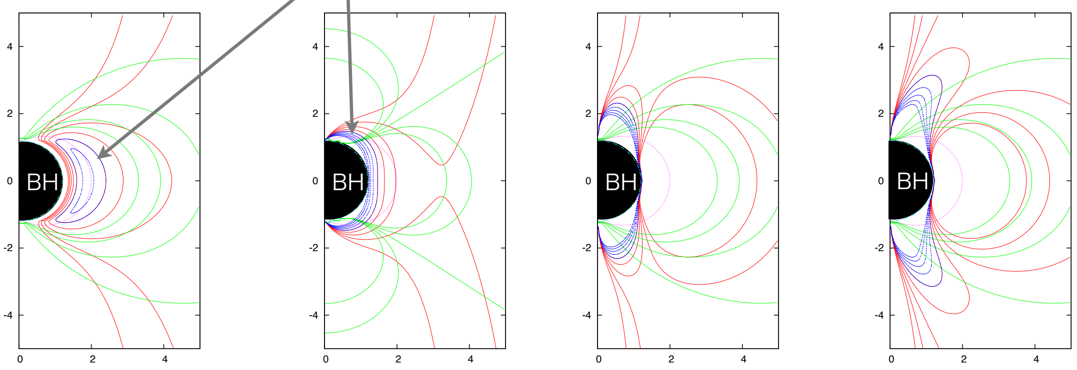

$L = -0.7m$	$L = -0.7m$	$L = -2.0m$	$L = 2.0m$
$Q_c = -3.0$	$Q_c = \ 3.0$	$Q_c = 20.0$	$Q_c = 20.0$

Negative Potential region

magnetic moment ↑ (left) and ↓ (right)

$$a = 0.98M, \quad V_{\rm min} = -2.0m, \quad V_{\rm max} = 2.0m$$

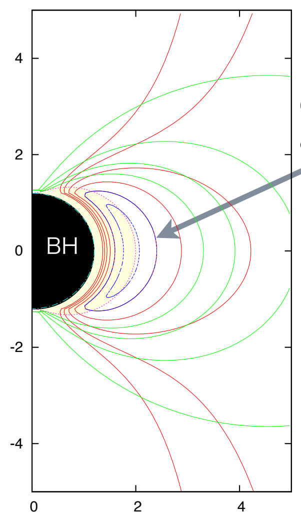

Charged particles are trapped !

Chaotic orbit !

↓

Cosmic-ray formation ?

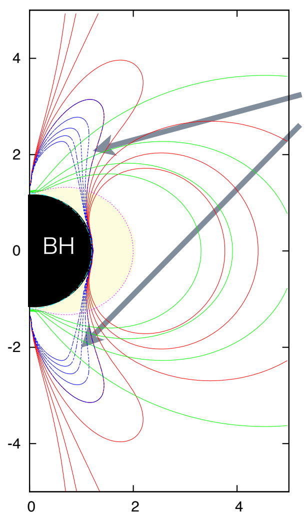

Off-equatorial regions

⇩

Jet formation ?

Near equatorial plane :
Negative potential region (bule line)

High-latitude area :
Negative potential region (blue line)

Motion of a Test Charge

Chaotic motion !

Takahashi & Koyama (2009)

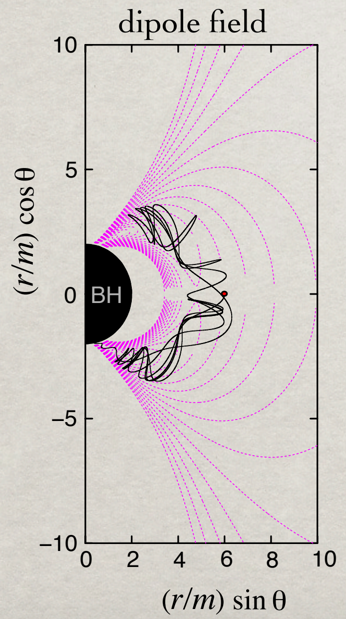

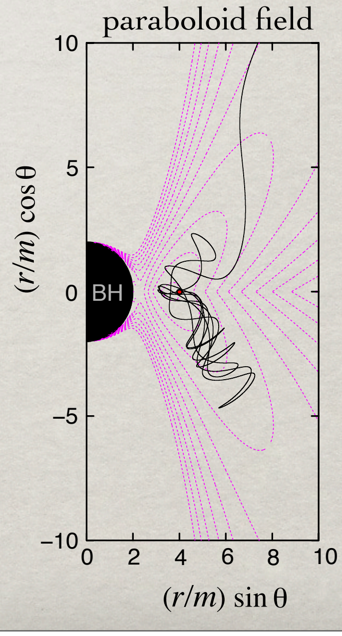

2013年12月7日土曜日

BH in a Uniform Magnetic Field

Wald (1974)

Uniform magnetic field of strength

BH charge
in a uniform magnetic field

$$A_\mu = \frac{B_0}{2}\left(m_\mu + \frac{2J}{M}k_\mu\right) - \frac{Q}{2M}k_\mu$$

In the case of Kerr BH,
Electrostatic potential A_t
is generated.

BH is charged with electricity
when BH rotates in a magnetic field.

m_μ the axial Killing vector

k_μ the timelike Killing vector

J the angular momentum of the BH spacetime

M the mass of the BH spacetime

A_ϕ magnetic field lines

A_t electrostatic potential

2013年12月7日土曜日

Restrictions on Magnetic Penrose Process

Uniform magnetic field (Wald solution)

Effective potential

Limit to the relative velocity is relaxed !

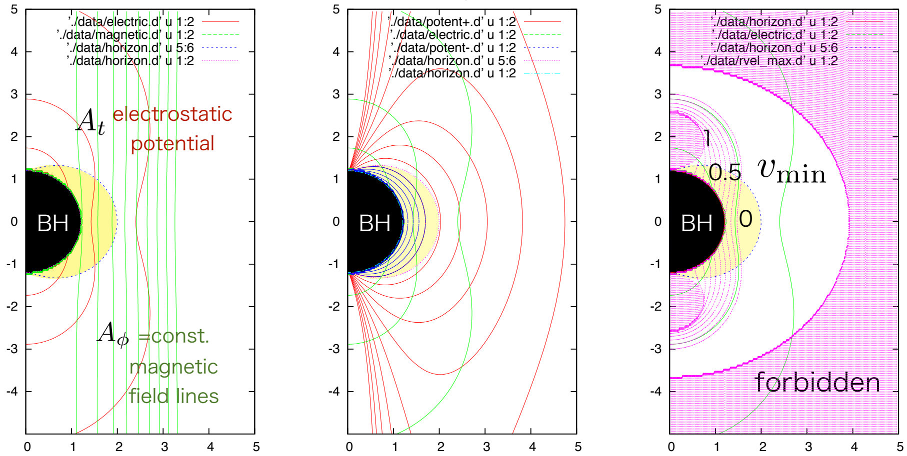

$a = 0.98M,\ E_1 = 0.7m,\ L = -6.0/Mm,\ \boxed{B_0 = 2.0,}\ Q_{\rm BH} = 0.2$

2013年12月7日土曜日

Restrictions on Magnetic Penrose Process

Uniform magnetic field (Wald solution)

Effective potential

Limit to the relative velocity is relaxed !

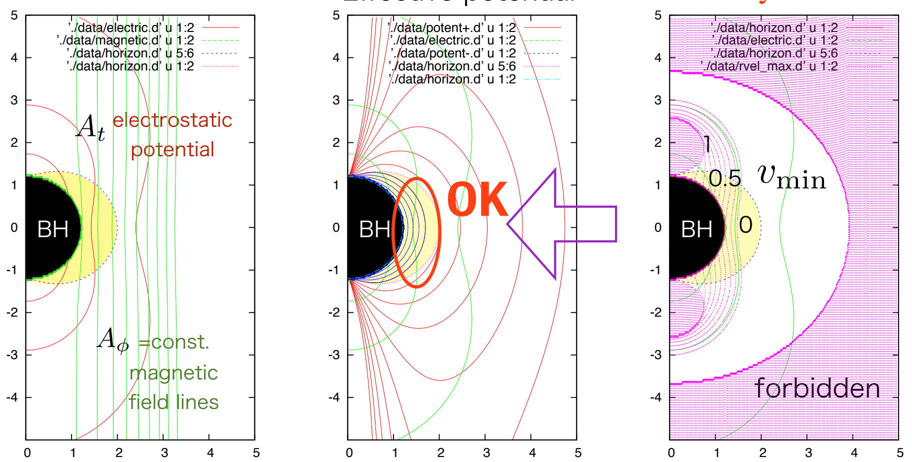

$a = 0.98M,\ E_1 = 0.7m,\ L = -6.0/Mm,\ \boxed{B_0 = 2.0,}\ Q_{\rm BH} = 0.2$

2013年12月7日土曜日

Restrictions on Magnetic Penrose Process

Uniform magnetic field (Wald solution) riverse direction

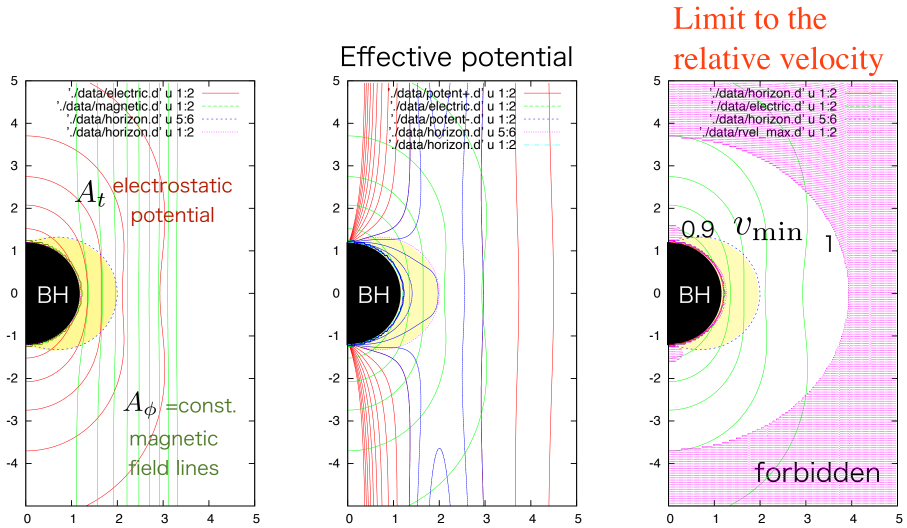

$$a = 0.98M,\ E_1 = 0.7m,\ L = -6.0/Mm,\ \boxed{B_0 = -3.0,}\ Q_{\rm BH} = 0.2$$

2013年12月7日土曜日

Restrictions on Magnetic Penrose Process

Uniform magnetic field (Wald solution) riverse direction

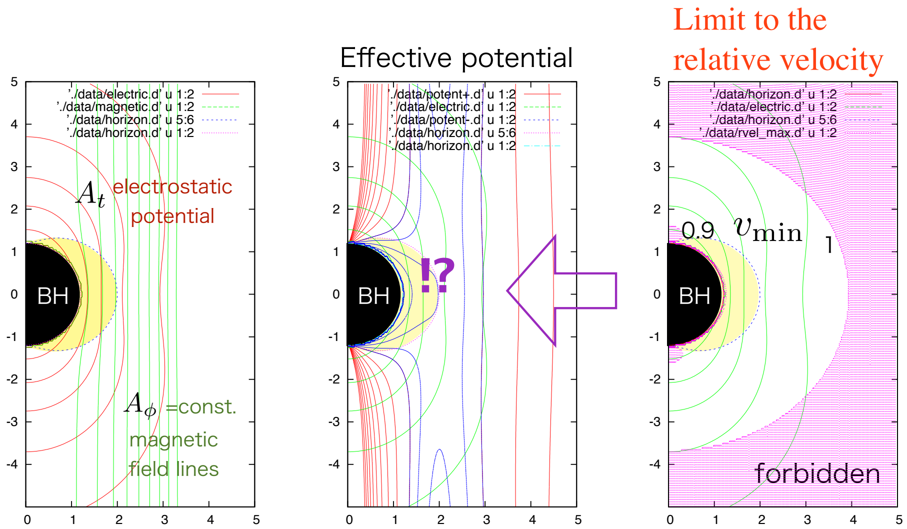

$$a = 0.98M,\ E_1 = 0.7m,\ L = -6.0/Mm,\ \boxed{B_0 = -3.0,}\ Q_{\rm BH} = 0.2$$

2013年12月7日土曜日

Negative Potential region

Wald solution (Black Hole-**Uniform**) $a = 0.98M$

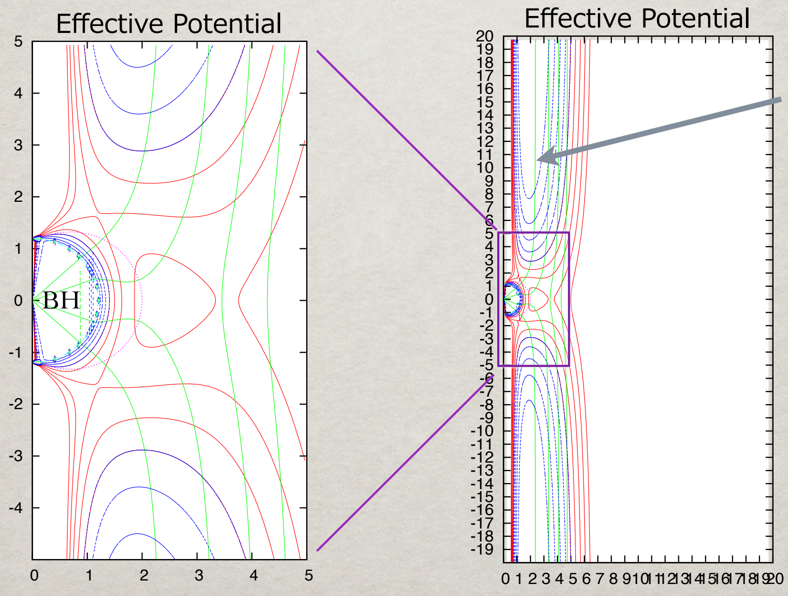

Acceleration of a charged particle is possible in this area.

Jet formation ?

Information of the black hole space-time

Accretion Disk --- The radiation is emitted from outside of ISCO.
(radio ~ X-ray, gamma-ray)

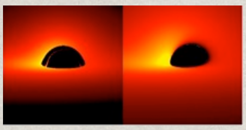

BH - Aurora --- The **HE emission** from very close to the Event Horizon is possible.

BH - Van Allen radiation belt --- The plasma can be trapped in this zone, which may be related to a **cosmic ray** .

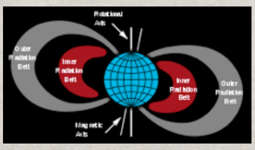

Magnetic Penrose Process !

END

“Gravitational waves generated during slow-roll inflation in Lorentz-violating Weyl gravity”

by Kohji Yajima

[JGRG23(2013)P31]

Gravitational waves generated during slow-roll inflation in Lorentz-violating Weyl gravity

Kohji Yajima
Rikkyo University, Japan
in collaboration with Tsutomu Kobayashi (Rikkyo University)

JGRG23 in Hirosaki Nov. 5 - 8, 2013

Abstract: We study gravitational waves generated during inflation in the ghost-free but Lorentz-violating Weyl gravity. This is the one of the theories about higher orders of curvature invariants in Einstein-Hilbert action as a quantum correction. Using this theory, we calculate the power spectrum of gravitational waves generated during power-law inflation, as an example of slow-roll inflation. We compare our results with the study about de Sitter expansion and the case of general relativity.

1 Lorentz-violating Weyl gravity

N. Deruelle, M. Sasaki, Y. Sendouda and A. Youssef , JHEP **09**, 009 (2012)
We use the model:

$$S[g_{ab},\chi]=\frac{1}{2\kappa}\int d^4x\sqrt{-g}\left(R+2\gamma C_{abcd}C_{efgh}\gamma^{ae}\gamma^{bf}\gamma^{cg}u^du^h\right)+S_\chi[g_{ab},\chi]\,,$$

where

$$u_a\equiv\frac{\partial_a\chi}{\sqrt{-\partial_b\chi\partial^b\chi}}\qquad\text{and}\qquad\gamma_{ab}\equiv g_{ab}+u_au_b\,.$$

$$C_{abcd}\equiv R_{abcd}-\frac{2}{n-2}\left\{g_{a[c}R_{d]b}+g_{b[d}R_{c]a}-\frac{1}{n-1}g_{a[c}g_{d]b}R\right\}\qquad(n\geq 3)\,.$$

We use units: $c=\hbar=1$. $\kappa{=}8\pi G$. γ has dimension of length^2. The action of the scalar field χ, $S_\chi[g_{ab},\chi]$, is arbitrary, but we assume $\partial_a\chi$ everywhere timelike and future-directed. The vector u^a determines a preferred time direction and then in this theory the solution breaks local Lorentz symmetry spontaneously. This model has no ghost degrees of freedom.

2 Metric perturbations

We consider the constant χ surfaces are flat and take a flat Friedmann-Robertson-Walker (FRW) spacetime as a background,

$$g_{ab}dx^adx^b=a^2(\eta)(-d\eta^2+\delta_{ij}dx^idx^j)\,,$$

where η is conformal time: $d\eta=dt/a$. We expand metric perturbations around a flat FRW spacetime

$$\begin{aligned}\delta g_{ab}dx^adx^b=a^2\big[&-2Ad\eta^2+2(\partial_iB+B_i)d\eta dx^i\\&+(2C\delta_{ij}+2\partial_i\partial_jE+\partial_iE_j+\partial_jE_i+h_{ij})dx^idx^j\big]\,.\end{aligned}$$

The dynamical perturbation from Weyl term in the action is only the tensor perturbation h_{ij}. We write down the action for the tensor perturbations:

$$S_T[h_{ij}]=\frac{1}{8\kappa}\int d\eta d^3x\left[a^2(h'_{ij}h'^{ij}-\partial_kh_{ij}\partial^kh^{ij})+4\gamma\partial_kh'_{ij}\partial^kh'^{ij}\right]\,.$$

3 Gravitational waves generated during inflation

E.O.M. of tensor perturbations in Wely gravity is

$$\ddot{h}_k+H\left(\frac{3a^2+4\gamma k^2}{a^2+4\gamma k^2}\right)\dot{h}_k+\frac{k^2}{a^2+4\gamma k^2}h_k=0\,,$$

where dot stands for derivative with respect to cosmic time t.

3.1 Sub-horizon limit

To consider the behavior of the mode in sub-horizon, we take the limit, $\frac{k}{aH}\gg 1$, and then E.O.M. of the mode is

$$\ddot{h}_k+H\dot{h}_k+\frac{1}{4\gamma}h_k=0\,.$$

3.2 Power-law inflation

We consider power-law inflation $a(t)\propto t^p$ $(p>1)$ as an example of slow-roll inflation. Then $H=p/t$ and the sub-horizon E.O.M. can be solved analytically as

$$h_k=t^{-\mu}\left\{\alpha H_\mu^{(1)}\left(\frac{t}{2\sqrt{\gamma}}\right)+\beta H_\mu^{(2)}\left(\frac{t}{2\sqrt{\gamma}}\right)\right\}\qquad(\alpha,\beta=\ \text{const.})\,,$$

where

$$\mu\equiv\frac{p-1}{2}>0\,.$$

4 Quantization

From the analysis of de Sitter expansion, modes are oscillating at $t>t_1$, t_1 is the time when the length scale $\sqrt{\gamma}$ at which the Lorentz-violating Weyl term operates is equal to the Hubble radius H^{-1}. We take the positive frequency mode in $t>t_1$ and quantize tensor perturbations. From the action for the tensor perturbations, the momentum conjugate to h_{ij} is

$$\pi^{ij}=\frac{\partial\mathcal{L}}{\partial h'_{ij}}=\frac{1}{4\kappa}(a^2h'^{ij}-4\gamma\triangle h'^{ij})\,.$$

We impose the commutation relation

$$[\hat{h}_{ij}(\eta,\vec{x}_1),\hat{\pi}^{ij}(\eta,\vec{x}_2)]=2i\delta(\vec{x}_1-\vec{x}_2)\,.$$

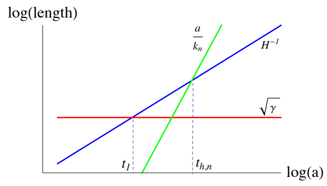

Figure 1: the length scale $\sqrt{\gamma}$ on which the Lorentz-violating Weyl term operates, the Hubble radius H^{-1}, and an arbitrary mode a/k_n. t_1 is the time when $\sqrt{\gamma}=H^{-1}$, and $t_{h,n}$ is the time when a mode a/k_n exits the Hubble radius.

5 Numerical analysis

5.1 Initial condition

We take the initial condition of mode functions as

$$h_k=\left(\frac{\kappa\pi}{4\gamma}\right)^{\frac{1}{2}}\frac{1}{k}t^{-\mu}H_\mu^{(2)}\left(\frac{t}{2\sqrt{\gamma}}\right)\,.$$

This form is chosen to be the Minkowski positive frequency modes at $\sqrt{\gamma}\ll t$ on sub-horizon scales.

5.2 Power spectrum

We calculate the power spectrum of gravitational waves in Weyl gravity and general relativity in power-law inflation.

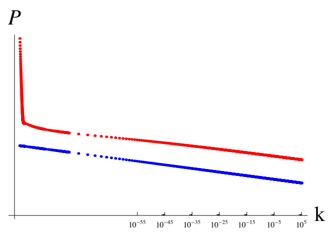

Figure 2: The power spectrum of gravitational waves in Weyl gravity and general relativity in power-law inflation. The red line is in Weyl gravity and blue line is in general relativity. A vertical axis is arbitrary.

6 Conclusion

We calculate the power spectrum of gravitational waves generated in power-law inflation in Lorentz-violating Weyl gravity. That is differ from the power spectrum in general relativity on large scales. The situation is the following: the modes with small k exit Lorentz-violating scale $\sqrt{\gamma}$ and soon cross horizon. So the effect of Lorentz-violation is large.

“An exact solution describing a closed membrane

without spherical symmetry”

by Hiroshi Kozaki

[JGRG23(2013)P32]

Closed membranes without spherical symmetry

Hiroshi Kozaki (Ishikawa national college of technology) <kozaki@ishikawa-nct.ac.jp>
with H. Ishihara and T. Koike

Introduction and conclusion

Introduction

Extended objects have been providing various topics in cosmology. The dynamics, however, is still not well clarified since equations of motion (EOMs) are given in non-linear partial differential equations. Cohomogeneity one symmetry, which means that $(p+1)$-dimensional world volume Σ is foliated by p-dimensional orbits of isometries, is helpful to study the dynamics because the EOMs are reduced to ordinary differential equations. In particular, the Nambu-Goto EOMs for strings ($p=1$) and membranes ($p=2$) are reduced to geodesic equations in certain quotient spaces.

Conclusion

A closed membrane solution without spherical symmetry is obtained in Minkowski spacetime by assuming a particular cohomogeneity one symmetry. While the membrane itself is closed, the intrinsic geometry of the world volume is a $2+1$ dimensional flat FLRW universe, which is nots spatially closed. This result, which seems contradictory, is due to the peculiarity of the assumed symmetry. The cosmological singularity corresponds to a singular orbit of isometries, which is given as a null line.

The world volume (z-direction is omitted).

dashed lines : snapshots of the closed membrane.
solid lines : foliating orbits of isometries.
two dimensional homogeneous and isotropic surface with zero constant curvature.
jagged line : singular orbit of the isometries.
null line.

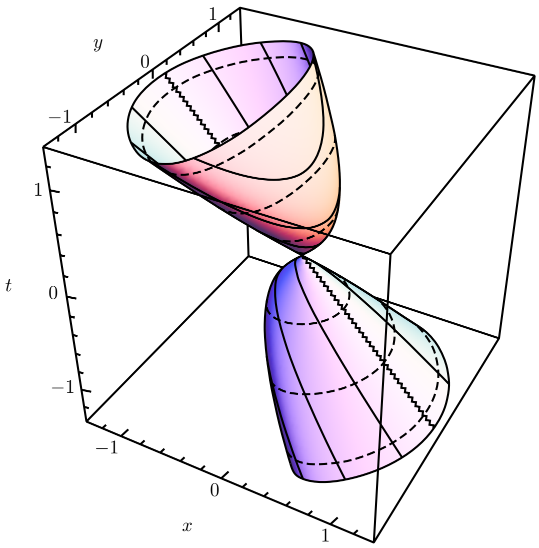

The solution

Cohomogeneity one symmetry

The world volume is assumed to be foliated by the orbits of the isometries generated by the commuting Killing vectors:

$$K_y + L_z,\ K_z - L_y$$

K_i : Lorentz boost $\quad$ L_j : rotation

Foliating orbits

The embedding of the orbit is solved as

$$t = \frac{u}{2}\vec{y}^2 + \frac{u+v}{2},\quad x = -t+u,\quad y = u\,y^1,\quad z = u\,y^2$$

$\vec{y} := (y^1, y^2)$: coordinates on the orbit
$u,\ v$: constants

These equations are written in the implicit forms:

$$-(t-\frac{v}{2})^2 + (x+\frac{v}{2})^2 + y^2 + z^2 = 0,\quad t+x = u.$$

The orbit is, therefore, the intersection of the light cone and the null plane.

Coordinate system and ansatz

We consider $(u,\ v,\ y^1, y^2)$ as coordinates in Minkowski spacetime, where the metric is written as

$$ds^2 = -dudv + u^2 d\vec{y}^2$$

and then take the following ansatz to impose the cohomogeneity one symmetry

$$u = u(\tau),\ v = v(\tau),\ y^1 = \sigma^1,\ y^2 = \sigma^2$$

$(\tau,\ \sigma^1, \sigma^2)$: coordinates on the world volume

Solution

The Nambu-Goto equations are reduced to the geodesic equations in two dimensional spacetime with the metric

$$ds^2_{\text{2-dim}} = u^4(-dudv)$$

This is readily solved as

$$v = C^2 u^5. \quad C : \text{integration constant}$$

The embedding of the world volume is implicitly given as

$$-t^2 + x^2 + y^2 + z^2 + C^2(t+x)^6 = 0$$

Induced metric on the world volume Σ

$$ds^2_\Sigma = -d\tau^2 + u^2(\tau)d\vec{\sigma}^2, \qquad u(\tau) \propto \tau^{1/3}$$